



# 5<sup>TH</sup> VIRTUAL GEOSCIENCE CONFERENCE

## BOOK OF ABSTRACTS



TECHNISCHE  
UNIVERSITÄT  
DRESDEN

contact:



**HiF**

HELMHOLTZ-INSTITUT FREIBERG  
FÜR RESSOURCENTECHNOLOGIE



# Table of contents

<b>Session 1 – Point Cloud Processing: Workflows, Geometry &amp; Semantics</b>	<b>9</b>
<b>Extending geodetic geo-monitoring networks by supervised point cloud matching</b>	<b>10</b>
<i>Lukas Raffl<sup>1*</sup> &amp; Christoph Holst<sup>1</sup> .....</i>	<i>10</i>
<b>A new open source software to design models for automatic 3D point cloud classification in environmental studies: cLASpy_T</b>	<b>12</b>
<i>Xavier Pellerin Le Bas<sup>1*</sup>, Laurent Froideval<sup>2</sup>, Christophe Conessa<sup>2</sup>, Laurent Benoit<sup>2</sup> .....</i>	<i>12</i>
<b>Time Series Analysis of 3D/4D Point Clouds within the Open-Source Online Course E-TRAINEE</b>	<b>14</b>
<i>Katharina Anders<sup>1,2*</sup>, Bernhard Höfle<sup>1</sup>, Sina Zumstein<sup>1</sup>, Jakub Dvořák<sup>3</sup>, Krzysztof Gryguc<sup>4</sup>, Lucie Kupková<sup>3</sup>, Adriana Marcinkowska-Ochtyra<sup>4</sup>, Andreas Mayr<sup>5</sup>, Adrian Ochtyra<sup>4</sup>, Markéta Potůčková<sup>3</sup> &amp; Martin Rutzinger<sup>5</sup> .....</i>	<i>14</i>
<b>Testing Theory for Identification of Aeolian Sand Transport Trends in 4D Data from Permanent Laser Scanning</b>	<b>16</b>
<i>Mieke Kuschnerus<sup>1*</sup>, Sander Vos<sup>2</sup>, Sierd de Vries<sup>2</sup>, José A. Á. Antolínez<sup>2</sup>, Roderik Lindenbergh<sup>1</sup> .....</i>	<i>16</i>
<b>Assessing dune dynamics from Dutch airborne laser scanning products</b>	<b>18</b>
<i>Roderik Lindenbergh<sup>1</sup>, Christa van Ijzendoorn<sup>2</sup>, Jinhu Wang<sup>3</sup> .....</i>	<i>18</i>
<b>Optimizing colour-schemes for 3D point cloud visualization: the case of classified point clouds, surface normal representations and engineering defect diagnostics</b>	<b>20</b>
<i>Laure Manceau<sup>1*</sup>, Thomas JB Dewez<sup>2</sup>, Hugues Fournier<sup>3</sup>, Julien Vallet<sup>3</sup> .....</i>	<i>20</i>
<b>Session 2 – Visualisation, communication &amp; Teaching</b>	<b>22</b>
<b>Virtual geoscience 3D modelling quality: experience from three years of V3Geo</b>	<b>23</b>
<i>Simon J. Buckley<sup>1*</sup>, Conor Lewis<sup>1</sup>, John A. Howell<sup>2</sup>, Magda Chmielewska<sup>2</sup>, Nicole Naumann<sup>1</sup>, Jess Pugsley<sup>2</sup>, Kari Ringdal<sup>1</sup>, Joris Vanbiervliet<sup>1</sup>, Thomas J.B. Dewez<sup>3</sup> .....</i>	<i>23</i>
<b>Using 360° video to create immersive virtual reality teaching materials: A virtual field trip to the Swiss Alps to assess stream water sources</b>	<b>26</b>
<i>Professor Ian Maddock<sup>1*</sup> and Harry Ormonde<sup>1</sup> .....</i>	<i>26</i>
<b>Does time really matter? A comparison between virtual and physical field trips</b>	<b>28</b>
<i>Pugsley J.<sup>1</sup>, Howell J.<sup>1</sup>, Hartley A.<sup>1</sup>, Buckley S.<sup>2,3</sup>, Chmielewska M.<sup>1</sup>, Naumann N.<sup>2</sup>, .....</i>	<i>28</i>

<b>The effectiveness of Virtual Reality Field Trips (VFTs) in Field Geology education</b>	<b>29</b>
<i>Jan van Bever Donker<sup>1*</sup>, Rudy Maart<sup>1</sup>, Delia Marshall<sup>1</sup>, Luyanda Mayekiso<sup>1</sup>, Matthew S. Huber<sup>1</sup>, Henok Solomon<sup>1</sup> &amp; Nompumelelo Mgabisa<sup>1,2</sup></i> .....	29
<b>Using VR to make in-person fieldwork in the environmental sciences more inclusive</b>	<b>30</b>
<i>Derek A McDougall<sup>1*</sup>, Lynda Yorke<sup>2</sup> &amp; Simon Hutchinson<sup>3</sup></i> , .....	30
<b>Session 3 – Applying Machine Learning in Geosciences</b>	<b>31</b>
<b>Unlocking the Potential of Historical Aerial Imagery for the Antarctic Peninsula: Automating 3D Reconstruction using Python and MicMac</b>	<b>32</b>
<i>Felix Dahle<sup>1</sup>, Roderik Lindenbergh<sup>1</sup>, Bert Wouters<sup>1</sup></i> .....	32
<b>Advanced Glacier Monitoring with ICEpy4D: A Python Toolkit for Multi-Epoch Analysis using Deep-Learning Photogrammetry</b>	<b>34</b>
<i>F. Ioli<sup>1*</sup>, F. Nex<sup>2</sup> &amp; L. Pinto<sup>1</sup></i> .....	34
<b>Deep learning of topographic anomalies for the detection of regions of interest in 3D point clouds</b>	<b>36</b>
<i>Reuma Arav<sup>1*</sup>, Dennis Wittich<sup>2</sup>, Franz Rottensteiner<sup>2</sup></i> .....	36
<b>Machine Learning Approach on Dynamic Interactions between Air Pollutants and Forest Health using Open-access Remote Sensing Data: A Case study of the Białowieża Forest</b>	<b>40</b>
<i>Luka Mamić<sup>1*</sup>, Francesco Pirotti<sup>2,3</sup></i> .....	40
<b>Automatic boulder detection applied to the Stone Garden (Altai Mountains, Russia): techniques and outcomes</b>	<b>42</b>
<i>Sergei Medvedev<sup>1</sup>, Dmitry Zastrozhnov<sup>2,3,4*</sup>, Viktor Spiridonov<sup>3,5</sup>, Nils Charles Prieur<sup>4,6</sup>, Andrei Zastrozhnov<sup>3</sup> &amp; Sverre Planke<sup>2,4</sup></i> .....	42
<b>Session 4 – Digital Outcrop Characterisation &amp; Analysis</b>	<b>44</b>
<b>Using outcrop digital models to guide subsurface studies for CO<sub>2</sub> storage: An example from the Amellago Oolitic Ramp (Morocco) as an analogue for the Paris Basin Dogger Reservoir</b>	<b>45</b>
<i>A. Bordenave<sup>1,2*</sup>, E. Dujoncquoy<sup>3</sup>, P. Razin<sup>4</sup>, P. Daguinos<sup>4</sup>, B. Issautier<sup>1</sup> &amp; J. Kenter<sup>3</sup></i> .....	45
<b>Digital outcrop mapping of the Puga geothermal field, Ladakh, India</b>	<b>47</b>
<i>Sam T Thiele<sup>1*</sup>, Horthing V Zimik<sup>2,3</sup>, Aditya Naik<sup>4</sup>, Daudayal Sharma<sup>3</sup>, Pankaj Khanna<sup>3</sup></i> .....	47
<b>How high-resolution DOM &amp; VR boost unravelling and modelling of complex fault zones?</b>	<b>49</b>
<i>Lamarche J.<sup>1*</sup>, Richard P.<sup>2</sup>, Touré K. <sup>1</sup>, Viseur S. <sup>1</sup>, Fleury J. <sup>1</sup>, Civet F. <sup>3</sup></i> .....	49
<b>A new 1:50.000 scale map of the Nuussuaq basin: unveiling the dynamic earth with digital methods</b>	<b>51</b>
<i>Erik Vest Sørensen <sup>1*</sup>, Asger Ken Pedersen<sup>2</sup></i> .....	51
<b>Session 5 – Airborne &amp; Remote Mapping</b>	<b>53</b>
<b>A manmade disaster - The vulnerability of managed forests in the disastrous southern summer wildfires 2023 in Chile – A remote sensing approach</b>	<b>54</b>
<i>Benedikt Hora<sup>1</sup> and Constanza Gonzalez-Mathiesen <sup>2</sup></i> .....	54

<b>Unlocking the Potential: Bridging the Gap Between Remote Sensing Science and User Uptake in Environmental Applications. An Eastern Austrian Case Study</b>	<b>56</b>
<i>Anna Iglseder<sup>1</sup>, Christian Prochaska<sup>2</sup>, Lorenz Schimpl<sup>1</sup>, Nils Berger<sup>1</sup>, Hannes Hoffert-Hösl<sup>2</sup>, Michael Lechner<sup>3</sup>, Markus Immitzer<sup>3</sup>, Christine Rottenbacher<sup>4</sup>, Tanja Lumetsberger<sup>5</sup>, Christoph Bauerhansl<sup>6</sup>, Markus Hollaus<sup>1</sup> .....</i>	
	<i>56</i>
<b>Mapping Wildfire Scores – NDVI vs. NBR vs. AFRI</b>	<b>58</b>
<i>Arnon Karnieli<sup>1*</sup> &amp; Manuel Salvoldi<sup>1</sup> .....</i>	
	<i>58</i>
<b>Extending QGIS towards collaborative analysis and interpretation of geospatial data</b>	<b>60</b>
<i>Sebastian Mikolka-Flöry<sup>1*</sup>, Norbert Pfeifer<sup>1</sup> .....</i>	
	<i>60</i>
<b>Mobile mapping and GeoSLAM for the characterisation and modelling of karst morphologies at the conduit scale</b>	<b>61</b>
<i>Tanguy Racine<sup>1*</sup>, Celia Trunz<sup>1</sup>, Julien Straubhaar<sup>1</sup>, Philippe Renard<sup>1</sup> .....</i>	
	<i>61</i>
<b>High-resolution aerial imagery for early detection of climate-induced natural hazards at a mountain range scale</b>	<b>62</b>
<i>Natalie Barbosa<sup>1,2*</sup>, Juilson Jubanski<sup>3</sup>, Ulrich Münzer<sup>4</sup>, Florian Siegert<sup>1,3</sup> .....</i>	
	<i>62</i>
<b>Session 6 – Recent Developments in Geomorphic Process and Hazard Monitoring</b>	<b>64</b>
<b>Geological Monitoring processes with small laser scanners. Examples in Montserrat, Puigcerçós, Croscat volcano (Catalonia, Spain) and analogic models</b>	<b>71</b>
<b>Complexity and precision of topographic change detection in active volcanic craters using close-range airborne imagery and SfM-MVS photogrammetry</b>	<b>73</b>
<b>Enriching Geohazard Education through Virtual Field Trips using VR and 3D Outcrop Models</b>	<b>75</b>
<b>Session 7 – Applications in Hydrology &amp; Ecology</b>	<b>77</b>
<b>Revolutionising Natural Flood Management with SCALGO Live, SCIMAP, and Drones</b>	<b>78</b>
<i>Josie Lynch<sup>1*</sup>, Dr Derek McDougall<sup>1</sup> and Professor Ian Maddock<sup>1</sup> .....</i>	
	<i>78</i>
<b>Monitoring streamflow with drones</b>	<b>80</b>
<i>Westerberg, I. K. <sup>1*</sup>, Mansanarez, V.<sup>1</sup>, Lyon, S.W.<sup>2,3,4</sup>, Huseby Karlsen, R.<sup>1</sup> &amp; Lam, N.<sup>2</sup> .....</i>	
	<i>80</i>
<b>UAV- and handheld-hyperspectral imaging for <i>Sphagnum</i> discrimination and vegetation modelling</b>	<b>81</b>
<i>Franziska Wolff<sup>1*</sup>, Sandra Lorenz<sup>2</sup>, Pasi Korpelainen<sup>1</sup>, Anette Eltner<sup>3</sup> &amp; Timo Kumpula<sup>1</sup> .....</i>	
	<i>81</i>
<b>Mapping Pb/Zn-stressed plant communities: challenges of centimetre- to millimetre-scale UAV sensing for training deep-learning schemes</b>	<b>83</b>
<i>Thomas JB Dewez<sup>1*</sup>, Adrien Breton<sup>1</sup>, Gaël Bellenfant<sup>1</sup>, Marie de Boisvilliers<sup>2</sup>, Marion Houlès<sup>2</sup>, Florent Guiotte<sup>2</sup>, Bruno Roux<sup>2</sup>, Sébastien Lefèvre<sup>3</sup>, Javiera Castillo-Navarro<sup>3</sup>, Guglielmo Fernandez Garcia<sup>3</sup>, Felix Kröber<sup>3</sup>, Thomas Corpetti<sup>3</sup>, Florian Delerue<sup>4</sup> .....</i>	
	<i>83</i>
<b>An index representing geomorphological disturbance for Alpine plants based on airborne laser scan data</b>	<b>85</b>
<i>Andreas Mayr<sup>1*</sup>, Martin Rutzinger<sup>1</sup>, Lukas Müller<sup>1</sup>, Andreas Kollert<sup>1</sup>, Stefan Dullinger<sup>2</sup>, Karl Hülber<sup>2</sup> ....</i>	
	<i>85</i>

<b>Poster Contributions</b>	<b>87</b>
<b>Virtual field trips for teaching rock mechanics and tunnelling using CoSpaces – summary of 4 years of experiences</b>	<b>88</b>
<i>Luis Jordá Bordehore*</i> , <i>Salvador Senent Dominguez</i> , <i>Ruben Angel Galindo Aires</i> , <i>Jesús González Galindo</i> .....	88
<b>Advancing Geology Education through Immersive Virtual Reality Training Modules</b>	<b>90</b>
<i>Jian Yang</i> <sup>1*</sup> , <i>Maximilian Hallenberger</i> <sup>2</sup> & <i>Florian Wellmann</i> <sup>1</sup> .....	90
<b>Integrating Rapid Geomodeling with Mixed-Reality for Enhanced Geoscientific Applications</b>	<b>92</b>
<i>Miguel de la Varga</i> <sup>1,2</sup> , <i>Dr Simon Virgo</i> <sup>1</sup> .....	92
<b>Towards an automated workflow for assessing effects of forest disturbance on land surface temperature in low mountain ranges of Central Germany using GEE and the Landsat archive</b>	<b>94</b>
<i>Simon Grieger</i> <sup>1*</sup> , <i>Daniel Wyss</i> <sup>1</sup> & <i>Birgitta Putzenlechner</i> <sup>1</sup> .....	94
<b>UAV LiDAR-based tree detection and structural parameter estimation with a focus on the treeline ecotone</b>	<b>95</b>
<i>Alex Šroller</i> <sup>1*</sup> , <i>Markéta Potůčková</i> <sup>1</sup> & <i>Václav Trem</i> <sup>2</sup> .....	95
<b>SfM method for underground corridors modelling – Kletno mine example</b>	<b>97</b>
<b>Workflow of unmanned aerial vehicle (UAV) application to railways geotechnical asset management</b>	<b>99</b>
<i>Oriol Pedraza</i> <sup>1*</sup> , <i>Marc Janeras</i> <sup>1</sup> , <i>Iván Garcia</i> <sup>1</sup> & <i>Toni Gil</i> <sup>2</sup> .....	99
<b>Sensing Mountains – Learning about the Observation of Environmental Processes in a Changing World</b>	<b>101</b>
<i>Martin Rutzinger</i> <sup>1</sup> , <i>Katharina Anders</i> <sup>2</sup> , <i>Magnus Bremer</i> <sup>1,3</sup> , <i>Anette Eltner</i> <sup>4</sup> , <i>Caroline Gaever</i> <sup>5</sup> , <i>Bernhard Höfle</i> <sup>2</sup> , <i>Roderik Lindenbergh</i> <sup>6</sup> , <i>Andreas Mayr</i> <sup>1*</sup> , <i>Sander Oude Elberink</i> <sup>5</sup> , <i>Francesco Pirotti</i> <sup>7</sup> , <i>Marco Scaioni</i> <sup>8</sup> , <i>Thomas Zieher</i> <sup>1,9</sup> .....	101
<b>Comparing the in situ and SfM methods for brittle tectonics analysis – a case study of the Strzegom-Sobótka granite massif</b>	<b>103</b>
<i>Bartłomiej Grochmal</i> <sup>1*</sup> , <i>Mariusz Fialkiewicz</i> <sup>1</sup> , <i>Marcin Olkowicz</i> <sup>1</sup> & <i>Marcin Dąbrowski</i> <sup>1</sup> .....	103
<b>Structural analysis in the quarries and outcrops of the Moravo-Silesian fold and thrust belt: a case study using photogrammetry methods</b>	<b>104</b>
<i>Mariusz Fialkiewicz</i> <sup>1*</sup> , <i>Bartłomiej Grochmal</i> <sup>1</sup> , <i>Marcin Olkowicz</i> <sup>1</sup> & <i>Marcin Dąbrowski</i> <sup>1</sup> .....	104
<b>Semi-automatic discontinuity detection using density in point cloud data</b>	<b>106</b>
<i>Antonin Chalé</i> , <i>Michel Jaboyedoff</i> , and <i>Marc-Henri Derron</i> .....	106
<b>Integration of remote sensing techniques for slopes monitoring</b>	<b>108</b>
<i>M<sup>a</sup> Amparo Núñez-Andrés</i> <sup>1*</sup> , <i>Felipe Buill</i> <sup>1</sup> , <i>Francisco Javier Muñoz</i> <sup>1</sup> , <i>Oriol Pedraza</i> <sup>2</sup> & <i>Marc Janeras</i> <sup>1,2</sup> .....	108
<b>Cliff overhang mapping on 3D point clouds with Cloud Compare</b>	<b>110</b>
<i>Thomas JB Dewez</i> <sup>1*</sup> , <i>Clara Lévy</i> <sup>1</sup> , <i>Claire Myr</i> <sup>2</sup> .....	110

<b>Updating of Rockfall inventory in the Montserrat massif (Spain): attributes in Point clouds for hazard assessment using Machine Learning techniques.</b>	<b>112</b>
<i>Garcia-Sellés, D.<sup>1*</sup>, Blanco, L.<sup>2</sup>, Janeras, M.<sup>3</sup>, Pedraza, O.<sup>3</sup> .....</i>	<i>112</i>
<b>Quantifying slope movements: Tree trunk tracking using long-range stationary 4D laser scanning point clouds</b>	<b>114</b>
<i>Ronald Tabernig<sup>1*</sup>, Katharina Anders<sup>2</sup>, Patrick Fritzmann<sup>3</sup>, Hannah Weiser<sup>2</sup>, Vivien Zahs<sup>2</sup>, Bernhard Höfle<sup>2,4,5</sup> &amp; Martin Rutzinger<sup>1</sup> .....</i>	<i>114</i>
<b>Using Machine Learning to filter point clouds from artificial rainfall simulations</b>	<b>116</b>
<i>Oliver Grothum*, Anne Bienert, Mikesch Blümlein &amp; Anette Eltner.....</i>	<i>116</i>
<b>Processing large amounts of time-lapse imagery for geomorphic research: an AI-based approach</b>	<b>118</b>
<i>Hanne Hendrickx<sup>1*</sup>, Xabier Blanch<sup>1</sup>, Mario Kummert<sup>2</sup>, Antonio Abellan<sup>3</sup>, Reynald Delaloye<sup>4</sup>, Anette Eltner<sup>1</sup> .....</i>	<i>118</i>
<b>Surface elevation monitoring in northern Tunisia using multi-temporal photogrammetric imagery</b>	<b>122</b>
<i>Imen Brini<sup>1,2*</sup>, Denis Feurer<sup>1</sup>, Riadh Tebourbi<sup>2</sup>, Damien Raclot<sup>1</sup>, Fabrice Vinatier<sup>1</sup>, Riadh Abdelfattah<sup>2</sup> .....</i>	<i>122</i>
<b>Assesment of Soil Degradation: Water Erosion under Systematic UAV Supervision</b>	<b>124</b>
<i>Tomáš Laburda<sup>1*</sup>, Josef Krása<sup>1</sup>, Jakub Stašek<sup>1</sup>, Markéta Báčová<sup>1</sup> &amp; Tomáš Dostál<sup>1</sup> .....</i>	<i>124</i>
<b>Improving Soil Infiltration Assessment with Deep Learning for Water Segmentation Applied to Time-Lapse Imagery</b>	<b>126</b>
<i>Mikesch Blümlein<sup>1</sup>, Pedro Zamboni<sup>2</sup>, Jonas Lenz<sup>1</sup>, Anette Eltner<sup>1</sup> .....</i>	<i>126</i>
<b>Investigating the interrelations between of rainfall characteristics and gully erosion processes</b>	<b>128</b>
<i>Fentahun Bezie<sup>1,2</sup>, Kwinten Van Weverberg<sup>2</sup>, Amaury Frankl<sup>2,*</sup> .....</i>	<i>128</i>
<b>Generating ensembles of karst conduit surfaces of varying roughness and complexity with Gaussian random fields</b>	<b>129</b>
<i>Celia Trunz*, Tanguy Racine, Julien Straubhaar, Philippe Renard.....</i>	<i>129</i>
<b>Improving the resolution of mineralogical maps through the use of ANN with hyperspectral datasets of different resolution</b>	<b>130</b>
<i>Yehor Surkov<sup>1*</sup> &amp; Urs Mall<sup>1</sup> .....</i>	<i>130</i>
<b>Integrating surface spectral and subsurface geophysical data for comprehensive resource characterisation of mining residues</b>	<b>132</b>
<i>Moritz Kirsch<sup>1*</sup>, Ana Bautista Gascueña<sup>1,5</sup>, Samuel Thiele<sup>1</sup>, Akshay Kamath<sup>1</sup>, Andrea Viezzoli<sup>2</sup>, Arianna Rapiti<sup>2</sup>, Roberto De La Rosa<sup>1,5</sup>, Per Gisselø<sup>3</sup>, Angelo Farci<sup>4</sup> &amp; Richard Gloaguen<sup>1</sup> .....</i>	<i>132</i>
<b>Digitalising Svalbard with Svalbox: towards a baseline survey of one of the world's fastest warming places</b>	<b>133</b>
<i>Kim Senger<sup>1,*</sup>, Lilith Kuckero<sup>1</sup>, Peter Betlem<sup>1,2</sup>, Rafael Kenji Horota<sup>1,3</sup>, Aleksandra Smyrak-Sikora<sup>1</sup>, Nil Rodes<sup>1</sup>, Anna Sartell<sup>4,1</sup>, Anders Dahlin<sup>1,2</sup>, Tereza Mosociova<sup>1</sup>, Marius Jonassen<sup>1</sup> .....</i>	<i>133</i>
<b>Creative and Funny Use of Unmanned Aerial Systems and Mobile Devices in Hydraulic: A Project-Based Learning Approach</b>	<b>135</b>

<i>Hana Nekrep<sup>1</sup>, Matjaž N. Perc<sup>2*</sup></i> .....	135
<b>Water level estimation comparison: UAV vs satellite altimetric data</b>	<b>136</b>
<i>Grzegorz Walusiak<sup>1*</sup> &amp; Matylda Witek<sup>1</sup></i> .....	136
<b>Multi-drone experimental campaign for shallow river bathymetry</b>	<b>137</b>
<i>Matylda Witek<sup>1*</sup> &amp; Grzegorz Walusiak<sup>1</sup></i> .....	137
<b>Exploring the potential of UAV for plant biodiversity monitoring in farmland</b>	<b>138</b>
<i>Caterina Barrasso<sup>1</sup>, Robert Krüger<sup>2*</sup>, Lisanne Hölting<sup>1</sup>, Anette Eltner<sup>2</sup> &amp; Anna Cord<sup>1</sup></i> .....	138
<b>Demonstrating the OPTRAM soil moisture model over pasture areas in drylands</b>	<b>140</b>
<i>Arnon Karnieli* &amp; Micha Silver</i> .....	140

**Session 1 – Point Cloud Processing: Workflows, Geometry & Semantics**

A large, faint, light gray globe is centered in the background of the slide.

# **SESSION 1**

## **POINT CLOUD PROCESSING: WORKFLOWS, GEOMETRY & SEMANTICS**

# Extending geodetic geo-monitoring networks by supervised point cloud matching

Lukas Raffl<sup>1\*</sup> & Christoph Holst<sup>1</sup>

<sup>1</sup> Technical University of Munich (TUM), TUM School of Engineering and Design, Chair of Engineering Geodesy, Arcisstraße 21, 80333 Munich, Germany, lukas.raffl@tum.de

**Key words:** geo-monitoring, laser scanning, Monte Carlo Simulation, congruence model, 3D deformation vectors

Geo-monitoring plays a crucial role in risk prevention, particularly in mountainous regions such as the Alps, where climate change has led to an increase in gravitational mass movements. To address this challenge, geodetic monitoring systems are essential for understanding geological processes, detecting deformations, and forecasting potential events. The goal is to provide precise 3D deformation vectors with high accuracy and spatial coverage while ensuring the quality of the results through redundancy and statistical significance tests.

In geodetic monitoring, we use point-based as well as point-cloud-based methods for deformation analysis. In the case of point-based monitoring, geodetic network measurements and adjustments allow for the most consistent error propagation and thus a trustworthy statistical significance calculation. However, a spatial discretization of the object has to be made, and the installation of a sufficient number of targets is especially difficult in inaccessible hazardous areas in the mountains.

To overcome these limitations, we introduce a workflow for supervised point cloud matching that allows the inclusion of point clouds into a conventional geodetic monitoring network. Our approach is based on virtual targets represented by local scan patches. Each patch is matched between overlapping stations and across different measurement epochs using the Iterative Closest Point Algorithm (ICP) (Fig. 1). Thus, similar to feature points, a number of homologous points are created that overcome the challenge of missing point identities in laser scans. This enables the creation of a combined monitoring network consisting of signalized and non-signalized points and improves the spatial resolution as well as the network geometry. However, supervised patch selection is necessary as the accuracy of ICP matching strongly depends on the point distribution within the patches. In our workflow, each patch is evaluated within a Monte Carlo Simulation to ensure that the patch fulfils the quality requirements.

We apply our method to two datasets. The first is a monitoring setup in the laboratory, where we establish the parameters for the supervised patch selection and demonstrate how the network geometry is improved. The second is the real case study of Mt. Hochvogel, where the proposed method helps to clearly enhance the spatial resolution of deformation vectors (Fig. 2). The results show that the integration of point clouds into monitoring networks by supervised point cloud matching improves the accuracy and reliability of the subsequent rigorous deformation analysis, thus allowing for an early identification of deformations in geo-monitoring applications.

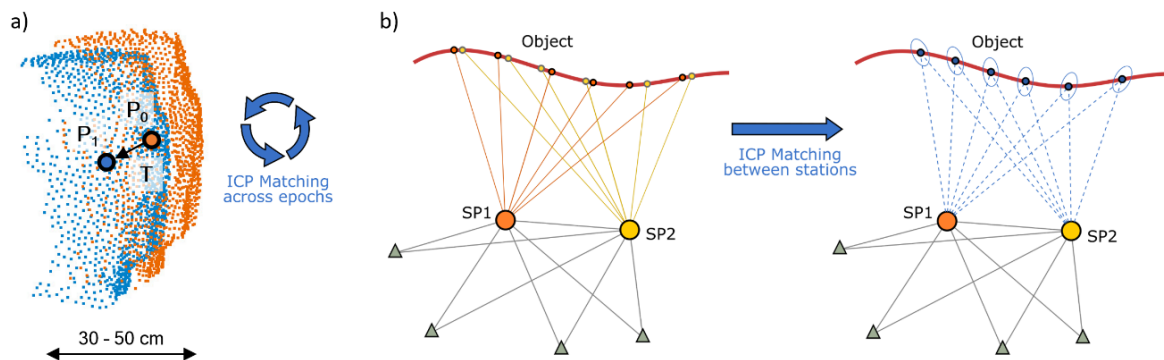


Figure 1: a) Creation of corresponding virtual targets using ICP matching and b) integration into the geodetic monitoring network.

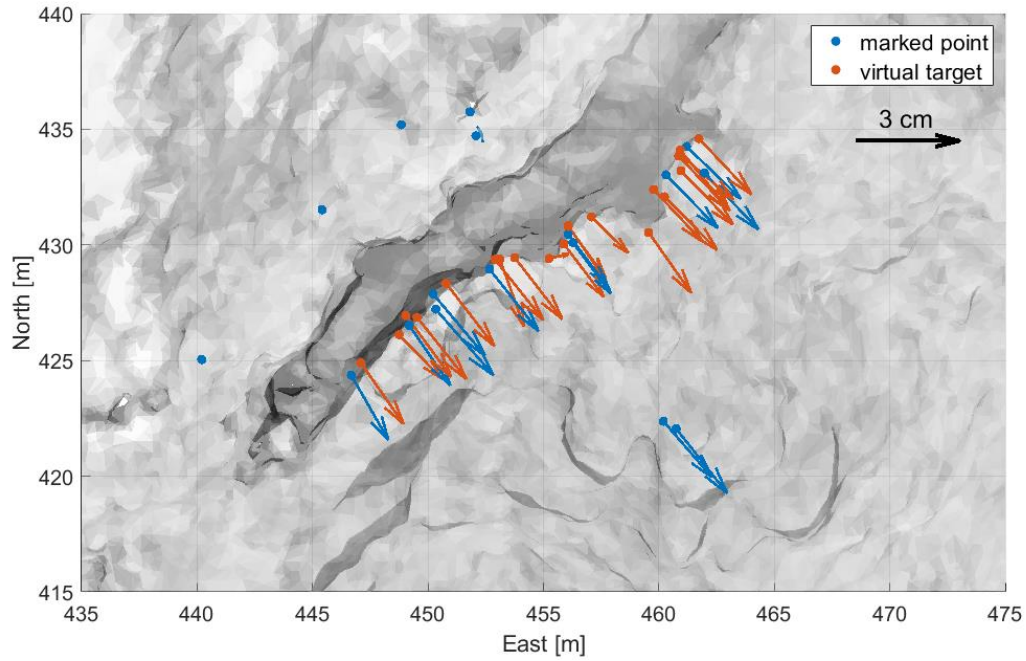


Figure 2: Deformation vectors on Mt. Hochvogel between 2018 and 2019.

**Acknowledgements:** This research is done within the research project “AlpSenseRely” financed by the Bavarian State Ministry of the Environment and Consumer Protection.

## A new open source software to design models for automatic 3D point cloud classification in environmental studies: cLASpy\_T

Xavier Pellerin Le Bas<sup>1\*</sup>, Laurent Froideval<sup>2</sup>,  
Christophe Conessa<sup>2</sup>, Laurent Benoit<sup>2</sup>

<sup>1</sup>Scienteama, 4 av. de Cambridge 14200 Hérouville-St-Clair, France, xavier.pellerin@scienteama.fr

<sup>2</sup>Normandie Univ, UNICAEN, UNIROUEN, CNRS, M2C, 14000 Caen, France

**Key words:** machine learning, classification, environmental data, photogrammetry, airborne LiDAR, hyperspectral data.

We introduce a new open source software, cLASpy\_T, that helps classify environmental 3D point clouds. cLASpy\_T means ‘Tools for classification of LAS files with Python’. Its primary mission is to assist those who have to try out various machine learning algorithms on their point clouds. These could be derived from photogrammetry or LiDAR scanners enhanced with geometric features and/or spectral information from colors (RGB), multi- or hyperspectral bands. cLASpy\_T transforms LAS files with additional features to make it compatible with the scikit-learn library. The software is divided into three modules: ‘training’, ‘predict’ and ‘segment’. These modules respectively train supervised classification models, make predictions with these models, and segment point clouds into clusters.

Currently, three supervised algorithms from scikit-learn API are used for training and prediction: two based on decision trees, RandomForestClassifier or GradientBoostingClassifier, and one based on feed-forward neural networks, MLPClassifier. The segmentation module is performed by the unsupervised K-Means algorithm. Geometric features or spectral information can be added to a LAS file as extra dimensions. Extra and standard dimensions of the LAS format can both be used with cLASpy\_T. Our first example shows how to classify 3D photogrammetric data of a limited area over a coastal dike in 3 different classes (sand, rocks, blocks), thanks to geometric features and RGB (Fig. 1). An overall accuracy of 95% is reached, with a training set of 300,000 points and a test set of 10 million points.

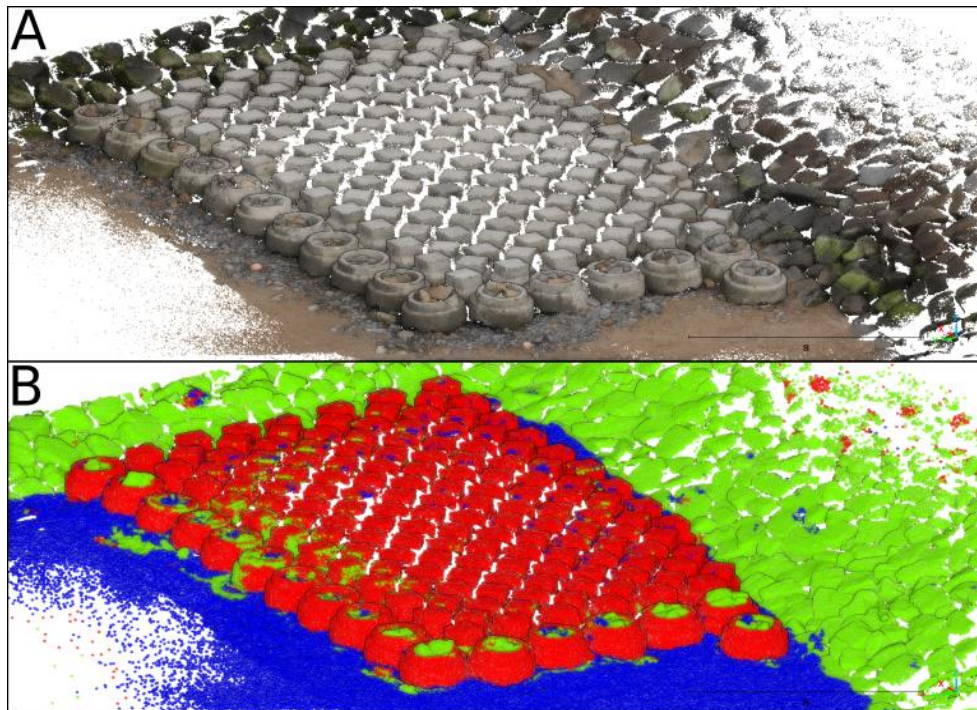


Figure 3: A. SfM point cloud over a coastal dike;  
B. Classified point cloud, sand in blue, rocks in green and blocks in red.

The second example classifies two airborne LiDAR datasets with RGB information acquired over the Orne estuary in Normandy, France into 9 different classes: water, wet sand, dry sand, mud, mix, schorre/grass, high vegetation/buildings, low vegetation, roads. Depending on the algorithm, an overall accuracy of 90% can be exceeded with a training set of 500,000 points and a test set of 20 million points.

Finally, we show how to design a model for the Belon river (Brittany, France) based on 3D airborne LiDAR data fused with hyperspectral data. Geometric and spectral features are used to classify the point cloud into 9 classes. An overall accuracy of 95% is achieved with a training set of 50,000 points and a test set of 4 million points.

## Time Series Analysis of 3D/4D Point Clouds within the Open-Source Online Course E-TRAINEE

Katharina Anders<sup>1,2\*</sup>, Bernhard Höfle<sup>1</sup>, Sina Zumstein<sup>1</sup>, Jakub Dvořák<sup>3</sup>, Krzysztof Gryguc<sup>4</sup>, Lucie Kupková<sup>3</sup>, Adriana Marcinkowska-Ochtyra<sup>4</sup>, Andreas Mayr<sup>5</sup>, Adrian Ochtyra<sup>4</sup>, Markéta Potůčková<sup>3</sup> & Martin Rutzinger<sup>5</sup>

<sup>1</sup>*3DGeo Research Group, Heidelberg University, Germany, katharina.anders@uni-heidelberg.de*

<sup>2</sup>*Department of Aerospace and Geodesy, TUM School of Engineering and Design, Technical University of Munich, Germany*

<sup>3</sup>*Department of Applied Geoinformatics and Cartography, Faculty of Science, Charles University, Czech Republic*

<sup>4</sup>*Department of Geoinformatics, Cartography and Remote Sensing, Faculty of Geography and Regional Studies, University of Warsaw, Poland*

<sup>5</sup>*Department of Geography, University of Innsbruck, Austria*

**Key words:** *change analysis, topographic monitoring, remote sensing, teaching, e-learning*

Analyzing time series of remote sensing data has become an essential but challenging task of current research and many applications of environmental monitoring and understanding human-environment interactions. Besides global Earth observation programs which provide extensive image archives, point cloud data are becoming increasingly available at local to national scales. Depending on the survey purpose and properties (i.e., sensor and platform), laser scanning or photogrammetric acquisitions are repeated at annual or seasonal timescales, down to daily and hourly observations in fixed monitoring settings (EITEL *et al.*, 2016). The generated 3D time series, or 4D point clouds in case of near-continuous acquisition, require processing and analysis at different spatial and temporal scales, often combining different data sources, and using a variety of computational methods for filtering, classification, and change analysis. Such methodological knowledge and practical skills are hence gaining increasing importance in remote sensing and geoinformatics curricula. To meet this need, we have developed a comprehensive research-oriented open e-learning course on time series analysis in remote sensing for environmental monitoring, called E-TRAINEE (POTŮČKOVÁ *et al.*, 2023). The E-TRAINEE course connects themes from computer science, geography, and environmental research within modules on (1) methods of time series analysis in remote sensing, (2) satellite multispectral images time series analysis, (3) 3D/4D geographic point cloud time series analysis, and (4) airborne imaging spectroscopy time series analysis. This contribution focusses on module 3.

In the module on geographic 3D/4D point cloud analysis, participants learn about the theory of point cloud processing and concepts of change analysis, accompanied by exercises in state-of-the-art open-source graphical software (CloudCompare) and Python tools, such as PDAL and the dedicated library for change analysis in 4D point clouds py4dgeo (PY4DGEO DEVELOPMENT CORE TEAM, 2022). Topics comprise methods of multitemporal and time series-based 3D change analysis, machine learning methods for point cloud classification, laser scanning simulation, and overall the automatization of workflows through Python scripting. The module includes two research-oriented case studies of topographic monitoring with 4D point clouds, namely the observation of rock glacier dynamics through multisource, multitemporal point clouds, and coastal monitoring using permanent terrestrial laser scanning. All practical parts exclusively use open data and open tools, and are designed to be feasible on standard personal computers, so that they are accessible to a broad group of participants for self-learning.

The course material is hosted in an open-source Git repository, which is automatically compiled into a public course website. Interactive material, such as Jupyter Notebooks, can be directly downloaded from the website or accessed in the repository. The E-TRAINEE course is openly released in August 2023 on this GitHub repository: <https://github.com/3dgeo-heidelberg/etrainee>.

**Acknowledgements:** This work is funded by the project E-TRAINEE (E-learning course on Time Series Analysis in Remote Sensing for Understanding Human-Environment Interactions) in the framework of the Erasmus+ program of the European Union (strategic partnership project ID 2020-1-CZ01-KA203-078308).

## References

EITEL, J. U. H., HÖFLE, B., VIERLING, L. A., ABELLÁN, A., ASNER, G. P., DEEMS, J. S., GLENNIE, C. L., JOERG, P. C., LEWINTER, A. L., MAGNEY, T. S., MANDLBURGER, G., MORTON, D. C., MÜLLER, J., & VIERLING, K. T., 2016. Beyond 3-D: The new spectrum of lidar applications for earth and ecological sciences. *Remote Sensing of Environment*, 186: 372-392.

POTŮČKOVÁ, M., ALBRECHTOVÁ, J., ANDERS, K., ČERVENÁ, L., DVOŘÁK, J., GRYGUC, K., HÖFLE, B., LHOTÁKOVÁ, Z., MARCINKOWSKA-OCHTYRA, A., MAYR, A., NEUWIRTHOVÁ, E., OCHTYRA, A., RUTZINGER, M., ŠEDOVÁ, A., ŠROLLERŮ, A., & KUPKOVÁ, L., 2023. E-TRAINEE: Open e-learning course on time series analysis in remote sensing. *ISPRS Archives of the Photogrammetry, Remote Sensing and Spatial Information Sciences (accepted)*. Proceedings of the ISPRS Geospatial Week 2023.

PY4DGEO DEVELOPMENT CORE TEAM, 2022. py4dgeo: library for change analysis in 4D point clouds [Source Code]. <https://github.com/3dgeo-heidelberg/py4dgeo>.

# Testing Theory for Identification of Aeolian Sand Transport Trends in 4D Data from Permanent Laser Scanning

Mieke Kuschnerus<sup>1\*</sup>, Sander Vos<sup>2</sup>, Sierd de Vries<sup>2</sup>, José A. Á. Antolínez<sup>2</sup>, Roderik Lindenbergh<sup>1</sup>

<sup>1</sup> *Geoscience and Remotesensing Department, Delft University of Technology, Stevinweg1, 2628 CN Delft, The Netherlands, {m.kuschnerus, r.c.lindenbergh}@tudelft.nl*

<sup>2</sup> *Hydraulic Engineering Department, Delft University of Technology, Stevinweg1, 2628 CN Delft, The Netherlands, {s.e.vos, j.a.a.antolinez, sierd.devries}@tudelft.nl*

**Key words:** *Permanent Laser Scanning, Hypothesis Testing, Aeolian Sand Transport, Time Series, Coastal Remote Sensing*

Long-term coastal monitoring is essential in the study of effects of climate change on urban sandy beaches. Slow processes such as gradual erosion or accretion due to aeolian sand transport are difficult to observe and quantify with incidental in-situ or remote sensing methods, such as satellite observations or airborne laser scanning. Permanent laser scanning (PLS), a laser scanner installed long term on a fixed location and scanning in regular intervals (hourly), provides a unique opportunity to monitor and analyse these processes.

As an example for a typical urban beach in the Netherlands, the location on the beach in Noordwijk is studied for a period of three years (see Figure 1). Hourly scans with a Riegl VZ-2000 laser scanner provide a large 4D spatio-temporal data set (Vos, 2023) providing the opportunity for an in-depth case study.

Figure 2 shows ten example time series located on the upper beach (indicated in Figure 1 with a red bar) over the entire observation period of nearly three years. As indicated with the arrows in Figure 2, possible causes for gaps or change points in time series can be caused by failing of the instrument, heavy storms or unusual high tides among others. Instead of manually analysing time series, we automatically segment the time series at each change point or gap and classify each part independently using multiple hypothesis testing (Chang, 2016).

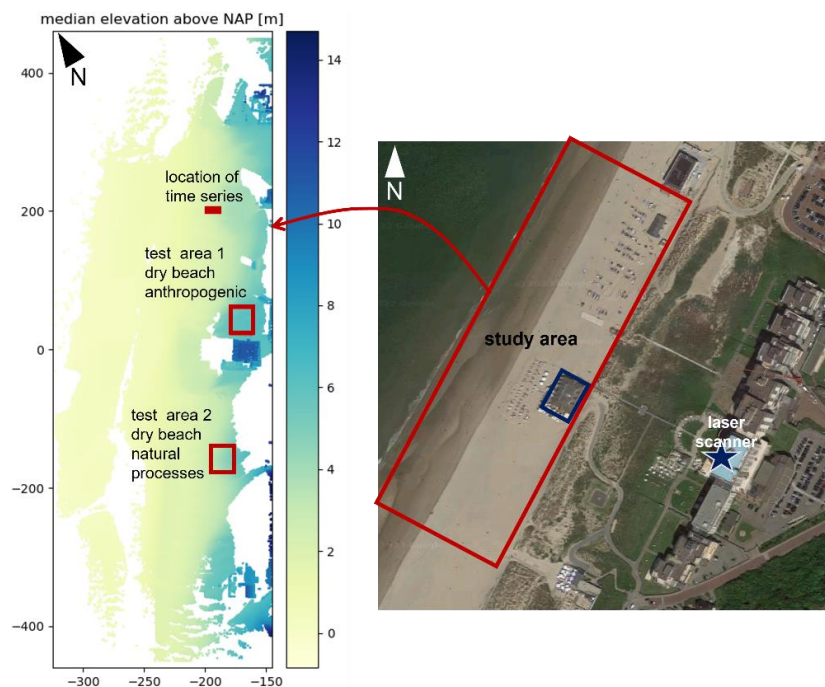


Figure 1: Overview of study site with aerial image (© Googlemaps) and point cloud of the beach area colored according to elevation. Two test areas are marked with red squares and the location of the time series in Figure 2 are indicated with a red bar.

With the help of multiple hypothesis testing, each segment of elevation time series from the PLS data set is tested for the most likely statistical model: no statistical change, step function (indicating a missing change point) or linear change, which yields a slope estimate. The slope estimates allow to identify especially slow moving, gradual changes at levels of millimetre per day. We then classify all identified sudden and gradual changes considering the estimated parameters, according to their most likely cause: anthropogenic, aeolian, tidal, storm induced or other. Other possible causes include errors in the observation data set or processing or human objects such as boats or tents placed in the observation area.

In this way we provide a method to identify and quantify processes such as aeolian sand transport or human activities, which play a vital part in coastal evolution and management.

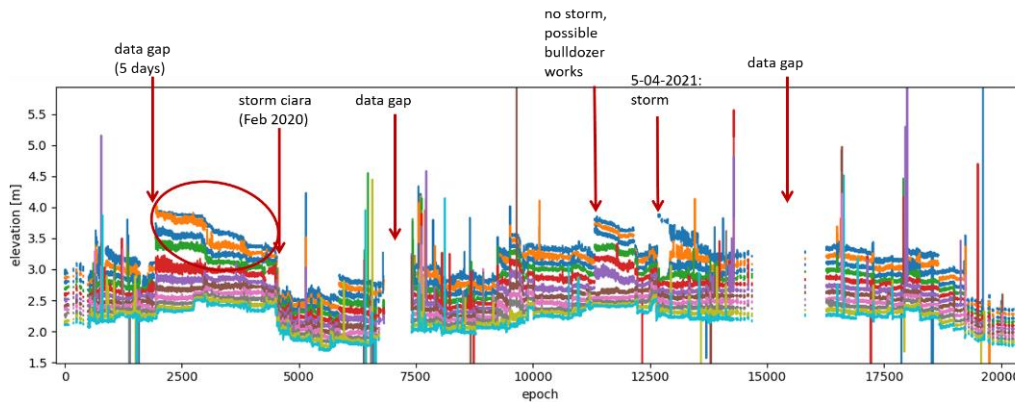


Figure 2. Three year time series of elevation values at 10 locations across the beach. Some events are marked with red arrows and the ellipse shows a period of gradual change that can most likely be attributed to aeolian sand transport.

**Acknowledgements:** The authors would like to thank Grand Hotel Huis ter Duin for their cooperation. This research has been supported by the Netherlands Organization for Scientific Research (NWO, grant no. 16352) as part of the Open Technology Programme and by Rijkswaterstaat (Dutch Ministry of Infrastructure and Water Management).

## References

VOS, S., KUSCHNERUS, M., LINDENBERGH, R., & DE VRIES, S., 2023. 4D spatio-temporal laser scan dataset of the beach-dune system in Noordwijk, NL (Version 2) [Data set]. *4TU.ResearchData.*, doi: 10.4121/1AAC46FB-7900-4D4C-A099-D2CE354811D2.V1.

L. CHANG & R. F. HANSSSEN, 2016. A Probabilistic Approach for InSAR Time-Series Postprocessing. *IEEE Transactions on Geoscience and Remote Sensing*, vol. 54, no. 1, pp. 421-430, doi: 10.1109/TGRS.2015.2459037.

## Assessing dune dynamics from Dutch airborne laser scanning products

Roderik Lindenbergh<sup>1</sup>, Christa van Ijzendoorn<sup>2</sup>, Jinhu Wang<sup>3</sup>

<sup>1</sup> Dept. GRS, TU Del9, [r.c.lindenbergh@tudel9.nl](mailto:r.c.lindenbergh@tudel9.nl)

<sup>2</sup> Dept. HE, TU Del9, [C.O.vanIjzendoorn@tudel9.nl](mailto:C.O.vanIjzendoorn@tudel9.nl)

<sup>3</sup> IBED, University of Amsterdam, [j.wang7@uva.nl](mailto:j.wang7@uva.nl)

Dutch dunes are essential coastal features that protect the hinterland from flooding, while providing nature and recreational values in a heavily populated region. Dune morphology changes due to natural causes, e.g., sand blown in from the beaches, but also due to human intervention, like the creation of artificial blowouts in the first dune row adjacent to the beach, compare Figure 1. Dutch dunes are sampled by systematically acquired airborne LiDAR data, from two different projects. First, The Netherlands as a whole, is covered at intervals of ~7 years by the Dutch national LiDAR data set Actueel Hoogtebestand Nederland (AHN), which is so done for four different epochs, from AHN-1 until AHN-4. Second, Dutch coasts are in addition monitored at yearly intervals in the framework of the so-called JarKus measurements (yearly coastly measurements), since ~2000. Due to the spatial and temporal coverage of the dataset, it can be exploited to assess dune dynamics, e.g. (Van Ijzendoorn et al., 2021). Goal of the proposed work is to compare two recently developed methodologies to extract elevation changes from multi-temporal LiDAR data.

The first method (Kuschnerus et al., 2021) derives clusters of similarly looking time series of elevation data. If necessary, elevation data is gridded to ensure that heights are available at the same locations through time. This allows to construct grid-wise time series. Similarly behaving time series are next clustered using k-means. The second, Principal Component Analysis (PCA) based method (Frantzen, 2022), first reorganizes a grid of time series in a deformation-time array, where each time series is represented as list of deviations from the mean elevation or a reference epoch. Next, similar variations in these deviations occurring at different epochs are highlighted by applying PCA on the deviations, which basically reprojects the deviations w.r.t. to a basis of mutual orthogonal maximal variations. Both methods have shown promising results on so-called Permanent Laser Scanning data, obtained by a terrestrial scanner automatically scanning from a fixed location, but the case studies considered were different: one considered changes on a beach, the other changes in high mountain terrain.

To enable comparison, both methods we will be applied to the same cases. First, on AHN data of the carved dunes of Figure 1, and second, on JarKus data of the sand engine, (Stive et al, 2013), a peninsula of sand erected at the South-West of The Hague, The Netherlands, where currently new dunes are forming. Results are expected to give insight in the dynamics in those two areas, and in the type of dune morpho-dynamics that can be highlighted by the two discussed methods.

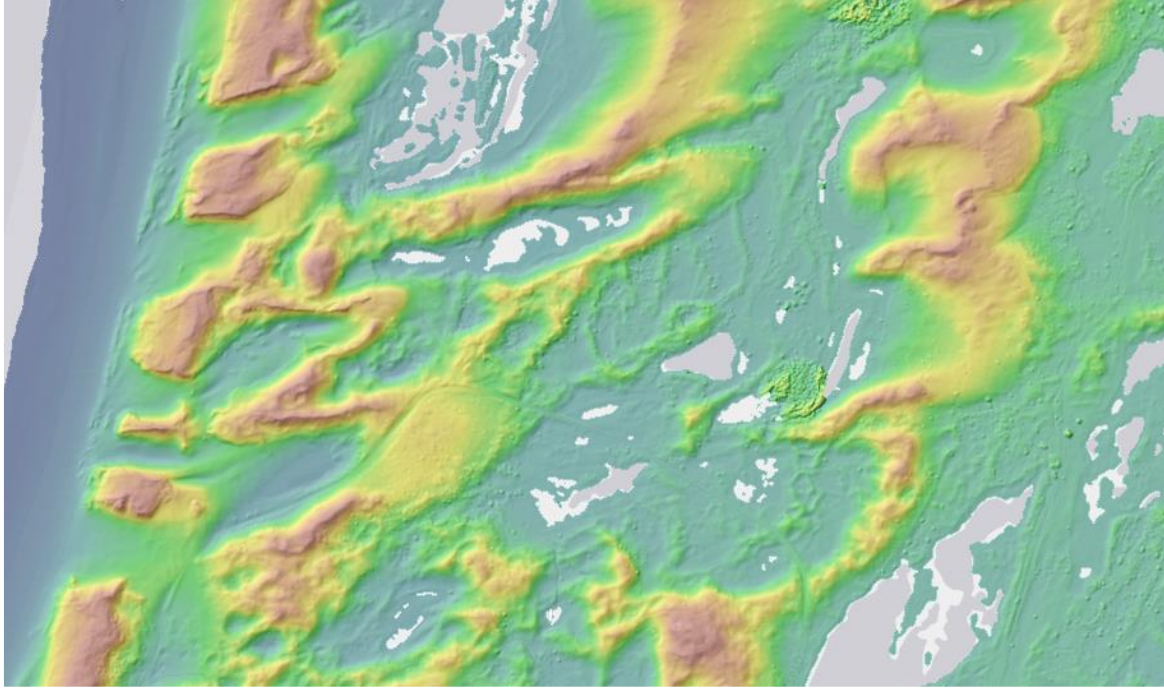


*Figure 1. Dune field west of Amsterdam, The Netherlands as represented by the Dutch national LiDAR altimetry data set AHN. Traditionally, a continuous first ridge of dunes is separating the sea (at the left of the image) from the rest of the dunes. Here this dune ridge got carved using bulldozers to increase dynamics.*

## References

KUSCHNERUS, M., LINDENBERGH, R., & VOS, S. (2021). COASTAL CHANGE PATTERNS FROM TIME SERIES CLUSTERING OF PERMANENT LASER SCAN DATA. *EARTH SURFACE DYNAMICS*, 9(1), 89-103.

FRANTZEN, P., (2022). IDENTIFYING HIGH ALPINE GEOMORPHOLOGICAL PROCESSES USING PERMANENT LASER SCANNING TIME SERIES, MSc THESIS, DELFT UNIVERSITY OF TECHNOLOGY.

STIVE, M. J., DE SCHIPPER, M. A., LUIJENDIJK, A. P., AARNINKHOF, S. G., VAN GELDER-MAAS, C., VAN THIEL DE VRIES, J. S., ... & RANASINGHE, R. (2013). A NEW ALTERNATIVE TO SAVING OUR BEACHES FROM SEA-LEVEL RISE: THE SAND ENGINE. *JOURNAL OF COASTAL RESEARCH*, 29(5), 1001-1008.

VAN IJZENDOORN, C.O., DE VRIES, S., HALLIN, C. ET AL., (2021). SEA LEVEL RISE OUTPACED BY VERTICAL DUNE TOE TRANSLATION ON PROGRADING COASTS. *SCI REP* 11, 12792, [hCps://doi.org/10.1038/s41598-021-92150-x](https://doi.org/10.1038/s41598-021-92150-x)

# Optimizing colour-schemes for 3D point cloud visualization: the case of classified point clouds, surface normal representations and engineering defect diagnostics

Laure Manceau<sup>1\*</sup>, Thomas JB Dewez<sup>2</sup>, Hugues Fournier<sup>3</sup>, Julien Vallet<sup>3</sup>

<sup>1</sup> IPGP – F-75005 Paris, France, [lauremanceau0411@free.fr](mailto:lauremanceau0411@free.fr)

<sup>2</sup> BRGM – Direction des Risques et Prévention, F-45060 Orléans, France, [t.dewez@brgm.fr](mailto:t.dewez@brgm.fr)

<sup>3</sup> Helimap Sixense, CH-1066 Epalinges, Switzerland, [hugues.fournier@helimap.ch](mailto:hugues.fournier@helimap.ch) [julien.vallet@helimap.ch](mailto:julien.vallet@helimap.ch)

**Key words:** *Point cloud visualization, colour ramps, surface normal representation*

LiDAR provides visually rich information on the environment, the nature of measured objects and the geometric properties of their surfaces. For interpreting a scene, plotting 3D points in display is insufficient to leverage its content. Complementary scalar values can substantially improve understanding.

There exists plenty possibilities for representing scalar values as graduated colours. Even if colour representations are often subjective, colour mapping is not just a matter of taste. The scientific stake is to identify all there is to grasp in the data for drawing correct conclusions. Many colour ramps, most notably rainbow, lack perceptual uniformity (KOVESI, 2015) which distorts data structure perception and lead to interpretations errors (ROGOWITZ & KALVIN, 2001). Rainbow ramps must be banned at all costs. Instead, optimal colour ramps can be chosen based on data type (BREWER, 1999, ROGOWITZ *et al.*, 1996). Our brain intuitively interprets data ordering through a colour's grey level (called lightness). The spatial variations of scalar values are a second important aspect. Does the data juxtapose large homogenous domains or small blobs of highly variable values? With low spatial frequency data, choose colour ramps that vary hue and saturation. Prefer colour ramps with lightness variations for high spatial frequency data. Additionally, adjacent colours are distinguishable only if they are furthest apart than 40 units in the CIELab colour space (CARTER & CARTER, 1982).

This presentation will detail theory and optimal solutions for representing 3D point cloud properties commonly used in geoscience: discrete object class, surface normals and local relief visualizations.

Unordered categorical data, e.g. point classes require distinct colours. But one should prefer mapping darker shades (i.e. low lightness) to low-lying points and lighter colours to elevated or higher roughness class. We propose revising the current lidar industry scheme to improve object class visual separability (Fig. 1).

On geological outcrops, fracture planes, in a broad sense, stand out as patches of similar surface orientation, skirted by abruptly changing values around their edges. The first notion is that dip direction is a circular variable, bounded between 0° and 360°. The colour ramps ought to share the same colour at both ends. Second, the angle between two adjacent facture sets is very often determined by the geological setting. For instance, angular spacing comes crudely at 90° in diaclosed sedimentary rocks and 60°/120° in compressive contexts. Optimal colour ramps should thus contain either 4 (for sedimentary) or 6 (for compressive) dominant shades to maximize visual separability. Third, the dominant colours of the ramp should match dip direction modes to enhance family distinction (Fig. 2).

To visually emphasize surface damage, such as ruts on roads or defects on concrete dam surfaces, signed roughness is a pertinent proxy. As ratio-type variable, roughness optimally maps to a continuous diverging color ramp, where the central ramp colour maps to 0. Opposite ends are best distinguished with opposed hues in the CIELab colour space. People with colour-blindness will appreciate a ramp based on the blue/yellow pair. Kovesi's [colorcet.com](http://colorcet.com) repository offers both light and dark-centered diverging ramps as well as colour-blind-friendly schemes.

**Acknowledgements:** we thank Peter Kovesi for expanding [colorcet.com](http://colorcet.com) with ramps in Cloud Compare format, upon our request. Fabio Cramereri created and distributes complementary colour schemes at [fabiocramereri.ch](http://fabiocramereri.ch).

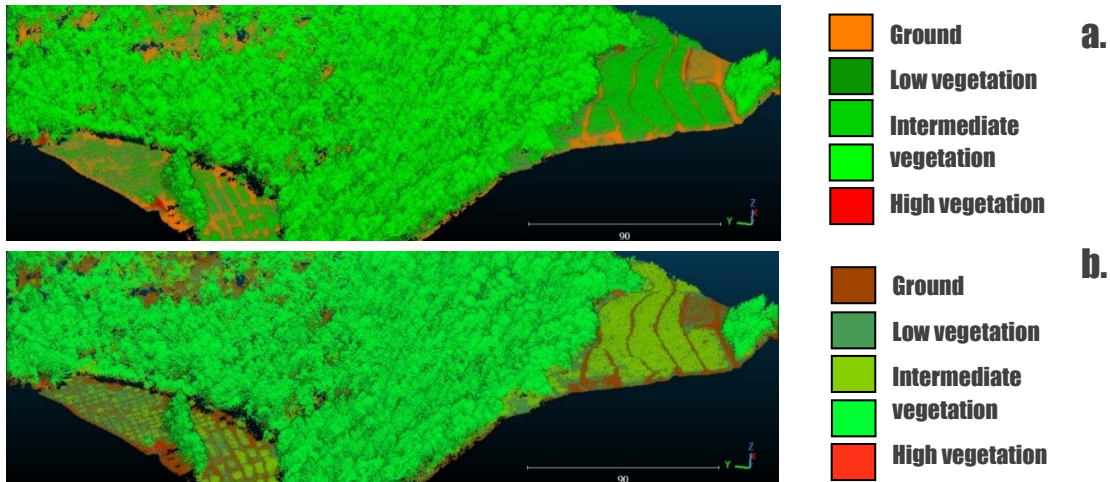


Figure 1: Representation of classes using discrete colours of a countryside landscape close to Sion (Switzerland). a: colours from an industrial standard (TerraScan). b: our colour ramp improves visual class contrasts (at least 40 CIELab space units) and lightness ordering is coherent with above-ground elevation (lighter is higher).

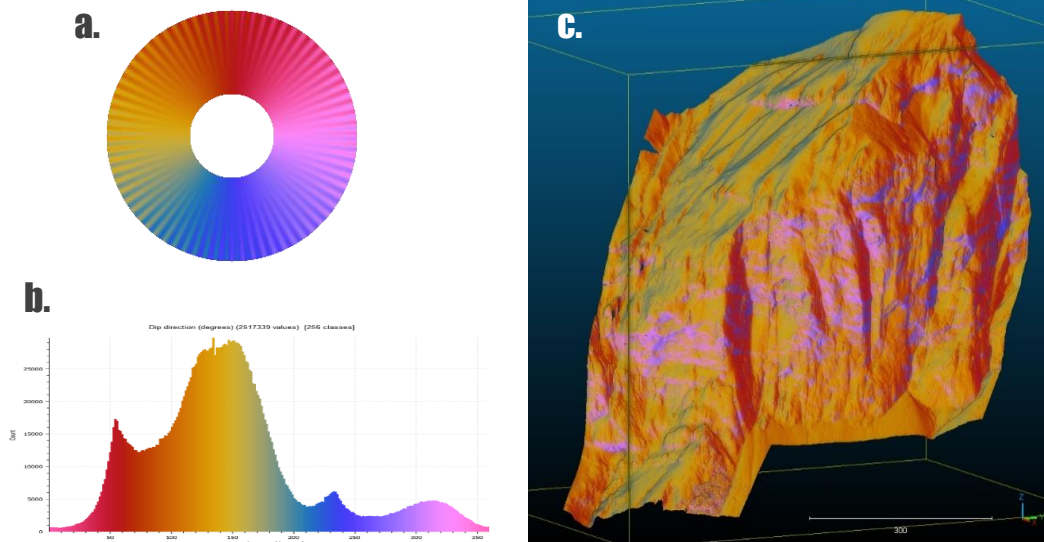


Figure 2: Representation of a diaclosed rock outcrop surface normals. a: Circular CET-C1 color ramp with 4 dominant colours (Kovesi). b: Dip-direction histogram with rotated circular ramp to match the outcrop's principal poles. c: Point cloud of a Swiss cliff with our optimized dip-direction ramp. Two orthogonal planes dominate in dark red and yellow. Pink surfaces correspond to a minor mode made by shallow overhangs.

## References

- BREWER C.A., 1999. Color use guidelines for data representation, *Proc. Sect. On Stat. Graphics. Ann. meet. Am. stat. assoc.*, Baltimore, Maryland, USA, 55-60, accessible [here](#)
- CARTER, R.C., CARTER, E.C., 1982. High-contrast sets of colors. *Applied Optics*. 21: 2936-2939.
- CRAMERI, F., n.d. Fabiocrameri/colourmaps, URL <https://www.fabiocrameri.ch/colourmaps/>
- KOVESI, P., 2015. Good colour maps: how to design Them. arXiv e-prints, <http://arxiv.org/abs/1509.03700>.
- KOVESI, P., n.d., Colorcet, URL <https://colorcet.com/>
- ROGOWITZ, B.E., KALVIN A.D., 2001. The "Which Blair Project": a quick visual method for evaluating perceptual color maps. *Proceedings Visualization 2001. VIS '01.*, San Diego, CA, USA, 183-556, accessible [here](#)
- ROGOWITZ, B.E., TREINISH, L.A., BRYSON, S., 1996. HOW NOT TO LIE WITH VISUALIZATION. *COMP. IN PHYS.* 10(3): 268-273.

## **Session 2 – Visualisation, communication & Teaching**

A large, faint, light gray globe is centered in the background of the page, behind the main title text.

# **SESSION 2**

# **VISUALISATION, COMMUNICATION & TEACHING**

## Virtual geoscience 3D modelling quality: experience from three years of V3Geo

Simon J. Buckley<sup>1\*</sup>, Conor Lewis<sup>1</sup>, John A. Howell<sup>2</sup>, Magda Chmielewska<sup>2</sup>, Nicole Naumann<sup>1</sup>, Jess Pugsley<sup>2</sup>, Kari Ringdal<sup>1</sup>, Joris Vanbiervliet<sup>1</sup>, Thomas J.B. Dewez<sup>3</sup>

<sup>1</sup> NORCE Norwegian Research Centre, Bergen, Norway, [simon.buckley@norceresearch.no](mailto:simon.buckley@norceresearch.no)

<sup>2</sup> Department of Geoscience, University of Aberdeen, UK

<sup>3</sup> BRGM-French Geological Survey, Orléans, France

**Key words:** 3D modelling, virtual outcrop, photogrammetry, lidar, open data, visualisation, sharing

3D modelling in geoscience has undergone a step change over the last 15 years, as photogrammetry coupled with drone platforms and low-cost software has made acquisition and processing methods widely accessible. The result is an increasing number of 3D models – from laboratory to field scale – being used for quantitative and qualitative purposes for a wide range of applications in virtual geoscience. Coupled with open science requirements being developed by public funding bodies, there is a growing need for the geoscience community to be able to publish high quality 3D models as part of communication, dissemination and exploitation of study results. Repositories such as V3Geo (BUCKLEY et al., 2022) and commercial web services such as Sketchfab (CAWOOD & BOND, 2019) are currently being used for sharing 3D model results in geology and geoscience. These sites allow models to be uploaded to cloud storage and visualised in web viewers. This allows the geoscience community to be able to publish and share their results with colleagues, others in the community or the public, making it easier than ever to achieve the guiding ideals of FAIR (WILKINSON et al., 2016).

There is one critical issue associated with publishing 3D models as a resource for the community: data quality and reliability. In the past, scientific publications reported results derived from 3D model acquisition and processing, but without other scientists being able to independently access the model datasets for repetition of experiments or for use in their own studies. Now, with online sharing sites and the move towards open data, available 3D models can be easily accessed. A problem arises when the published 3D models are affected by data quality issues. Any derived use is dependent on the accuracy and reliability of the published dataset, including issues associated with source data, coordinate systems, processing, or formatting prior to publication. This is particularly important in quantitative studies or interpretation, where data accuracy or artefacts can significantly affect the quality of measurements, interpretations or analysis. However, qualitative studies are also affected.

Many authors have discussed the issues associated with acquisition and processing of lidar or photogrammetric 3D models in geology and geoscience (e.g. CHANDLER, 1999; BUCKLEY et al., 2008; ELTNER et al., 2016) and their effect on the accuracy of analysis, offering “guidelines” on how to avoid pitfalls in their 3D modelling approaches. This has resulted in a general increase in quality of models as geoscientists improve and recognise quality issues in their own models. However, the abundance and ease of sharing can create issues with provenance if authors rely on published data, without being aware of potential quality issues that may be inherent in any 3D model they utilise.

In this contribution, we examine some of the common issues affecting 3D models in geoscience, based on experience gained over three years of receiving community contributions in the V3Geo model repository (V3Geo, 2023). Since its inception in 2020, V3Geo has received over 150 models from organisations worldwide. Each is subject to a simple technical quality control, based on a set of published guidelines (Buckley et al., 2022). Despite this, quality of submissions can be variable, with common issues including georeferencing, resolution (of 3D geometry and texture), and processing or orientation artefacts. Several V3Geo model localities have been independently acquired by different authors and published on Sketchfab. This gives a further opportunity to highlight quality issues, which may not be apparent by simple visual inspection of a model within the 3D web viewer. Here, we highlight some of the common issues affecting community 3D models, and provide thoughts on common acquisition, processing and quality control procedures that can help to improve the quality of 3D modelling in the geoscience community.

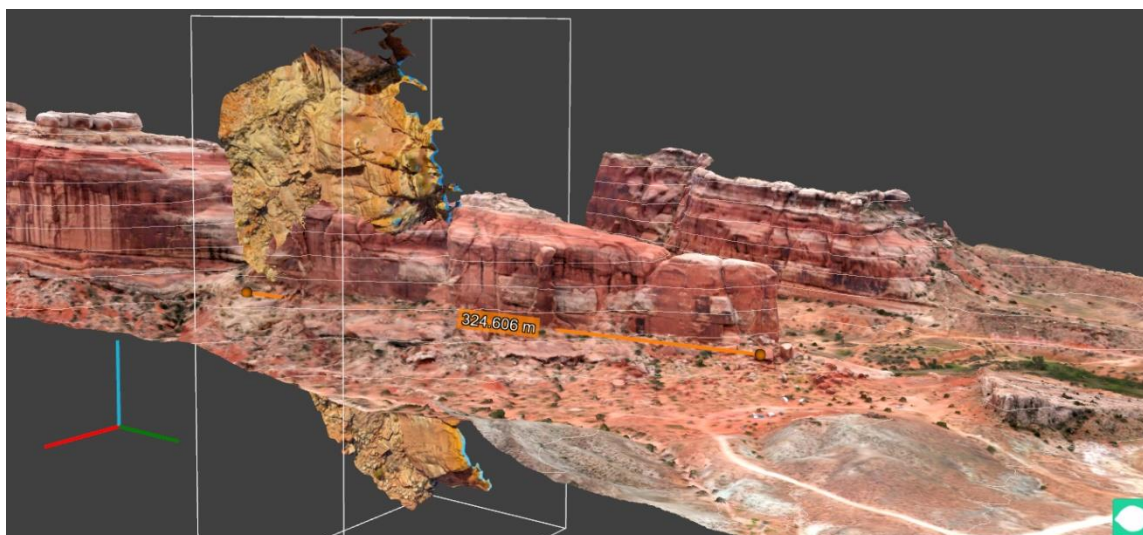


Figure 1: Comparison of 3D outcrop models of Courthouse Rock, Utah from V3Geo (<https://v3geo.com/model/111>; wider area, shown with 10m contours) and Sketchfab (<https://sketchfab.com/3d-models/courthouse-rock-abe6b7f6e279401292995dbed3dacb97>; outlined with bounding box) co-visualised in LIME (Buckley et al., 2019). The latter has incorrect positioning and orientation while the V3Geo model is correctly georeferenced. In the figure, the Sketchfab model has been transformed from its original location in local coordinates to be within the bounding box of the V3Geo model.

**Acknowledgements:** The SAFARI consortium (<https://safaridb.com>) is thanked for its continued support throughout the development of the V3Geo repository. We acknowledge the individuals, groups and organisations who are making their 3D model datasets available to the geoscience community in repositories such as V3Geo and Sketchfab. Examples are used to raise the awareness of published data quality in the scientific and professional community, without any criticism being intended. Finally, model authors providing active feedback on the V3Geo repository are particularly thanked for their engagement.

## References

- BUCKLEY, S.J., HOWELL, J.A., ENGE, H.D. & KURZ, T.H., 2008a, Terrestrial laser scanning in geology: Data acquisition, processing and accuracy considerations: *Journal of the Geological Society*, 165: 625–638, [doi:10.1144/0016-76492007-100](https://doi.org/10.1144/0016-76492007-100).
- BUCKLEY, S.J., RINGDAL, K., NAUMANN, N., DOLVA, B., KURZ, T.H., HOWELL, J.A. & DEWEZ, T.J.B., 2019. LIME: Software for 3-D visualization, interpretation, and communication of virtual geoscience models, *Geosphere*, 15: 222–235. [doi:10.1130/GES02002.1](https://doi.org/10.1130/GES02002.1).
- BUCKLEY, S.J., HOWELL, J.A., NAUMANN, N., LEWIS, C., CHMIELEWSKA, M., RINGDAL, K., VANBIERVELIET, J., TONG, B., MULELID-TYNES, O.S., FOSTER, D., MAXWELL, G. & PUGSLEY, J., 2022. V3Geo: a cloud-based repository for virtual 3D models in geoscience, *Geoscience Communication*, 5: 67–82, [doi:10.5194/gc-5-67-2022](https://doi.org/10.5194/gc-5-67-2022).
- CAWOOD, A. & BOND, C., 2019. eRock: An open-access repository of virtual outcrops for geoscience education, *GSA Today*, 29: 36–37, [doi:10.1130/GSATG373GW.1](https://doi.org/10.1130/GSATG373GW.1).
- CHANDLER, J., 1999. Effective application of automated digital photogrammetry for geomorphological research. *Earth Surface Processes and Landforms*, 24: 51–63.
- ELTNER, A., KAISER, A., CASTILLO, C., ROCK, G., NEUGIRG, F. & ABELLÁN, A., 2016. Image-based surface reconstruction in geomorphometry – merits, limits and developments, *Earth Surface Dynamics*, 4, 359–389, <https://doi.org/10.5194/esurf-4-359-2016>.
- V3GEO, 2023. Virtual 3D geoscience. <https://v3geo.com>, last accessed 05 June 2023.
- WILKINSON, M. D., DUMONTIER, M., AALBERSBERG, et al., 2016. The FAIR guiding principles for scientific data management and stewardship, *Scientific Data*, 3: 160018, [doi:10.1038/sdata.2016.18](https://doi.org/10.1038/sdata.2016.18).

# Integrating Drone Data, Photogrammetry, and Virtual Reality Geological Studio Software for Enhanced Outcrop Analysis and Visualization

Tiina Harak<sup>1</sup>

<sup>1</sup>University of Tartu, Ülikooli 18, 50090 Tartu, Estonia, tiina.harak@ut.ee

**Key words:** drone, photogrammetry, Virtual Reality Geological Studio Software, outcrop

Geological fieldwork plays a vital role in understanding Earth's complex geology. However, traditional fieldwork approaches often face logistical and accessibility challenges when studying remote or hazardous outcrops. This abstract explores the integration of drone data, photogrammetry techniques, and Virtual Reality Geological Studio software to overcome these limitations and enhance outcrop analysis and visualization.

The model was created using drone photos of an impressive outcrop located on the Pakri Peninsula in Estonia (59° 23' 9" N, 24° 2' 9" E). Rising 25 meters high, this remarkable geological formation exposes a fascinating combination of sandstones and limestones from the Lower Cambrian, Upper Cambrian, and Ordovician periods. Situated as part of the Baltic klint, which is exposed to the forces of sea waves, this outcrop offers valuable insights into the effects of undulations and fluctuating water levels. Through the application of photogrammetry, it becomes possible to study and analyze these dynamic changes on the outcrop in detail.

By importing the reconstructed 3D models into the Virtual Reality Geological Studio software, geoscientists can explore and interact with virtual outcrops in a realistic and intuitive manner. Users can navigate the outcrop, examine geological structures, annotate features of interest, and conduct measurements with enhanced accuracy and precision, which would otherwise be difficult, considering the height and location of the cliff.

By using the remote sensing methods, it becomes feasible to virtually recreate and conserve ever-changing outcrops, while also predicting their future development. The Pakri outcrop boasts a historic old lighthouse, constructed in the 17th century, with its foundation now exposed on the cliff's edge. By creating a virtual tour of the outcrop, it becomes possible to digitally preserve this significant structure and ensure its longevity for generations to come.

In conclusion, the integration of drone data, photogrammetry, and data processing represents a powerful and transformative approach to outcrop analysis and visualization. This integrated workflow allows geoscientists to overcome logistical and accessibility challenges, providing a safe, efficient, and highly interactive platform for studying and understanding Earth's geological formations. As technology advances and the software continues to evolve, this integration will play an increasingly vital role in advancing geoscientific research, education, and exploration.

# Using 360° video to create immersive virtual reality teaching materials: A virtual field trip to the Swiss Alps to assess stream water sources

Professor Ian Maddock<sup>1\*</sup> and Harry Ormonde<sup>1</sup>

<sup>1</sup> Department of Geography and Environmental Management, University of Worcester, Henwick Grove, Worcester, UK, i.maddock@worc.ac.uk

**Key words:** Virtual reality, 360° video, 360° camera, drone, Google Earth, education

The use of 360° video embedded within teaching materials has seen increasing use due to its immersive and interactive features. Embedding 360° video into virtual reality teaching materials creates a more realistic experience of dynamic environments than photos and photo panoramas because of their ability to capture motion and therefore creates a richer virtual experience within the learning resource. They also provide a more interactive experience than using 2D videos because of the need for students to engage with the resource rather than passively watch the video, though they suffer from being lower resolution than their 2D counterparts. However, capturing, editing, and sharing 360° video requires an element of technical skills to develop educational materials. This talk will discuss some of these technical issues and describe how to create teaching resources using 360° video that can enrich the learning process, enhance students' motivation and enjoyment and promote active participation in the classroom.

This presentation describes the outcomes of a University of Worcester 'Students as Academic Partners' (SAP) Scheme project that aimed to create a virtual field trip to the Arolla and Moiry Valleys in the Swiss Alps to identify the water source of mountain streams (e.g., glacial meltwater, groundwater or snowmelt) (Fig. 1). The virtual field trip visits nine field sites and allows students to assess their physical characteristics (i.e., width, depth, velocity, substrate and gradient) and their water quality (i.e., water temperature and specific conductance). These field measurements were collected, plus 360° videos captured in the Arolla and Moiry Valleys in September 2022 using ground-based (pole-mounted) and aerial (drone-mounted) cameras and 360° photo panoramas were obtained by drone at each location.



Figure 1: A screenshot of the Virtual Field Trip in Google Earth

One key limitation of 360° videos is their relatively poor resolution compared to traditional 2D video. For this resource, 360° video resolution was enhanced upto 8K using AI software and then edited to embed field site information to overcome some of this limitation. The finished videos were then uploaded to YouTube for hosting and viewing. The virtual field trip was created using Google Earth Web which was chosen because it is freely available and relatively simple to use. The virtual field trip starts by providing some contextual information and then guides students to visit each site, highlighting the location of each on a map and enables them to view the 360° photo panorama (hosted externally on the Kuula web-hosting service) to assess the local setting. Then students interact with 360° videos to explore the features of each site and extract data from the videos (Fig. 2). They then carry out data analysis on the field data to identify stream sources. Future developments will include the addition of 360° ambisonic VR audio and the integration of 3D models into the virtual field trip produced from drone imagery and Structure-from-Motion (SfM) photogrammetry.

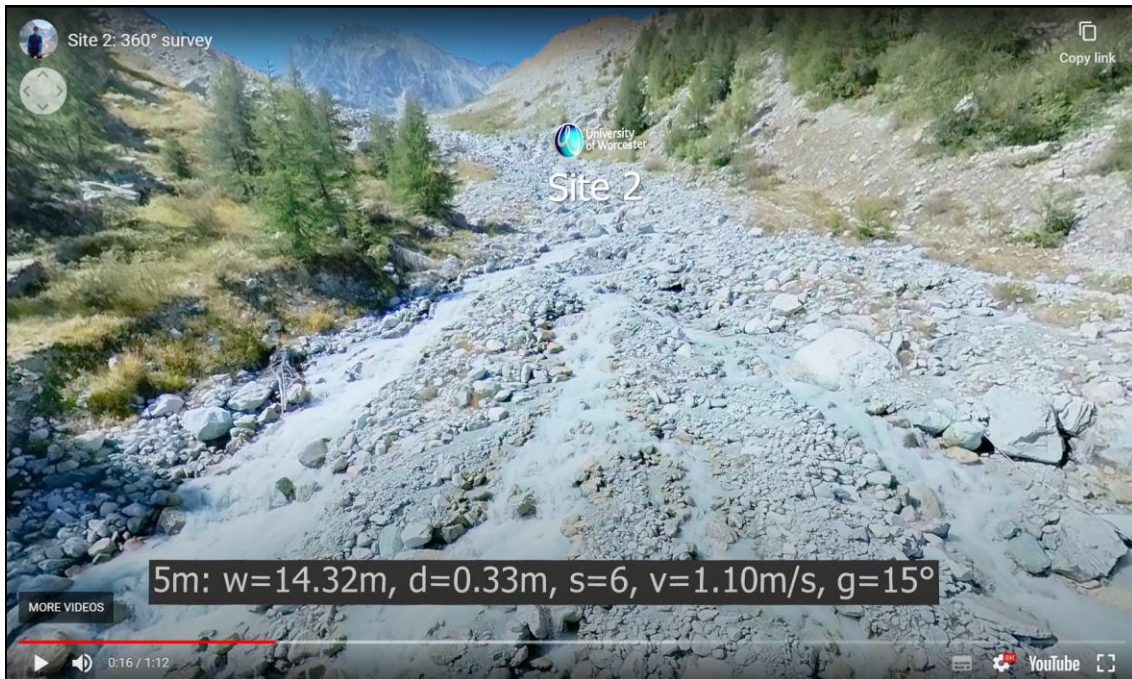


Figure 2. A screenshot of a 360° video with field data embedded within it ( $w$ =width,  $d$ =depth,  $s$ =dominant substrate (coded),  $v$ =velocity,  $g$ =gradient)

## Does time really matter? A comparison between virtual and physical field trips

Pugsley J.<sup>1</sup>, Howell J.<sup>1</sup>, Hartley A.<sup>1</sup>, Buckley S.<sup>2,3</sup>, Chmielewska M.<sup>1</sup>, Naumann N.<sup>2</sup>,

<sup>1</sup> *Department of Geology and Geophysics, University of Aberdeen, Aberdeen, AB24 3EU, jessica.pugsley@abdn.ac.uk*

<sup>2</sup> *NORCE Norwegian Research Centre AS, P.O. Box 22, N-5838 Bergen, Norway*

<sup>3</sup> *Department of Earth Science, University of Bergen, P.O. Box 7803, N-5020 Bergen, Norway*

**Key words:** *Virtual Field Trip, Virtual Outcrop, LIME, Fieldwork*

Virtual field trips (VFTs) became widespread during the 2020 COVID-19 pandemic, though as travel restrictions and social distancing measures slowly fade from the global populations memory, the value of VFTs within the education system requires further evaluation. During the pandemic several VFTs were constructed and delivered to MSc. students studying Integrated Petroleum Geoscience at the University of Aberdeen, Scotland. These VFTs were a direct replacement for physical trips, including a 10-day long trip to Utah, USA, which utilised virtual outcrops initially collected for research purposes prior to the pandemic. A cohesive dataset was provided to the students within LIME consisting of multiple virtual outcrops alongside DEMs, field photos, 360° photo spheres, maps, cross sections, and schematic diagrams which enabled students to explore, analysis and interpret within a virtual environment. The VFTs were delivered in real time, were tutor led and location based, and followed a format that aimed to emulate traditional fieldwork. The duration of the various activities (e.g. independent student work, groupwork, staff explanation and discussion) were recorded over the course of the VFT.

In April 2023 the field trip physically returned to Utah for the first time in 3 years, where students visited many of the same localities with similar learning goals and assessments to the virtual trips of previous years and pre-pandemic physical trips. The duration of activities with equivalent categories were recorded for the physical trip to allow comparison between the two trips. At the end of each course a questionnaire was distributed that was designed to appraise the quality of the fieldtrip to the students, with a goal of addressing the effectiveness of the delivery, student experience, and the learning outcomes.

Preliminary analysis of the results shows several notable differences in timings between virtual and physical fieldtrip formats. Firstly, travel time (e.g. driving and walking) is not recorded for VFT given students attended the trip from their homes, or travelled to and from the university before and after the trip in their own time. However, for the physical fieldtrip an average of 25% of the total teaching time was spent driving and a further 8% walking between localities. The VFT involved on average 13% more groupwork than the physical trips, whereas the physical trip had a 6% increase in individual work (e.g. exploring the outcrop or virtual outcrop). Lunch and break time for the VFT also contributed to an additional 11% compared to physical trips.

Here we will discuss the results and the implications from the duration analysis of the various activities on the efficacy of fieldtrips in general, when related to detailed student feedback. Overall students benefited from true emersion within the landscape, culture and outdoor environment that the physical trip enabled. The VFT however, had many benefits including improvements in 3D and geospatial understanding. Given their time efficiency, we argue VFTs could be an under-utilized resource post-pandemic and could be implemented as a powerful means of introducing students to a greater variety of sedimentary basins and stratigraphy during their studies, adding to what they learn on physical trips.

# The effectiveness of Virtual Reality Field Trips (VFTs) in Field Geology education

Jan van Bever Donker<sup>1\*</sup>, Rudy Maart<sup>1</sup>, Delia Marshall<sup>1</sup>, Luyanda Mayekiso<sup>1</sup>, Matthew S. Huber<sup>1</sup>, Henok Solomon<sup>1</sup> & Nompumelelo Mgabisa<sup>1,2</sup>

<sup>1</sup>*Department of Earth Sciences, University of the Western Cape, Cape Town, South Africa,  
jvanbeverdonker@uwc.ac.za*

<sup>2</sup>*Department of Water and Sanitation, Pretoria, South Africa*

**Key words:** *High-Definition; Fieldwork; 3-D models; Spatial awareness*

The ability for virtual reality and augmented reality to immerse the user into an alternate environment has been greatly improved in recent years, allowing for digitization of traditional geological field trips for use in creating virtual field trips (VFTs). These VFTs allow for students to visit sites that are otherwise inaccessible, and also allow for a combination of virtual and in-person field trips, whereby students are able to visit key sites virtually before an in-person field trip.

Our group has constructed VFTs from 3 locations in South Africa for use in courses at the University of the Western Cape. In this work, we evaluate the impact of VFTs in the teaching of geological fieldwork.

We created a set of four small scale VFTs covering a major unconformity near Table Mountain, sedimentary structures and deformation features, as well as features related to the interaction of the basement rocks with the intrusion of the Cape Granite near Cape Town, a single tour looking at slope stability at a dam near the town of Clanwilliam, and a large-scale VFT from the Tanqua Karoo fan complex. These tours were presented to 1<sup>st</sup>, 2<sup>nd</sup>, 3<sup>rd</sup>, and 4<sup>th</sup> year university students. VFTs were assembled from high-resolution photography, 360° photography, and drone photography. High-definition images were taken using a Canon-EOS R5 High Resolution camera on a panoramic camera head with various lenses and an Insta360-X1 for low resolution 360° panoramas as landing pages. A Mavic 3 Cine was used for drone photography. The Pano2VR software was used to assemble the data into VFTs, including annotations, overlays, drone images, and videos.

The VFTs were developed in conjunction with geo-cognition principles while considering the path a novice takes to become an expert (PETCOVIC & LIBARKIN, 2007) and designed to guide the students to combine taught features and definitions into an understanding of geological concepts that comes with the natural progression from novice to expert, focusing on concepts such as geological processes and spatial relationships.

The average scores of questionnaire responses and assessment scores of post fieldwork reports were used to assess learning gain. The responses of 109 1<sup>st</sup> year students were analysed using a Paired Samples t-Test, showing that participants' level of understanding of 11 different geological concepts significantly increased from pre-VFT ( $M = 4.71$ ,  $SD = 1.94$ ) to post-VFT ( $M = 7.06$ ,  $SD = 3.20$ ;  $t = 6.67$ ,  $p = 0.00$ ,  $d = 0.64$ ). The pooled variability is slightly larger than twice the mean difference. This suggests that VFTs are effective in preparing students for in-person field trips.

Based on our results, VFTs are effective where students are given virtual exposure to a field area that they will visit in person in the future, causing them to be better prepared for in-person field work, so that they can better benefit from the time in the field.

**Acknowledgements:** The authors wish to thank DSI CIMERA for funding this project and Dr De Ville Wickens of Georoutes for tirelessly explaining the Tanqua geology to us.

## References

PETCOVIC, H. L. & LIBARKIN, J.C., 2007. Research in Science Education: The Expert-Novice continuum. *Journal of Geoscienc Education*, 55: 333-339.

## Using VR to make in-person fieldwork in the environmental sciences more inclusive

Derek A McDougall<sup>1\*</sup>, Lynda Yorke<sup>2</sup> & Simon Hutchinson<sup>3</sup>,

<sup>1</sup> *School of Science and the Environment, University of Worcester, Worcester, UK,  
d.mcdougall@worc.ac.uk*

<sup>2</sup> *School of Natural Sciences, Bangor University, Bangor, Gwynedd, UK*

<sup>3</sup> *School of Science, Engineering & Environment, University of Salford, Salford, UK*

**Key words:** VR, virtual fieldwork, inclusion, accessibility, pedagogy

Highly valued by staff and students alike, fieldwork is a defining characteristic of most taught courses in geography, earth, and environmental sciences. Nevertheless, fieldwork can present challenges for some people – including those with disabilities, seen and unseen. The *More Inclusive Fieldwork* (MIF) project, funded by the Natural Environmental Research Council, explores how virtual reality (VR) can be used to support in-person field experiences for all participants, ideally as part of a broader accessibility and inclusion strategy.

There are three parts to the MIF project. Firstly, a review of published literature and unpublished case studies demonstrates different pedagogical approaches and benefits to using immersive (VR-based) virtual fieldwork to support the ‘real’ thing. For example, whilst all students gain from the opportunity to preview a field site and revisit it later, students with disabilities (e.g., anxiety, restricted mobility) greatly benefit from being able to do so. This may reduce anxiety and allow a more informed discussion around adjustments where the terrain may present obstacles. However, virtual fieldwork can provide additional advantages. These include: i) extending the field experience by providing virtual access to less accessible sites (e.g., on top of a mountain); ii) extending the field experience by allowing participants to observe changes over time (where the destination is a rapidly changing environment, such as a glacier terminus or braided river); and (iii) providing a fallback in the event of wet weather or other circumstances that limit or prevent fieldwork, including global pandemics.

The second stage of the project takes the form of a website and accompanying workshops, which provides pedagogic and technical advice on different approaches to VR-based virtual fieldwork. This work, which remains ongoing, emphasizes the value of developing resources that are sustainable and not reliant on external platforms. Having said that, external platforms and software can provide functionality that cannot easily be reproduced without software developers. Good examples of these more sophisticated approaches are provided by some digital outcrop models, which allow users to collect data.

The third stage, which is just beginning, focusses on creating a community of practice, where interested individuals working in different institutions collaborate in the development of new resources. There are many benefits to collaboration; it can be an efficient use of time and resources, including an opportunity to draw on experience elsewhere.

## **Session 3 – Applying Machine Learning in Geosciences**

A large, faded globe of the Earth is centered in the background of the page.

# **SESSION 3**

# **APPLYING MACHINE**

# **LEARNING IN**

# **GEOSCIENCES**

# Unlocking the Potential of Historical Aerial Imagery for the Antarctic Peninsula: Automating 3D Reconstruction using Python and MicMac

Felix Dahle<sup>1</sup>, Roderik Lindenbergh<sup>1</sup>, Bert Wouters<sup>1</sup>

<sup>1</sup> Dept. of Geoscience & Remote Sensing, Delft University of Technology, the Netherlands  
 F.Dahle@tudelft.nl, R.C.Lindenbergh@tudelft.nl, Bert.Wouters@tudelft.nl

**Key words:** *Historical Imagery, Photogrammetry, Structure from Motion, Antarctica, Aerial Imagery*

The US Geological Survey (USGS) has made available a vast collection of historical aerial imagery from Antarctica, known as the TMA archive, captured by the U.S. Navy between 1946 and 2000. Our project aims to leverage this valuable resource to generate Digital Elevation Models (DEMs) of the region, enabling us to assess long-term changes in ice elevation on the Antarctic Peninsula. To achieve this, we employ Structure from Motion (SfM), a photogrammetric technique that constructs 3D structures from two-dimensional images by identifying tie-points between them.

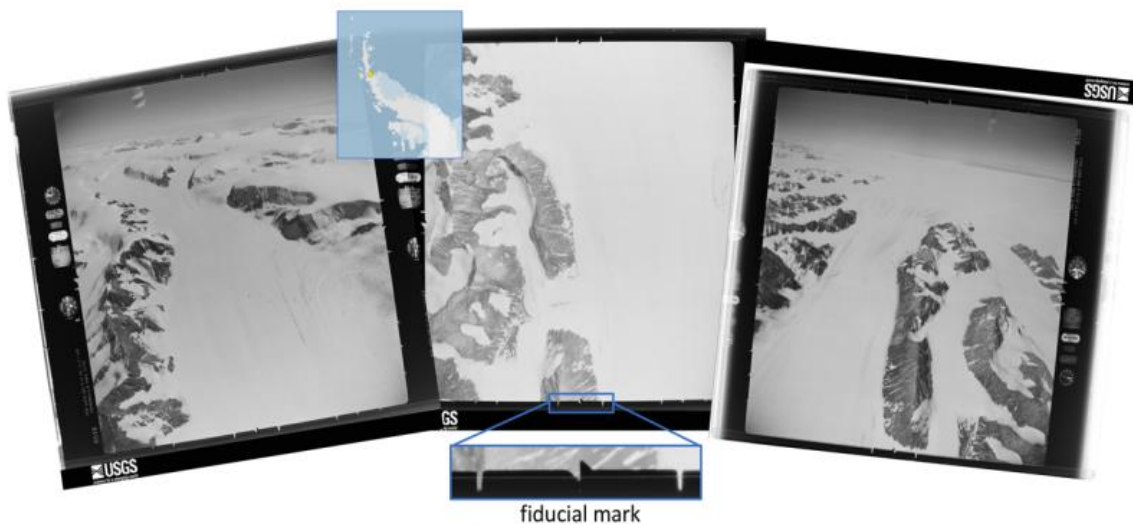


Figure 4: Example for historical images from the TMA archive

While this task is typically straightforward, the unique challenges posed by the historical nature of the TMA archive necessitate innovative approaches. The archival data lacks complete or even accurate image and camera information, such as focal length, height, or camera position, which must be inferred from various sources. Additionally, the grayscale images depict diverse scenes of Antarctica, featuring challenges such as clouds over snow (white on white pixels) extensive water and snow areas. Manual intervention in the SfM process to enhance the model quality is infeasible due to the archive's scale, consisting of approximately 300,000 images.

To overcome these challenges, we propose automating the entire SfM process using Python and MicMac, a photogrammetry toolbox developed by IGN. Although the project is currently ongoing, we have made significant progress in mitigating the complexities of the data. First, we developed a machine learning-based method to automatically identify fiducial marks in the images and normalize them, considering that the historical images are scans from film. Second, we trained a segmentation model to semantically segment the images, allowing us to exclude unsuitable areas (e.g., clouds, water, sky) during tie-point detection. Third, we devised techniques to extract missing or erroneous metadata, such as focal length and height, directly from altimeters and handwritten notes on the images, when available. Lastly, as the exact positions of the images are only approximately known, we are currently developing an algorithm to automatically derive their precise locations.



By generating accurate 3D models, we will compare them with contemporary elevation data, including satellite stereo-photogrammetry and altimetry (e.g., ICESat-2), enabling us to gain detailed insights into elevation and mass changes over the past five decades. This comprehensive analysis will contribute to our understanding of the Antarctic Peninsula's dynamic environment and provide valuable information for climate and glaciological studies.

**Acknowledgements:** This work was funded by NWO-grant ALWGO.2019.044.

# Advanced Glacier Monitoring with ICEpy4D: A Python Toolkit for Multi-Epoch Analysis using Deep-Learning Photogrammetry

F. Ioli<sup>1\*</sup>, F. Nex<sup>2</sup> & L. Pinto<sup>1</sup>

*1 Dept. of Civil and Environmental Engineering (DICA), Politecnico di Milano, Milan, Italy – (francesco.ioli, federico2.barbieri, federica.gaspari, livio.pinto)@polimi.it*

*2 Dept. of Earth Observation Science (EOS), Faculty ITC, University of Twente, Enschede, The Netherlands – f.nex@utwente.nl*

**Key words:** *Time-lapse cameras, low-cost, stereo reconstruction, sfm, 4D monitoring*

Time-lapse cameras are commonly used to capture high-frequency images of glacier flow, providing qualitative and quantitative data with minimal maintenance. However, the use of a single cameras hinders the possibility to compute 3D models, estimate volumetric changes, and apply change detection algorithms. Existing software packages such as ImGraft (Messerli and Grinsted, 2015), Pointcatcher (James et al., 2016), and PyTrx (How et al., 2020) allow the calculation of glacier velocities from oblique time-lapse images by feature tracking, but are limited to monoscopic camera systems. SfM software packages for multicamera systems, such as Agisoft Metashape or Colmap, rely on traditional Feature-Based Matching (FBM) that may not be suitable for wide camera baselines (Yao et al., 2021). This work presents ICEpy4D, a Python-based toolkit that integrates deep learning-based wide baseline matching with multi-epoch 3D reconstruction for glacier monitoring. ICEpy4D is available at <https://github.com/labmgf-polimi/icepy4d/>.

ICEpy4D is a modular tooling that allows for the following processing steps (Figure 1): (i) identifying corresponding features and solving relative and absolute camera orientations; (ii) tracking features in single camera time series to automatically detect targets in consecutive images, (iii); performing Bundle Adjustment (BA) and generating dense reconstruction by using external libraries, (iv) process time series of point cloud. ICEpy4D uses pre-trained SuperPoint+SuperGlue neural networks (Sarlin et al., 2020) for feature matching, which have demonstrated superior performance over traditional FBM with wide baselines (Yao et al., 2021). The BA currently relies on the Agisoft Metashape Python API, which is seamlessly integrated into the ICEpy4D workflow. Alternatively, COLMAP can be used for BA, but without GCP support. Similarly, densification can be performed by Metashape or COLMAP. Point cloud processing is implemented using the open source libraries Open3D and CloudComPy.

A low-cost stereoscopic system was installed on Belvedere Glacier in summer 2021 (Ioli et al., 2023). It consisted of two time-lapse cameras placed respectively 180 m and 340 m apart from the glacier terminus, with a baseline of 260 m. Daily stereo pairs acquired by the cameras were processed using ICEpy4D. Camera positions were assumed to be fixed, while camera rotations, caused by wind gusts, were estimated by BA, including GCPs located in stable areas. Ice volume loss was computed by DEM of Differences (DOD) between pairs of point clouds spaced by five days to increase the signal-to-noise ratio, resulting in a loss of  $6.3 \times 10^4 m^3$  of ice (Figure 2a) and a glacier retreat of 17.6 m (Figure 2b) from May to November 2022.

ICEpy4D is a promising toolkit for 4D glacier monitoring using affordable stereo/multi-camera setups, that incorporate a 3D component into multi-temporal glacier monitoring, ICEpy4D, enabling volume variations computation. ICEpy4D is under active development and new features are planned for the near future, including testing the open-source CERES library as a replacement for Agisoft Metashape for BA and deep learning techniques for dense reconstruction. Furthermore, ICEpy4D will be extended to interface with other libraries such as py4dgeo (Anders et al., 2021) for 4D point cloud processing and PyTrx (How et al., 2020) for monoscopic feature tracking.

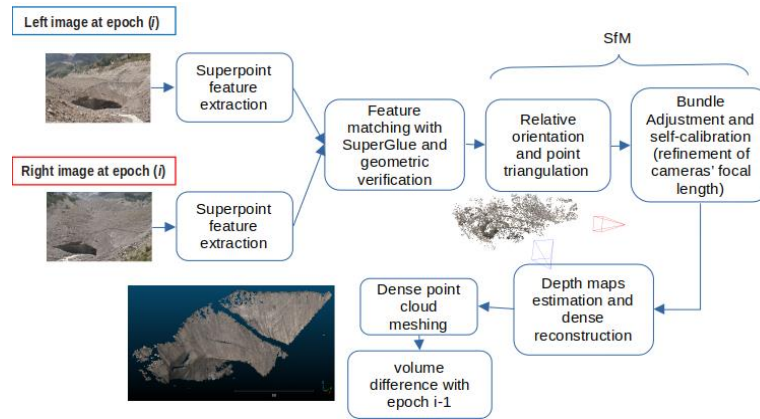


Figure 1. Scheme of the main workflow that can be performed with ICEpy4D.

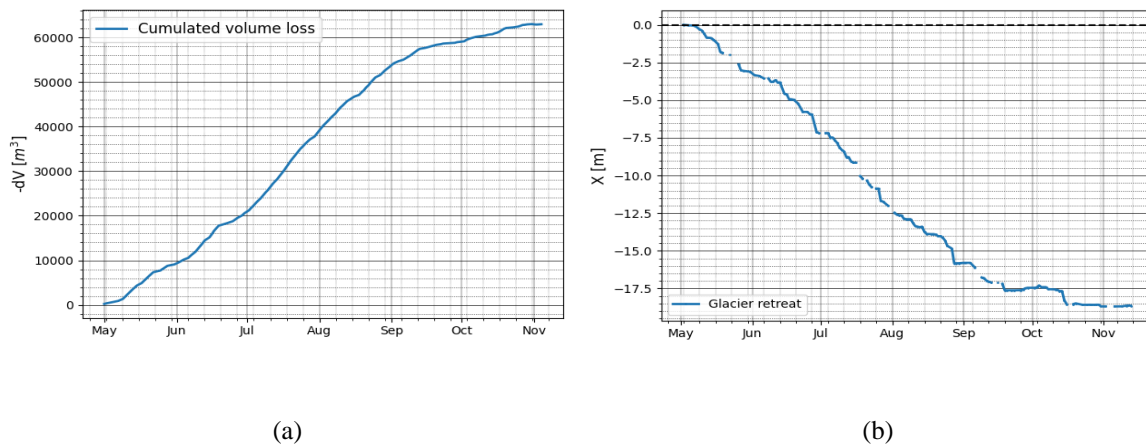


Figure 2. (a) Cumulative ice volume lost at the terminus of Belvedere Glacier from May to November 2022; (b) Belvedere Glacier retreat between May and November 2022, estimated as the location of the terminal ice-cliff upper boundary along a cross section parallel to the streamwise direction (labeled as  $X$ ) and located at the center of the glacier terminus.

## References

- How, P., Hulton, N. R. J., Buie, L. & Benn, D. I., 2020. PyTrx: A Python-Based Monoscopic Terrestrial Photogrammetry Toolset for Glaciology. *Frontiers Earth Sci.*, 8.
- Ioli, F., Bruno, E., Calzolari, D., Galbiati, M., Mannocchi, A., Manzoni, P., Martini, M., Bianchi, A., Cina, A., De Michele, C. & Pinto, L. 2023. a Replicable Open-Source Multi-Camera System for Low-Cost 4d Glacier Monitoring. *ISPRS Int. Arch. Photogramm.*, 48, 137-144.
- Messerli, A. & Grinsted, A., 2015. Image georectification and feature tracking toolbox: ImGRAFT. *Geosci. Intrum. Meth.*, 4(1), 23–34.
- James, M. R., How, P. & Wynn, P. M., 2016. Pointcatcher software: analysis of glacial time-lapse photography and integration with multitemporal digital elevation models. *J. Glaciol.*, 62(231), 159–169.
- Sarlin, P.-E., DeTone, D., Malisiewicz, T. & Rabinovich, A., 2020. SuperGlue: Learning feature matching with graph neural networks. *Proc. CVPR IEEE*
- Yao, G., Yilmaz, A., Meng, F., & Zhang, L., 2021. Review of Wide-Baseline Stereo Image Matching Based on Deep Learning. *Remote Sens.*, 13(16), 3247.
- Anders, K., Winiwarter, L., Mara, H., Lindenbergh, R., Vos, S.E. & Höfle, B. 2021: Fully automatic spatiotemporal segmentation of 3D LiDAR time series for the extraction of natural surface changes. *ISPRS J. Photogramm. Remote Sens.*, 173, pp. 297-308.

# Deep learning of topographic anomalies for the detection of regions of interest in 3D point clouds

Reuma Arav<sup>1\*</sup>, Dennis Wittich<sup>2</sup>, Franz Rottensteiner<sup>2</sup>

<sup>1</sup> Dept. of Geodesy and Geoinformation, TU Wien, 1040 Vienna, Austria, reuma.arav@geo.tuwien.ac.at

<sup>2</sup> Institute of Photogrammetry and GeoInformation, Leibniz University Hannover, Hannover, Germany

**Keywords:** visual saliency, geomorphological entities, natural environment, lidar, photogrammetry, deep neural network.

Three-dimensional point clouds are ubiquitous in the study of natural environments. These point clouds hold extensive datasets that pose challenges for analysis. This is particularly because the collected data contains a diverse set of objects, at varying shapes and sizes, that are distributed throughout the data, and intricately intertwined within the topography. In such cases, it is difficult to focus on the important regions and perform the required analyses. In this presentation, we draw inspiration from visual perception phenomena to highlight regions of interest. In visually perceptive animals, the visual system filters and allocates more attention to attractive and interesting regions to enable further processing (Cong et al., 2018). In point clouds, visual saliency has been previously suggested as a preliminary stage to localize complex processing procedures, e.g., detection, simplification, registration and others (e.g., Arav et al., 2022). Here we propose to evaluate visual saliency in order to differentiate the objects of interest from the cluttered environment while emphasize their presence within the overall context. Previous approaches suggested handcrafted attributes that signify saliency (e.g., Ding et al., 2019; Arav & Filin, 2020). However, such methods are affected by the surface roughness pattern and by measurement noise.

Instead, we propose in this presentation to learn the landscape shape and then search for anomalies. We assume that any change from the prevalent surface would suggest a salient object. Since the topography not necessarily regular, we first train a deep neural network to reconstruct the surface. Specifically, we train a network designed to process a voxel grid's shell and generate a reconstructed voxel grid as an output. In scenarios where the reconstructed part deviates from regularity, the resulting reconstruction error will be significant, indicating high saliency. To showcase the effectiveness of our proposed approach, we search for salient features within a 2 km long point cloud of the Pielach River (Austria). Figure 1 shows an example of the identification of objects along the riverbed and river banks by using the proposed method. Through qualitative and quantitative analysis, we establish a strong correlation between the reconstruction error and salient objects. We compare the results to other saliency evaluation methods and show the advantage of the proposed method.

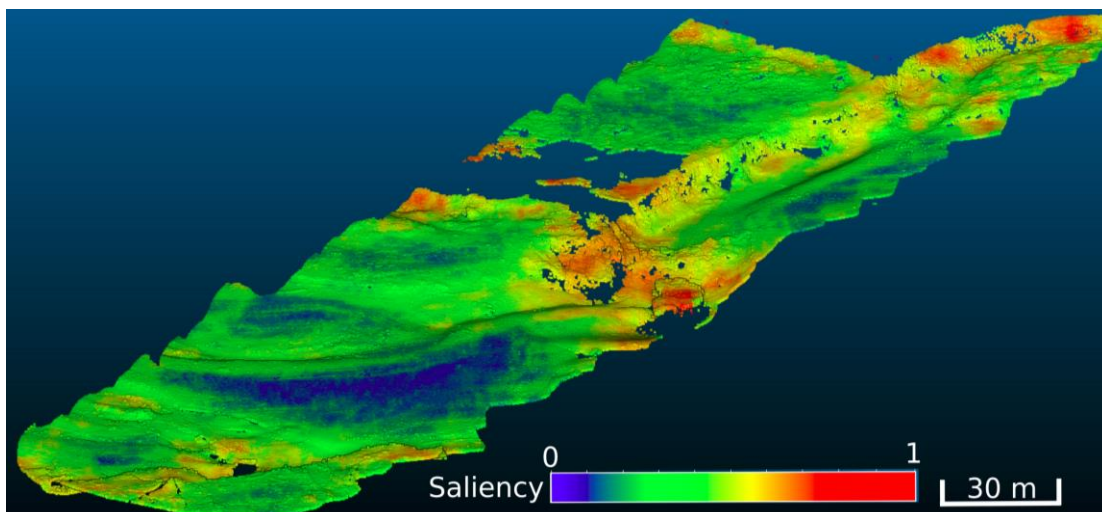


Figure 1: An extract of saliency evaluation by learning surface reconstruction of a point cloud in the Pielach River (Austria).

**Acknowledgements:** This project has received funding from the European Union’s Horizon 2020 research and innovation programme under the Marie Skłodowska-Curie grant agreement No. 896409. The authors would also like to thank Ass.Prof. Gottfried Mandlbürger and Riegl LMS for the permission to use the test data.

## References

CONG, R., LEI, J., FU, H., CHENG, M. -M., LIN, W. AND HUANG, Q., 2019. Review of Visual Saliency Detection With Comprehensive Information. *IEEE Transactions on Circuits and Systems for Video Technology*, vol. 29, 10:2941-2959, doi: 10.1109/TCSVT.2018.2870832.

ARAV, R., FILIN, S., AND PFEIFER, N., 2022. Content-Aware Point Cloud Simplification of Natural Scenes. *IEEE Transactions on Geoscience and Remote Sensing*, vol. 60:1-12, doi: 10.1109/TGRS.2022.3208348.

ARAV, R., AND FILIN, S., 2020. Saliency of subtle entities within 3-d point clouds. *ISPRS Annals of the Photogrammetry, Remote Sensing and Spatial Information Sciences, Volume V-2-2020, 2020*, doi: 10.5194/isprs-annals-V-2-2020-179-2020.

DING, X., LIN, W., CHEN, Z. AND ZHANG, X., 2019. Point Cloud Saliency Detection by Local and Global Feature Fusion. *IEEE Transactions on Image Processing*, vol. 28, no:5379-5393, 2019, doi: 10.1109/TIP.2019.2918735.

# Workflow automation for SfM change-detection: an application to rockfalls

Xabier Blanch<sup>1,3\*</sup>, Antonio Abellan<sup>2</sup>, Marta Guinau<sup>3</sup>, Anette Eltner<sup>1</sup>

<sup>1</sup> Institute of Photogrammetry and Remote Sensing, Technische Universität Dresden, 01062 Dresden, Germany. [xabier.blanch@tu-dresden.de](mailto:xabier.blanch@tu-dresden.de)

<sup>3</sup> Center for Research on the Alpine Environment (CREALP), Sion, CH1950 Valais, Switzerland,

<sup>3</sup> RISKINAT Research Group, GEOMODELS Research Institute, Universitat de Barcelona, 08028 Barcelona, Spain,

**Key words:** Rockfall monitoring, change detection, machine learning, Structure from Motion

The workflow for change detection from point clouds is well known and used in various scientific fields for monitoring processes. This method was extensively developed in the last two decades with the introduction of LiDAR (Light Detection and Ranging) technology, which allows point clouds to be acquired with exceptional accuracy and speed. However, the advent of SfM-MVS (Structure from Motion - Multi-View Stereo) algorithms, which enables the generation of point clouds at very low cost, makes this method a suitable alternative and one of the most widely used tool for monitoring in the geosciences.

The technological facilities that allow the permanent installation of these instruments, together with the ease of data transmission from the field to the laboratory, especially in the case of cameras, make it increasingly easy to obtain 3D data with at very high temporal frequency (Blanch et al., 2023). This apparent advantage can become a limitation when parts of the processing workflow involve manual steps that require user intervention. For this reason, process automation is one of the new steps in the improvement of 3D change detection workflows (Blanch 2022).

The usual workflow for 3D change detection processes for movement/deformation monitoring consists of: a) capturing (LiDAR) or generating (SfM-MVS) point clouds, b) aligning the point clouds of two epochs (e.g., ICP algorithm, Chen & Medioni (1992)), c) obtain the distances between the points of the two point clouds (e.g. M3C2 algorithm, Lague et al., 2013), d) clustering the points that have a distance value higher than a defined accuracy threshold (Tonini & Abellan, 2014), and e) manually filter these clusters to remove points that do not correspond to a real deformation/movement (e.g. vegetation, animals, shadows that could be identified as movement/strain) (Figure 1).

The final filter step, which is very important for determining the quality and actual usability of the change detection result, is usually performed manually. Proposed alternatives to avoid a manual step tend to use very

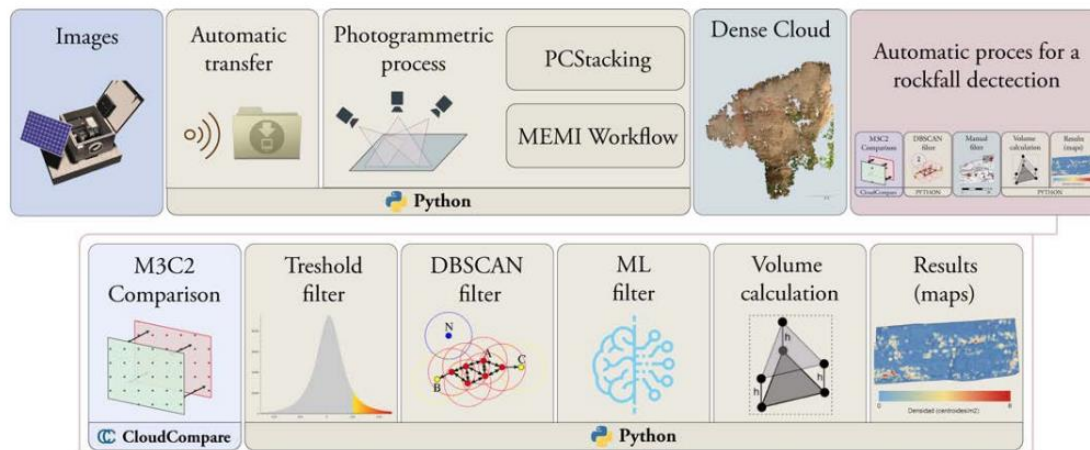


Figure 1: Classic workflow to obtain a change detection comparison from two different point cloud. In this example, the SfM-MVS photogrammetric process (first row) is used to obtain the point clouds

conservative parameters that, although they remove the bad clusters, overestimate the monitored movement/deformation, especially when its magnitude is small.

Our introduced, new approach uses Machine Learning (ML) algorithms that allow us to maintain restrictive detection parameters and thus identify all possible magnitudes of change. By training a Random Forest classifier model on a dataset containing 135 manually labelled rockfalls, we achieved an automatic ML classifier that, on an evaluation dataset of 35 rockfalls, has shown an accuracy of 97% in identifying clusters that do not correspond to rockfalls (true negatives), and an accuracy of 89% in identifying clusters that do correspond to a rockfall (true positives) (Figure 2).

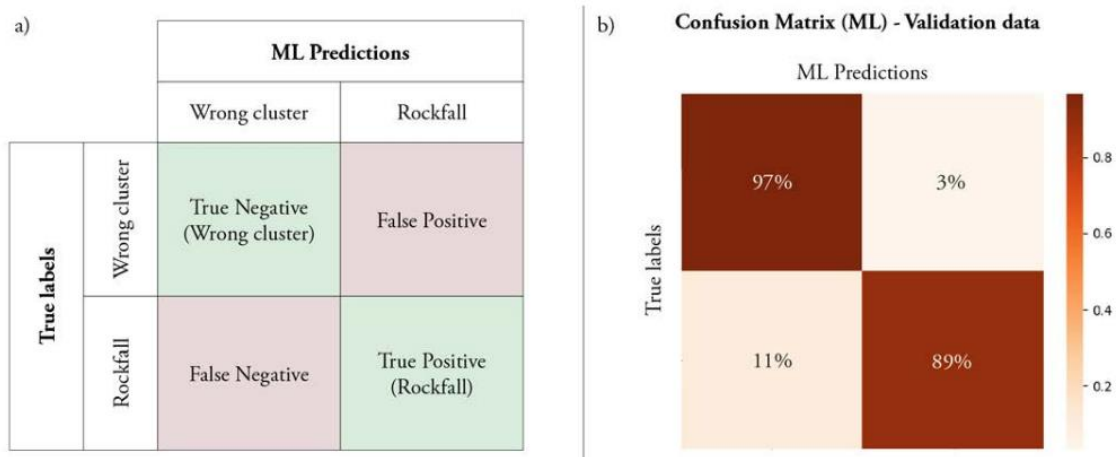


Figure 2: a) Explanation of the confusion matrix obtained in the training. Positive results are the True Negative and True Positive quadrants. b) Accuracy obtained in each quadrant for the best iteration. Evaluated on the evaluation dataset (35 rockfalls).

## References

- BLANCH, X., GUINAU, M., ELTNER, A., AND ABELLAN, A. (2023): Fixed photogrammetric systems for natural hazard monitoring with high spatio-temporal resolution, Nat. Hazards Earth Syst. Sci. Discuss. [preprint], <https://doi.org/10.5194/nhess-2023-79>, in review
- BLANCH, X., (2022). Developing Advanced Photogrammetric Methods for Automated Rockfall Monitoring. Doctoral dissertation. Universitat de Barcelona. Retrieved from: <http://hdl.handle.net/10803/675397>
- CHEN, Y., & MEDIONI, G. G. (1992). Object modelling by registration of multiple range images. Image and Vision Computing, 10(3), 145–155. [https://doi.org/10.1016/0262-8856\(92\)90066-C](https://doi.org/10.1016/0262-8856(92)90066-C)
- LAGUE, D., BRODU, N., & LEROUX, J. (2013). Accurate 3D comparison of complex topography with terrestrial laser scanner: Application to the Rangitikei canyon (N-Z). ISPRS Journal of Photogrammetry and Remote Sensing, 82, 10–26. <https://doi.org/10.1016/j.isprsjprs.2013.04.009>
- TONINI, M., & ABELLÁN, A. (2014). Rockfall detection from terrestrial LiDAR point clouds: A clustering approach using R. Journal of Spatial Information Science, 8(8), 95–110. <https://doi.org/10.5311/josis.2014.8.123>

# Machine Learning Approach on Dynamic Interactions between Air Pollutants and Forest Health using Open-access Remote Sensing Data: A Case study of the Białowieża Forest

Luka Mamić<sup>1\*</sup>, Francesco Pirotti<sup>2,3</sup>

<sup>1</sup> Sapienza University of Rome, Department of Civil, Building and Environmental Engineering, Via Eudossiana 18, 00184 Rome, Italy, [lmamic@uniroma1.it](mailto:lmamic@uniroma1.it)

<sup>2</sup> University of Padua, Department of Land, Environment, Agriculture and Forestry (TESAF), Viale dell'Università 16, 35020 Legnaro, Italy

<sup>3</sup> University of Padua, Interdepartmental Research Centre in Geomatics (CIRGEO), Viale dell'Università 16, 35020 Legnaro, Italy

**Key words:** air pollutants, forest health, machine learning, remote sensing, Sentinel-2, Sentinel-5P.

The Białowieża Forest, a UNESCO World Heritage Site, is an important ecosystem known for its rich biodiversity and ecological significance. However, increasing air pollution poses a potential threat to the health of this unique forest. This study aims to investigate the dynamic interactions between air pollutants and forest health by integrating Sentinel-2 and Sentinel-5P remote sensing data with machine learning algorithms.

Using QGIS software, the boundaries of the Białowieża Forest protected area were extracted from a map obtained from the UNESCO website (Fig. 1). The resulting layer was transformed to the WGS84 coordinate system and uploaded to Google Earth Engine, defining the study's area of interest.

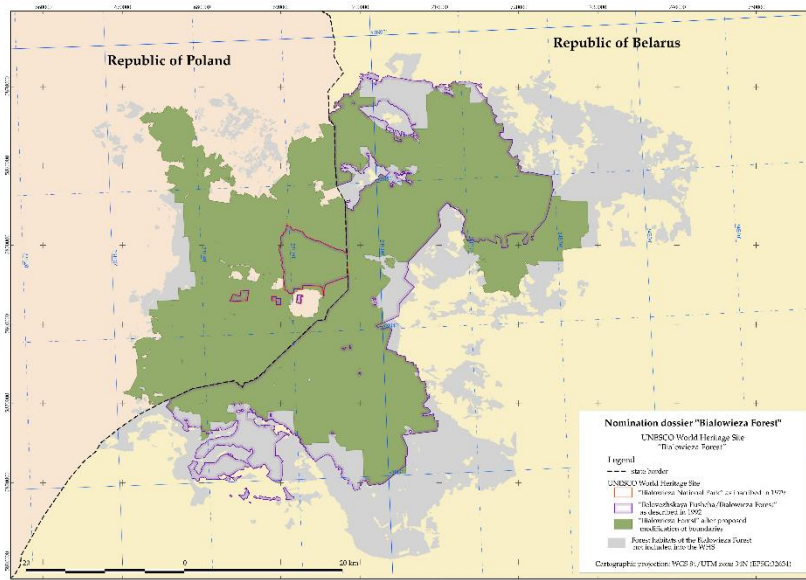


Figure 1: Map of UNESCO World Heritage Site "Białowieża Forest" (UNESCO, 2023)

Monthly mean values of the Normalized Difference Vegetation Index (NDVI) from Sentinel-2 and various air pollutants, including ozone (O<sub>3</sub>), aerosol index (AI), carbon monoxide (CO), formaldehyde (HCHO), nitrogen dioxide (NO<sub>2</sub>), sulphur dioxide (SO<sub>2</sub>), and methane (CH<sub>4</sub>), from Sentinel-5P were resampled to 1000x1000m pixels covering the study area. Data were collected from January 2019 to December 2022, resulting in 48 images, each containing eight bands (NDVI, O<sub>3</sub>, AI, CO, HCHO, NO<sub>2</sub>, SO<sub>2</sub> and CH<sub>4</sub>) and representing one month. These images were used to train a random forest (RF) model for predicting NDVI and investigating the influence of air pollutants on forest health. The RF model employed 500 trees and underwent 10-fold cross-validation. Accuracy assessment was performed using Pearson correlation coefficient ( $r$ ), mean absolute error (MAE), and root mean square error (RMSE).

The results demonstrated that using the mentioned air pollutants, the RF model achieved a high accuracy in predicting NDVI ( $r = 0.9507$ ,  $MAE = 0.0308$ ,  $RMSE = 0.0419$ ). Variable importance analysis revealed  $O_3$  and AI as the most influential variables in the trained model (Fig. 2).

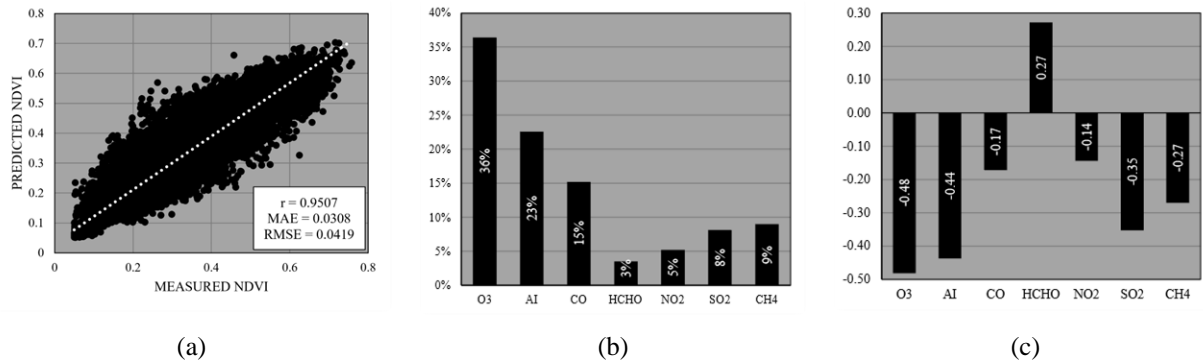


Figure 2. Results of the study: (a) trained RF model for predicting NDVI, (b) variable importance analysis of the developed model, (c) correlation coefficient ( $r$ ) of each variable to the NDVI.

Further investigation of the correlation between each variable and NDVI revealed that  $O_3$  has the strongest negative correlation ( $r = -0.48$ ). This finding aligns with our previous study on the relation between  $O_3$  and NDVI on common wheat crops. It is not yet clear if the observed relationship is related to NDVI because of health or because of other causes, and more investigation is required. Additionally, the study unveiled the detrimental effect of AI ( $r = -0.44$ ) on forest health, potentially linking research on AI's association with  $PM_{2.5}$  and  $PM_{10}$  (CHEN ET AL., 2016) to their harmful impact on vegetation health (RAI, 2016).

This study contributes to a better understanding of the impact of air pollutants on the health of the Białowieża Forest and sheds light on the broader implications for global vegetation. By revealing the intricate links between air pollution and forest dynamics, this research emphasizes the importance of digital methods and remote sensing technologies in understanding and addressing environmental challenges.

## References

CHEN, W., TANG, H., ZHAO, H., & YAN, L., 2016. Analysis of Aerosol Properties in Beijing Based on Ground-Based Sun Photometer and Air Quality Monitoring Observations from 2005 to 2014. *Remote Sensing*, 8(2):110, <https://doi.org/10.3390/rs8020110>.

UNESCO WORLD HERITAGE CONVENTION, 2023, Białowieża Forest – map of inscribed extension, accessed 29 May 2023, <https://whc.unesco.org/en/list/33/maps/>.

RAI, P. K., 2016. Impacts of particulate matter pollution on plants: Implications for environmental biomonitoring. *Ecotoxicology and environmental safety*, 129, 120-136, <https://doi.org/10.1016/j.ecoenv.2016.03.012>.

## Automatic boulder detection applied to the Stone Garden (Altai Mountains, Russia): techniques and outcomes

Sergei Medvedev<sup>1</sup>, Dmitry Zastrozhnov<sup>2,3,4\*</sup>, Viktor Spiridonov<sup>3,5</sup>, Nils Charles Prieur<sup>4,6</sup>,  
Andrei Zastrozhnov<sup>3</sup> & Sverre Planke<sup>2,4</sup>

<sup>1</sup>Medvedev Consulting, Oslo, Norway, [sergeimed@yahoo.com](mailto:sergeimed@yahoo.com)

<sup>2</sup>Volcanic Basin Energy Research, Oslo, Norway, [zastrozhe@gmail.com](mailto:zastrozhe@gmail.com)

<sup>3</sup>A.P. Karpinsky Russian Geological Research Institute (VSEGEI), Saint Petersburg, Russia

<sup>4</sup>Department of Geosciences, University of Oslo, Norway

<sup>5</sup>Russian Geological Research Oil Institute (VNIGNI), Moscow, Russia

<sup>6</sup>Stanford University, Stanford, CA, USA

**Key words:** boulder detection, deep learning, GIS, Altai Mountains

The demand for surface and sub-surface detection of boulder fields is growing. While being most developed for planetary sciences (e.g. HOOD *et al.*, 2022), in Earth studies it is mainly useful for offshore spatial planning (e.g., wind farms, platforms, pipelines) and ecosystem research. However, most offshore areas lack high-resolution non-confidential bathymetric and acoustic imagery data to apply and evaluate boulder detection techniques. In our project, we examine a large boulder field in the Altai Mountains (“Stone Garden”), which provides an ideal location to test different techniques and design robust detection workflows. These outcomes can be further applied to offshore studies.

The Stone Garden is a large boulder field (~2 km<sup>2</sup>) located in the Altai Mountains on the left bank of the Katun’ river, near the village of Inja, along the Chuya Highway. It lies on the middle terrace of the Katun’ river, and its origin has mainly been attributed to hypothetical Altai megafloods, related to catastrophic drainage of ice-dammed lakes existing in the Chuja and Kuraj depressions in the late Quaternary (e.g. HERGET, 2005). However, several authors dispute its catastrophic nature, claiming glaciers were the main transport agents of the boulder material (e.g. OKISHEV, 2011). To advance our understanding of the origin of the Stone Garden, a quantitative analysis of the properties of boulder populations is required.

During the 2021 field campaign, we applied structure-from-motion photogrammetry to UAV photography data collected over the Stone Garden to compute a high-resolution (13 cm/px) digital surface model (DSM) and orthophoto imagery mosaic (6 cm/px). Our study involves two major parts: (i) boulder detection and outlining, and (ii) analysis of boulder population properties.

For boulder detection, we used three methods: (1) Deep learning technique to analyse high-resolution orthophoto images of the area (PRIEUR *et al.*, 2022a, 2022b); (2) Advanced combination of standard GIS methods and manual tuning of DSM and orthophoto images; (3) Numerical recognition of topographic singularities on DSM. The analysis of boulder sizes demonstrates identical power-law distribution (CLAUSET *et al.*, 2009) for all three methods with power-law exponent between 3 and 4. This dependence breaks for boulders smaller than ~2-3 m in effective diameter. This defines the completeness of the detection only for boulders of larger dimensions (2-10 m), if no additional geological mechanism exists that removes average size boulders (0.5-2.5 m) from the area.

The boulder detection not only recognizes boulders position and concentration, but also allows us to analyse their individual and statistical properties. The spatial distribution of boulders shows differences in size depending on relative elevation. Orientation of elongated boulders is not well-defined statistically, but major axes tend to be orthogonal to the average topographic trend. We also develop DSM-based methods to detect boulders characterized by distinct stoss slope, which allows us to build a map of the distribution of stoss slopes orientation.

The combination and comparison of different methods increases the analysis robustness. The three methods in our study show comparable boulder detection results. We also developed routines for in-depth analysis of statistical and individual properties based on DSM. Offshore areas without acoustic imagery data can also benefit from these workflows.

**Acknowledgements:** We thank V. Zykin, V. Zykina, S. Golovanov and E. Malikova (Sobolev Institute of Geology and Mineralogy, Novosibirsk, Russia) for their assistance in the field.

## References

Clauset, A., Shalizi, C. R., & Newman, M. E., 2009. Power-law distributions in empirical data. *SIAM review*, 51(4), 661-703. Herget J., 2005. Reconstruction of Pleistocene ice-dammed lake outburst floods in Altai Mountains, Siberia. *Geol. Soc. Am. Spec. Publ.*, V. 386. 118 p.

Okishev P.A., 2011. Relyef i oledneniye Russkogo Altaya [Relief and Glaciation of the Russian Altai]. Tomsk University Press, 382 p. In Russian.

Prieur, N. C., Rubanenko, L., Xiao, Z., Kerner, H., Werner, S. C., & Lapôtre, M. G. A., 2022a. A Large Training Dataset of Boulder Sizes and Shapes as a First Step Towards the Automated Detection of Rock Fragments on Planetary Surfaces. *LPI Contributions*, 2678, 1835.

Prieur, N. C., Amaro, B., Gonzalez, E., Rubanenko, L., Xiao, Z., Kerner, H., Werner, S. C., & Lapôtre, M. G. A., 2022b. Deep Learning for Boulder Detection on Planetary Surfaces. *American Geophysical Union (AGU) Conference*. P23A-02.

## **Session 4 – Digital Outcrop Characterisation & Analysis**

A large, faded globe of the Earth is centered in the background of the page.

# **SESSION 4**

# **DIGITAL OUTCROP**

# **CHARACTERISATION &**

# **ANALYSIS**

# Using outcrop digital models to guide subsurface studies for CO<sub>2</sub> storage: An example from the Amellago Oolitic Ramp (Morocco) as an analogue for the Paris Basin Dogger Reservoir

A. Bordenave<sup>1,2\*</sup>, E. Dujoncquoy<sup>3</sup>, P. Razin<sup>4</sup>, P. Daguinos<sup>4</sup>, B. Issautier<sup>1</sup> & J. Kenter<sup>3</sup>

<sup>1</sup>BRGM - Bureau de Recherches Géologiques et Minières, Orléans, France. a.bordenave@brgm.fr

<sup>2</sup>AGeoS - Applied Geology and Sedimentology, Helioparc, 64000 Pau – France

<sup>3</sup>TotalEnergies S.A, CSTJF, Pau, France

<sup>4</sup>Univ. Bordeaux, CNRS, Bordeaux INP, EPOC, UMR 5805, F-33600 Pessac, France

**Key words:** Subsurface analogue, Sequence stratigraphy, Jurassic, Morocco, Oolitic system, CCS

Understanding subsurface reservoirs remains an important objective for the future when considering carbon capture and storage (CCS) solutions for reducing greenhouse gas emissions. As with traditional subsurface studies, methods and techniques to characterise reservoirs for CCS are the same; utilising cores, well logs and/or seismic data, overseen by conceptual geological model. However, the lack of data for characterising geobodies, at the core of the reservoir, oblige geologists to use outcrop analogues. Furthermore, with the objective of having a true analogy, seismic-scale outcrop analogues are preferred (PLAYTON et al., 2010). One of the main problems of these objects is limited accessibility and it remains a challenge for the full assessment of outcrop analysis. The development of drone technologies in recent decades, followed by the improvement of image processing, photogrammetry, and software interpretations, allows us to remove the issue of outcrop accessibility and enables the accurate determination of the 3D architecture of seismic-scale outcrops. Here we present a high resolution integrated interpretation of a 15km long UAV-based digital outcrop model (DOM) of the Amellago Limestone (Jurassic, High Atlas Morocco), with the objective to accurately understand the Dogger Formation of the Paris Basin, a principal target for CO<sub>2</sub> storage.

The Amellago cliffs are considered a world-class reference outcrop for oolitic carbonate ramp systems with a seismic-scale, continuous and structurally undeformed geometry (Figure 1). This Lower to Middle Jurassic ooid-dominated ramp system is exposed along a 37 km long series of steep cliffs which allow reliable geological interpretation. A drone-based photogrammetric acquisition was performed in 2018 with a novel workflow, integrating self-developed and commercial (UGCS) software solutions to obtain automatised, efficient, and accurate vertical flight paths with an UAV quadcopter (DJI Phantom 4 pro) (DUJONCQUOY et al., 2019). The model has been anchored with 33 ground control points and then generated from 21000 photos with the Agisoft Metashape Professional software. The digital outcrop model has a 1.54 cm/pix resolution and has been interpreted with the Virtual Reality Geological Studio software (Fig 1). The geological interpretation of the model was initially based on a (field-based) pre-existing interpretation (PIERRE et al., 2010) in order to guide the determination of the stratigraphic framework at large scale. Subsequently, “seismic” sequence stratigraphy principles were applied to identify bedding surface terminations as toplap, downlap or onlap to understand the true internal architecture.

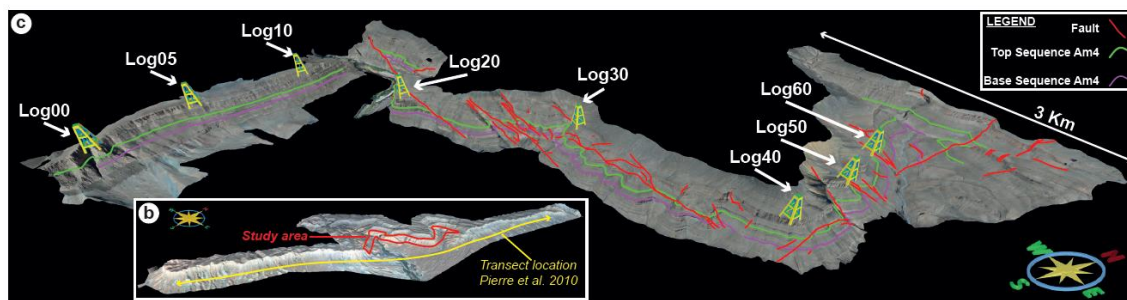


Figure 1: Third order sequence mapping along the km long photogrammetric model of the Amellago limestone.

In this study, the work concentrated on the sequence Am4, one of the nine 3rd order stratigraphic sequences; described in the literature within the area of interest (Pierre et al., 2010). The latter is limited by major maximum regressive surfaces (MRS) defined from the distal part of the sedimentary system and tracked inwards along the DOM. Transgressive and regressive intervals were defined based on the identification of major maximum flooding intervals, characterised by massive recessive intervals. Thickness variations and stratigraphy on the proximal-distal profile were quantified by serial digital logs, which have been calibrated to fieldwork data. The regressive stages show a thickening outward (20m) and slightly inclined geometries ( $0.1^\circ$ ) while the transgressive stage is tabular. Eleven HF cycles are identified in the sequence Am4. These cycles are bounded by higher frequency MRS. Even if these HF cycles seem relatively tabular at large scale, they show complex internal architecture with onlap, toplap and downlap surface geometry terminations. The detailed mapping of the surfaces and internal geometries resulted in the identification of sequence stratigraphic motifs associated to retrogradation, aggradation-progradation and pure-progradation prism. These motifs are faciologically calibrated by field observations, sampling and existing literature. Finally, detailed sedimentological observations made of individual geobodies allow us to partition and classify oolitic dunes along different sequence stratigraphic motifs and propose an accurate facies model along this oolitic ramp. A systematic analysis of these objects showed a variety of dune characteristics (extension, thickness, stacking, contact, dip etc.) on a proximal-distal profile. The proximal part is composed of multiple kilometre wide shoal complexes with successive thin (3m) and wide (>1km) dunes, present along both retrograding and aggrading-prograding prism. In contrast oolitic dunes from the distal part are isolated, thicker (5m), poorly extended (<100m) and only distributed at the top of aggrading-prograding and pure-progradation prisms.

All results obtained from the interpretation of the Amellago outcrop model have been used for a subsurface CO<sub>2</sub> storage reservoir characterisation in the Paris Basin. Owing to a large and unique dataset for CO<sub>2</sub> storage assessment, such as newly acquired 3D seismic data, well logs and cores, a complete reservoir characterisation was possible. However, the lack of intermediate scale resolution associated with oolitic dunes, oblige us to use results and concepts developed on the Amellago study. After a comparison of sedimentary facies, stacking patterns (facies and sequence) and general sequence stratigraphic architecture, we identify some similarities between the Dogger Platform and Amellago Cliff. Results obtained can guide us to target specific seismic sub-units and drive specific static modelling for an accurate CO<sub>2</sub> injection.

In conclusion, the Amellago case study provides a good example of how highly detailed photogrammetric acquisitions and interpretations of seismic-scale outcrop analogues can enable access to accurate reconstructions of stratal framework and associated facies partitioning, which can be directly applied for subsurface characterisation. The next objective of this study will be to integrate results from hyperspectral scanning (DUJONCQUOY *et al.*, submitted), showing diagenetic reservoir intervals, in order to generate forward modelling for an immediate application during subsurface reservoir modelling.

**Acknowledgements:** Author and co-authors would like to thank TotalEnergies and specifically the PIT (Projet d'Innovation Technologique) for project funding.

## References

- Dujoncquoy, E., Forge, A., & Kenter, J., 2019. UAV-based photogrammetric acquisition along large-scale cliffs: novel workflow for seismic-scale 3D outcrop studies. *1, 57. Mallorca, SPAIN.*
- Dujoncquoy, E., Bourillot, R., Thiele, S., Kenter, J., Bordenave, A., Ransinangue, A., Champagne, J., Lorenz, S., & Gloaguen, R., *Submitted.* Resolving Stratigraphic Control on Seismic-Scale Dolomitization from Digital-Outcrop and Hyperspectral Mapping. *Geology*
- Pierre, A., Durllet, C., Razin, P., & Chellai, E. H., 2010. Spatial and temporal distribution of ooids along a Jurassic carbonate ramp: Amellago outcrop transect, High-Atlas, Morocco. *Geological Society, London, Special Publications*, 329(1), 65.
- Playton, T., Kenter, J., Levy, M., Pierre, A., Jones, G. D., & Harris, P. M., 2010. Strategies for modeling depositional heterogeneity of carbonate ramps using outcrop analogs and multiple point statistics. *GEO 2010, cp-248-00453.*

## Digital outcrop mapping of the Puga geothermal field, Ladakh, India

Sam T Thiele<sup>1\*</sup>, Horthing V Zimik<sup>2, 3</sup>, Aditya Naik<sup>4</sup>, Daudayal Sharma<sup>3</sup>, Pankaj Khanna<sup>3</sup>

<sup>1</sup>Helmholtz-Zentrum Dresden-Rossendorf, Helmholtz Institute Freiberg for Resource Technology, 09599 Freiberg, Germany, [s.thiele@hzdr.de](mailto:s.thiele@hzdr.de)

<sup>2</sup>Chemical Oceanography Division, National Institute of Oceanography, Goa 403004, India

<sup>3</sup>Discipline of Earth Sciences, Indian Institute of Technology Gandhinagar, Gujarat-382355, India

<sup>4</sup>Department of Earth & Environmental Sciences, Indian Institute of Science Education and Research, Mohali, Punjab-140306, India

**Key words:** Puga, geothermal energy, digital outcrop mapping, magmatic hydrothermal

The Puga geothermal field, located at ~4400 m elevation within exhumed ultra-high pressure gneisses of the Tso Morari nappe (Ladakh, western Himalayas), presents one of the most prospective high-enthalpy geothermal energy resources in India (GUPTA *et al.*, 1974). It has been extensively characterised with geophysical and hydrogeochemical methods, but remains relatively poorly understood from a geological perspective.

Recent uplift and glacial denudation of the Puga area has resulted in several ~250 m high cliffs north and east of the Puga geothermal site. Given the dome-shaped geometry of the Tso Morari nappe (EPARD & STECK, 2008), the lithologies and structures exposed in these cliffs are likely analogous to the subsurface below Puga to depths of at least several kms. We have surveyed these cliffs using a DJI Mavic Air 2 to collect ~2800 12 Megapixel images at ~1 to 5 cm ground sampling resolution, and applied the structure from motion multi-view stereo (SfM-MVS) workflow implemented in Agisoft Metashape to derive a 3D digital outcrop model (DOM). This DOM was georeferenced using the onboard UAV GPS and iterative closest point alignment to a 12.5 m resolution ALOS PALSAR DEM, and interpreted using the Compass plugin in CloudCompare (THIELE *et al.*, 2017; GIRARDEU-MONTAUT, 2016) to map geological structures including faults, fractures, foliations and lithological contacts (Fig. 1).

This mapping has allowed us to link a variety of structures with paleo-fluid flow, and derive a conceptual model for the modern geothermal system. Outcomes of this mapping include the following:

1. Gneissic foliation is well developed across the area, varying locally between two orientations, analogous to a decameter scale S-C shear fabric. This foliation dips shallowly (10-30°) to the north-east on the northern side of the Puga valley, and horizontally to gently southwards on the southern side of the valley, defining a broad antiform.
2. Several sets of brittle fractures crosscut the gneissic foliation (Fig. 1), including multiple neotectonic NW-dipping normal faults (EPARD & STECK, 2008). These faults show significant evidence of past fluid flow, including m-thick quartz-tourmaline veins, and appear spatially associated with the hot-springs.
3. Large (5-25 m thick) lenses of sericite and tourmaline alteration are exposed on both sides of the Puga valley, associated with regions of intense foliation (Fig. 2a, b). Further characterization of this alteration is in progress, but it could represent partial greisenisation by magmatic fluids within a moderately deep geothermal reservoir. This may be analogous to the modern reservoir imaged at 2-3 km depth by geophysical surveys (GUPTA, 1974).
4. Various types of fracture fill and associated wall-rock alteration occur throughout the DOM, including advanced argillic and alunitic alteration associated with recent but now-extinct fumarolic systems (Fig. 2c, d), quartz-tourmaline veins and, locally, fine grained sulfide precipitates. Travertine deposits within larger joints are also common.

We conclude that the cliffs north and east of the Puga hot springs preserve a fossilized geothermal system that can be studied to better predict reservoir properties for future energy projects.

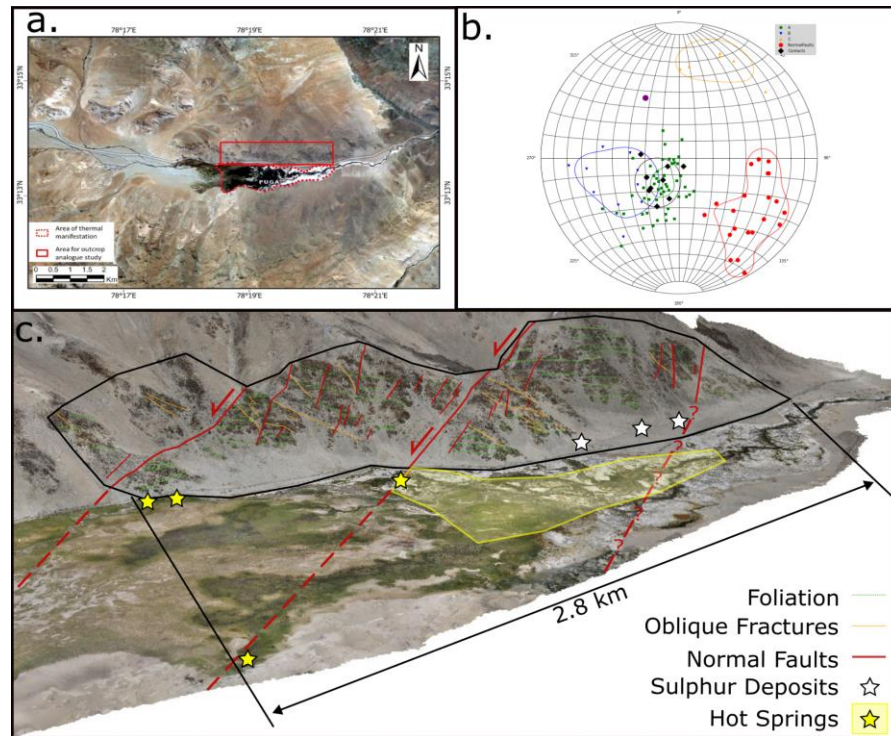


Figure 1: Reservoir analogue outcrop adjacent to the Puga hot springs site (a). Structural measurements (b) extracted from the digital outcrop model (c) have been plotted using a lower-hemisphere stereographic projection, and highlight several sets of fractures and faults that likely controlled fluid circulation prior to their exhumation.

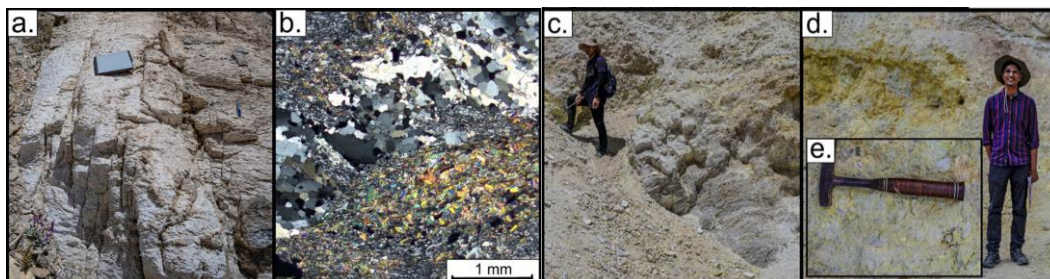


Figure 2. Examples of sericitic (a, b), advanced argillic (c) and solfataric (alunite) alteration (d, e) observed at Puga. This appears to be controlled by fracture zones (a) and foliation (c) in the gneiss, while also forming polymictic breccias (e) that are interpreted to be welded valley fill and scree deposits.

**Acknowledgements:** The authors would like to acknowledge the Paired Early Career Fellowship in Applied Research (PECFAR) awarded to STT and PK for facilitating the research exchange that allowed this research.

## References

- EPARD, J.L. & STECK, A., 2008. Structural development of the Tso Moriri ultra-high pressure nappe of the Ladakh Himalaya. *Tectonophysics*, 451(1-4), pp.242-264.
- GIRARDEU-MONTAUT, D., 2016. CloudCompare. *EDF R&D Telecom ParisTech*, 11, France
- GUPTA, M.L., RAO, G.V., & NARAIN, H., 1974. Geothermal Investigations in the Puga Valley Hot Spring Region, Ladakh, India. *Geophys. Res. Bull.* 12 (2-3): 119-36.
- THIELE, ST., GROSE, L., SAMSU, A., MICKLETHWAITE, S., VOLLGGER, SA., & CRUDEN, AR., 2017. Rapid, Semi-Automatic Fracture and Contact Mapping for Point Clouds, Images and Geophysical Data. *Solid Earth* 8 (6): 1241-53. <https://doi.org/10.5194/se-8-1241-2017>.

# How high-resolution DOM & VR boost unravelling and modelling of complex fault zones?

Lamarche J.<sup>1\*</sup>, Richard P.<sup>2</sup>, Touré K.<sup>1</sup>, Viseur S.<sup>1</sup>, Fleury J.<sup>1</sup>, Civet F.<sup>3</sup>

<sup>1</sup> Aix-Marseille Université, CNRS, IRD, INRAE, Cerege, Um 34, 3 Place Victor Hugo (Case 67), 3331, Marseille, Cedex 03, France, lamarche@cerege.fr

<sup>2</sup> PRGeology, <https://prgeology.com/>

<sup>3</sup> VR2Planet 2 rue du chateau de l'Éraudière 44300 Nantes (FRANCE)

**Key words:** Fault Zones, Photogrammetry, DFN, permeability, VR

Modelling fault zone is a real challenge because fault zones are complex imbricated structures in 3D and at multiple scales. They include heterogenous faults and fractures patterns as well as damage zones and fault cores. Their structure, imbrication and evolution are essential for fluid flows prediction in sub-surface. The recent development of drone surveys and virtual geology is a chance for geologists to better capture the multi-scale complexity of kilometre long faults zones. However, the switch from DOM to 3D structural model is still not an easy game.

The aim of this project is to create a workflow that accurately capture faults structure in 3D and in VR in order to support the modelling of fluid flow along complex fault zones.

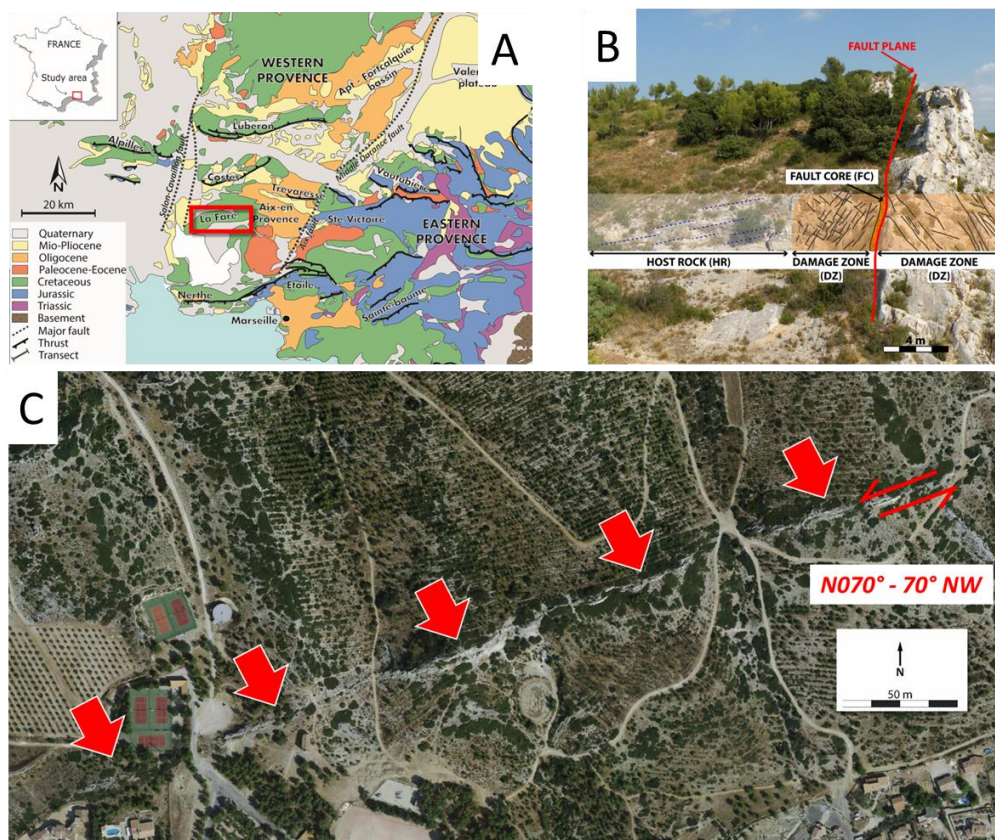


Figure 1: Location and geological context of Castellans Fault Zone. A: Location in SE France, B: host rock, damage zone and core of the Castellans fault; C: aerial view of the 1km long Castellans fault.

The targeted fault crops out in SE-France (Fig. 1). It is ~1 km long, N070 striking and 70°N dipping. It affects Lower Cretaceous carbonates (Urgonian facies). The fault initiated as a normal during mid-Cretaceous, then reactivated as strike-slip during the Pyrenean shortening (Aubert et al., . Its structural style is a mix between normal and strike-slip, giving rise to complex features and lateral variability. The main fault zone is composed

of imbricated fault surfaces. Major faults are several hundred meters long with numerous relays between segments. Minor faults are conjugate to major ones. The fault zone bears a damage zone of variable width. It is composed of fractures organized into 2 to 4 sets.

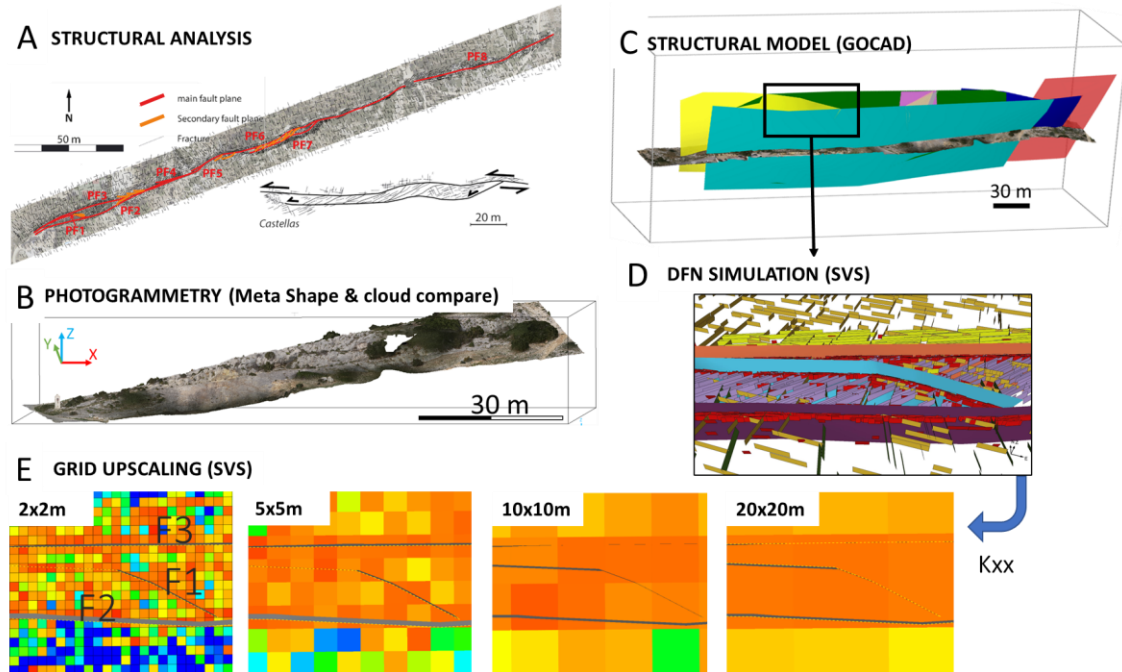


Figure 2: Workflow for fault zones analysis, fractures simulation and permeability calculation. A: field structural analysis; B: Digital Outcrop Model, C: Structural fault model, D: Discrete Fracture Network simulation, E: Permeability calculation in 4 grids with increasing cell size.

**Acknowledgements:** We acknowledge Shell for the software SVS, as well as VR2Planet for VRExplorer.

## References

Irène Aubert, Juliette Lamarche, Pascal Richard, Philippe Leonide, (2022) Imbricated structure and hydraulic path induced by strike slip reactivation of a normal fault, Journal of Structural Geology, Volume 162

## A new 1:50.000 scale map of the Nuussuaq basin: unveiling the dynamic earth with digital methods

Erik Vest Sørensen <sup>1\*</sup>, Asger Ken Pedersen<sup>2</sup>

<sup>1</sup> Geological Survey of Denmark and Greenland, Øster Voldgade 10, DK-1350, Copenhagen K, Denmark, [evs@geus.dk](mailto:evs@geus.dk)

<sup>2</sup> Natural History Museum of Denmark, Øster Voldgade 5–7, DK-1350, Copenhagen K, Denmark

**Key words:** photogrammetry, feature extraction and mapping, volcanology, mineralogy and minning

Photogeological mapping is a classical remote sensing discipline used in geological map production. It has been fundamental to the exploration and mapping of the volcano-sedimentary Nuussuaq basin in central west Greenland since the mid 70'ties. As a technique, the methodology has developed enormously, and digital outcrop models are now produced routinely across different geoscience disciplines. As the “image” is the central background data we, as a principle, strive to collect overlapping images of the landscape whenever doing field work. With the Nuussuaq basin as an example, this has resulted in a unique and growing image archive that date back to the 90'ties. The archive now consists of c. 20.000 overlapping images collected through time and we are currently producing a new 1:50.000 scale map of the Nuussuaq basin based on these images (Fig.1). With this as an example we demonstrate our photogrammetric workflow and give examples of dynamic volcanic processes (Fig. 2) that can be documented by carefully investigating the images.

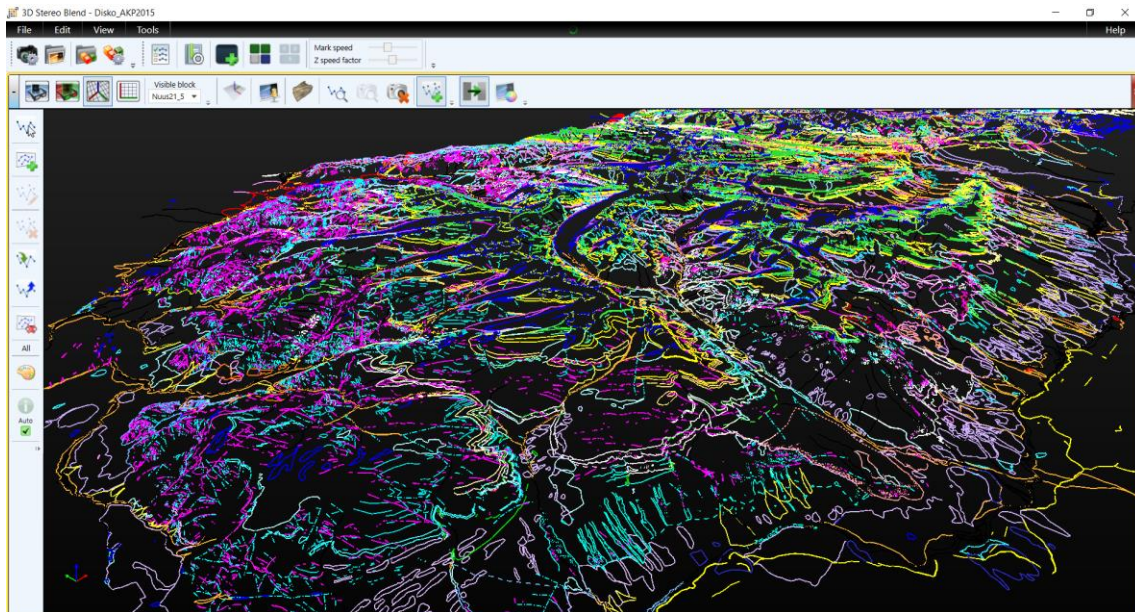
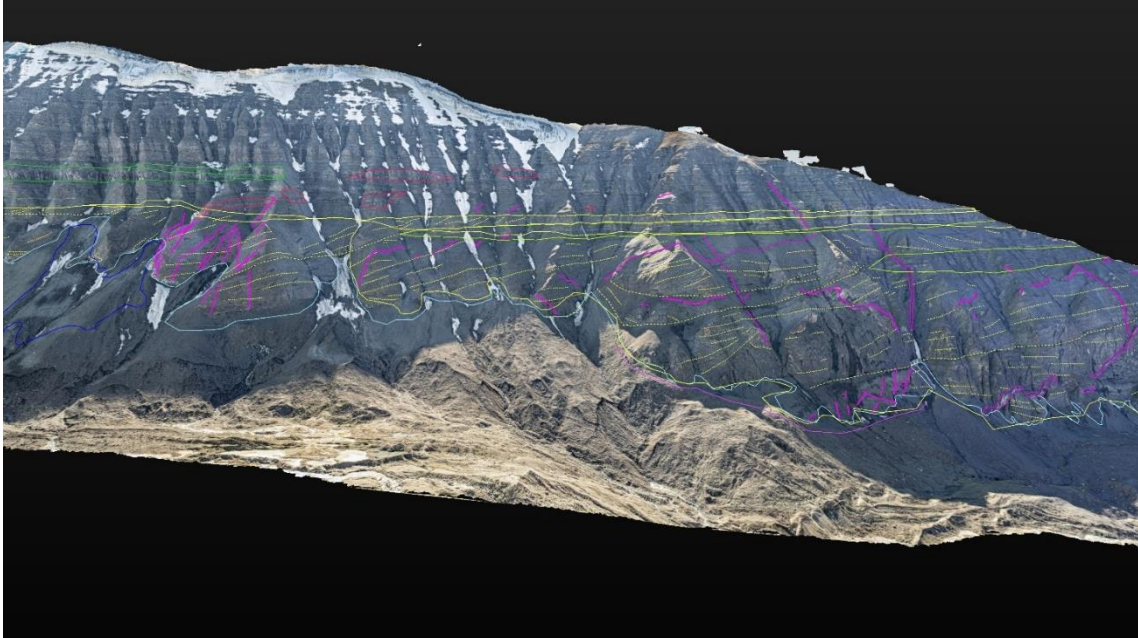


Figure 1: Perspective view showing the more than 80.000 3d polylines that have been mapped and annotated from available images during the map production. Field of view is approximately 60 x 40 km



*Figure 2. Virtual outcrop model showing examples of mapped complexed picritic intrusive patterns and eruption sites from central Nuussuaq. Purple coloured lines indicate trace of dyke intrusion, red coloured lines indicate eruption sites, yellow coloured indicate trace of foreset-bedding in hyaloclastite. Field of view is approximately 1300 x 600 m.*

## **Session 5 – Airborne & Remote Mapping**

A large, faded, light gray globe of the Earth is centered in the background of the page, behind the main title text.

# **SESSION 5**

# **AIRBORNE & REMOTE**

# **MAPPING**

# A manmade disaster - The vulnerability of managed forests in the disastrous southern summer wildfires 2023 in Chile – A remote sensing approach

Benedikt Hora<sup>1</sup> and Constanza Gonzalez-Mathiesen<sup>2</sup>

<sup>1</sup> Instituto de Historia y Ciencias Sociales, Universidad Austral de Chile, Valdivia 5090000, Chile

<sup>2</sup> Facultad de Arquitectura y Arte, Universidad del Desarrollo, Concepción, Chile

**Key words:** Valdivian temperate rainforest, forestry, Chilean summer wildfire 2023, biodiversity hotspots, wildfire prevention

The Valdivian temperate rainforest (VTR) is one of the world’s 36 biodiversity hotspots. These are defined as having at least 1500 endemic plant species and having lost 70% or more of their original habitat extent (Mittermeier et al 2013). This ecosystem is a temperate biome, located in Chile and western Argentina between 33 S and 48S, which includes different types of forests, shrublands, wetlands, rivers, and lakes. Its general biogeographical features are its location on the South American continent, its Neotropic affinities, and the legacy of the Gondwana supercontinent. Its isolation from other forest biomes has given it its strong endemism (Tecklin 2011 et al.) Strong human induced transformations, including climate change and landscape alterations, especially towards forest plantations of introduced species have increased the occurrence of wildfires which were especially destructive in the dry southern summer January 2022 – March 2023 (Peña-Fernández, E., & Valenzuela-Palma, L. 2008; Sánchez et al. 2023). Most affected areas were plantations areas of Eucalyptus y Pino Oregon in the Coastal Mountain range. In this recent wildfire season 310.000 ha have been burnt which is seven times more than during an average wildfire season in Chile (Conaf 2023; Coper 2023) (Figure 1).

In this study we want to show the correlation between landcover and wildfire events in the southern summer months of 2023. In order to quantify land use on large areas data of PROBA-V satellite mission was used (Buchhorn 2020 et al.). To differentiate between primary forest and managed forests the global planted tree extends of 2015 was applied (Lesiv 2022). We derived wildfire data from FIRMS 2023 database (Fire Information for Resource Management System) using a timescale of 15 January till 15 March 2023. We used this period because in this span the catastrophic wildfires in Chile were at their greatest. We delimited the analysis from the Maule region in the north to the northern part of the Los Lagos region.

The map shows that wildfires occur mainly in low-mountain areas in the Coastal Mountain range and that managed forest ecosystems are the most affected (Figure 1).

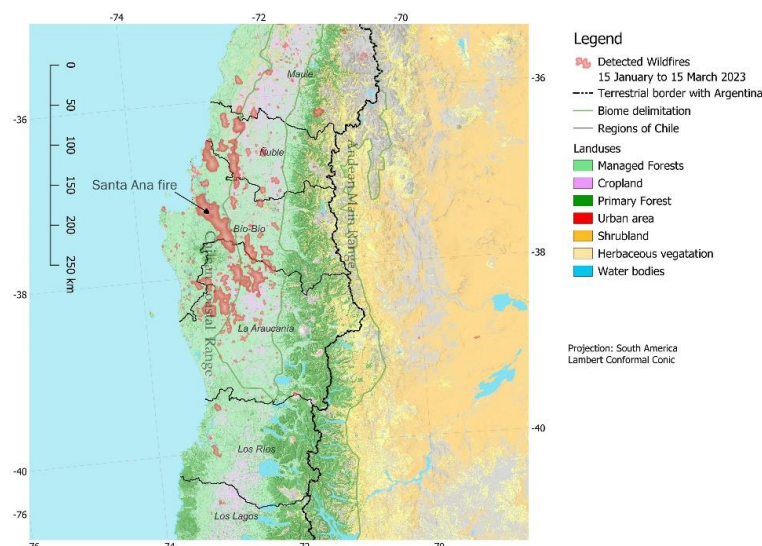


Figure1 Wildfires detected between 15 January and 15 March 2023 and land use distribution in southern Chile Source: Own illustration out of databases of Buchhorn et al. 2020, Lesiv 2022 and FIRMS 2023

We calculated from the FIRMS database an area of nearly 900,000 ha affected areas which is significant overestimation of the burned area. However, for overview analysis this data is still useful. Crossing data with previous land uses with the polygons of the wildfire fire events of 2023 shows that especially managed forest with nearly 77 % of the affected land use must draw special attention. Primary forest with only 4,8 % of affected area were far less affected by the 2023 Chilean wildfires (Table 1). Special attention must be drawn to managed forest areas (plantations) nearby population centres in future fire prevention plans. These interface areas represent zones where more lives and properties are exposed to wildfires; accordingly, this is where the biggest lost in life and infrastructure occur. For instance, the “Santa Ana” fire (2023), that affected the municipalities of Nacimiento, Santa Juana, Coronel and San Pedro de la Paz, resulted in 85,801 ha burned, 904 houses destroyed, 4,773 people displaced and 19 fatalities.

Managed forest	Cropland	Primary forest	Built up	other	Total area affected
76,89	11,4	4,8	1,7	5,2	898,600 ha

Table 1: Distribution patterns of land uses affected by wildfires between 15 January to 15 March 2023 in Chile

**Acknowledgements:** We thank CIGIDEN Centro de Investigación para la Gestión Integrada del Riesgo de Desastres for supporting this study.

## References

- BUCHHORN, M.; SMETS, B.; BERTELS, L.; ROO, B.D.; LESIV, M.; TSENDBAZAR, N.-E.; HEROLD, M.; FRITZ, S. 2022 Copernicus Global Land Service: Land Cover 100m: Collection 3: Epoch 2018: Globe 2020. Available online: <https://viewer.vito.be/2018> (accessed on 15th of April 2023).
- CONAF. 2023. *Situación nacional de incendios forestales*. <https://www.conaf.cl/situacion-nacional-de-incendios-forestales/>. Revised 20th May
- COPER, M. J. Análisis (CR) 2 - Meteorología extrema: uno de los factores tras los incendios de febrero 2023 en el centro-sur de Chile.
- ECHEVERRÍA, C.; NEWTON, A.C.; LARA, A.; BENAYAS, J.M.R.; COOMES, D.A. 2007 Impacts of Forest Fragmentation on Species Composition and Forest Structure in the Temperate Landscape of Southern Chile. *Glob. Ecol. Biogeogr.*, 16, 426-439.
- FIRMS. 2023 Global fire map <https://firms.modaps.eosdis.nasa.gov/> (accessed on 20<sup>th</sup> of May 2023)
- HERSBACH, H.; BELL, B.; BERRISFORD, P.; HIRAHARA, S.; HORÁNYI, A.; MUÑOZ-SABATER, J.; NICOLAS, J.; PEUBEY, C.; RADU, R.; SCHEPERS, D. 2020 The ERA5 Global Reanalysis. *Q. J. R. Meteorol. Soc.*, 146, 1999–2049.
- HORA, B., ALMONACID, F., & GONZÁLEZ-REYES, A. (2022). Unraveling the Differences in Landcover Patterns in High Mountains and Low Mountain Environments within the Valdivian Temperate Rainforest Biome in Chile. *Land*, 11(12), 2264.
- LARA, A.; SOLARI, M.E.; PRIETO, M.D.R.; PEÑA, 2012 M.P. Reconstrucción de La Cobertura de La Vegetación y Uso Del Suelo Hacia 1550 y Sus Cambios a 2007 En La Ecorregión de Los Bosques Valdivianos Lluviosos de Chile (35\_–43\_30' S). *Bosque Valdivia* 2012, 33, 13–23.
- LESIV, M.; SCHEPASCHENKO, D.; BUCHHORN, M.; SEE, L.; DÜRAUER, M.; GEORGIEVA, I.; JUNG, M.; HOFHANSL, F.; SCHULZE, K.; BILOUS, A.; ETAL 2022. Global Forest Management Data for 2015 at a 100 m Resolution. *Sci. Data* 9, 199
- MITTERMEIER, R.A.; TURNER, W.R.; LARSEN, F.W.; BROOKS, T.M.; GASCON, C. 2011 Global Biodiversity Conservation: The Critical Role of Hotspots. In *Biodiversity Hotspots: Distribution and Protection of Conservation Priority Areas*; Zachos, F.E., Habel, J.C., Eds.; Springer: Berlin/Heidelberg, Germany; pp. 3–22. ISBN 978-3-642-20992-5.
- PEÑA-FERNÁNDEZ, E., & VALENZUELA-PALMA, L. 2008. Incremento de los incendios forestales en bosques naturales y plantaciones forestales en Chile. In *Memorias del segundo simposio internacional sobre políticas, planificación y economía de los programas de protección contra incendios forestales: Una visión global* (pp. 595-612).
- SÁNCHEZ, R., BRIONES, M. J., GAMBOA, A., MONSALVE, R., BERROETA, D., & VALENZUELA, L. 2023. Delimitación de áreas quemadas en Chile a partir de umbrales dNBR ajustados según región y cubiertas del suelo. *Revista de Teledetección*, (61), 43-58.
- TECKLIN, D.; DELLASALA, D.A.; LUEBERT, F.; PLISCOFF, 2011 P. Valdivian Temperate Rainforests of Chile and Argentina. In *Temperate and Boreal Rainforests of the World: Ecology and Conservation*; Springer: Berlin/Heidelberg, Germany, 132–153.

# Unlocking the Potential: Bridging the Gap Between Remote Sensing Science and User Uptake in Environmental Applications. An Eastern Austrian Case Study

Anna Iglseider<sup>1</sup>, Christian Prochaska<sup>2</sup>, Lorenz Schimpl<sup>1</sup>, Nils Berger<sup>1</sup>, Hannes Hoffert-Hösl<sup>2</sup>, Michael Lechner<sup>3</sup>, Markus Immitzer<sup>3</sup>, Christine Rottenbacher<sup>4</sup>, Tanja Lumetsberger<sup>5</sup>, Christoph Bauerhansl<sup>6</sup>, Markus Hollaus<sup>1</sup>

<sup>1</sup> Research Group Photogrammetry, Department of Geodesy and Geoinformation, TU Wien, Vienna, Austria, [anna.iglseider@geo.tuwien.ac.at](mailto:anna.iglseider@geo.tuwien.ac.at),

<sup>2</sup> Georaum GmbH, St. Anton an der Jeßnitz, Austria

<sup>3</sup> University of Natural Resources and Life Sciences, Vienna (BOKU), Institute of Geomatics, Vienna, Austria,

<sup>4</sup> Center for Environmental Sensitivity, University for Continuing Education Krems, Austria,

<sup>5</sup> Department for Knowledge and Communication Management, University for Continuing Education Krems, Austria,

<sup>6</sup> Unit Remote Sensing, Austrian Research Centre for Forests, Vienna, Austria,

**Key words:** Natural Protection Areas, Data Fusion, Stakeholder Integration, Applied Remote Sensing Science, Habitat Mapping, Green Space Monitoring

The great potential to use remotely sensed data to address various questions of landscape ecology and vegetation monitoring has been shown in numerous studies. As highlighted in a recent review paper by FASSNACHT *et al.* (2023), remote sensing science frequently prioritizes specific data sources or methodological advancements over the significance and usability of the derived information, which is actually more critical for user acceptance. In reality, even applied research often fails to reach the stakeholder who could gain the greatest advantages if the outcomes are solely shared through scientific communication channels and developed methods and workflows are not matching with the practitioners needs.

In our ongoing project, we aim to address this very challenge. In collaboration with a regional consortium comprising project partners from universities, government agencies and an engineering and planning consultancy we are rearranging the project workflow to prioritize practitioners' needs at the beginning of the project. After identifying potentially interested stakeholders, we invited three regional management authorities of natural and cultural protection areas (Donau-Auen National Park, Vienna Woods Biosphere Reserve, World Heritage Site Wachau) and two city governments (Vienna and Krems in Lower Austria) to serve as associated stakeholders in our project. In initial workshops, the stakeholder's desires and needs regarding landscape monitoring, reporting obligations, and inventory assessments, particularly in the context of protected areas and sustainable development strategies, were collected. In addition, potential contributions of the stakeholders, especially in situ and reference data or personal expertise were identified. These workshops were followed by gathering available remote sensing data, including airborne laser scanning (ALS), multispectral orthophotos, point clouds from digital aerial photogrammetry (DAP) as well as Sentinel-1 (S1) and Sentinel-2 (S2) data on a multitemporal level. Based on the insights gained from stakeholder discussions and data analysis, applied use cases were extracted that appeared realistic in terms of their implementation into the stakeholders' professional routines. An overview of the selected use cases is shown in Figure 5.

The exploration and the analysis of the use cases are subject of ongoing research. Therefore, a wide methodological toolbox including pixel- and segment-based machine learning, expert-based classification approaches or point cloud structure analysis is considered. Results of a preliminary feasibility study show e.g. potential for training machine learning models on a combination of ALS and multitemporal Sentinel data for classification and monitoring of Natura 2000 forest and grassland habitats (IGLSEIDER *et al.*, 2023) or establishing an expert-based classification approach based on a combination of ALS and DAP data for detailed green roof monitoring in cities.

The presentation will reflect the process of stakeholder engagement, present the application fields of interest for the stakeholders, the feasibility discussion within the project consortium and first results how to approach the selected use cases.

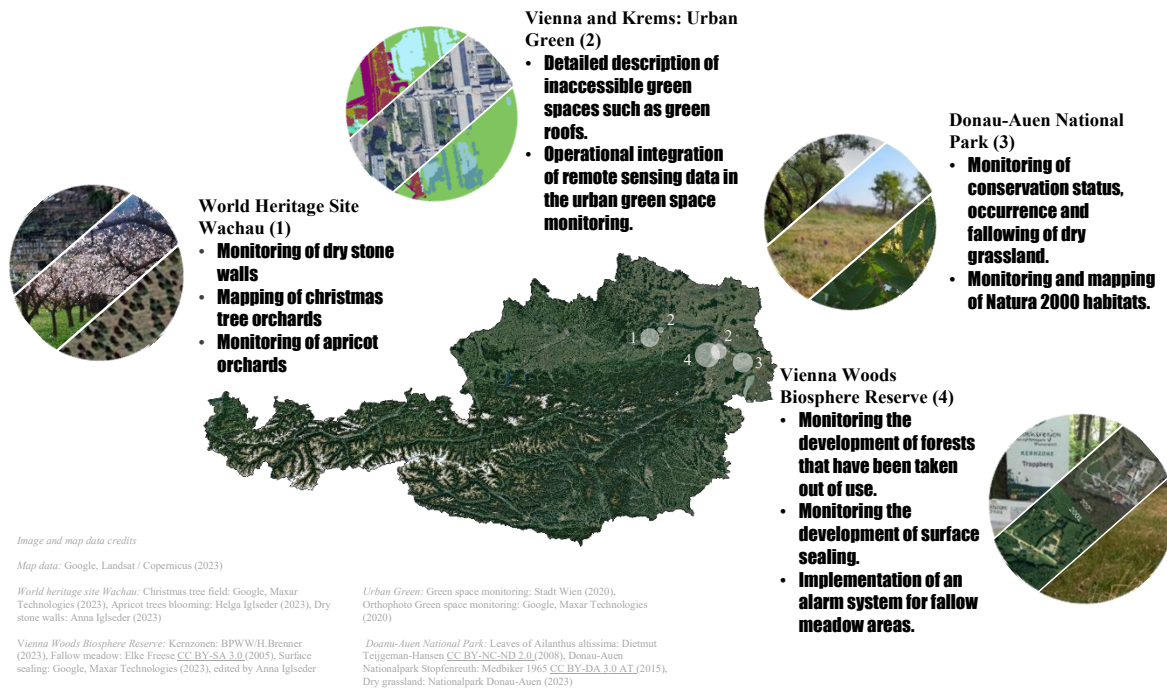


Figure 5: Study cases for integration of remote sensing based approaches in applied monitoring concepts

## References

- FASSNACHT, F.E., WHITE, J.C., WULDER, M.A. & NÆSSET, E., 2023. Remote sensing in forestry: current challenges, considerations and directions. *Forestry: An International Journal of Forest Research*, cpad024. <https://doi.org/10.1093/forestry/cpad024>
- IGLSEDER, A., IMMIZER, M., DOSTÁLOVÁ, A., KASPER, A., PFEIFER, N., BAUERHANSL, C., SCHÖTTL, S. & HOLLAUS, M., 2023. The potential of combining satellite and airborne remote sensing data for habitat classification and monitoring in forest landscapes. *International Journal of Applied Earth Observation and Geoinformation*, 117: 103131. <https://doi.org/10.1016/j.jag.2022.103131>

## Mapping Wildfire Scores – NDVI vs. NBR vs. AFRI

Arnon Karnieli<sup>1\*</sup> & Manuel Salvoldi<sup>1</sup>

<sup>1</sup> *The Remote Sensing Laboratory, Institutes for Desert Research, Ben Gurion University of the Negev, karnieli@bgu.ac.il, salvoldi@post.bgu.ac.il*

**Keywords:** *Burn severity; Change detection; Sentinel-2, Multi-temporal.*

In recent years, wildfires have become serious human and environmental concerns for several reasons. Most importantly, they threaten human life, flora, and fauna, as well as properties and economic losses. Wildfires are considered one of the worst ecological disturbances to long-term records of vegetation phenology, since land-cover alterations are the basis for understanding the biological responses to climate change, such as impacting carbon emissions, at regional to continental scales. The effect of wildfires on biodiversity, plant reproduction, forest succession, habitat quality, hydrologic regimes, and soil characteristics, such as nutrient cycling, is also worth mentioning. For all the reasons mentioned above, different technologies have been developed for detecting and monitoring various aspects of wildfire, including risk assessment, active fire detection, gas and aerosol emission, smoke penetration, and temporal dynamics of burned areas. Among all technologies, there is a general agreement that remote sensing techniques are essential for providing valuable data for detecting, monitoring, interpreting, and responding to wildfires from local to global scales. The current project strives to develop and use an advanced Earth observation approach for accurate post-fire spatial and temporal assessment shortly after fire events while eliminating the influence of biomass-burning smoke on the ground signal. The Aerosol-Free Vegetation Index (AFRI), Eq. 1, which has a meaningful advantage in penetrating an opaque atmosphere influenced by biomass-burning smoke, was used to fulfill this goal (Karnieli et al. 2001; Salvoldi et al. 2020). The relative difference AFRI (RdAFRI), Eq. 2, set of algorithms was implemented at the same procedure commonly used with the Relative difference Normalized Burn Ratio (RdBRN). Similar to the NBR, the Aerosol-Free Vegetation Index (AFRI) is also based on the correlation between the visible-red and the SWIR2 band:

$$AFRI = (\rho_{NIR} - 0.5\rho_{SWIR2}) / (\rho_{NIR} + 0.5\rho_{SWIR2}) \quad (1)$$

where  $\rho$  is the reflectance value of the indicated spectral band – NIR, and SWIR2 (around 2.1  $\mu\text{m}$ ).

The study was conducted nine months when Israel experienced massive pyro-terrorism attacks of more than 1100 fires from the Gaza Strip. 25 Sentinel-2 Level-2A products were selected with cloud coverage inferior to 15% from 6 April 2018 to 22 December 2018, in order to monitor the study area during the kite and balloon attacks period. The NIR band (B8) and the SWIR2 (B12), at 10 and 20 m spatial resolution, respectively, were used to calculate the relevant spectral indices.

Similar to the procedures developed for the NBR-based set of algorithms, the most intuitive burned area-mapping indicator consists of an absolute change detection methodology obtained by subtracting a post-fire AFRI image from a pre-fire AFRI image to derive the difference AFRI (dAFRI):

$$dAFRI = AFRI_{t_0} - AFRI_{t_1} \quad (2)$$

Then, the dAFRI, for two successive images collected in this study, can be formulated as:

$$dAFRI(i-1, i) = AFRI(i-1) - AFRI(i), \quad \text{with } i = 2, \dots, 25 \quad (3)$$

where (i) indicates the i-th image in the database. The dAFRI(i-1, i) can present problems in the cases with low vegetation values for the image taken at (i-1): the absolute change will be small, and the index will not be able to detect the burned area. In order to avoid this issue, the relative differenced AFRI (RdAFRI) was defined as:

$$RdAFRI(i-1, i) = \frac{dAFRI(i-1, i)}{\sqrt{|AFRI(i-1)|} / 1000} \quad (4)$$

Positive RdAFRI(i-1, i) values represent a decrease in vegetation cover, while negative values represent an increase in vegetation cover.

For comparing the performance of the NBR, NDVI, and AFRI indices, a section of the S2 Level-2A image obtained on 10 July 2018, is presented in Fig. 1.

The transects represent a common situation when smoke, at different intensities, covers a variety of substrates—cultivated, bare soils, fire scars, and more. The true-color composite image ( $RGB = 0.665, 0.56, 0.49 \mu\text{m}$ ) shows the open fire (light-orange hue), the biomass burning smoke (white hue), as well as burned scars that are a few days old (dark surfaces). The three indices were produced at 10-m spatial resolution, according to Equations (1), (2), and (5), from the surface reflectance values along a cross-section of 2771 m (Figure 6, line A-A). This line was selected since it passes cultivated fields, bare soil, and was overcast by light smoke that characterized the entire region along the whole study period. This line is subdivided into several segments. From pixel 0 to 50 (and similarly from pixel 180 to 190) over the agricultural field where no smoke exists, the AFRI values accurately mimic those of the NDVI, but the NBR values are significantly lower. From pixel 50 to 180, over the bare soil, AFRI values are somehow higher than those of the NDVI. However, the NBR values are negative and much lower. From pixel 180 to 318, under the smoke, the AFRI values of the crops remain at the same high level as in the smoke-clear section, while both the NDVI and NBR produce low values.

While validating with ground observations, the RdAFRI-based algorithms produced an overall accuracy of 87% against the 80% obtained by the RdNBR-based algorithm. Furthermore, the RdAFRI maps were smoother than the equivalent RdNBR, with noise levels two orders of magnitude lower than the latter (Fig. 2). However, due to different cloud covers on the two consecutive dates, an automatic determination of a threshold level was not possible. Therefore, two threshold levels were considered through visual inspection and manually assigned to each imaging date.

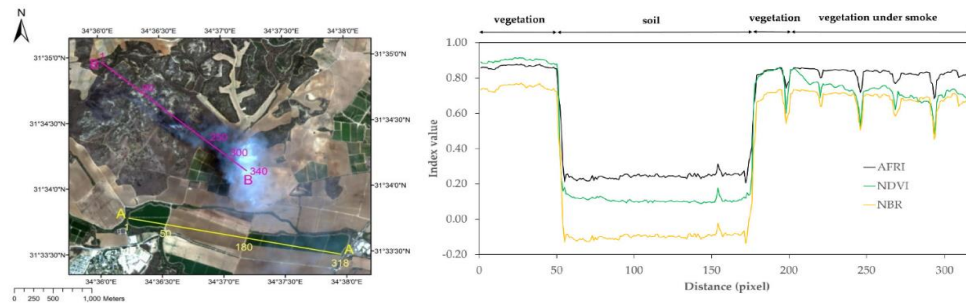
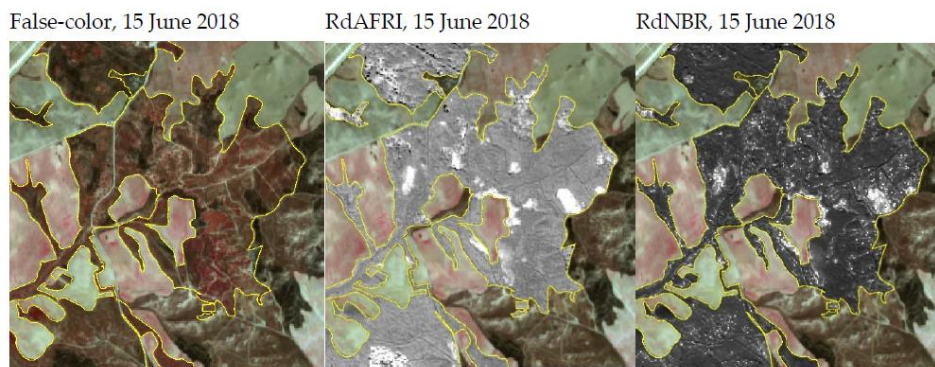


Figure 1: (a) A true-color ( $RGB = 0.665, 0.56, 0.49 \mu\text{m}$ ) daily surface reflectance image of the Israeli territory on 10 July 2018. The open fire appears in a light-orange hue, the burn scars are dark, and the smoke is a white hue; (b) AFRI, Normalized Difference Vegetation Index (NDVI), and Normalized Burn Ratio (NBR) values along a cross-section on 10 July 2018. The x-axis numbers represent the pixels' distance along line A-A in accordance with Figure 1(a).

Figure 3: False-color image with the corresponding RdAFRI and RdNBR images.



## References

- Karnieli, A., Kaufman, Y.J., Remer, L., & Wald, A. (2001). AFRI - aerosol free vegetation index. *Remote Sensing of Environment*, 77, 10-21
- Salvoldi, M., Siaki, G., Sprintsin, M., & Karnieli, A. (2020). Burned Area Mapping Using Multi-Temporal Sentinel-2 Data by Applying the Relative Differenced Aerosol-Free Vegetation Index (RdAFRI). *Remote Sensing*, 12

# Extending QGIS towards collaborative analysis and interpretation of geospatial data

Sebastian Mikolka-Flöry<sup>1\*</sup>, Norbert Pfeifer<sup>1</sup>

<sup>1</sup> TU Wien, Department of Geodesy and Geoinformation, Research Unit Photogrammetry,  
*sebastian.floery@geo.tuwien.ac.at*

**Keywords:** *collaborative, spatial analysis, QGIS, virtual meetings*

The last few years have had drastic impacts on our personal and working lives, especially on the way we communicated and interacted with each other. With the sudden measures to limit social contacts, everyone was forced to find ways to communicate and interact virtually. While common tasks (e.g. meetings) could easily be held virtually using existing tools, these proved to be insufficient for various tasks but especially when working with geospatial data.

To collaboratively analyze, discuss and interpret geospatial data within virtual meetings, the screen of one participant, showing relevant datasets in e.g. QGIS, is typically shared. However, as only this person can directly interact with the data, all others are only passive participants which cannot directly control what is displayed. In many cases this situation leads to more confusion for everyone involved than to an improvement of the situation: “Could you show that previous screen section again? You mean that structure on the left, that one? No, the other one where your mouse was before. No no no, I meant the other one. If you zoom out a little bit, I can show it to you. Oh no, that was too much.” Does this appear familiar?

As virtual meetings have become an integral part of everyone’s working life by now, there exists an urgent need to overcome these problematics. Based on our experiences with using QGIS in virtual meetings, we investigated how collaborative elements can be integrated to improve the way we collaboratively discuss and analyze geospatial data within virtual meetings. Hence, we developed a small QGIS plugin building upon Socket.IO, which enables real-time communication between clients and a server. This allows us to integrate collaborative elements like synchronized screens, sharing one’s current view, showing the mouse cursor of all participants and real time annotations within QGIS.

While still experimental and hence, not yet publicly released, our approach already shows that the experience of collaboratively analyzing geospatial data within virtual meetings can be significantly improved. Furthermore, overcoming the purely passive form of interaction among participants leverages the effectiveness of such meetings. Hence, we believe that the developed plugin is a major step towards the collaborative interpretation and analysis of geospatial data within virtual meetings.

# Mobile mapping and GeoSLAM for the characterisation and modelling of karst morphologies at the conduit scale

Tanguy Racine<sup>1\*</sup>, Celia Trunz<sup>1</sup>, Julien Straubhaar<sup>1</sup>, Philippe Renard<sup>1</sup>

<sup>1</sup> University of Neuchâtel, 11 Rue Emile Argand, 2000 Neuchâtel, Switzerland, [tanguy.racine@unine.ch](mailto:tanguy.racine@unine.ch)

**Key words:** karst, SLAM, cave mapping, hydrogeology

Predicting contaminant and solute transport, forecasting floods and modelling speleogenetic stages are key questions of karst hydrogeology for which some theoretical foundations are still missing. In karst hydrological models, cave passages are treated as tubular segments in which turbulent fluid transport is approximated using the Darcy-Weisbach formula (BROWN, 2002).

However karstic cave systems have highly variable geometry and rugosity at the conduit scale, ranging from smooth passages with circular or elliptical cross-sections in the (epi-) phreatic zone, key-hole shaped canyons in the vadose zone, to much more complex anastomotic mazes, or passages whose morphology is overprinted by collapse or sedimentary fill. Each of these types of passages is characterised by multi-scale roughness which may not be accounted for by a single parameter e.g., normalized rugosity from the Colebrook-White formula. The solutional morphology of cave conduits chiefly depends on the distance to base-level and hence the speleogenetic process, the type of bedrock or the presence and orientation of fractures or bedding planes (DE WAELE & GUTIÉRREZ, 2022). There is thus a need to infer physical laws at the conduit scale across the wide spectrum of actual cave conduits.

To achieve this, mapping of relevant cave morphology is carried out at test in caves in Switzerland and Slovenia. Cave surveys are performed using a handheld mobile-mapping device and the Simultaneous Localisation and Mapping (SLAM) algorithm (SMITH & CHEESEMAN, 1986), allowing dense point clouds and triangulated surfaces representing the cave walls to be reconstructed.

We present the result of preliminary conduit mapping in different hydrogeological settings. We characterise a set of triangulated 3D surfaces, targeting a suite of typical conduit geometries, ranging from phreatic to vadose, to account for the complexity of speleogenetic process.

**Acknowledgements:** This research is funded by the ERC Project 101071836 — KARST.

## References

- BROWN, G. O. (2002). The history of the Darcy-Weisbach equation for pipe flow resistance. In *Environmental and water resources history* (pp. 34-43).
- DE WAELE, J., & GUTIÉRREZ, F. (2022). *Karst hydrogeology, geomorphology and caves*. John Wiley & Sons.
- SMITH, R. C., & CHEESEMAN, P. (1986). On the representation and estimation of spatial uncertainty. *The international journal of Robotics Research*, 5(4), 56-68.

## High-resolution aerial imagery for early detection of climate-induced natural hazards at a mountain range scale

Natalie Barbosa<sup>1,2\*</sup>, Juilson Jubanski<sup>3</sup>, Ulrich Münzer<sup>4</sup>, Florian Siegert<sup>1,3</sup>

<sup>1</sup> Department of Earth and Environmental Sciences, Faculty of Earth Sciences, GeoBio Center, Ludwig-Maximilians-University, Munich, 80333, Germany, [barbosa@biologie.uni-muenchen.de](mailto:barbosa@biologie.uni-muenchen.de)

<sup>2</sup> Chair of Landslide Research, Technical University of Munich, Munich, 80333, Germany

<sup>3</sup> 3D RealityMaps GmbH, Munich, 81673, Germany

<sup>4</sup> Department of Earth and Environmental Sciences, Section Geology, Ludwig-Maximilians-University, Munich, 80333, Germany.

**Key words:** High resolution aerial imagery, topographic change detection, climate induced natural hazards.

The rise in temperatures and rainfall due to climate change is expected to lead to higher rates and magnitudes of geomorphic processes. To better understand these changes, our study used high-resolution aerial imagery to analyse spatiotemporal patterns of topographic changes across the Zillertal Alps, a mountain range on the border of Austria and Italy.

With rugged, rocky terrain, numerous peaks, and deep valleys with intense glaciation above 2,500m, the Zillertal Alps have experienced a significant decline in glacier extent over time. Currently, the glacier extent represents less than 40% of their LIA glacier extent (FISCHER *et al.*, 2015), and associated natural hazards and cascading processes are of societal concern.

Our study generated five digital surface models (DSMs) using photogrammetric reconstruction from aerial imagery acquired by BEV (Bundesamt für Eich- und Vermessungswesen) and made available via TIRIS (Tiroler Rauminformationssystem) over an area of 810 km<sup>2</sup> with a spatial resolution of 20 cm. We identified 70 'hotspots' where geomorphic changes exceed a 10 m elevation difference in the last decade (2010-2019). These hotspots indicate areas of potentially increased natural hazards due to glacier retreat and moraine instability, sediment transport, landslides, debris flows and rockfalls, rock glaciers, and debris cover glaciers. A generalization of the location of these hotspots is presented in Figure 1.

To better understand the spatiotemporal evolution of relevant processes, we analysed time series of geomorphic change with a temporal resolution of 3 years (2010-2013, 2013-2016, 2016-2019, 2019-2022). This analysis allowed us to better constrain the temporal evolution of natural hazards and cascading processes, providing insights into the complex morphodynamics in alpine catchments and their relation to climate. For example, Figure 2 exemplifies a multiple pulses debris flow at the Mörchnerkar (schwarzensteinkes glacier catchment) initiated in 2013 that eroded a total of 249,911 m<sup>3</sup> and deposited 206,799 m<sup>3</sup> modifying the river morphology and dynamic.

Overall, the results achieved as part of the AlpSenseRely project - Alpine remote sensing of climate-induced natural hazards, provide a valuable understanding of the impact of rapid climate change on Alpine environments. High-resolution spatial and temporal photogrammetry allowed us to identify areas of potentially increased natural hazards at a mountain range scale and understand the spatiotemporal evolution of earth surface processes in the context of a rainier and warmer climate. Such understanding is critical for the sustainable development of high-alpine regions.

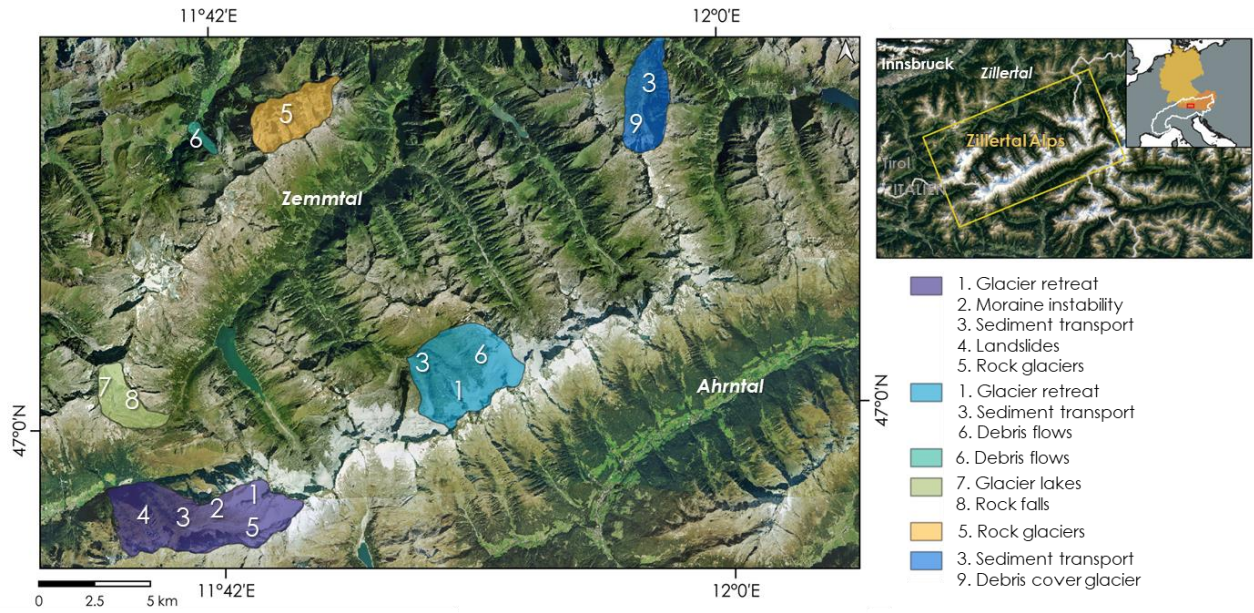


Figure 1: Areas of potential increased future natural hazard at the Zillertal mountain range.

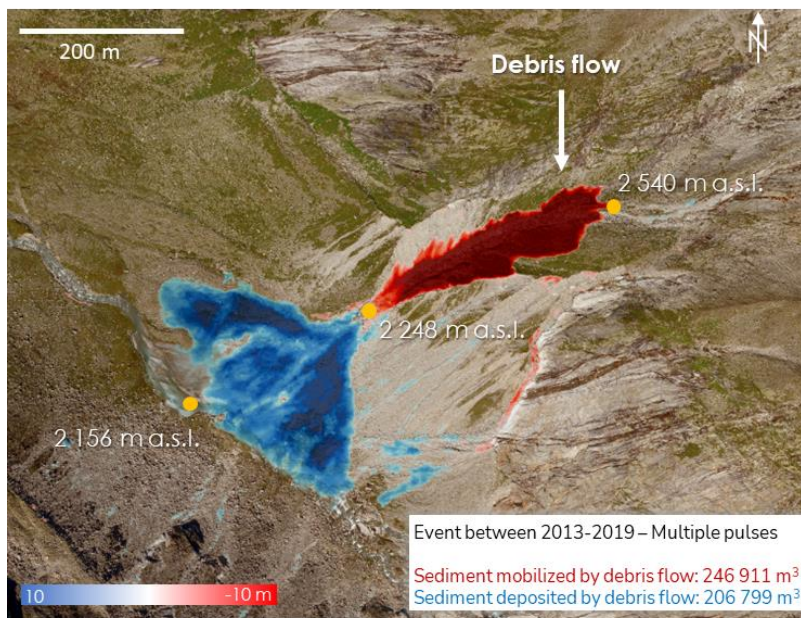


Figure 2. Spatio-temporal evolution of relevant natural hazards. Debris flow at the Mörchnerkar, schwarzensteinkees glacier catchment.

**Acknowledgements:** We thank the Bavarian Ministry of Environment and Consumer Protection for the funding of the project ‘AlpSenseRely’ (Teilprojekt LMU TUSO1UFS-77318), to Land Tyrol for the open sharing of the aerial imagery and to the colleagues at 3D RealityMaps GmbH, Munich for the outstanding support with the implementation of the 3D models used for visualization, visual interpretation, and figures.

## References

FISCHER, A., SEISER, B., STOCKER WALDHUBER, M., MITTERER, C., & ABERMANN, J., 2015. Tracing glacier changes in Austria from the Little Ice Age to the present using a lidar-based high-resolution glacier inventory in Austria. *The Cryosphere*, 9: 753-766.

**Session 6 – Recent Developments in Geomorphic Process and Hazard Monitoring**



**SESSION 6**  
**RECENT DEVELOPMENTS**  
**IN GEOMORPHIC**  
**PROCESS AND HAZARD**  
**MONITORING**

## From measured radar LOS displacement to real displacement: Case study of Cima del Simano (Switzerland)

Charlotte Wolff<sup>1</sup>, Tiggi Choanji<sup>1</sup>, Marc-Henri Derron<sup>1</sup>, Li Fei<sup>1</sup>, Amalia Guttirez<sup>1</sup>, Michel Jaboyedoff<sup>1</sup>, Andrea Pedrazzini<sup>2</sup>, Carlo Rivolta<sup>3</sup>

<sup>1</sup>ISTE - University of Lausanne, Lausanne, Switzerland, (charlotte.wolff@unil.ch)

<sup>2</sup>Sezione forestale- Repubblica e Cantone Ticino, Bellinzona, Switzerland

<sup>3</sup>Ellegi Srl - operational and administrative headquarters, Milano, Italy

**Key words:** Rockslide, InSAR, LOS displacement, failure scenarios, SLBL

The satellite (Interferometric Synthetic Aperture Radar) InSAR monitoring technique is a very convenient and non-intrusive technique to assess large extent and low movements areas such as those occurring during subsidences, pre-irruption volcano activities or deep-seated landslides or rockslides. This technique can help delimitating the unstable surface where displacements occur. In the case of deep-seated instabilities, once the moving area is defined, scenarios of failure, defined by an extent, a volume and a potential mechanism, can be suggested. If the failure mechanism is a wedge sliding, the discontinuity sets forming the wedge are determined with an analysis of the Lidar DEM with COLTOP and the volume of the sliding compartment rebuild in Cloud Compare\* (Jaboyedoff et al., 2019). In the case of a rotational sliding, the volume and the base level of the instability are calculated with the SLBL\* algorithm (Jaboyedoff et al., 2020).

Thus, it is possible to make assumptions on the sliding direction, for both sliding mechanisms:

- (1) Wedge sliding: it corresponds to the intersection line of the two planes forming the wedge,
- (2) Rotational sliding: the dip and dip direction of the local base provide information on the sliding direction.

One of the main disadvantages of the InSAR technique is that the measure of displacement is only given in one direction: along the Line Of Sight (LOS) of the radar device. To calculate the real displacement, at least three radar acquisitions along three non-colinear LOS are mandatory; for example, one Ground-Based InSAR acquisition and two satellite InSAR acquisitions, one with an ascending orbit and one with a descending orbit.

However, a displacement along a single LOS is sufficient if an assumption on the direction of the movement is made. Therefore, the LOS displacement vector can be reprojected onto the real displacement vector. This corresponds to applying the following equation:

$$\overrightarrow{Displacement}_{Real} = \overrightarrow{Displacement}_{LOS} \cdot \overrightarrow{Displacement}_{unit\_Real} \quad (1)$$

With

- $\overrightarrow{Displacement}_{LOS}$  the vector of real displacement (known from InSAR acquisition),
- $\overrightarrow{Displacement}_{unit\_Real}$  the vector of displacement along the LOS (from the assumption held),
- $\overrightarrow{Displacement}_{Real}$  the unit vector of real displacement.

This method was used to study the movements at the Cima del Simano instability (Ticino, Switzerland). The latter, at an altitude of 2500m, is characterized by one main opened crack and several smaller active fractures. Cima del Simano is monitored by satellite and GB-InSAR since 2021 and displacements along the radar LOS of about 1cm/year have been measured. Based on the observed movements, the topography and the discontinuity sets, scenarios of failure were proposed and their sliding direction defined (Figures 1 and 2). The equation 1 was applied to the displacement measured along GB- and satellite InSAR LOS to better assess the activity of the instability.

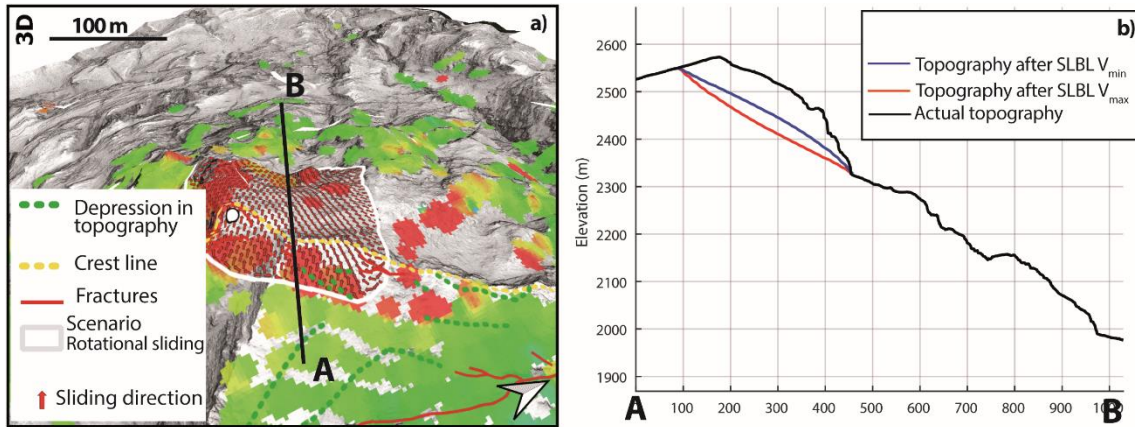


Figure 1: Failure scenario proposed in the case of a rotational sliding defined by SLBL. (a) Delimitation of the scenario and sliding direction (b) Profile of the sliding base level

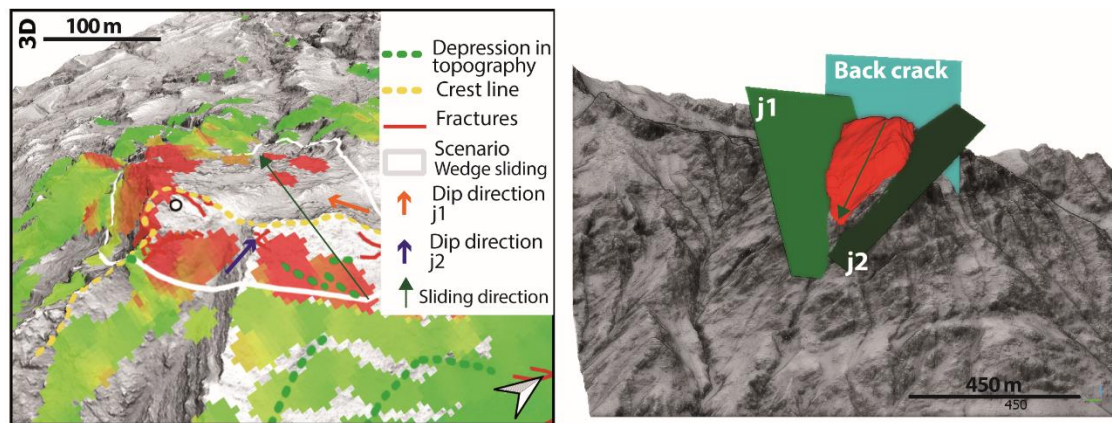


Figure 2: Failure scenario proposed in the case of a wedge sliding structurally constrained by two joint sets  $j_1$  and  $j_2$ . (a) Delimitation of the scenario (b) Planes delimitating the sliding volumes, constructed in Cloud Compare

## References

JABOYEDOFF, M., GUERIN, A., NOËL, F., FEI, L., DERRON, M.H., TROILO F., BERTOLO D., THUEGAZ D., 2019. Structural and hazard assessment of the Brenva rockslide scar (Mont-Blanc massif, Aosta Valley, Italy)

JABOYEDOFF, M., CARREA, D., DERRON, M.H., OPPIKIFER, T., PENNA, I.M., RUDAZ, B., 2020. A Review of Methods Used to Estimate Initial Landslide Failure Surface Depths and Volumes, *Engineering Geology*, 267.

## High Spatial Resolution method for 3D Landslide Monitoring by feature tracking and histogram analyses using point clouds

Kourosh Hosseini<sup>1\*</sup>, Christoph Holst<sup>2</sup>

<sup>1</sup> *2 Technical University of Munich (TUM), TUM School of Engineering and Design, Chair of Engineering Geodesy, Arcisstraße 21, 80333 Munich, k.hosseini@tum.de*

<sup>2</sup> *Technical University of Munich (TUM), TUM School of Engineering and Design, Chair of Engineering Geodesy, Arcisstraße 21, 80333 Munich*

**Key words:** *Landslide, Feature tracking, Histogram analyses*

Landslides represent a significant natural hazard that is observed across various geographical locations worldwide, with potential impacts that include damage to infrastructure and property, as well as threats to human life. According to the World Health Organization, between 1998 and 2017, landslides affect an estimated 4.8 million people and cause more than 18000 deaths. Due to the potential severity of these events, extensive research has been undertaken to better understand the occurrence and underlying mechanisms of landslides. One of the most crucial areas of investigation relates to the prediction of landslides, which seeks to provide timely and accurate warnings of impending events to minimize damage and loss of life. Achieving a landslide prediction system with high spatial resolution requires the effective detection of landslides through advanced methods. There are several methods for monitoring landslides which were discussed in [Angeli MG et al, 2000]. Recently, feature-based methods have been proposed to provide the required high spatial resolution. Compared to other pointwise and point-cloud-based methods, the advantages of using this method have been investigated in [C. Holst et al, 2021]. In this study, some of the shortcomings of this method are discussed, and the following goals are pursued:

1. Reducing the errors caused by the matching process, especially in the border sections of the point cloud, by histogram analysis.
2. Maintaining proper distribution of vectors throughout the study areas
3. Using various data to check the performance of the presented method more precisely. These data sets are different in terms of size, type of deformation, density of point clouds and direction of displacement.
4. Evaluation of the accuracy of the presented method using the available data

However, one of the key challenges associated with these methods is the high number of outliers produced during the matching algorithm, which can lead to reduced efficiency and increased computational complexity. To address this challenge, this research presents a novel approach for high spatial resolution landslide detection that involves the removal of outliers. This is accomplished through the application of histogram analysis on the displacement arrows, which enables the identification and removal of outliers (Figure 1).

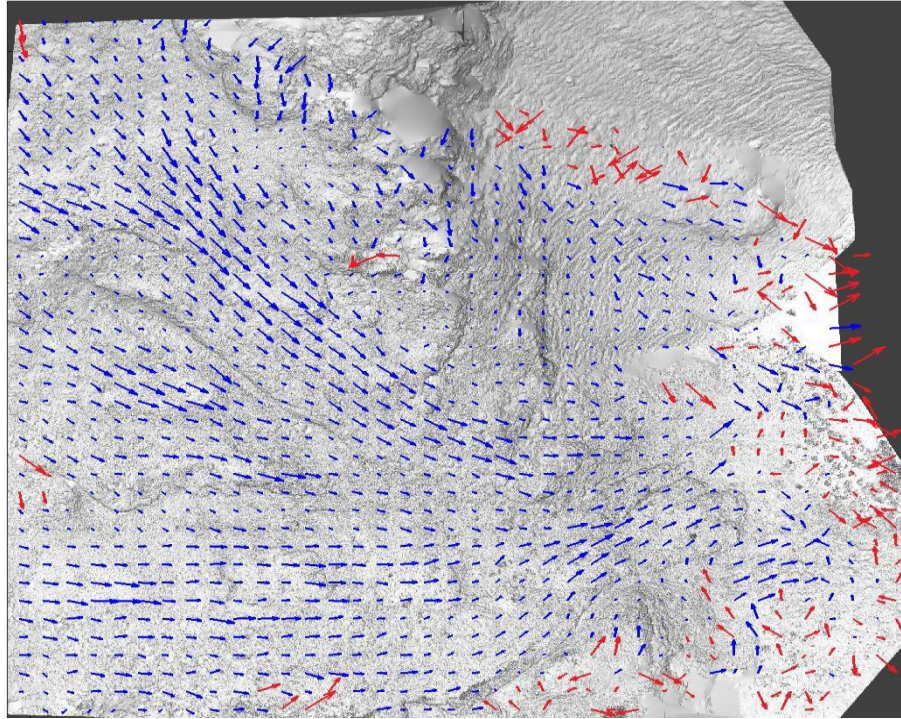


Figure 1: The red arrows indicate the displacements that are considered outliers based on histogram analysis.

The proposed method has been tested on three different datasets in several terms including size, texture, and collection quality. These data sets were collected by RTC360 and P50 laser scanners. The results demonstrate that the removal of outliers does not compromise the distribution of displacement arrows and improve the accuracy of detecting landslide behaviors. Finally, the presented approach represents an effective method for achieving high spatial resolution landslide detection, while also minimizing computational complexity and improving efficiency.

## References

- ANGELI, M.G., PASUTO, A. AND SILVANO, S., 2000. A CRITICAL REVIEW OF LANDSLIDE MONITORING EXPERIENCES. *ENGINEERING GEOLOGY*, 55(3), PP.133-147.
- HOLST, C., JANßEN, J., SCHMITZ, B., BLOME, M., DERCKES, M., SCHOCH-BAUMANN, A., BLÖTHE, J., SCHROTT, L., KUHLMANN, H. AND MEDIC, T., 2021. INCREASING SPATIO-TEMPORAL RESOLUTION FOR MONITORING ALPINE SOLIFLUCTION USING TERRESTRIAL LASER SCANNERS AND 3D VECTOR FIELDS. *REMOTE SENSING*, 13(6), P.1192.

## Multi-method monitoring of a failing rock face, Swiss Alps

Hanne Hendrickx <sup>1\*</sup>, Gaëlle Le Roy <sup>2</sup>, Agnès Helmstetter <sup>3</sup>, Eric Pointner <sup>4</sup>, Eric Larose <sup>5</sup>,  
Luc Braillard <sup>6</sup>, Jan Nyssen <sup>7</sup>, Reynald Delaloye <sup>8</sup>, Amaury Frankl <sup>9</sup>

<sup>1</sup> *Institute of Photogrammetry and Remote Sensing, Technische Universität Dresden, Dresden, Germany  
(hanne.hendrickx@tu-dresden.de)*

<sup>2</sup> *Univ. Grenoble Alpes, Univ. Savoie Mont Blanc, CNRS, IRD, Univ. Gustave Eiffel, ISTERre, Grenoble,  
France / Géolithe, Crolles, France (gaelle.le-roy@univ-grenoble-alpes.fr)*

<sup>3</sup> *Univ. Grenoble Alpes, Univ. Savoie Mont Blanc, CNRS, IRD, Univ. Gustave Eiffel, ISTERre, Grenoble,  
France (agnes.helmstetter@univ-grenoble-alpes.fr)*

<sup>4</sup> *Rovina & Partner AG, Visp, Switzerland (eric.pointner@rpgeol.ch)*

<sup>5</sup> *Univ. Grenoble Alpes, Univ. Savoie Mont Blanc, CNRS, IRD, Univ. Gustave Eiffel, ISTERre, Grenoble,  
France (eric.larose@univ-grenoble-alpes.fr)*

<sup>6</sup> *Department of Geosciences, University of Fribourg, Switzerland (luc.braillard@unifr.ch)*

<sup>7</sup> *Department of Geography, Ghent University, Belgium (jan.nyssen@ugent.be)*

<sup>8</sup> *Department of Geosciences, University of Fribourg, Switzerland (reynald.delaloye@unifr.ch)*

<sup>9</sup> *Department of Geography, Ghent University, Belgium (amaury.frankl@ugent.be)*

**Key words:** *Terrestrial laser scanner, time-lapse camera, photogrammetry, seismology, structural predisposition, rockfall*

Rockfall, a significant geomorphic process in cold-climate high mountains, is influenced by lithology and geological structure orientation. However, the impact of climate change on precipitation and temperature is anticipated to modify the frequency and scale of rockfall incidents. Rising temperatures lead to weakened ice-filled joints, contributing to the escalation of rockfall events. In the European Alps, permafrost degradation has been linked to a rise in rockfall incidents over the past three decades (FISCHER ET AL., 2011), posing a threat to nearby communities.

Studying rockfall in these environments is challenging due to the inaccessibility of mountain ridges and the complex interaction between controlling factors. In order to enhance our comprehension of rockfall incidents and their underlying conditions, we conducted a four-year monitoring study at the Grosse Grabe rock face (2700 m above sea level, Fig. 1) in the Mattertal region of the Western Swiss Alps, spanning from 2017 to 2021 (HENDRICKX ET AL., 2022). Due to the challenging accessibility of the study site, we employed a combination of various close-range remote sensing techniques to analyse morphological and morphometric changes. The monitoring initiative was initiated in 2011 with the installation of a fixed automatic camera, originally intended for monitoring nearby rock glaciers. Notably, this dataset is exceptional as data collection commenced prior to any significant rockfall occurrence. Following the detection of the initial rockfall activity during the observation period, more detailed surveys were conducted using Terrestrial Laser Scanning (TLS) and Uncrewed Aerial Vehicles (UAVs). This enabled us to quantify pre-failure displacement (Fig. 2), determine rockfall locations, and estimate volumes. By utilising seismic data obtained from a nearby rock glacier study site, we were able to establish a comprehensive dataset encompassing all individual rockfall events, including precise timing and estimated volumes.

By integrating multiple techniques, we overcame limitations related to sensor capabilities and monitoring intervals, achieving a high level of temporal and spatial resolution in monitoring rockfall incidents. This integration of diverse datasets provided us with multiple lines of evidence, enhancing the robustness of our findings. Consequently, the collected high-resolution rockfall record offers unprecedented detail on short-term rock wall destabilisation, contributing to our understanding of high mountain geomorphology in a changing climate. Ongoing monitoring at the site reveals preliminary results from 2022 and 2023, which strongly suggest a high likelihood of future rockfall events (Fig. 2).

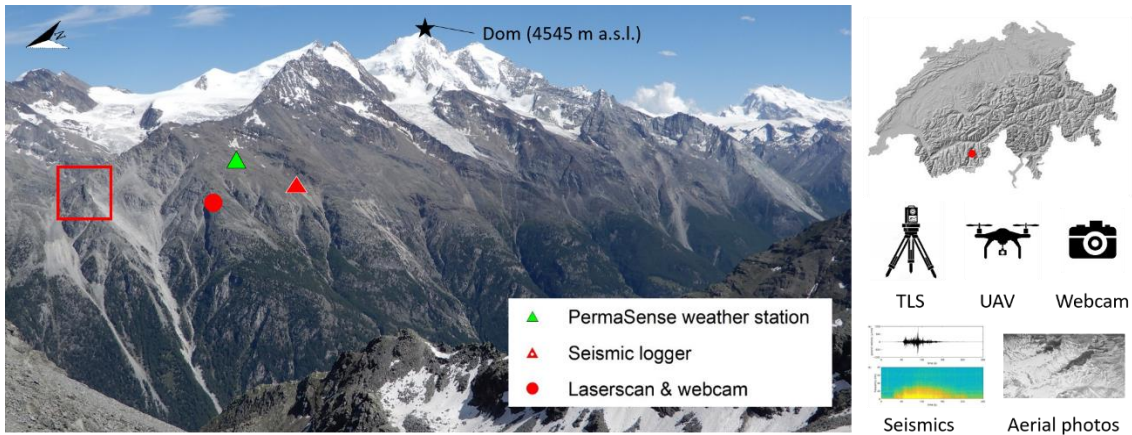


Figure 1: The study site of Grosse Grabe in the Matter valley (Western Swiss Alps) and the multi-method monitoring strategy.

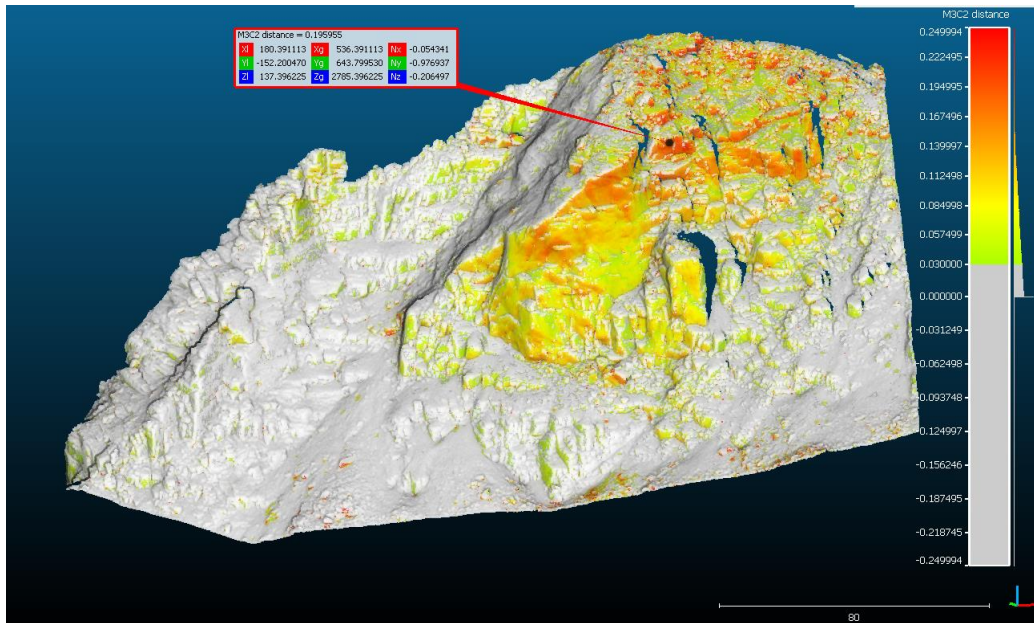


Figure 2: Displacements of the rock face in the summer of 2022, reaching up to 20 cm, as measured by differencing two consecutive laser scans at the beginning and end of the summer.

**Acknowledgements:** The following organisations provided funding for this study: ANR LabCom GEO3iLab; Municipality of St. Niklaus (VS); FWO Flanders, Grant/Award Numbers: V4.248.19 N, V4.253.18 N, V4.321.17 N°

## References

FISCHER, L. ET AL. (2011) 'Monitoring topographic changes in a periglacial high-mountain face using high-resolution DTMs, Monte Rosa East Face, Italian Alps', *Permafrost and Periglacial Processes*. John Wiley & Sons, Ltd, 22(2), pp. 140–152. doi: 10.1002/ppp.717.

HENDRICKX, H. ET AL. (2022) 'Timing, volume and precursory indicators of rock- and cliff fall on a permafrost mountain ridge (Mattertal, Switzerland)', *Earth Surface Processes and Landforms*, 47(6), pp. 1532–1549. doi: 10.1002/esp.5333.

## Geological Monitoring processes with small laser scanners. Examples in Montserrat, Puigcerçós, Croscat volcano (Catalonia, Spain) and analogic models

Garcia-Sellés, D.<sup>1\*</sup>, Guinau, M.<sup>1</sup>, Eras, M.<sup>1</sup>, Montesinos, P.<sup>1</sup>, Ramos, M.<sup>2</sup>, Ferrer, O.<sup>2</sup>

<sup>1</sup> *Departament de Dinàmica de la Terra I de l'Oceà, GRC RISKMAT, UB-Geomodels, Facultat de Ciències de la Terra, Universitat de Barcelona (UB). 08028 Barcelona, Spain [dgarcia@ub.edu](mailto:dgarcia@ub.edu), [mguinau@ub.edu](mailto:mguinau@ub.edu)*

<sup>2</sup> *Departament de dinàmica de la Terra I de l'Oceà, Grup de Geodinàmica I Anàlisi de Conques (GGAC), UB-Geomodels, Facultat de Ciències de la Terra, Universitat de Barcelona, 08028 Barcelona, Spain*

**Key words:** *TLS, Rockfall, Monitoring*

In recent years, the appearance of new laser scanners with LIDAR technology are installed in small size and price devices (Velodyne, Innoviz, Livox (GLENNIE et al., 2019, ORTIZ ARTEAGA et al., 2020)), in comparison with the already consolidated topographic scanners (Rigel, Leica Geosystems, Optech), make it possible new applications. In this document, we show the different results for the Livox models, Mid-40 and Avia (Figure 1), in monitoring rockfalls, landslides, and the evolution of analog models in the laboratory. The results obtained with those small-size laser scanners from different field examples at distances from 3 to 350 m are shown and compared with data captured by photogrammetry. The possibilities offered by these devices with low consumption and fast data acquisition (200,000 pts/sec) are also presented. The study cases presented are the first results of the adaption of monitoring the Montserrat massif (Barcelona, Spain) with a Livox Avia from a range of 200m and compared with a Leica P50 lidar; the monitored of the escarpment of Puigcerçós (Lleida, Spain) with a Livox Mid-40 from a range of 85 m and compared with an ILRIS-3D model; and the comparison erosion of the Croscat volcano (Girona, Spain) monitored with an ILRIS-3D TLS, obliques photogrammetry, and Avia model from a range of 300m. Also, it commented on the first results of a close-range scanning of a Sand-Box tectonic model to analyze the evolution with the Livox Mid-40 model.



*Figure 1: Livox Avia and DSLR camera equipment.*

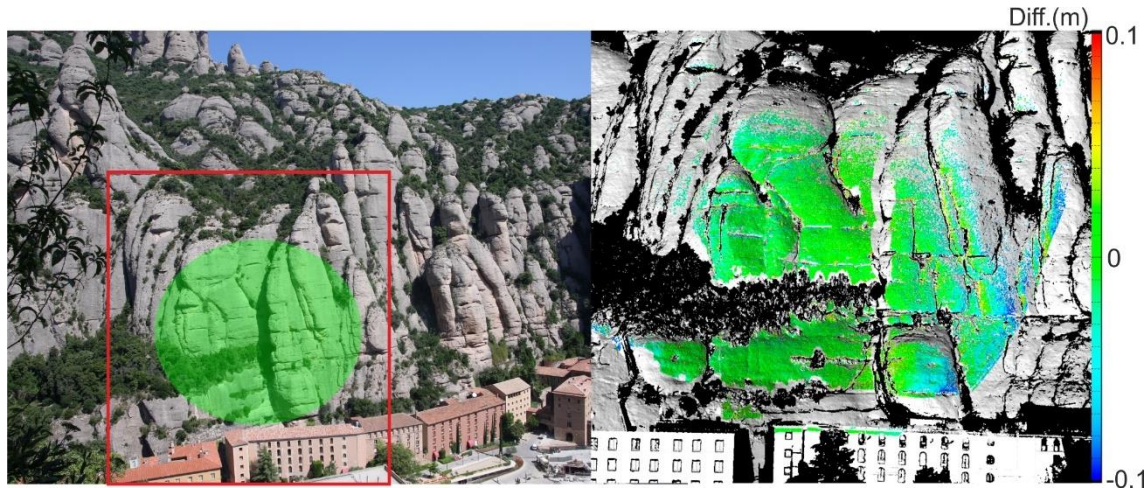


Figure 2: Use example of TLS Avia. Left: Montserrat mountain (Barcelona, Spain) showing the compared area between TLS Iiris-3D and TLS Livox Avia (green circle), the red box frames the image on the right image. Right: Results and scale of the differences.

The purpose of these devices is the continuous monitoring of the escarpments to detect deformations previous to the rockfalls and the comparison of the surfaces after the rockfall in order to calculate rock volumes (BLANCO et al., 2022). The nature of the deformation process in each escarp conditioned the applicability of these devices and the detection accuracy for each escenario.

## References

- BLANCO, L., GARCIA-SELLÉS, D., GUINAU, M., ZOUPEKAS, T., PUIG, A., SALAMÓ M., GRATACÓS, O., MUÑOZ, J.A., JANERAS, M. & PEDRAZA, O., 2022. Machine Learning-Based Rockfalls Detection with 3D Point Clouds, Example in the Montserrat Massif (Spain). *Remote Sensing*, 14, 4306.
- GLENNIE, C.L. & HARTZELL, P.J., 2020. Accuracy assesment and calibration of low-cost autonomous Lidar sensors. *The International Archives of the Photogrammetry, Remote Sensing and Spatial Information Sciences*, 43: 371-376.
- ORTIZ ARTEAGA, A., SCOTT, D. & BOEHM, 2019. Initial investigation of a low-cost automotive lidar system. *The International Archives of the Photogrammetry, Remote Sensings and Spatial Information Sciences*, XLII-2/W17: 6<sup>th</sup> International Wokshop LowCost 3D- Sensors, Algorithms, Applications, 2-3 December 2019, Strasbourg, France.

# Complexity and precision of topographic change detection in active volcanic craters using close-range airborne imagery and SfM-MVS photogrammetry

Benoît SMETS<sup>1,2\*</sup>, Pierre-Yves TOURNIGAND<sup>2</sup> & Louise DELHAYE<sup>3</sup>

<sup>1</sup> *Natural Hazards and Cartography Service, Royal Museum for Central Africa, 13 Leuvensesteenweg, B-3080 Tervuren, Belgium, benoit.smets@africamuseum.be*

<sup>2</sup> *Cartography and GIS Research Group, Dpt. Geography, Vrije Universiteit Brussel, 2 Pleinlaan, B-1050 Brussels, Belgium*

<sup>3</sup> *Operational Directorate Natural Environment, Royal Belgian Institute of Natural Sciences, 29 Rue Vautier, B-1000 Brussels, Belgium*

**Key words:** UAV, SfM, MVS, Photogrammetry, Co-alignment, Volcano

Active volcanic craters can display fast changing topography, especially at open-vent volcanoes. Their evolution through time holds information about the eruptive activity and the pressure state of the shallow plumbing system, while local geomorphological changes can potentially affect the eruption style of the volcano. Measuring these changes and the evolution of construction and destruction episodes in craters is therefore relevant for volcano monitoring.

Digital cameras onboard Unoccupied Aerial Vehicles (UAV) are increasingly used for that purpose, as they offer cost-effective way to observe volcanic activity and reconstruct the topography of active craters using Structure-from-Motion Multi-View Stereo (SfM-MVS) photogrammetry. However, challenges remain for the processing of time-series. The classical multi-epoch co-alignment technique (e.g., Li et al., 2017; Feurer and Vinatier, 2018) commonly used for accurate 3D change detection is frequently prevented on active volcanoes (Delhaye and Smets, 2021), for three main reasons. First, the context of image acquisition can drastically differ between epochs. The steep and complex topography makes the texture of the crater strongly dependent on the sun illumination (i.e., shadow orientation and size, contrast between sunny and shadow areas). The atmospheric transparency can vary due to volcanic outgassing, water vapor, dust and humidity. Water can change the colour and apparent texture of volcanic rocks. Second, it is often difficult to obtain the same image acquisition geometry during each survey. Automatic flights are frequently impossible due to the steep and complex topography. The orientation of outgassing and its dynamics during a survey may influence the paths followed by the UAV. Field and weather conditions sometimes influence the flight plan, its duration and the number of images that can be acquired. The platform carrying the camera may differ between epochs (i.e., helicopter versus multirotor UAV versus fixed-wing UAV acquisitions), forcing preferential view geometries during surveys. Finally, the camera and/or lens used can be different between surveys, leading to epochs with different image quality, resolution and camera distortions.

In the present work, we take advantage of three on-going investigations on Nyiragongo (D.R. Congo), Ol Doinyo Lengai (Tanzania) and Stromboli (Italy) volcanoes to highlight the complexity of multi-temporal photogrammetry on active craters and show examples of precision reached to measure volcano-related topographic changes. The Nyiragongo dataset provides suggestions to best co-align epochs when the geometry of acquisition and the camera equipment strongly differ. The Ol Doinyo Lengai dataset shows the potential of crowdsourcing to create usable time-series and assess lava accumulation and emission rate. On Stromboli, data acquired at a daily to sub-daily frequency show the precision we could expect from multi-temporal photogrammetry to measure small-scale topographic changes.

**Acknowledgements:** This work is based of different scientific investigations performed by the authors in the frame of the VeRSUS (BELSPO STEREO-III Programme, Grant n° SR/00/382), MORPHEUS (FWO postdoc scholarship, Grant n° FWOTM996) and GuiDANCE (BELSPO FED-tWIN Programme, Grant n° Prf-2019-066) research projects.

## References

DELHAYE, L., & SMETS, B., 2021. Time-series in Structure-from-Motion photogrammetry: Testing co-registration approaches for topographic change analysis. *IGARSS 2021 – 2021 IEEE International Geoscience and Remote Sensing Symposium*: 4648-4651.

FEURER, D., & VINATIER, F., 2018. Joining multi-epoch archival aerial images in a single SfM block allows 3-D change detection with almost exclusively image information. *ISPRS journal of photogrammetry and remote sensing*, 146: 495-506.

LI, W., SUN, K., LI, D., BAI, T., & SUI H., 2017. A new approach to performing bundle adjustment for time series UAV images 3D building change detection. *Remote Sensing*, 9(6): 625.

## Enriching Geohazard Education through Virtual Field Trips using VR and 3D Outcrop Models

Ryan Kromer<sup>1\*</sup>, Suzanne Bickerdike<sup>2</sup>, Jason Williams<sup>1</sup>, Buena Galleposa<sup>2</sup>, Matthew Wilson<sup>2</sup>, Ben Pierce<sup>2</sup>, Johanna Fenton<sup>2</sup>

<sup>1</sup>*School of Earth and Environment, University of Leeds, r.a.kromer@leeds.ac.uk*

<sup>2</sup>*Digital Education Service, University of Leeds*

**Key words:** *Geohazards, virtual field trips, immersive environment, 3D models, Jurassic Coast*

There are many exciting opportunities to create immersive learning experiences using rich 3D digital data of the environment. Immersive virtual field trips can be designed to be student-centred, problem-based, collaborative, and fun. Virtual field trip elements can be introduced as an asynchronous component prior to an in-person field trip as a preparation tool or as a post field trip resource. Virtual trips are also more inclusive, allowing a wide range of students to participate regardless of ability or location. With these benefits in mind and aligning them with University of Leeds' digital education and sustainability strategies, we created a virtual geohazards field trip for the MSc Engineering Geology programme exploring the Jurassic Coast in SW England. The aim of this contribution is to share the development of the resource and an initial assessment of student learning.

We can develop unique insights into geohazard processes using virtual and VR field resources as the spatio-temporal and multi-dimensional aspects can be better explored, understood, and communicated as compared to a field visit alone (HAVENITH *et al.*, 2019). For this reason, we developed learning activities using both VR and multi-temporal digital outcrop models. The main learning outcome of the virtual geohazards trip was to enable students to evaluate geohazards and assess risk at a variety of scales using qualitative and quantitative approaches.

Data for the virtual field trip was collected over a three-day period in March 2023 at three sites in Dorset, England. This consisted of collection of terrestrial lidar, high resolution photos for photogrammetry model generation, 360 videos and images, UAV video footage, and piece to camera videos at sites of interest. The VR component was constructed using 360 videos and images of the site using CenarioVR (ELB LEARNING, 2022). UAV video footage and the teaching videos were embedded within application allowing for an immersive learning experience. Students could move around and explore the coastline, explore on top of and below the cliffs, and travers landslides without exposing themselves directly to the hazards (Fig. 1). We found ArcGIS Storymap to be an effective tool for tying together geospatial resources, introducing learning activities, and acting as a springboard to enter the VR experience. Learning activities consisted of exploring the geology, structural mapping, geohazard characterization, and change analysis, which was facilitated using photogrammetry, terrestrial lidar, and airborne lidar models (Fig 2.).

Student evaluations revealed both high engagement and high perceived educational value of the resource. They found the 3D models and change detection enhanced their understanding of geohazard processes as it allowed them to explore the terrain in a unique way. Student marks were also higher on their risk assessment as compared year's with an in person trip. Engagement with the virtual trip was high following the synchronous session showing its value as an ongoing resource. Most notably, 82% of the students on the MSc Engineering Geology programme wanted more VR or virtual field trip experiences as part of their education. Future work will consist of developing pre and post field trip resources for in person trips and further evaluating various aspects of the student learning experience.



Figure 1: Virtual field trip to the Jurassic Coast in SW England. The VR experience allows exploration of the coast from base of the cliff, top of the cliff, the surrounding area and from drone footage. There is also the ability to navigate and get information from embedded media content.

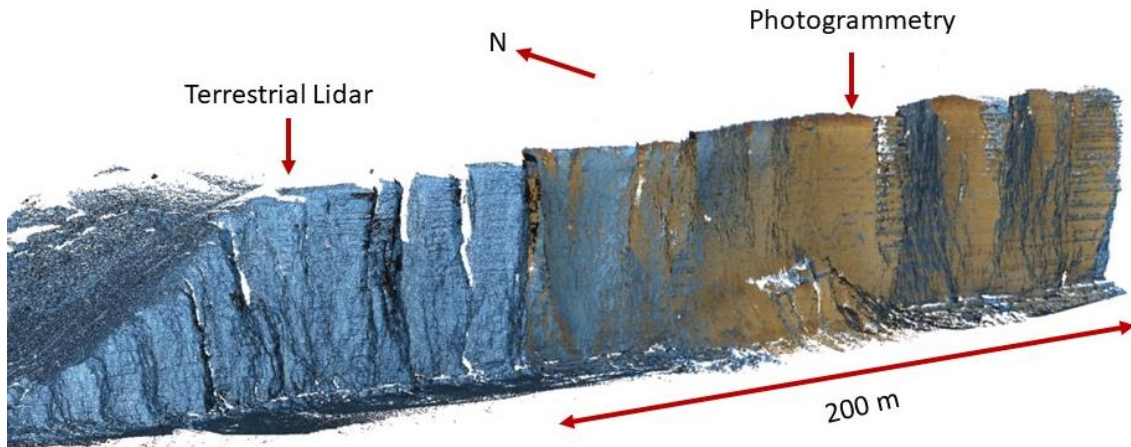


Figure 2: Terrestrial lidar, photogrammetry, and multi-temporal airborne models were used to support learning exercises involving structural and hazard characterization.

## References

HAVENITH, H.B., CERFONTAINE, P. & MREYEN, A.S., 2019. How virtual reality can help visualise and assess geohazards. *International Journal of Digital Earth*, 12(2):173-189.

ELB LEARNING. 2022. CenarioVR [Computer Software], American Fork, UT.

## **Session 7 – Applications in Hydrology & Ecology**



# **SESSION 7 APPLICATIONS IN HYDROLOGY & ECOLOGY**

# Revolutionising Natural Flood Management with SCALGO Live, SCIMAP, and Drones

Josie Lynch<sup>1\*</sup>, Dr Derek McDougall<sup>1</sup> and Professor Ian Maddock<sup>1</sup>

<sup>1</sup> *Department of Geography and Environmental Management, University of Worcester, Henwick Grove, Worcester, UK, j.lynch@worc.ac.uk*

**Key words:** *Natural Flood Management, Nature-based Solutions, SCALGO Live, SCIMAP, drone, GIS*

Natural Flood Management (NFM) is a Nature-based Solution (NbS) that aims to restore natural river functions for flood risk management by slowing the flow and storing water, intercepting rainfall, and increasing soil infiltration. This is becoming increasingly important due to the devastating impacts of flooding as a result of climate change. A challenge associated with implementing NFM is the absence of a systematic approach to determine the most appropriate locations within a catchment to implement these measures. Instead, the existing approach focuses on identifying farmers or landowners who are willing to participate in NFM projects, rather than locating areas in the catchment where NFM is most effective in reducing the risk of flooding downstream.

This presentation describes a strategic identification of NFM sites in catchments in Worcestershire, Herefordshire, and Gloucestershire, UK, in collaboration with the Environment Agency (EA), Severn Rivers Trust, Worcestershire / Gloucestershire County Council(s). This approach uses web-based software (SCALGO Live and SCIMAP), GIS, and drone data (DJI Phantom 4 RTK) to create high-resolution Digital Elevation Models (DEM) and orthophoto mosaics together to map and model the river catchment to identify the most suitable locations for NFM. SCALGO Live is an online flood risk platform which provides rapid mapping of watercourses, in depressions or from the sea, presenting an overview of the flood risk for a single property, an entire city, or catchment. In this research, SCALGO Live was used to identify main and dense flow paths, as well as areas suitable for water storage, for example. The Sensitive Catchment Integrated Modelling and Prediction (SCIMAP) web-based software was used to identify sources of



*Figure 1. Hydrological connectivity map generated with SCIMAP (<https://scimap.org.uk/>). Red displays areas which connect most frequently with the floodplain, pink areas show areas that connect frequently, but less often than red (SCIMAP 2023).*

environmental pressures in the catchment, focusing on sediment, nitrates, phosphates, and flood hazard generation. Outputs used from SCIMAP for this research include i) the hydrological connectivity map (figure 1) to prioritise areas in the catchment for floodplain NFM interventions, such as floodplain reconnection, or creating online/offline storage ponds, ii) the soil erosion risk map to highlight areas of agricultural land that are most susceptible to erosion, helping determine the most appropriate locations for agricultural land management.

The outcomes from SCIMAP and SCALGO Live were validated by comparing EA 1m resolution Light Detection and Ranging (LiDAR) data and 1.84cm/pix drone data (figure 2) obtained with a DJI Phantom 4 RTK. The results showed that LiDAR 1m is satisfactory for displaying the overall trends of runoff, but higher resolution data from the drone is required to identify where overland flow is concentrating in tractor tracks and rills. The research findings provide local authorities with the necessary information to prioritise the most appropriate and effective locations for NFM in the catchments. This research also highlights the importance of using scientific evidence and data-driven approaches to identify NFM sites effectively, promoting the use of NbS to mitigate the effects of flood risk due to climate change whilst improving biodiversity and human wellbeing.



Figure 2. Validation of modelled flow paths in SCALGO Live (<https://scalgo.com/>) between EA 1m LiDAR data (pink) and 1.84cm/pix resolution drone data from DJI Phantom 4 RTK (blue) in Herefordshire, UK. The drone orthophoto is overlaid on the base map sourced from Mapbox (SCALGO Live 2023).

## Monitoring streamflow with drones

Westerberg, I. K.<sup>1\*</sup>, Mansanarez, V.<sup>1</sup>, Lyon, S.W.<sup>2,3,4</sup>, Huseby Karlsen, R.<sup>1</sup> & Lam, N.<sup>2</sup>

<sup>1</sup> IVL Swedish Environmental Research Institute, Stockholm, Sweden, [ida.westerberg@ivl.se](mailto:ida.westerberg@ivl.se)

<sup>2</sup> Bolin Centre for Climate Research, Stockholm University, Stockholm, Sweden

<sup>3</sup> Department of Physical Geography, Stockholm University, Stockholm, Sweden

<sup>4</sup> School of Environment and Natural Resources, Ohio State University–OARDC, Wooster, OH, USA

**Key words:** streamflow monitoring, rating curves, structure from motion, drone lidar, hydraulic modelling

Streamflow monitoring data are needed for many new locations to tackle water problems related to climate change and other societal challenges. However, when using traditional empirical streamflow monitoring methods, it typically takes many years to establish reliable data and in particular for extreme flows that are creating increasingly severe impacts on society. This gap between increasing data needs and current monitoring capabilities calls for new monitoring methods to be developed.

Drones provide an unprecedented ability to measure both the physical and hydraulic characteristics of a river in an efficient manner. Topography, water surface slope, surface water velocity and even bathymetry can be derived from drone images and drone lidar data. Traditionally, streamflow is monitored indirectly using a rating curve (a model of the relation between streamflow and water level at the gauging station) that is fitted to empirical control gaugings and then used to calculate continuous streamflow data time series from measured water level time series. Using drone-based data of river physical and hydraulic characteristics together with hydraulic modelling makes it possible to model rating curves with much fewer control gaugings.

We exploited this potential by incorporating drone data into the framework for Rating curve Uncertainty estimation using Hydraulic Modelling (RUHM). The RUHM framework combines a one-dimensional hydraulic model with Bayesian inference and together with drone data it allows us to efficiently estimate a reliable rating curve and its associated uncertainty based on as few as three calibration gaugings.

We present our results from applying RUHM to Swedish gauging stations where we model rating curves and streamflow based on drone data. We primarily used low-cost camera drones to collect both the input (DEM, vegetation and bathymetry) and calibration data (water surface slope and surface velocity) for the hydraulic model, but also tested the capabilities of drone lidar data. Our aim was to estimate reliable rating curves with RUHM based only on data from the drone flights. We assessed the uncertainty in the drone-derived model input and calibration data compared to traditional fieldwork techniques, as well as their impact on the RUHM-modelled rating curves and streamflow results.

Careful planning of when to fly the drone was important for obtaining good-quality model input and calibration data and different conditions were needed for different types of data. Using a combination of drone camera and drone lidar data we were able to obtain all the data needed for RUHM from the drone flights. Extreme low and high flows were reliably modelled with RUHM with constrained uncertainty based on as few as three low and middle flow gaugings, without the need for gauging extreme flows. Our results show that using RUHM with drone data is an efficient and promising alternative to traditional streamflow monitoring methods, being much less time-consuming and costly, as well as involving fewer risks to field staff.

## UAV- and handheld-hyperspectral imaging for *Sphagnum* discrimination and vegetation modelling

Franziska Wolff<sup>1\*</sup>, Sandra Lorenz<sup>2</sup>, Pasi Korpelainen<sup>1</sup>, Anette Eltner<sup>3</sup> & Timo Kumpula<sup>1</sup>

<sup>1</sup> Department of Geographical and Historical Studies, University of Eastern Finland, Yliopistokatu 2, P.O. Box 111, Joensuu, 80101, Finland, franziska.wolff@uef.fi

<sup>2</sup> Division Exploration Technology, Helmholtz-Institute Freiberg for Resource Technology (HZDR), Chemnitzer Straße 40, Freiberg, 09599, Germany, s.lorenz@hzdr.de

<sup>3</sup> Institute of Photogrammetry and Remote Sensing, Technische Universität Dresden, Dresden, 01062, Germany, anette.eltner@tu-dresden.de

**Key words:** mires, spectral properties, narrow-band, imaging spectroscopy

Sensor development advances accurate vegetation classification, enhancing a comprehensive understanding of species spatial distribution and diversity. Applying hyperspectral imaging particularly benefits the understanding of biodiversity based on the spectral properties acquired over a larger, spatial scale. This is interesting for mire ecosystems, where especially *Sphagnum* mosses pose a challenge regarding spectral separability. The separability of peat mosses can help to assess the current state and dynamics in peatland ecosystems, which in turn reveal information about ecological processes, such as carbon storage. This study evolves around the question if and which benefits hyperspectral sensors provide over conventional RGB and multispectral sensors in the context of *Sphagnum* discrimination and vegetation modelling. Therefore, we investigated if hyperspectral imaging under unsteady field conditions can provide reliable data for this. Our study site Ilajansuo mire, located in North Karelia, Finland, is an aapa mire situated at the border of southern and main aapa mire zone. These mire types are characterized by fen and bog elements forming a complex of distinct micropatterns, such as wet flarks, strings, and hummocks. Each of those elements is formed by specialized plant communities along the water table gradient, including *Sphagnum* mosses. Using vegetation plot imagery captured with Specim IQ hyperspectral handheld camera (400 – 1000 nm) and species inventory, we established a spectral library with spectral signatures of dominant species. Secondly, we applied this data to model *Sphagnum* and vegetation distribution across the entire study site based on hyperspectral Uncrewed Aerial Vehicle (UAV) imagery acquired with Specim AFX10 (400 – 1000 nm). We examined the spectral breakdown of individual signatures and the potential linkage to mixed pixels of the UAV hyperspectral imagery. Preliminary results show that (*Sphagnum* moss) species can be discriminated, partly even in the visible region of the electromagnetic spectra using the handheld device. Varying moisture conditions and the phenological stage, however, affected the spectral reflectance. Our preliminary results suggest plot recording from the same moss species under apparent varying water level influence to provide separate library entries according to the different wetness stages. The spatial resolution of approximately eight centimetres of the UAV-hyperspectral data captures largely mixed pixels and not only pure *Sphagnum* regions, emphasizing the need for downscaling of the Specim IQ images to the resolution of the UAV-imagery and to consider general vegetation entities besides species level. Under these premises, hyperspectral imaging with a handheld camera can be used to establish a spectral library, which in turn benefits UAV-hyperspectral data classification for those sites, where *Sphagnum* carpets and lawns prevail to a great extent. The findings generally emphasise the benefit of hyperspectral imaging over the use of conventional multispectral and RGB sensors in the context of species separation at plot scale, whereas peatland drying stages can be assessed at full-scale with UAV-hyperspectral information. Further studies could therefore include moisture measurements across the peatland and the computation of (narrow-band) indexes that relate to the water holding capacities of mosses to investigate plant stress in relation to microtopography.

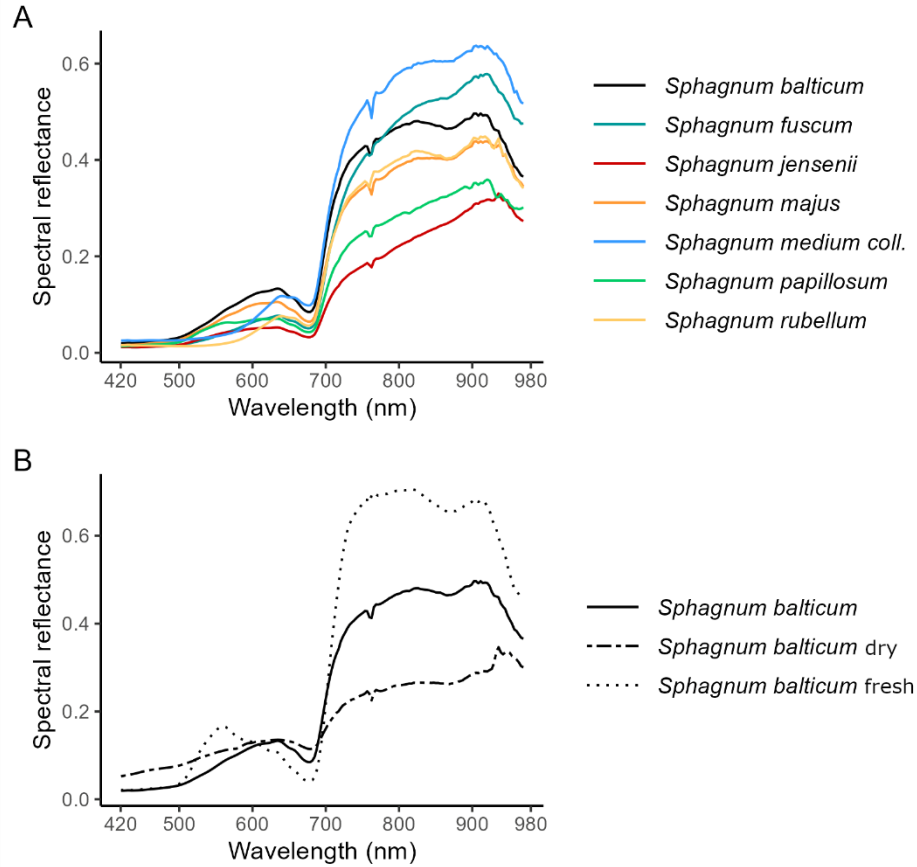


Figure 1: Spectral profile (420 – 980 nm) of all *Sphagnum* mosses present in the study area (A) and of three different site-conditions for *Sphagnum balticum* (B). Established, yellow-brown *Sphagnum balticum* carpets grow at a water table depth of 2-3 cm, while “dry” refers to bleached out patches with a water table depth of 8 cm. “Fresh” *Sphagnum* are young, clearly greenish sprouts at 4 cm water table depth. Hyperspectral imagery was captured with Specim IQ handheld hyperspectral camera.

**Acknowledgements:** This study was funded by Kone foundation, Helsinki, Finland, in the context of the PhD project of F. Wolff.

## Mapping Pb/Zn-stressed plant communities: challenges of centimetre- to millimetre-scale UAV sensing for training deep-learning schemes

Thomas JB Dewez<sup>1\*</sup>, Adrien Breton<sup>1</sup>, Gaël Bellenfant<sup>1</sup>, Marie de Boisvilliers<sup>2</sup>, Marion Houlès<sup>2</sup>, Florent Guiotte<sup>2</sup>, Bruno Roux<sup>2</sup>, Sébastien Lefèvre<sup>3</sup>, Javiera Castillo-Navarro<sup>3</sup>, Guglielmo Fernandez Garcia<sup>3</sup>, Felix Kröber<sup>3</sup>, Thomas Corpetti<sup>3</sup>, Florian Delerue<sup>4</sup>

<sup>1</sup> BRGM, Direction des Risques et Prévention, F-45060 Orléans, France, [t.dewez@brgm.fr](mailto:t.dewez@brgm.fr)

<sup>2</sup> L'Avion Jaune, F-32480 St Clément de rivièrè, France

<sup>3</sup> IRISA, Université Bretagne Sud (UBS), F-56000 Vannes, France

<sup>4</sup> Univ. Bordeaux, CNRS, Bordeaux INP, EPOC, UMR 5805, F-33600 Pessac, France

**Key words:** *plant ecosystem functioning, UAV, lidar, photogrammetry, plant mapping, ground-truth, class image classification, neural network*

Plant interactions play a pivotal role in ecosystem functioning. In stressed ecosystems, dominant plants often mitigate environmental stress in their immediate vicinity enabling maintenance of low stress-tolerant species. In that case beneficiary plants are clustered around their benefactors. This process increases plant diversity and develops corresponding plant communities. Metals/metalloids rich environments challenge vegetation development making their remediation intricate. The ANR-funded SixP project investigates the role of facilitation in Zn/Pb contaminated sites as a potential tool for their remediation. Plant mapping is a key project component to discover clumped spatial distributions. For this, a set 24 459 plants spread over 352 m<sup>2</sup>, split in 24 distinct sampling patches were identified, located with differential GNSS and measured. That is 30 full man-days of effort. UAV acquisition could presumably ease the mapping endeavor in three ways: (i) surveying much larger surfaces, hence broadening statistical and environmental representativeness; (ii) archiving land cover state when the manual survey is performed; (iii) providing continuous explanatory variable layers such as topographic context and multispectral surface response to feed seemingly effortless deep-learning classification algorithms. This contribution means to highlight the challenges of providing accurate and trustworthy labels for training AI schemes.

A lead/zinc mining district, in Sentein, central Pyrenees mountains (southern France) was active up until the 1960's. Remaining toxic wastes act as stress control variable, while the vertical distribution of mining activities, over 1000 m of elevation, bring climate control on plant ecosystems. L'Avion Jaune company performed Uncrewed Aerial Vehicle (UAV) flights, before the growing season (march/june 2020) and at full growth (june/july 2020). Lidar was used for overview ground topography (with canopy top density ca. 50 pts/m<sup>2</sup>) and SfM-photogrammetry at two resolutions for land cover: 20 mm/pixel (RGB) before growth and 2-3 mm/pixel (RGB+near-infrared) at full growth season. Millimetric resolution is justified by metallic toxicity constraining dwarf plant development. Full growth mm-resolution covered 7 zones for a total of 1.34 ha (40 times the ground-truth surface), while overview cm-resolution data covered 36.6 ha, 1000 times the reference.

The first lesson: differential-GNSS survey in mountain terrains is not trivial. No phone coverage meant no real-time corrections, nor accurate national geodesic network tie. A GNSS base station was freely deployed alongside a rover unit to broadcast real-time corrections. Base-to-reference-network post-processing tied surveys to IGN's RGP network, but only with a limited accuracy (ca. 20 cm). Stationing a known benchmark with the base station would have improved accuracy. Fortunately, plant and UAV surveys were performed in a common spring-summer 2020 reference frame, with temporary UAV targets positioned by the plant-mapping teams. GNSS plant positions are coherent with UAV data to within 10-30 mm.

The second lesson: producing UAV photogrammetric coverages at 2-3 millimeter pixels of plants is incredibly challenging. The UAV flew 10-m above ground to reach image resolution. But flying low strains photographic and photogrammetric processing to the limit. The UAV blew wind on the tiny gracile leaves and stems. Fast shutter speed of 1/1000 s counter-acted both motion blur and pixel ovalization due to UAV vibrations but

imposed a wide aperture ( $f/3.5$ ). This mitigated vignetting, refraction and diffraction issues of small apertures. Yet narrower apertures would have increased the depth-of-field, but at the cost of increasing image electronic noise to preserve shutter speed. Sensor sensitivity was set at 200 ISO. While with these settings, plants were reasonably sharp, the wind shifted the position of mobile plant organs between photos. This challenged photogrammetric surface reconstruction and orthophotos mosaicking. Finally, RGB and Near-Infrared imagers were flown simultaneously, back-to-back to generate 4-band ortho-imagery. But with two points of view, even if only 8 cm apart, the base-line was sufficiently large to generate differential parallax between images, challenging orthorectification along elevated object edges. This means that RGB pixel signatures do not always match the underlying NIR signal depending on the local topography.

The third lesson: training AI models for class (here species) segmentation requires a trustworthy training set. GNSS-tagged labels link a 1D position with a plant label and radius. In raster form, it is a label disk map. But the plant may not be exactly, at pixel scale, below the GNSS point, due to geometric imprecision. We innovated with a fuzzy edge labelling map to accounts for location uncertainty (Guiotte et al., in prep.)

Finally, can trained models be transposed to different sites? ImageNet feature mapping clustered with t-SNE (Castillo-Navarro *et al.*, 2022) maps image features to predict the chances of successful classification.

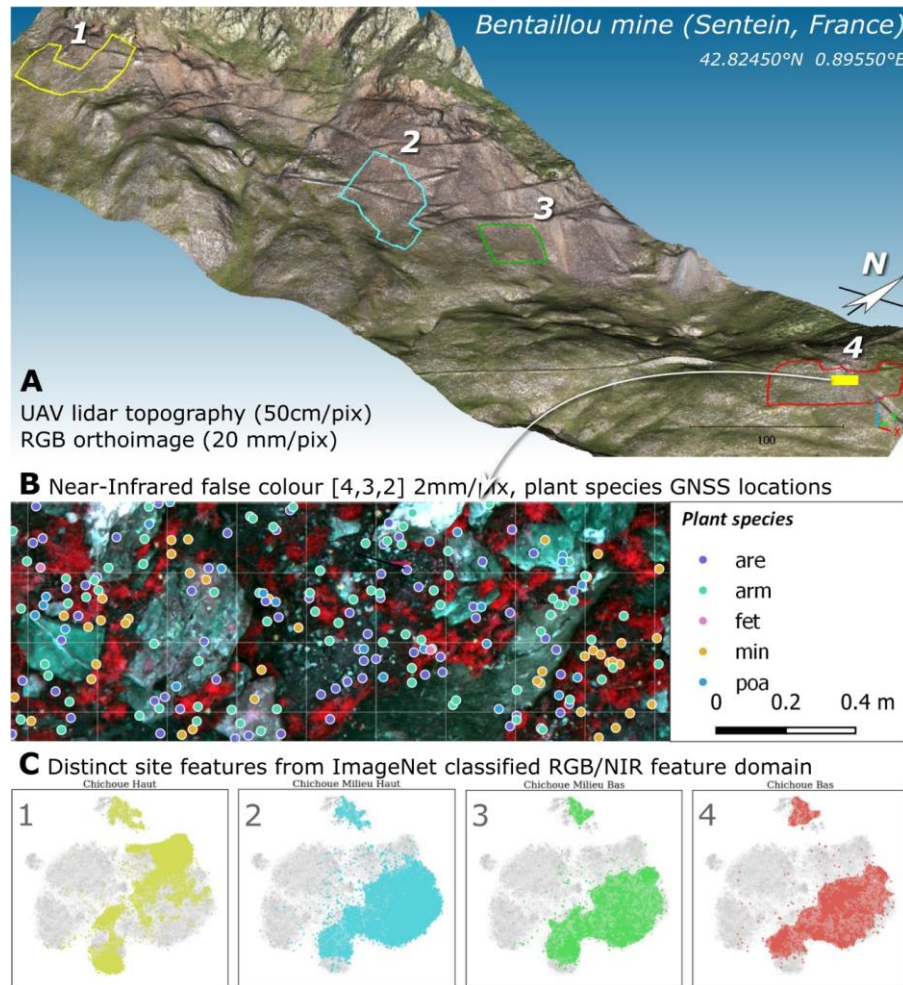


Figure 6 : From field data sensing (A) and GNSS plant mapping (B) to classification features (C). In C, distinct sites only contain a restricted set of ImageNet features. Site 1 does not contain a large part of features present in other sites (sectors to the right of feature space), which raises caution.

CASTILLO-NAVARRO, J., LE SAUX, B., BOULCH, A., AUDEBERT, N., LEFEVRE, S., 2022. Semi-supervised semantic segmentation in Earth Observation: the MiniFrance suite, dataset analysis and multi-task network study. *Mach Learn* 111, 3125–3160. <https://doi.org/10.1007/s10994-020-05943-y>

## An index representing geomorphological disturbance for Alpine plants based on airborne laser scan data

Andreas Mayr<sup>1\*</sup>, Martin Rutzinger<sup>1</sup>, Lukas Müller<sup>1</sup>, Andreas Kollert<sup>1</sup>, Stefan Dullinger<sup>2</sup>,  
Karl Hülber<sup>2</sup>

<sup>1</sup> Department of Geography, University of Innsbruck, Austria, andreas.mayr@uibk.ac.at

<sup>2</sup> Biodiversity Dynamics and Conservation Group, University of Vienna, Austria

**Key words:** *Geomorphology, Ecology, Laser Scanning, Process Path Modelling, Process Mapping, Plant Distribution*

The European Alps and other mountain regions are home for many cold-adapted plant species. It is not yet clear whether, in a warming climate, these species are at high risk of extinction or have a high chance to survive in microrefugia offered by the complex terrain. Exploring this question requires maps of environmental conditions at high spatial resolution (e.g., one meter). In addition to variables related to soil temperature and snow cover (e.g., duration and melt-out timing), the disturbance by geomorphic processes is a key factor controlling the growing conditions at many sites.

When assessing the susceptibility to geomorphic disturbance based on airborne laser scanning (ALS), two major challenges are encountered: First, some processes (e.g., avalanches) do not shape the terrain strongly enough to be detectable in ALS data but should be modelled as their occurrence is ecologically relevant and, hence, affects the performance of flora and fauna. Second, some geomorphic processes (e.g., landslides) cannot be represented by straightforward models without input data from extensive and costly field campaigns, yet they cause topographic change that can be derived from multitemporal ALS data and, thus, might be used for generating an indicator for disturbance.

We developed a novel geomorphic disturbance index (GDI) as a spatially explicit measure for the relative impact of geomorphic processes on plant occurrence. The GDI addresses the two aforementioned challenges by combining an empirical and a modelling component, both taking ALS data as input. The empirical component is based on topographic changes detected between two 3D point clouds spanning multiple years (in our case eleven years). Change is categorized by dominant geomorphic process domains (such as fluvial processes, channel erosion, rock glacier movement, landslides, and rockfall) in a semi-automatic classification (MÜLLER *et al.*, 2022). The modelling component delineates areas affected by avalanches and fluvial processes (including permanent or episodic flow in channels and episodic, diffuse sheet flow). Process paths and spatially varying, relative intensities are simulated by established, regional-scale models using a raster terrain model. The components are combined into a compound index (the GDI) using a disturbance rating scheme that is applied to the process categories and accounts for different, process-specific degrees of disturbance severity for vegetation.

We computed the GDI for a study area of approximately 20 km<sup>2</sup>, located in the Central Alps of Austria, covering elevations from c. 1800 m a.s.l. to 3500 m a.s.l.. The methods are parameterized by a visual interpretation of the resulting maps and plausibility checks including extensive field observations. Moreover, we compare the resulting GDI against (i) a manually produced, “traditional” geomorphological map and (ii) with in-situ estimates of geomorphic disturbance at 899 vegetation plots visited in the field. The presented approach is reproducible and, being based on widely available ALS data, it holds the potential for scaling to larger areas and for transferability to other regions with similar geomorphic and climatic conditions. By quantifying an important factor that is otherwise difficult to grasp, we expect the GDI to be a valuable contribution for studies of current and future vegetation cover and species distribution.

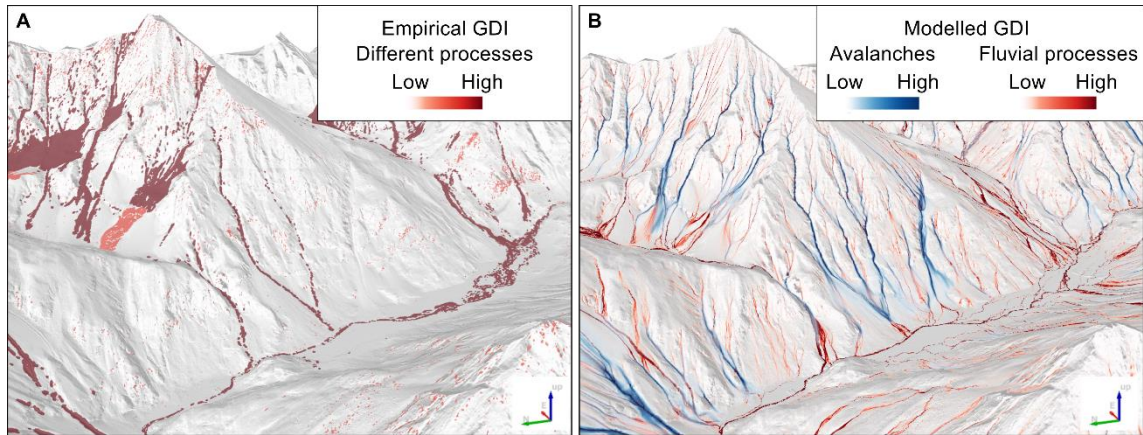


Figure 1: Complementary components of the Geomorphic Disturbance Index (GDI): (A) An empirical component derived from classified topographic changes (resulting from different geomorphic processes); (B) modelled components, here blended in two different colors for avalanches and fluvial processes, respectively.

**Acknowledgements:** This work has received funding from the European Research Council (ERC) under the European Union’s Horizon 2020 research and innovation programme (Grant agreement No. 883669).

## References

Müller, L., Rutzinger, M., Mayr, A., and Kollert, A. 2022: Airborne laser scanning change detection for quantifying geomorphological processes in high mountain regions. *ISPRS Ann. Photogramm. Remote Sens. Spatial Inf. Sci.*, V-2-2022, 391–398.

## **Poster Contributions**



# **POSTER CONTRIBUTIONS**

## Virtual field trips for teaching rock mechanics and tunnelling using CoSpaces – summary of 4 years of experiences

Luis Jordá Bordehore<sup>\*</sup>, Salvador Senent Dominguez, Ruben Angel Galindo Aires, Jesús González Galindo

*Technical Universitu of Madrid (UPM). Av Profesor Aranguren 3. Escuela Técnica Superior de Ingenieros de Caminos Canales y Puertos, Departamento de Ingeniería y Morfología del Terreno.*

*\* l.jorda@upm.es*

**Key words:** *Covid 19 pandemic, lockdown, flipped classroom, Virtual Reality, 360 images*

In 2019 we decided to change our classes, motivated by the rise of the flipped classroom model and the problems of going on field trips, which we considered very important in geosciences and ground engineering subjects. We start with the subjects of rock mechanics and tunnelling and the module of rock mass classifications. The idea was to prepare a series of virtual scenarios where students gather the data as if they were doing a field trip. Since the very beginning of the project we wanted an immersive tour, but with certain limitations so as not to overload the virtual world (metaverse). The information and geological data would be in the virtual scenario but the students would use physical templates that they would fill in with pencil as if they were on a field trip. We were looking for a type of platform that would allow us to easily upload content but at the same time not “time consuming” in programming time, after all, we are not programmers but geotechnical professors. For this, we chose the CoSpaces commercial platform that allows us a virtual tour based on 360 images and data that we are programming and uploading as pop up menus and active links.

This is how we started our first “product” a series of linked scenarios and pop up menus in the CoSpaces platform. We went to real field visits where we took data that we would later upload to the virtual scenario as drop-down information: these scenes have different degrees of difficulty: some in which the parameters are “too” clearly described and with their values ( UCS, GSI, etc.). We also developed other more advanced scenarios where we give clues so that the student can calculate the required parameters with the help of his class notes (RQD, GSI, UCS via sclerometer etc). These scenarios were in full development when the COVID 19 lockdown emerged in March 2019. Since then, and given the great success that these products had, we share them in an open format with other universities and researchers (GARCIA VELA et al 2012). We returned to presential classroom teaching in 2021. Since 2021 we had the opportunity to make the classes more interactive with these tools and develop the “blended learning”. We have developed virtual scenarios for kinematic slope calculations (JORDA et al 2017), RMR, Q, SMR and Q slope geomechanical classifications and other calculations for mining, tunneling and slopes (DELGADO et al 2023).

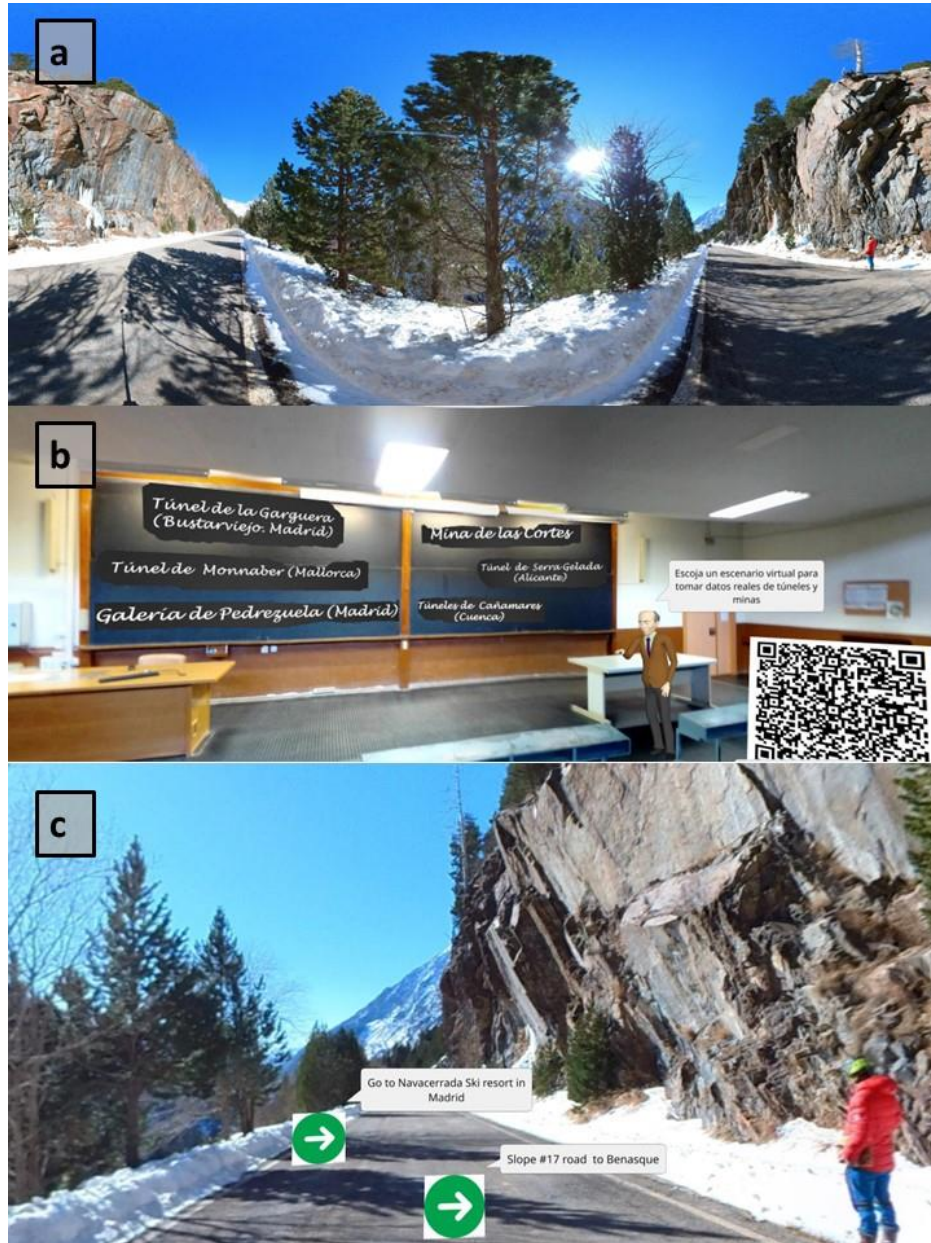


Figure 1: Several phases of elaboration of the scenarios and virtual tours: a) 360° spherical image taken on the frozen slopes of the Pyrenees, with icefalls that affect their stability (January 2023), b) Intermediate image: entrance scenarios (home page in CoSpaces), c) virtual tour in rock slopes to gather the field data.

## References

- JORDÁ BORDEHORE L., RIQUELME A., CANO M., & TOMÁS R., 2017. Comparing manual and remote sensing field discontinuity collection used in kinematic stability assessment of failed rock slopes, *International journal of rock mechanics and mining sciences*, 97, 24- 32.
- DELGADO-REIVAN, X.; PAREDES-MIRANDA, C.; LOAIZA, S.; ECHEVERRIA, M.D.P.V.; MULAS, M.; & JORDÁ-BORDEHORE, L., 2023. Stability Analysis of Rocky Slopes on the Cuenca-Girón-Pasaje Road, Combining Limit Equilibrium Methods, Kinematics, Empirical Methods, and Photogrammetry. *Remote Sensing*, 15, 862.
- M T GARCÍA-VELA, C P BORJA-BERNAL, L JORDÁ-BORDEHORE, R MEDINACELI-TORREZ, S LOAIZA, & D A FALQUEZ., 2021. Teaching rock mechanics using Virtual Reality: laboratory practices and field trips during the confinement of the Coronavirus COVID-19 in Ecuador, Bolivia, and Spain, *ISRM Symposium EUROCK 2021 – Mechanics and Rock Engineering from Theory to Practice*, IOP Conf. Ser.: Earth Environ. Sci. 833.

# Advancing Geology Education through Immersive Virtual Reality Training Modules

Jian Yang<sup>1\*</sup>, Maximilian Hallenberger<sup>2</sup> & Florian Wellmann<sup>1</sup>

<sup>1</sup> Computational Geoscience, Geothermics and Reservoir Geophysics, RWTH Aachen University, Aachen, Germany, [jian.yang@eonerc.rwth-aachen.de](mailto:jian.yang@eonerc.rwth-aachen.de)

<sup>2</sup> Energy and Mineral Resources Group (EMR), Geological Institute, RWTH Aachen University, Aachen, Germany

**Key words:** virtual reality, geoscience, gempy, geoscience education, immersive training modules

Virtual reality (VR) can enhance geoscience education by providing interactive and immersive learning experiences within 3D digital environments. Within this study, we developed and tested two immersive modules, leveraging the power of VR technology to provide students with realistic and interactive learning experiences.

Both scenarios have been integrated into the virtual teaching platform “MyScore”, developed by the Institute of Teaching & Research Field Engineering Hydrology (RWTH Aachen University), and extensively adopted by numerous universities across Germany.

The first module, “Virtual Geological Mapping Training” (Fig. 1), focuses on developing students' proficiency in structural mapping techniques. It comprises of 21 geological models converted from the standard issue textbook by G.M. Bennison (1990) using GemPy, an open-source 3D geological modelling tool developed in python (de la Varga et al., 2019). Through a virtual field environment, students can practice the identification and analysis of geological structures, such as faults, folds, and joints. The module offers a range of geological scenarios, each presenting unique challenges that require students to apply their knowledge of structural geology. Real-time feedback and guided exercises aid students in honing their skills, promoting accurate interpretation and effective communication of geological structures.

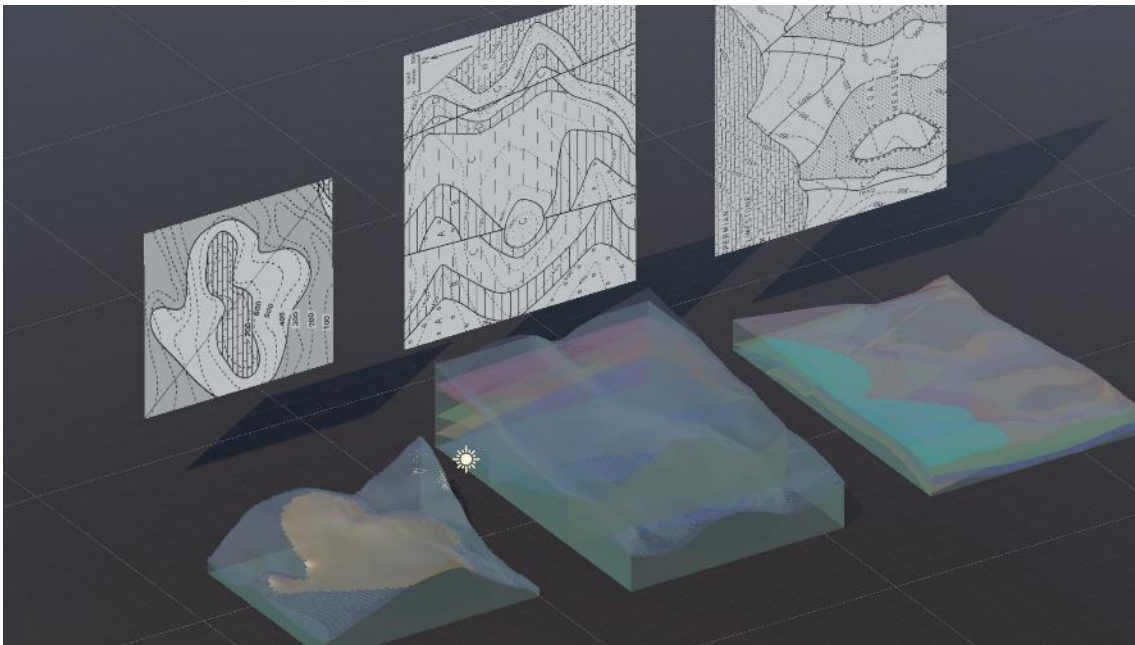


Figure 1: Virtual Geological Mapping Training built in Unity 3D game engine

The second module, “Rock Library Exploration”, immerses students in a comprehensive virtual rock library, designed to facilitate the identification of minerals and rocks. It includes over 70 specimens obtained through photogrammetry which have been either produced in-house or obtained from known online repositories. Students can navigate a vast collection of specimens, examining their physical properties, textures, and mineralogical composition. Interactive features allow students to rotate, magnify, and manipulate virtual specimens.

Preliminary evaluations of these immersive training scenarios have demonstrated their effectiveness in enhancing students' practical skills in geology. Students who engaged with these modules displayed improved accuracy in structural mapping and enhanced capabilities in identifying rocks and minerals. Furthermore, the immersive nature of the modules enhanced students' engagement, critical thinking, and spatial understanding of different geological concepts.

This research contributes to the evolving landscape of geology education, displaying the transformative potential of VR technology in developing practical skills. By immersing students in virtual field environments and interactive rock libraries, these training modules empower geology students to become proficient in structural mapping and mineral/rock identification, better preparing them for real-world geological exploration and research.

## References

DE LA VARGA, M., SCHAAF, A., & WELLMANN, F., 2019. GemPy 1.0: open-source stochastic geological modeling and inversion, *Geosci. Model Dev.*, 12, 1–32.

# Integrating Rapid Geomodeling with Mixed-Reality for Enhanced Geoscientific Applications

Miguel de la Varga<sup>1,2</sup>, Dr Simon Virgo<sup>1</sup>

<sup>1</sup>Terranigma Solutions GmbH, Aachen Germany

<sup>2</sup>Computational Geoscience, Geothermics and Reservoir Geophysics, RWTH University, Aachen Germany

**Key words:** *geomodeling, Mixed-Reality, Virtual Reality, Geosciences, Geodata Visualization, 3D*

Virtual and mixed reality technologies are reaching maturity for both professional and consumer applications, offering not only stereoscopic 3D visualization environments but also novel user interfaces with more immersive experiences of interacting with 3D content. Geosciences, which inherently deal with 3D complexities, can greatly benefit from these advancements. However, the potential benefits remain largely untapped for professional applications. Recent developments are bringing 3D geodata visualization with collaboration into virtual spaces. Nonetheless, the actual steps of 3D geological model creation and modification remain predominantly limited to workstation computers and 2D displays.

Addressing these limitations, we present LiquidEarth, a software solution that integrates rapid geomodeling with immersive mixed-reality environments. Utilizing a cloud-accelerated implicit modeling algorithm (powered by GemPy (DE LA VARGA *et al.*, 2019), LiquidEarth offers a dynamic experience of creating and updating 3D geological models in virtual spaces with real-time feedback (e.g., Fig 1). Cross-platform compatibility makes the solution device-agnostic, facilitating adoption in various geoscience applications and scenarios, including fieldwork.

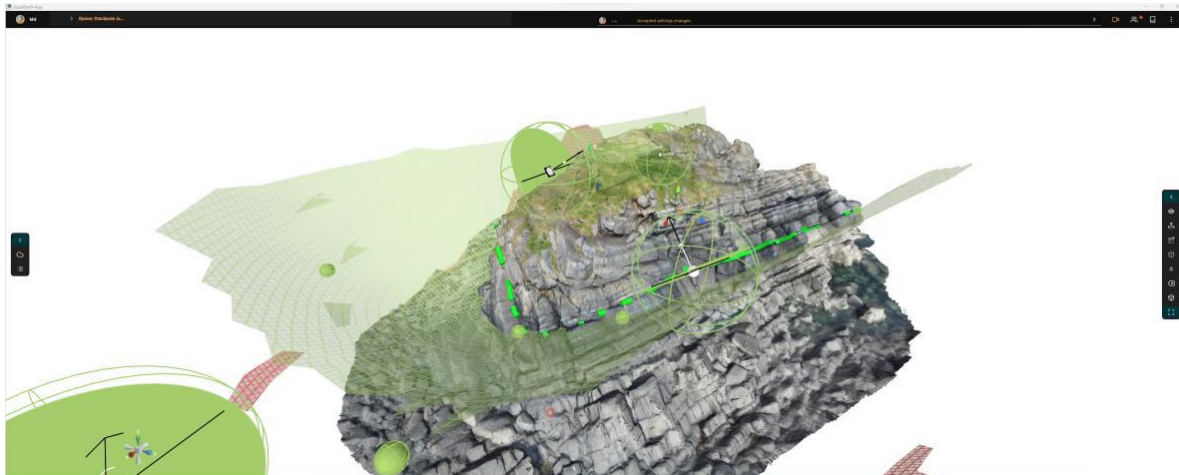


*Figure 1 Screenshot from the LiquidEarth platform showcasing the interpretation of an outcrop. The image highlights the application's capability to create and modify 3D geological models in an immersive mixed-reality environment*

The software combines features such as immersive visualization, real-time collaboration, field connectivity, workflow connectors, and flexible export options to create an integrated and versatile tool, making it ideal for geoscientific work in industry, research, and education. This holistic approach bridges the gap between immersive visualization of geological data and geological modeling, enabling geoscientists to harness the full potential of mixed reality technologies.

LiquidEarth signifies a substantial, yet initial, step towards the future of geomodeling by transcending traditional constraints. Its objective is to augment the geoscientific expert's ability to analyze and comprehend intricate geological 3D complexities while promoting the development of insightful conclusions.

## References

DE LA VARGA, M., SCHAAF, A., AND WELLMANN, F.: GemPy 1.0: open-source stochastic geological modeling and inversion, *Geosci. Model Dev.*, 12, 1–32, <https://doi.org/10.5194/gmd-12-1-2019>, 2019

# Towards an automated workflow for assessing effects of forest disturbance on land surface temperature in low mountain ranges of Central Germany using GEE and the Landsat archive

Simon Grieger<sup>1\*</sup>, Daniel Wyss<sup>1</sup>, Philipp Koal<sup>2</sup>, Ingolf Profft<sup>2</sup>, Lajos Blume<sup>1</sup> & Birgitta Putzenlechner<sup>1</sup>

<sup>1</sup> Georg August University of Göttingen, Institute of Geography, Dep. Cartography, GIS and Remote Sensing, Goldschmidtstr. 5, 37077 Göttingen, Germany

<sup>2</sup> Forestry Research and Competence Center (ThüringenForst AöR), Jägerstr. 1, 99867 Gotha, Germany  
\* [simon.grieger@uni-goettingen.de](mailto:simon.grieger@uni-goettingen.de)

**Key words:** forest disturbance, land surface temperature, time series analysis, forest monitoring, remote sensing, Landsat 8

Forests in Germany are under pressure due to drought stress and pest infestation, a trend which is projected to increase with global warming. In the spruce-dominated Southern Harz mountains in the German state of Thuringia, widespread forest disturbance caused defoliation and loss of forest cover. The same applies to other low mountain ranges in Central Germany. Shifts in forest vitality and vegetation cover can influence the land surface temperature (LST), an essential climate variable. LST derived from earth observation satellite data is used increasingly to study various processes related to climate change and land surface dynamics, in particular for research in vegetated and forested areas. For these areas, a loss of vitality or forest cover favours higher LST on summer days without cloud cover.

To assess the effects of forest disturbance on the LST on a regional scale, an automated workflow has been implemented to analyse a time series of the Landsat 8 Surface Temperature product, accessed via Google Earth Engine (GEE). On the level of individual Landsat raster cells with a spatial resolution of 30 m, an automated classification of forest disturbance level was performed using the phenology modelling approach by Löw & KOUKAL (2020), deriving forest disturbance from a time series of Sentinel-2 data. The addition of site-specific properties on the cell level allows for the identification of influencing factors, such as potential incoming solar radiation and potential soil water availability.

Results of this workflow applied to low mountain ranges in Thuringia indicate differences in the distributions of LST between disturbed and undisturbed forest stands, with a trend of higher temperatures in disturbed forest areas. Over the time series, the temperature difference between disturbed and undisturbed areas rises after forest disturbance events. The considered topographic and pedological site factors show varying influence depending on the level of forest disturbance.

The presented workflow is implemented to be applicable to other study areas, enabling assessment of the influence of forest disturbance on LST under different site conditions on a regional scale. Regarding increasing risk of forest disturbance and the necessity to adapt forest stands to a changing climate, knowledge of the factors influencing LST may aid in informed decision making in post-disturbance forest management.

## References

LÖW, M. & KOUKAL, T., 2020. Phenology Modelling and Forest Disturbance Mapping with Sentinel-2 Time Series in Austria. *Remote Sensing*, 12: 4191.

## UAV LiDAR-based tree detection and structural parameter estimation with a focus on the treeline ecotone

Alex Šrollerů<sup>1\*</sup>, Markéta Potůčková<sup>1</sup> & Václav Tremil<sup>2</sup>

<sup>1</sup> Charles University, Faculty of Science, Department of Applied Geoinformatics and Cartography, Albertov 6, Praha 2, Czechia, [srollera@natur.cuni.cz](mailto:srollera@natur.cuni.cz)

<sup>2</sup> Charles University, Faculty of Science, Department of Physical Geography and Geoecology, Albertov 6, Praha 2, Czechia

**Keywords:** LiDAR, ITD, UAV, parameters, treeline, forest

UAV LiDAR data (ULS) with a high point density ranging from tens to hundreds of points per square meter represents a versatile tool for forest inventory and environmental monitoring focused on conservation, biodiversity preservation, and proper functioning of forest ecosystem services. It is particularly suitable for smaller to medium-sized areas, less accessible locations, or when data must be acquired repeatedly at shorter time intervals. Due to the high dimensionality of the data and higher proportion of noise, the individual tree detection algorithms developed for airborne laser scanning (ALS) have limited transferability. Existing methods must be evaluated and, if necessary, modified over ULS data before they can be used reliably. Simultaneously, a comparison of individual methods using the same set of reference data, given stand type and area, is recommended so that the results are not influenced by these inputs and environmental variables. According to the results of the literature search, the use of individual tree detection methods in heterogeneous environments and for understory vegetation remains an unresolved topic for both ULS and ALS data.

Our study is focused on the comparison and development of ULS individual tree detection methods and the extraction of selected parameters (location, tree species, height, crown dimensions, diameter at breast height, crown height) at the tree level in a treeline ecotone, i.e., an environment characterized by stand heterogeneity in terms of vegetation density, height variability, and to a certain extent also species composition.

The area of interest is Krkonoše (50.75N, 15.58E) or the so-called Giant Mountains, a mountain range located in the north-western part of Czechia, stretching beyond the borders to Poland. The most valuable parts were declared a National Park in 1963 and 1952, on the Czech and Polish side, respectively. Ground elevation ranges from 400 to 1603 meters above sea level, with moderate to high relief. Highly endangered and rare treeless arctic-alpine tundra covers approximately 7.4 percent of the mountains. The ecosystem is affected by a continuous movement of the treeline to higher elevations.

Dendrometric measurements were carried out in 2018 and 2021 to monitor the dynamics of the upper forest boundary (Fig. 1). Throughout the summer months of 2023, new dendrometric measurements will be collected along with high-density LiDAR point clouds from a Riegl miniVUX-1 UAV laser scanner equipped with the APX-15 UAV GNSS/IMU and mounted on a hexacopter DJI M600. Data will be acquired throughout two gradients in the treeline ecotone with the aim of creating an open access database of sample plots covering a gradient of canopy closure, consisting of remote sensing data as well as reference measurements for testing and a more objective comparison of individual tree detection methods. First results of the research connected to the acquisition, processing of the data, and testing of the methods will be presented. High-density ULS point clouds will be compared to an existing ALS dataset (Fig. 1). From the point of view of physical geography, the knowledge gained will be applicable in the continuation of monitoring the dynamics of the treeline in the National Park and beyond.

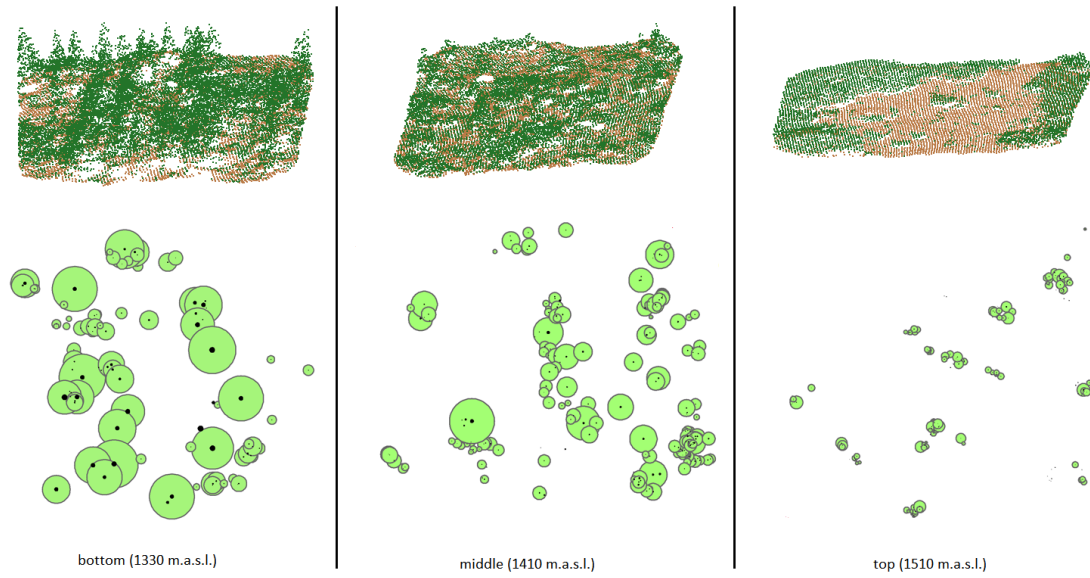


*Figure 1: ALS point cloud (top) and corresponding crown visualization from dendrometric measurements (bottom) throughout the gradient of the treeline ecotone – Modrý důl, Krkonoše mountains.*

**Acknowledgements:** The research is supported by the Grant Agency of Charles University (project No. 245023).

## SfM method for underground corridors modelling – Kletno mine example

Marcin Olkowicz<sup>1\*</sup>, Bartłomiej Grochmal<sup>1</sup>, Mariusz Fiałkiewicz<sup>1</sup>, Artur Sobczyk<sup>2</sup>, Paweł Zagożdżon<sup>3</sup> & Marcin Dąbrowski<sup>1</sup>

<sup>1</sup> Polish Geological Institute – National Research Institute, Lower Silesian Branch, Computational Geology Laboratory, al. Jaworowa 19, 53-122 Wrocław, Poland, molk@pgi.gov.pl

<sup>2</sup> Institute of Geological Sciences, University of Wrocław, Pl. M. Borna 9, 50-204 Wrocław, Poland

<sup>3</sup> Wrocław University of Science and Technology, Faculty of Geoengineering, Mining and Geology, Na Grobli St. 15, 50-421 Wrocław Poland

**Key words:** SfM, low light environment, underground objects reconstruction, fisheye photogrammetry

Low light and narrow space underground environments such as: caves, mines and other man-made tunnels are generally considered as photogrammetry-unfriendly. However, high quality models of such low accessible object are valuable source of information concerning tectonic and mining data, excavation stability, speleothem development, and other depending on the specific case. There are two major problems in photogrammetry based approaches to modelling underground objects. Firstly, lack of natural and usually insufficient artificial light, which affects image quality, and thereby quality of output model. Secondly, insufficient space for adequate camera positioning, which leads to increase in number of images required to cover entire corridor (walls, ceiling and floor). While applying classic close range photogrammetry approach, the above two issues combined make image acquisition difficult and time-consuming process, which also requires extra equipment to provide sufficient lighting.

To resolve those problems, we have prepared and tested a tailored approach, which minimizes hardware requirements, while at the same time allows for using simplified camera positioning schemes. On the hardware side, our approach needed two moderately expensive upgrades (~2500 EUR total). To deal with insufficient light conditions, we have used a custom battery powered handheld lamp, which provided diffused light. This allowed for an almost even illumination of the entire scenes, with amount of light sufficient to use low exposure times (below 1/50 s in our case) and allowing for taking shots directly from hand. This greatly decreased the time needed to take adjacent images. The problem of a proper coverage between images and insufficient space for camera positioning was resolved by using a diagonal fisheye lens with view angles 95°/140°/180° vertical/horizontal/diagonal. The fisheye lens allowed us to cover a sufficient area with a single shot even in narrow corridors. Simultaneously, we developed simplified camera positioning scheme, which consisted of twelve passes through the imaged corridor, with a roughly fixed camera to wall angle in each pass. Six passes were taken to image the walls, four for the ceiling and floor, and additionally two passes were executed with the camera directed parallel to the course of the corridor. The developed positioning scheme resulted in abundant, overlapping images taken at various angles and positions. The images evenly covered the walls, floor and ceiling, and thus reduced the chance of accumulating systematic errors along the corridor, which may lead to an overall deformation of the reconstructed object known from linear object reconstructions. Our approach required two people for image acquisition: one person to hold the lamp and the second to operate the camera. A low weight of the entire set - 1 kg for lamp, 1.5 kg per single battery allowing 3 hours of work, and 1.3 kg for DSLR camera with lens - makes the approach versatile for any underground works, especially in distant parts of underground objects such as caves, where the amount of taken gear is limited.

To test our approach, we performed a reconstruction of three adits located within the historical uranium mining region in Kletno, Lower Silesia, Poland, which have been inactive since the 50's. To validate our results, we compared the obtained models to available adit maps, including the original mine maps from the exploration period and some more recent compass and laser rangefinder based adit models. An example of the selected reconstructed adit is shown in Fig 1.

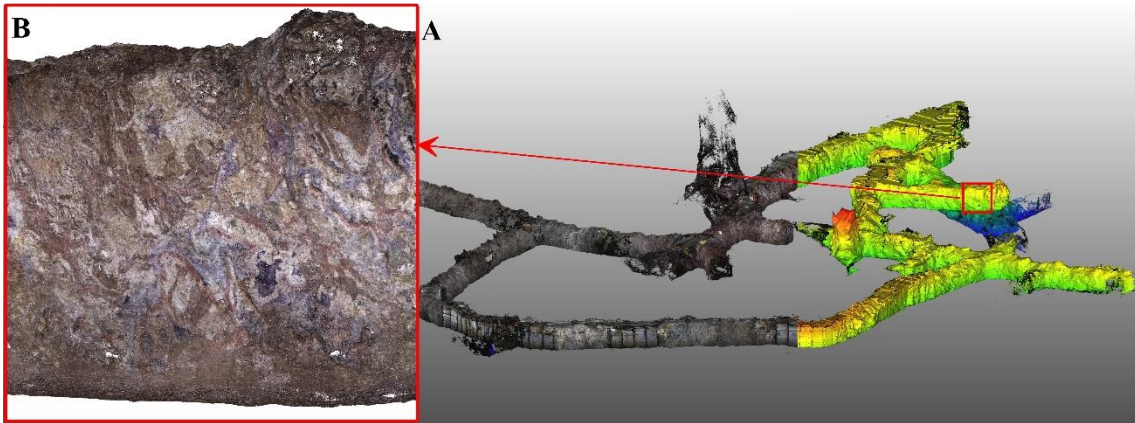


*Figure 1: An example of the reconstructed adit no. 18, A – an overall view of the 3d model; B – a closeup of a 2.5x2.5 m part of the corridor wall.*

## Workflow of unmanned aerial vehicle (UAV) application to railways geotechnical asset management

Oriol Pedraza<sup>1\*</sup>, Marc Janeras<sup>1</sup>, Iván García<sup>1</sup> & Toni Gil<sup>2</sup>

<sup>1</sup>Institut Cartogràfic i Geològic de Catalunya (ICGC), Parc de Montjuïc, 08038 Barcelona, Spain;

\*[oriol.pedraza@icgc.cat](mailto:oriol.pedraza@icgc.cat);

<sup>2</sup>Ferrocarrils de la Generalitat de Catalunya (FGC), C/ dels Vergós, 44, 08017 Barcelona, Spain.

**Key words:** UAV, geotechnical asset, railways, 3D point clouds, field survey.

The geotechnical assets are those components of the transportation infrastructure through which the ground has been adapted to the route (e.g., slopes, embankments, tunnels, retaining walls, rockfall fences, drains). These must be properly managed within the live-cycle operation of the infrastructure to offer permanent security conditions under control. In the case of the FGC rail network, more than 3,000 geotechnical assets are inventoried along 300 km of railways. ICGC is responsible for the geological and geotechnical monitoring of this network, covering the complete cycle of risk mitigation, from on-site surveys, asset condition analysis, maintenance, and investment planning, to project design and work management. In 2015, we started a digital migration of all this work, moving from reports to online interoperable geoinformation (SANTANA *et al.*, 2017) as the first steps, but this evolution has many applications to both field and office work, which are also aligned with the digital strategy of FGC with a 2030 horizon.

In 2018, ICGC incorporated the use of UAV as a working tool for the Geological Engineering Department to improve field surveys in all projects, including geotechnical asset management. The main objective of this innovation is to take advantage of new points of view for inspection by acquiring high-resolution and metric data to finally improve change detection capabilities. A workflow (Fig. 1) was developed to fully achieve this objective and cover the whole process up to sharing results with stakeholders in 3D geoinformation format.

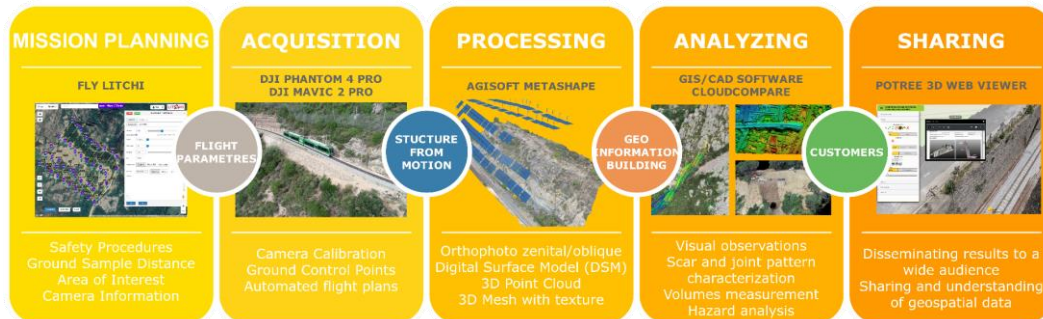


Figure 1: Workflow and results obtained when applying UAV to geotechnical assets in railways.

The workflow is distributed in three blocks. The first one consists of mission planning and data acquisition, designed following a logical approach that facilitates all the necessary steps to provide photographic material of the geotechnical asset. Mission planning includes legal authorization requirements for operations and the establishment of a safety check/protocol following the steps defined by the European Union Safety Agency (EASA). Once these requirements are in place, pre-flight mission preparation begins. For studies of rock massifs and rockfall fences, automated flight plans have been implemented with FlyLitchi drone software to cover the study area sequentially, capturing images repeatedly; however, for other geotechnical assets, such as slopes and retaining walls, where there may be poor GPS reception and magnetic interference from overhead lines, manual flights have been performed where experienced UAV pilots are required. The UAVs used are the DJI Phantom 4 Pro and DJI Mavic 2 Pro, which have sensors to avoid collisions, which is a great help in this type of flight.

Although the first objective is to capture images for a delayed inspection in the office or to generate a 3D point cloud, during a real-time inspection, it is also of great interest for expert technicians to obtain detailed photographs. The main disadvantage encountered in the use of UAVs with cameras in the inspection of geotechnical assets is the dense vegetation, which is an obstacle to the observation of elements of interest and to the quality of the images.

The second block consists of the processing and analysis of images acquired by UAVs and incorporated into the geotechnical asset management workflow. On the one hand, we have the images that are not processed and are used for the preparation of geological monitoring reports and construction management. On the other hand, sequentially captured images are used to generate 3D point clouds, generated by the software Agisoft Metashape, which combines photogrammetry and structure from motion (SfM) algorithms. Rockfall is the main geological risk on the railway network. Geometric analysis of the 3D point cloud allows kinematic and stability analysis (Tomás et al., 2020) and is of great help in the development of engineering projects for slope stabilization. Other products, such as orthophotos and digital surface models (DSM), allow detailed mapping and simulation of individual rock trajectories in 3D using software such as RockyFor 3D and RockGIS (Matas et al., 2023) for hazard analysis and fence design.

The last block deals with the communication of 3D geospatial data to improve its understanding and be able to share its contents with FGC in a simple way. Different web viewers have been generated with the Potree renderer to show more than 150 retaining walls distributed along three FGC railway lines (Fig. 2). These web viewers have been very useful to display a 3D point cloud of the geotechnical asset and to consult the proposed maintenance recommendations or improvement actions (PEDRAZA *et al.*, 2022). They also provide a set of measurement tools that can be exported into GIS and CAD programs.

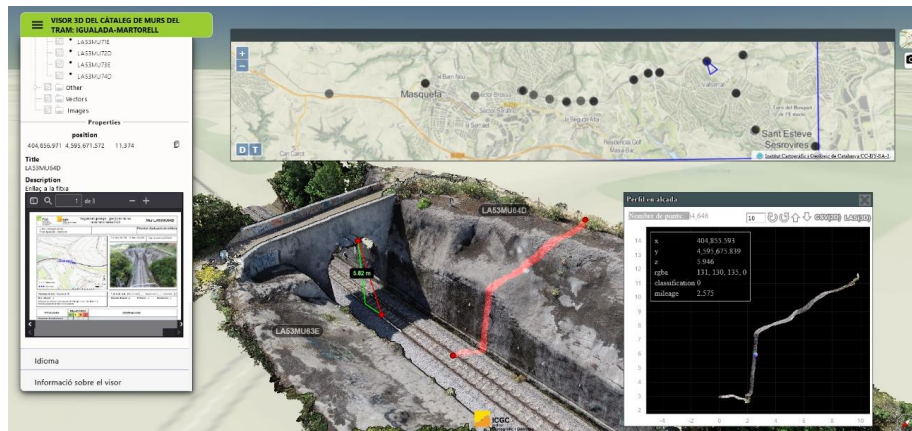


Figure 2. 3D web viewer of the catalog of retaining walls of the Llobregat-Anoia line of FGC, where some of the measurement tools present in the viewer are exemplified and the status of the asset can be consulted.

In conclusion, in these years of using UAVs, they have shown us that they are an inexpensive and fast solution for on-demand acquisition of detailed images of an area of interest and for the creation of 3D models. The use of UAVs on railways requires a good data processing base and good piloting skills, particularly in complex environments. Although the UAV workflow is exposed in this communication, it is our present duty to exploit it intensively. The future will lead to the incorporation of UAVs with LiDAR sensors and continuous data acquisition as mobile mapping.

**Acknowledgements:** The authors would like to especially acknowledge the colleagues of the Geological Engineering Team of the ICGC who are involved in this project.

## References

- MATAS, G., GILI, J., LANTADA, N. AND COROMINAS, J. 2023. The effect of rock fragmentation on rockfall barriers. *In 3<sup>rd</sup> JTCl Workshop on Impact of global changes on landslide risk. Oslo, Norway.*
- PEDRAZA, O., JANERAS, M., GILI, J.A., STRUTH, L., BULLI F., GUINAU, M., FERRÉ, A., ROCA, J., 2022. Comunicación de la geoinformación 3D mediante visores web y entornos inmersivos de realidad mixta en problemas de taludes y laderas. *In X Simposio Nacional sobre Taludes y Laderas Inestables. Granada, Spain. 537-548. ISBN 978-84-123222-7-9.*
- SANTANA, D., PONS, J., RODRÍGUEZ, H., PRAT, E., LÓPEZ, F., JANERAS, M., BUXÓ, P., FERRÉ, A., PARET, D., COMELLAS, J., 2017. Plataforma on-line para el seguimiento geológico y geotécnico de la red ferroviaria de FGC. *In IX Simposio Nacional sobre Taludes y Laderas Inestables. Santander, Spain. 674-685. ISBN 978-84-946909-5-2.*
- TOMÁS, R., RIQUELME, A., CANO, M., PASTOR, J.L., PAGÁN, J.I., ASENSIO, J.L., RUFFO, M. 2020. Evaluation of the stability of rocky slopes using 3D point clouds obtained from an unmanned aerial vehicle. *Revista de Teledetección, 55, 1-15. <https://doi.org/10.4995/raet.2020.13168>.*

## Sensing Mountains – Learning about the Observation of Environmental Processes in a Changing World

Martin Rutzinger<sup>1</sup>, Katharina Anders<sup>2</sup>, Magnus Bremer<sup>1,3</sup>, Anette Eltner<sup>4</sup>, Caroline Gaevert<sup>5</sup>, Bernhard Höfle<sup>2</sup>, Roderik Lindenbergh<sup>6</sup>, Andreas Mayr<sup>1\*</sup>, Sander Oude Elberink<sup>5</sup>, Francesco Pirotti<sup>7</sup>, Marco Scaioni<sup>8</sup>, Thomas Zieher<sup>1,9</sup>

<sup>1</sup> Department of Geography, University of Innsbruck, Innrain 52f, 6020 Innsbruck, Austria, martin.rutzinger@uibk.ac.at, magnus.bremer@uibk.ac.at, andreas.mayr@uibk.ac.at

<sup>2</sup> Institute of Geography, Heidelberg University, Im Neuenheimer Feld 368, 69120 Heidelberg, Germany, katharina.anders@uni-heidelberg.de, hoefle@uni-heidelberg.de

<sup>3</sup> Laserdata GmbH, Technikerstr. 21a, 6020 Innsbruck, Austria, bremer@laserdata.at

<sup>4</sup> Institute of Photogrammetry and Remote Sensing, Technische Universität Dresden, 01062 Dresden, Germany, anette.eltner@tu-dresden.de

<sup>5</sup> Faculty of Geo-Information Science and Earth Observation, University of Twente, Hallenweg 8, 7522 NH, Enschede, The Netherlands, c.m.gevaert@utwente.nl, s.j.oudeelberink@utwente.nl

<sup>6</sup> Dept. of Geosciences and Remote Sensing, Delft University of Technology, Stevinweg 1 / PO box 5048, 2628 CN Delft / 2600 GA Delft, The Netherlands, r.c.lindenbergh@tudelft.nl

<sup>7</sup> Department of Land, Environment, Agriculture and Forestry, Viale Dell'Università, 16 - Legnaro (PD), Italy, francesco.pirotti@unipd.it

<sup>8</sup> Department of Architecture, Built Environment and construction Engineering, Politecnico Milano, Via Ponzio 31, 20133 Milano, Italy, marco.scaioni@polimi.it

<sup>9</sup> Department of Natural Hazards, Austrian Research Centre for Forests (BFW), Rennweg 1, Hofburg, 6020 Innsbruck, Austria, thomas.zieher@bfw.gv.at

**Key words:** Remote Sensing, Close-range Sensing, Earth Observation, Mountain Research, Geomorphology, Landscape Ecology, Natural Hazard Research

The international summer school Sensing Mountains, which was held for the first time in 2015 in Obergurgl (Austria), is a biannual event for early career scientists bringing together international researchers from Geosciences, Biosciences and Engineering for mapping and analysing of geospatial data in mountain environments. The summer school takes up the rapid developments in sensor innovations in close-range and remote sensing and teaches participants how to apply methods for quantifying changes in a highly dynamic environment. A vital combination of input talks by invited keynote speakers, hands-on lectures and supervised practical assignments comprising project planning, sensor handling, data acquisition (Fig. 1), data analysis, reporting and presentation (Fig. 2) gives insights in both challenges in fundamental mountain research and tailored data acquisition for aiding in scientific reasoning (RUTZINGER et al. 2022). Practical assignments in 2022 comprised multitemporal 3D observation of geomorphic surface activity using point cloud-based change analysis and virtual laser scanning, monitoring long-term mountain river change based on point-cloud comparison techniques, comparison of close-range sensing approaches and sensors for extracting forest parameters, remote sensing of tree needle moisture content, analysing high resolution land surface structure and temperature, measuring river flow velocities with unteamed aerial vehicles, and implementing a digital twin of a natural environment. The long tradition of Sensing Mountains made it possible to build up monitoring data sets of selected sites around the venue comprising different phenomena of Alpine geomorphology and ecology, which are published as open access data sets at the pangaea.de platform. The next edition of #sensingmountains will take place from 22<sup>nd</sup> to 28<sup>th</sup> September 2024 (<https://www.uibk.ac.at/de/geographie/sensing-mountains/>).



*Figure 1: Measuring targets in the field for georeferencing 3d point clouds and orthophotos from photogrammetric unteamed aerial vehicle surveys.*

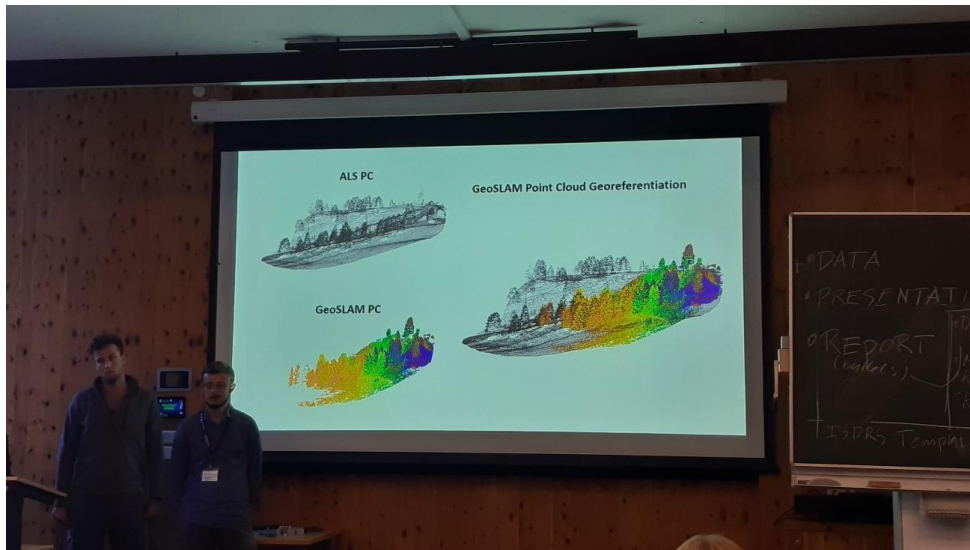


*Figure 2. Participants present their results of group assignments at the end of the course.*

**Acknowledgements:** The summer school organisational committee thanks for the financial support by the Faculty of Geo- and Atmospheric Sciences and the Department of Geography of the University of Innsbruck, 3DForEcoTech COST Action CA20118, RIEGL Laser Measurement Systems GmbH, LASERDATA GmbH, DMT GmbH & Co. KG, AllTerra Österreich GmbH. Furthermore, we thank the team of the University Centre Obergurgl for their professional and supportive hosting.

## References

RUTZINGER, M.; ANDERS, K.; BREMER, M.; ELTNER, A.; HÖFLE, B.; LINDENBERGH, R.; MAYR, A.; OUDE ELBERINK, S.; PIROTTI, F.; SCAIONI, M.; TOLKSDORF, H.; ZIEHER, T. (Eds.) (2022): Sensing Mountains. Innsbruck Summer School of Alpine Research 2022 – Close Range Sensing Techniques in Alpine Terrain. Innsbruck: innsbruck university press (IUP). <https://doi.org/10.15203/99106-081-9>

## Comparing the in situ and SfM methods for brittle tectonics analysis – a case study of the Strzegom-Sobótka granite massif

Bartłomiej Grochmal<sup>1\*</sup>, Mariusz Fiałkiewicz<sup>1</sup>, Marcin Olkowicz<sup>1</sup> & Marcin Dąbrowski<sup>1</sup>

<sup>1</sup> *Computational Geology Laboratory, Polish Geological Institute – National Research Institute, [bgroc@pgi.gov.pl](mailto:bgroc@pgi.gov.pl)*

**Key words:** *photogrammetry, structural geology, brittle tectonics, structural analysis, joints, UAVs*

This study aims to conduct a thorough comparison between classical field measurements of brittle structures and analysis of photogrammetric models of selected granite quarries using the CloudCompare software. The focus of investigation lies within the Strzegom – Sobótka granite massif, where 3D photogrammetric models have been derived from high-resolution aerial imagery captured by an unmanned aerial vehicle (UAV).

Strzegom – Sobótka granite massif is located in the Fore Sudetic block which lies in the NE part of the Bohemian Massif, about 50 km southwest from the city of Wrocław in SW Poland. Strzegom – Sobótka massif is composed of four main varieties: hornblende-biotite granite and biotite granite in the western part and biotite granodiorite and two-mica granite in the eastern part. This diversity indicates a complex evolution with variable contribution of mantle and crustal magma sources, fractional crystallization and mixing/mingling as main diversification factors. The main structural feature of these rocks are joints. Four sets of vertical joints were described from this region: NW-SE set, which was termed as “Q”, NE-SW set, termed as “S”, and two diagonal sets oriented N-S and W-E. Our results are generally compatible with these sets but greater complexity was observed. Initial paleostress analysis results for faults with slickensides show extension in the ENE-WSW to NE-SW direction.

Integration of photogrammetry holds the potential to overcome limitations of classical field measurements, especially when it comes to measurements of inaccessible and/or dangerous parts of quarries, providing enhanced accuracy and a more comprehensive understanding of structural data. Therefore we used a drone to capture high-resolution imagery of the quarries within the Strzegom – Sobótka granite massif. Utilizing photogrammetric techniques, the acquired imagery was then processed to generate a detailed 3D point cloud models. Subsequently, the CloudCompare software, equipped with a compass plugin, facilitated the measurement of joint and fault orientations within each analysed quarry.

Preliminary findings indicate that the integration of photogrammetry with structural geology analysis provides a valuable tool for obtaining measurements thus allowing for more in-depth analysis. This bears relevance to geological mapping, hazard assessment, and resource exploration, as accurate and exhaustive structural data plays a pivotal role in comprehending deformation processes and forecasting potential geological hazards.

## Structural analysis in the quarries and outcrops of the Moravo-Silesian fold and thrust belt: a case study using photogrammetry methods

Mariusz Fiałkiewicz<sup>1\*</sup>, Bartłomiej Grochmal<sup>1</sup>, Marcin Olkowicz<sup>1</sup> & Marcin Dąbrowski<sup>1</sup>

<sup>1</sup> *Computational Geology Laboratory, Polish Geological Institute – National Research Institute, [mfia@pgi.gov.pl](mailto:mfia@pgi.gov.pl)*

**Key words:** *Photogrammetry, tectonics, structural geology, structural analysis, 3D model, UAVs*

The Moravo-Silesian fold and thrust belt, which is located in northeastern part of Czech Republic and in southwestern Poland, at the eastern part of the Bohemian Massif, is renowned for its complex tectonic history and structural intricacies. This structure is made of a minor pre-orogenic Devonian sediments and up to 7.5 km thick syn-orogenic succession of Carboniferous sedimentary rocks, that constitute the deformed part of Variscan foreland basin (MAZUR *et al.* 2006). Four formations are distinguished within this unit: Andelska Hora Fm (shales, siltstones and greywackes, lower-middle Viséan), Horni Benesov Fm (mostly greywackes, middle Viséan), Moravice Fm (shales and siltstones with intercalations of greywackes, upper Viséan) and Hradec-Kyjovice Fm (shales, siltstones and greywackes, upper Viséan-Namurian A) (BABEK *et al.* 2004). Moravo-Silesian fold and thrust belt is elongated in the north-south to northeast-southwest direction with thrusts striking mainly northeast-southwest and fold axes trending mainly north-south (RAJLICH 1990). This structure is exposed in the Drahaný Uplands and Nizký Jeseník Mountains separated by the Olomuc Depression. This abstract presents a case study focused on the application of photogrammetry techniques to analyze tectonic structures at the quarry and outcrop scale within this geological region.

By employing aerial and regular imagery obtained through drone and cameras, and utilizing structure from motion (SfM) methods, we have successfully constructed detailed 3D models of the selected quarries and outcrops of the Moravo-Silesian fold and thrust belt rocks. Acquired images were processed using Agisoft Metashape software in which 3D models, that provide a high-resolution representation of the complex deformation pattern within given outcrop or quarry were constructed. We have used these models in CloudCompare software to extract quantitative data on the orientations of brittle structures such as faults (Fig. 1 (a)) and joints, and on the geometries of folds (Fig.1 (b)).

The utilization of photogrammetry has allowed us to overcome traditional limitations associated with field-based structural analysis and contribute to the growing body of knowledge on the application of photogrammetry methods in structural geology. Through our study, we aim to shed light on the tectonic evolution and deformation mechanisms that have shaped the Moravo-Silesian fold and thrust belt over geological time.

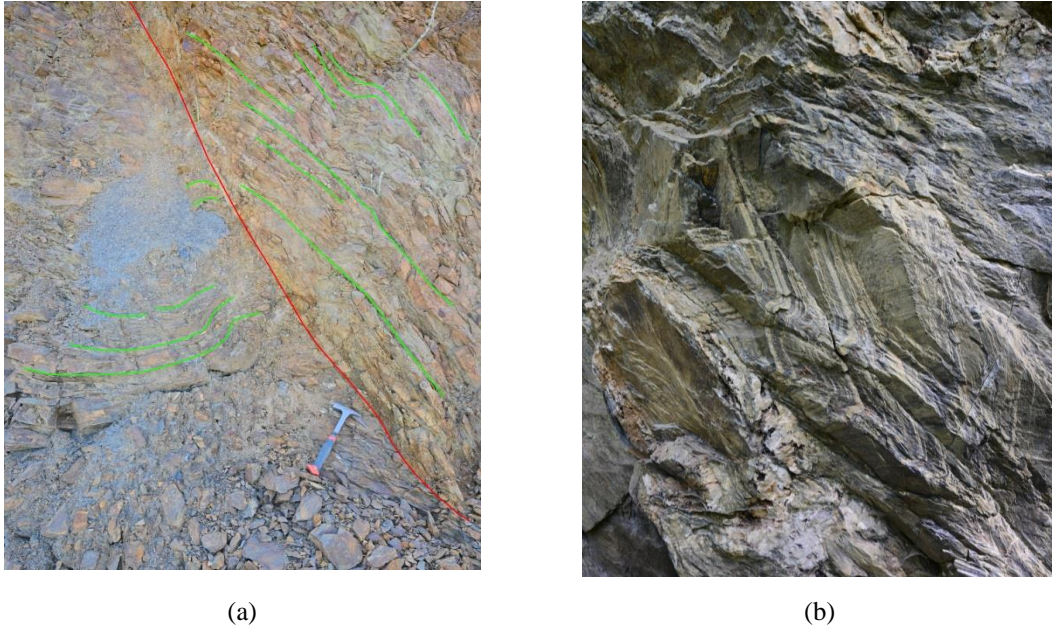


Figure 1: Examples of analysed structures: (a) fault and folded bedding, greywacke quarry "Dębowiec", Horni Benesov Formation, (b) folds in phyllites, Pokrzywno, Andelska Hora Formation

**Acknowledgements:** This research is a part of POLARIS project funded by National Science Centre of Poland, based on the decision number 2020/39/I/ST10/00818.

## References

- BABEK, O., MIKULAS, R., ZAPLETAL, J., & LEHOTSKY, T., 2004. Combined tectonic-sediment supply-driven cycles in a Lower Carboniferous deep-marine foreland basin, Moravice Formation, Czech Republic. *International Journal of Earth Sciences*, 93: 241-261.
- MAZUR, S., ALEKSANDROWSKI, P., KRYZA, R., & OBERC-DZIEDZIC, T., 2006. The Variscan Orogen in Poland. *Geological Quarterly*, 50: 89-118.
- RAJLICH, P., 1990. Strain and tectonic styles related to Variscan transpression and transtension in the Moravo-Silesian Culmian basin, Bohemian Massif, Czechoslovakia. *Tectonophysics*, 174: 351-367.

# Semi-automatic discontinuity detection using density in point cloud data

Antonin Chalé, Michel Jaboyedoff, and Marc-Henri Derron

*Institute of Earth Sciences, University of Lausanne, lausanne, Switzerland (antonin.chale@unil.ch)*

**Keywords:** *density map, point cloud (PC), structure from motion (SFM), Light Detection and Ranging (LiDAR)*

Studying and characterizing discontinuities is a fundamental step in hazard analysis for rock walls. Parameters such as the frequency and orientation of discontinuity families are crucial for evaluating the probability of rock volumes involved in potential movement, including sliding or toppling phenomena. The progress of techniques such as Structure-from-Motion (SFM) and Light Detection and Ranging (LiDAR) acquisition methods has revolutionized these surveys, enabling remote analysis entire cliffs. These acquisition methods provide access to high-density and accurate 3D point clouds (PC) data. However, detecting structural irregularities using PC data has faced challenges in achieving reliable results, especially for complex structures. For instance, the least square method can easily fit planar surfaces and has shown many good results. It is commonly used for semi-automatic discontinuity recognition. However, it still struggles in some cases, such as detecting curved discontinuities.

To overcome these limitations, we have developed a novel discontinuity detection algorithm. Our method focuses on emulating human perception of volume by detecting point alignments. The point cloud is scanned from multiple angles (viewpoints) to capture all possible visible planes representing discontinuities and faults, characterized by a densification of points from specific viewpoints. By leveraging point cloud optimization techniques, such as octree, and implementing effective multiprocessing, the scanning process achieves sufficient speed to process large amounts of data within a limited time frame. This initial analysis step adds a new dimension to our point cloud, allowing us to cluster different faulting systems using the DBSCAN method. The clustered faults are then stacked and polygonised to visualize the entire faulting system (figure 1).



*Figure 2: on the left picture of the real data scan of the yellow quarry Ferreyres. On the right density map of the yellow quarry in Ferreyres, generated using a specific viewpoint (angle of the viewpoint =  $\phi$ : 0,  $\theta$ : 0,  $\psi$ : 75). The color range indicates the point cloud density for this viewpoint.*

Our method has demonstrated effectiveness in detecting discontinuities expressed by surface on PC, as well as determining their number, orientation, and spatial frequency on simple synthetic models with variable point density and some variable noise input. Moreover, when applied to real LiDAR data our approach has yielded promising results on the yellow quarry of Ferreyres (Figure 2). Our current algorithm is at present limited to small point clouds. To further enhance the scanning efficiency, future improvements could include the application of gradient optimization or the implementation of GPU multiprocessing. By incorporating point density as an additional dimension (PC density), our method opens up new avenues for leveraging PC data. In

future work, we aim to further validate our algorithm and compare its outcomes with more traditional discontinuity detection methods.

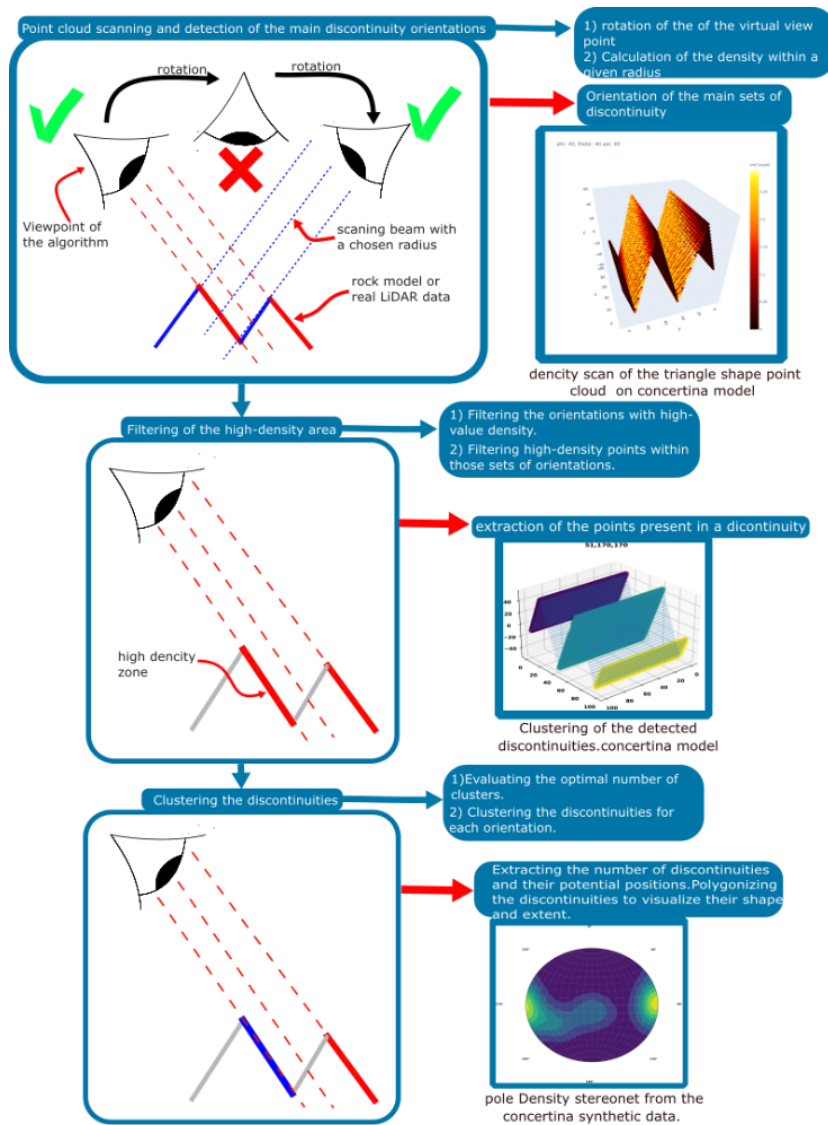


Figure 2: schema describing the 3 main step of the discontinuity detection algorithm.

## Integration of remote sensing techniques for slopes monitoring

M<sup>a</sup> Amparo Núñez-Andrés<sup>1\*</sup>, Felipe Buill<sup>1</sup>, Francisco Javier Muñoz<sup>1</sup>, Oriol Pedraza<sup>2</sup> & Marc Janeras<sup>1,2</sup>

<sup>1</sup> Department of Civil and Environmental Engineering, Universitat Politècnica de Catalunya-BarcelonaTech, C/Dr. Marañón 44-50, 08028 Barcelona, Spain \*m.amparo.nunez@upc.edu

<sup>2</sup> Institut Cartogràfic i Geològic de Catalunya (ICGC), Parc de Montjuïc, 08038 Barcelona, Spain

**Key words:** Terrestrial digital photogrammetry, UAV-laser scanning, TLS, UAV-photogrammetry, integration, vegetation, 3D models.

Geomatics techniques and methods have played a significant role in monitoring systems over the past two decades. The two most commonly utilized techniques are photogrammetry and laser scanning, which we find in both terrestrial and aerial versions usually from an unmanned aerial vehicle (UAV). These techniques provide 3D point clouds, allowing a multi-temporal analysis for both campaigns or continuous monitoring.

In the context of rockfall analysis, geomatics techniques are applied in characterizing hillslopes or cliffs, identifying unstable rock volumes, and monitoring their movement prior to potential falls (KROMER *et al.*, 2019) (BLANCH *et al.*, 2021) (NUÑEZ-ANDRÉS *et al.*, 2023). Additionally, they are used to detect rockfall activity and quantify detached volumes (ABELLAN, 2009). The information gathered through these methods is essential for establishing the magnitude-frequency relationship (JANERAS *et al.*, 2023) essential in the process of quantitative risk assessment.

One of the main challenges lies in determining the most suitable technique for each specific case. In Castellfollit de la Roca (Catalonia, Spain) we have observed the cliff composed of distinctive basaltic columns with all these techniques, Fig. 1:

- Terrestrial photogrammetry. Starting from September 2021, we have implemented a continuous mode terrestrial photogrammetry system equipped with three Canon EOS 6D Mark II cameras. This system serves for premonitory rockfall detection, capturing images with a ground sampling distance (GSD) of less than 10 mm, while for the models the GSD is approximately 20 mm.
- Terrestrial laser scanning (TLS). Since 2021, two campaigns per year have been conducted using the Leica ScanStation P50 to detect and characterize rockfalls. The GSD of the models is approximately 30 mm.
- UAV Photogrammetry. Annually, one campaign has been conducted since 2020 using the DJI Inspire 2 with the Zenmuse X4S camera. The resulting models have a GSD of 5 mm.
- UAV LiDAR. A pilot campaign was done in May 2022. The airborne laser scanning used is the Riegl VUX-1UAV. The GSD of the models is 50 mm in Z, and 100 mm in the horizontal component.

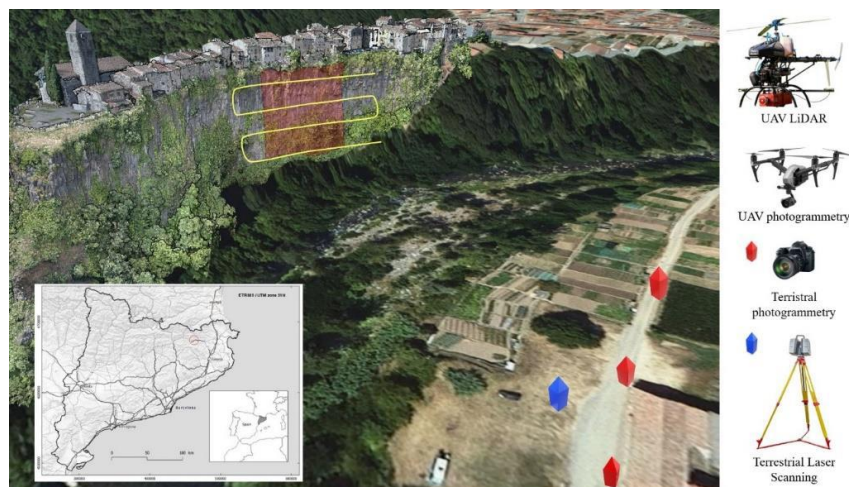


Figure 1: Techniques used in Castellfollit de la Roca (Girona, Spain)

This overlap allows us to make a complete comparison of the different techniques in extremely challenging terrain with significant limitations for some of them. The main drawback to the terrestrial techniques is the work distance due to the river. Moreover, the riparian vegetation limits the visibility of terrestrial devices located on the opposite side of the river Fluvià. In this comparison we consider factors such as accuracy, resolution, completeness, capture and processing time, versatility of the information and cost among others. Until now, the three techniques have allowed us to detect unstable basaltic column and monitor their movement before the fall. Fig. 2 shows the example using photogrammetry from UAV.



Figure 2. Example of change detection with UAV Photogrammetry comparing three campaigns.

Any technique is completely suitable, the black color of the basaltic cliff, the position and vertical structure of the prisms cause different problems in data capture and processing, such as unwanted brightness, homogeneity of the surfaces, cracks and wet surfaces, and the rapid growth of seasonal vegetation, etc. It makes it necessary to integrate data of different natures to get the best out of each of them for analysis. In this sense, before any processing, the vegetation must be filtered and we try to take advantage of the use of the mask obtained from terrestrial RGB or UAV images in the filtering process as it gives better results than the intensity of the LiDAR data. This mask will be used in the 3D point clouds to reduce the computation time in uninteresting areas and to avoid erroneous data.

**Acknowledgements:** This research has been developed in the frame of the project GeoRisk, “Advances in rockfall quantitative risk analysis (QRA) incorporating developments in geomatics (GeoRisk)”, grant number PID2019-103974RB-I00, funded by MCIN/AEI/10.13039/501100011033, Ministerio de Ciencia e Innovación and Agencia Estatal de Investigación of Spain

## References

- ABELLÁN, A. 2009. Improvements in Our Understanding of Rockfall Phenomenon by Terrestrial Laser Scanning: Emphasis on Change Detection and Its Application to Spatial Prediction. Ph.D. Thesis, Universitat de Barcelona, Barcelona, Spain. <https://diposit.ub.edu/dspace/handle/2445/27324>
- BLANCH, X., ELTNER, A., GUINAU, M. & ABELLAN, A. 2021. Multi-Epoch and Multi-Imagery (MEMI) Photogrammetric Workflow for Enhanced Change Detection Using Time-Lapse Cameras. *Remote Sensing* 13, no. 8: 1460. <https://doi.org/10.3390/rs13081460>
- JANERAS, M., LANTADA, N., NÚÑEZ-ANDRÉS, M.A., HANTZ, D., PEDRAZA, O., CORNEJO, R., GUINAU, M., GARCÍA-SELLÉS, D., BLANCO, L., GILI, J.A. & PALAU, J. 2023. Rockfall Magnitude-Frequency Relationship Based on Multi-Source Data from Monitoring and Inventory. *Remote Sensing* 15, no. 8: 1981. <https://doi.org/10.3390/rs15081981>
- KROMER, R., WALTON, G., GRAY, B., LATO, M. & GROUP, R. 2019. Development and Optimization of an Automated Fixed-Location Time Lapse Photogrammetric Rock Slope Monitoring System. *Remote Sensing* 11, no. 16: 1890. <https://doi.org/10.3390/rs11161890>
- NÚÑEZ-ANDRÉS, M.A., PRADES-VALLS, A., MATAS, G., BUILL, F. & LANTADA, N. 2023. New Approach for Photogrammetric Rock Slope Premonitory Movements Monitoring. *Remote Sensing* 15, no. 2: 293. <https://doi.org/10.3390/rs15020293>

# Cliff overhang mapping on 3D point clouds with Cloud Compare

Thomas JB Dewez<sup>1\*</sup>, Clara Lévy<sup>1</sup>, Claire Myr<sup>2</sup>

<sup>1</sup> BRGM – Direction Risques et Prévention, F-45060 Orléans, France, [t.dewez@brgm.fr](mailto:t.dewez@brgm.fr) [c.levy@brgm.fr](mailto:c.levy@brgm.fr)

<sup>2</sup> BRGM – Direction Régionale de Normandie, F-76130 Mont-Saint-Aignan, [c.myr@brgm.fr](mailto:c.myr@brgm.fr)

**Key words:** Point cloud processing, cliff, instability, overhang, cliff base cavity, MoveMin, MoveMax, Cloud Compare, rasterize tool, segmentation

Cliff geometry holds strong clues for future instabilities. Whether rock fall, rock sliding or wedge failure, all three phenomena require an unbuttressed downslope escape. At present, Cloud Compare implements two complementary tools for mapping potential failure planes from 3D cliff point clouds : the automated tool Facets (Dewez *et al.*, 2016) and the user-driven tool Compass (Thiele *et al.*, 2017). Facets assumes that fractures possess a sizeable surface expression on which a best-fit plane will adjust. Compass helps map either fracture surfaces or fracture traces. Both tools help dealing with potential failure planes constraining the geometry of rock slidings and wedge failures.

When it comes to anticipate rockfall failures, segmenting overhanging masses has not seen a mapping solution yet. In this communication, we propose a Cloud Compare approximated solution to resolve these geometries, demonstrate its use, successes and limits.

An overhang is a portion of unsupported cliff that can only be accurately rendered in full 3D, because several elevations Z do occur for a given XY position. An overhanging mass stands ahead of the deepest recess of the cliff. But where lies the deepest recess and can it be mapped automatically ? The Move Min/Move Max signal processing technique helps resolve this question. The function samples the signal with regular cells and assigns the maximum (or minimum) signal value to the cell centre. In Cloud Compare, the rasterize tool accomplishes this in 2.5D. When meshed, the minimum and maximum surfaces define the outcrop envelope. A Cloud2Mesh distance from each mesh to the original cloud expresses the distance in front of the minimum surface (overhang), or behind the maximum surface (recess) (Figure 7). Thresholding positive or negative Cloud2Mesh distances segments either cavity points or overhanging points.

This approach only approximates the vertical limits of overhanging masses or cavities on a grid. The exact near-vertical gradient is  $\text{atan}(dZ/[2*\text{grid step}])$ . The narrower the grid step, the steeper the gradient and the closer to true vertical. But grid steps cannot be too narrow or some cell will remain empty and miss data. Gridding also induces some degree of aliasing (jagged plan view edges of the overhang/cavity). To minimize aliasing issues, three solutions are at hand : (i) attributing the maximum (minimum) value to the actual point position instead of cell centre, (ii) reducing cell size yet making sure to maintain at least one point per cell, (iii) reducing grid obliquity with respect to cliff strike by aligning the local grid coordinate system to the cliff trend.

This method was applied to a coastal chalk cliff at Cape Fagnet, Fécamp Normandy (northern France). Cavities undermining the cliff occur at two elevations. The expected first level lies close to high tide level at the foot of the cliff. The second level sits near 15-20m elevation. The higher cavities are 10-15-m-high and 2-10-m-deep. They happen to be perched just above the Upper Cretaceous Turronian/Coniacian impermeable stratigraphic contact and undermine the upper section of the cliff (Figure 7). On 23 February 2023, an overhanging mass of 12 000 m<sup>3</sup>, as a first field estimate, collapsed from the cliff. The geometry before and after failure was constrained thanks to oblique aerial photographs (and their associated 3D topographic models) shot five years apart, on 16 April 2018 and 19 April 2023. This event is adequately predicted when applying our method to detect overhanging masses on the 2018 photogrammetric model of the cliff. The Move Min Move Max method is therefore a precious tool to help determine the likely magnitude of future rockfall events.

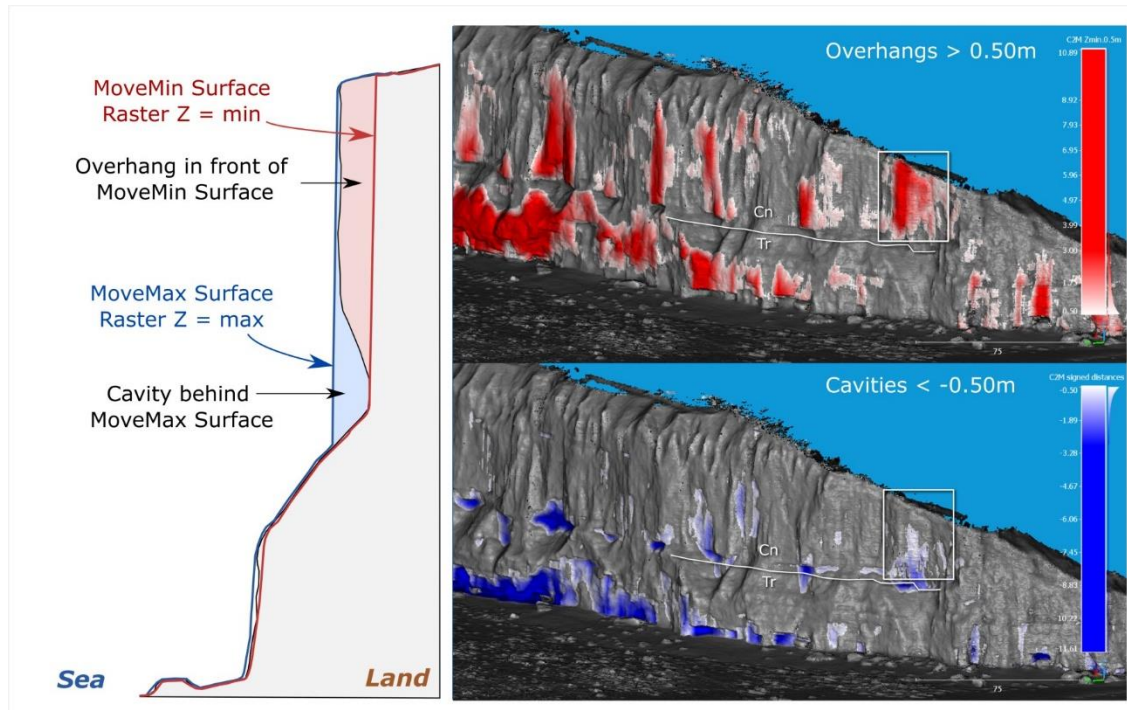


Figure 7 Principle of MoveMin and MoveMax point cloud filtering along Z coordinate. The MoveMin filter equates to rasterizing the point cloud, retaining only minimum Z values in each pixel. Overhangs stand in front of the raster Zmin mesh surface (in red). The MoveMax filter equates to rasterizing the points cloud retaining only the maximum Z value in each cell. Cavities stand behind the raster Zmax mesh surface (in blue). At Cape Fagnet chalk cliff site, the impermeable contact between Turonian (Tr) and Coniacian (Cn) (Upper Cretaceous) roots a level mid cliff cavities that decouples lower and upper cliff. White rectangle delineates the 23 Feb 2023 cliff collapse event. The collapsed mass only involved the upper cliff section undermined by mid-elevation cavities, not the entire height

**Acknowledgments:** This research was funded, in part, by ANR grant ANR-16-CE03-0008. A CC-BY public copyright license has been applied by the authors to the present document and will be applied to all subsequent versions up to the Author Accepted Manuscript arising from this submission, in accordance with the grant's open access conditions.



## References

- Dewez, T.J.B., Girardeau-Montaut, D., Allanic, C., Rohmer, J., 2016. FACETS: a CloudCompare plugin to extract geological planes from unstructured 3D point clouds. *The International Archives of the Photogrammetry, Remote Sensing and Spatial Information Sciences* XLI-B5, 799–804. <https://doi.org/10/gcc732>
- Thiele, S.T., Grose, L., Samsu, A., Micklethwaite, S., Vollgger, S.A., Cruden, A.R., 2017. Rapid, semi-automatic fracture and contact mapping for point clouds, images and geophysical data. *Solid Earth* 8, 1241–1253. <https://doi.org/10.5194/se-8-1241-2017>

# Updating of Rockfall inventory in the Montserrat massif (Spain): attributes in Point clouds for hazard assessment using Machine Learning techniques.

Garcia-Sellés, D.<sup>1\*</sup>, Blanco, L.<sup>2</sup>, Janeras, M.<sup>3</sup>, Pedraza, O.<sup>3</sup>

<sup>1</sup> *Departament de Dinàmica de la Terra i de l'Oceà, GRC RISKMAT, UB-Geomodels, Facultat de Ciències de la Terra, Universitat de Barcelona (UB). 08028 Barcelona, Spain [dgarcia@ub.edu](mailto:dgarcia@ub.edu)*

<sup>2</sup> *Anufra, soil & Water Consulting, 08028 Barcelona, Spain*

<sup>3</sup> *Institut Cartogràfic i Geològic de Catalunya (ICGC), 08038 Barcelona, Spain*

**Key words:** TLS, Rockfall, Monitoring

The monitoring of rockfalls in the vertical cliffs close to the infrastructures of the tourist-religious area of the Montserrat massif (Barcelona, Spain) is a project that began in 2007 and is still active. Terrestrial Laser Scanners (TLS) techniques and their continuous evolution for the identification of rockfalls have marked this project, where the importance of using the most recent techniques has been a constant. In recent years, the incorporation of Machine Learning techniques pursues the objective of automating the process of identifying rockfalls and optimizing the time required for this task. Initially, the methodology was applied in the Degotalls E cliff and later, in Degotalls N and actually the cliff closest to the Monastery is been processes. The update has also replaced the use of Optech's TLS ILRIS-3D model with Leica Geosystems' P50 model.

The contribution of the Leica P50 model consists of a higher speed of point capture and an increase in the spatial resolution of the outcrop. The methodology used (BLANCO et al., 2022) is based on variations of the M3C2 and DBSCAN algorithms and the classification of clusters by Machine Learning. The inventory has been used to achieve a complete characterization of the nature of the cliffs and to deepen the analysis of the data (JANERAS et al., 2023).

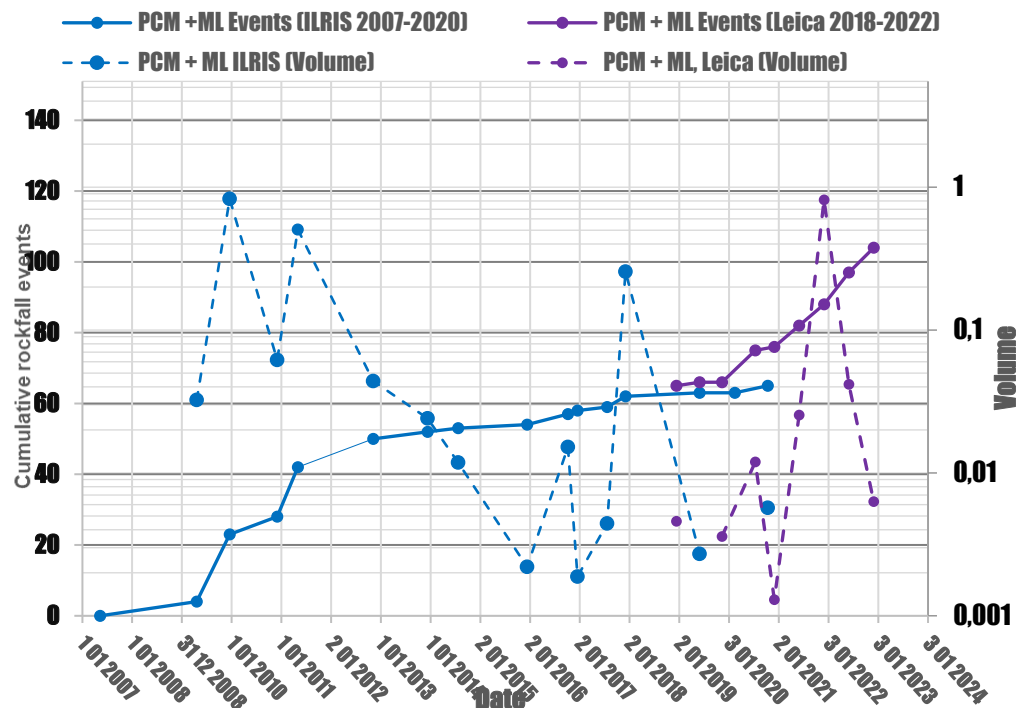


Figure 1: Graphic showing the cumulative number of events and total volume of rockfalls detected in Montserrat E.

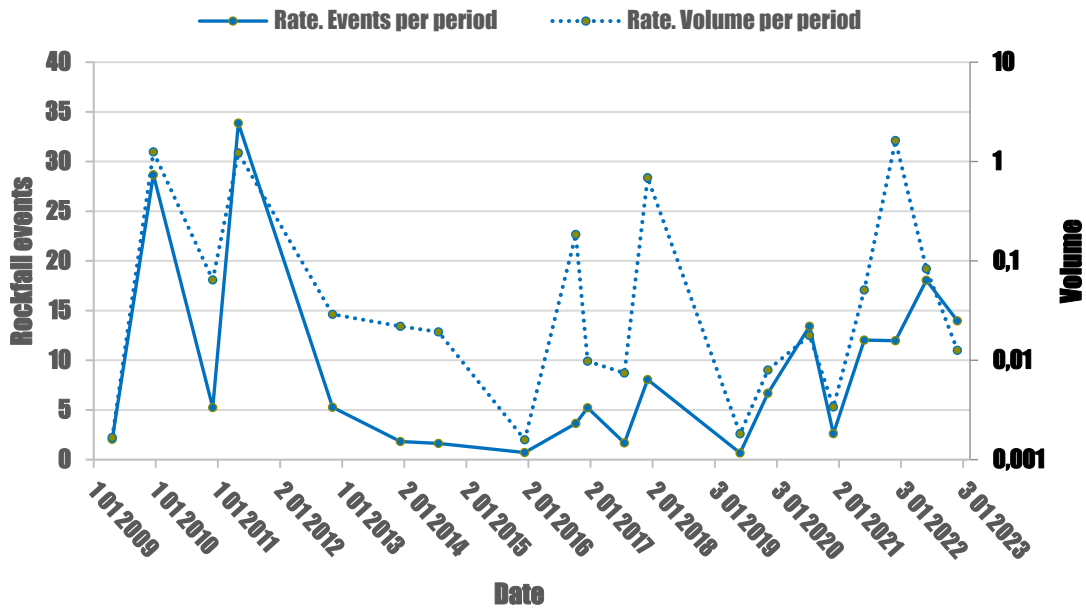


Figure 2: Rates of rockfall events and volumes for the different periods in Degotalls E cliff.

The inventory allows characterizing rockfall detachment hazardous conditions and reveal many of the underlying conditioning factors. Also, the appropriate data development allows create magnitude-frequency scenarios and some criteria for hazard assessment.

## References

BLANCO, L., GARCIA-SELLÉS, D., GUINAU, M., ZOUPEKAS, T., PUIG, A., SALAMÓ M., GRATACÓS, O., MUÑOZ, J.A., JANERAS, M. & PEDRAZA, O., 2012. Machine Learning-Based Rockfalls Detection with 3D Point Clouds, Example in the Montserrat Massif (Spain). *Remote Sensing*, 14, 4306.

JANERAS, M., LANTADA, N., NÚÑEZ-ANDRÉS M.A., HANTZ, D., PEDRAZA, O., CORNEJO, R., GUINAU, M., GARCIA-SELLÉS, D., BLANCO, L., GIL, J.A., & PALAU, J., 2023. Rockfall Magnitude-Frequency Relationship Based on Multi-Source Data from Monitoring and Inventory. *Remote Sensing*, 15(8):1981

## Quantifying slope movements: Tree trunk tracking using long-range stationary 4D laser scanning point clouds

Ronald Tabernig<sup>1\*</sup>, Katharina Anders<sup>2</sup>, Patrick Fritzmann<sup>3</sup>, Hannah Weiser<sup>2</sup>, Vivien Zahs<sup>2</sup>, Bernhard Höfle<sup>2,4,5</sup> & Martin Rutzinger<sup>1</sup>

<sup>1</sup> Department of Geography, University of Innsbruck, Innsbruck, Austria,  
ronald.tabernig@student.uibk.ac.at

<sup>2</sup> Institute of Geography, 3DGeo Research Group, Heidelberg University, Heidelberg, Germany

<sup>3</sup> Department of Geoinformation, Land Tirol, Innsbruck, Austria

<sup>4</sup> Interdisciplinary Centre of Scientific Computing (IWR), Heidelberg University, Heidelberg, Germany

<sup>5</sup> Heidelberg Center for the Environment (HCE), Heidelberg University, Heidelberg, Germany

**Key words:** time series analysis, change detection, landslide monitoring, tree trunks, terrestrial laser scanning

Large-scale landslides and secondary processes threaten human lives and infrastructure. Detecting, monitoring and understanding Alpine mass movements lay the foundation for the establishment of early warning systems and construction of protective structures.

Challenges of point cloud based change quantification (e.g., with M3C2) arise when point cloud density is generally low for the single epochs due to long measurement ranges. Additionally, in such monitoring setups with dense forest cover the slope surface is only sparsely represented by points. Thus, our novel approach uses temporal aggregation of point clouds to increase point density and uses 3D displacements of tree trunks as proxy for surface slope movements. Specifically, we are applying this technique to trees located above the Leckgalerie (Obergurgl, Austria), a stretch of an important connecting road.

Terrestrial laser scans were acquired every three hours from June to October in 2021 using a long-range stationary setup for the Riegl VZ-2000i. The segmentation and matching of tree trunks through all available point clouds allow to derive and compare displacement vectors of corresponding tree trunk objects throughout the scanning period. Three-dimensional distance measurements of three different methods are investigated: center of gravity (COG), iterative closest point (ICP), and trunk-ground-intersection (Intersection). The results of all three methods are compared to manual point-to-point measurements in the raw data to assess the accuracy of the developed method. Additionally, a simulation-based error margin is established based on more than 5000 simulated trunk displacements under varying conditions. These trunks are derived from laser scanning simulations on artificially generated scenes with the open-source scientific software HELIOS++ and Blender. Based on the results the area of interest can be classified into an unstable and a stable area.

Vertical displacements are prone to disproportional error margins and thus the displacements are inspected in 2D. During the active period of 56 days, the unstable area shows average displacements of 1.8 m (COG), 1.81 m (ICP), and 1.6 m (Intersection), with a weekly mean of 0.22 m, 0.23 m, and 0.2 m respectively. The simulation-based error margins are derived by the Mean Absolute Percentage Error (MAPE). These errors are 23.7 % (COG), 28.5% (ICP), and 39.2 % (Intersection). The calculated MAPE, when comparing the methods results to the manual point-to-point measurements from the first to the last epoch, are found to be consistent for both the COG and ICP methods at 9.5 %, and 3.4 % for the Intersection method.

The developed approaches deliver reasonable results demonstrating the potential of the utilisation of tree trunks as common and reoccurring objects for change detection. This provides additional information for forested areas on landslides that would otherwise be difficult to obtain.

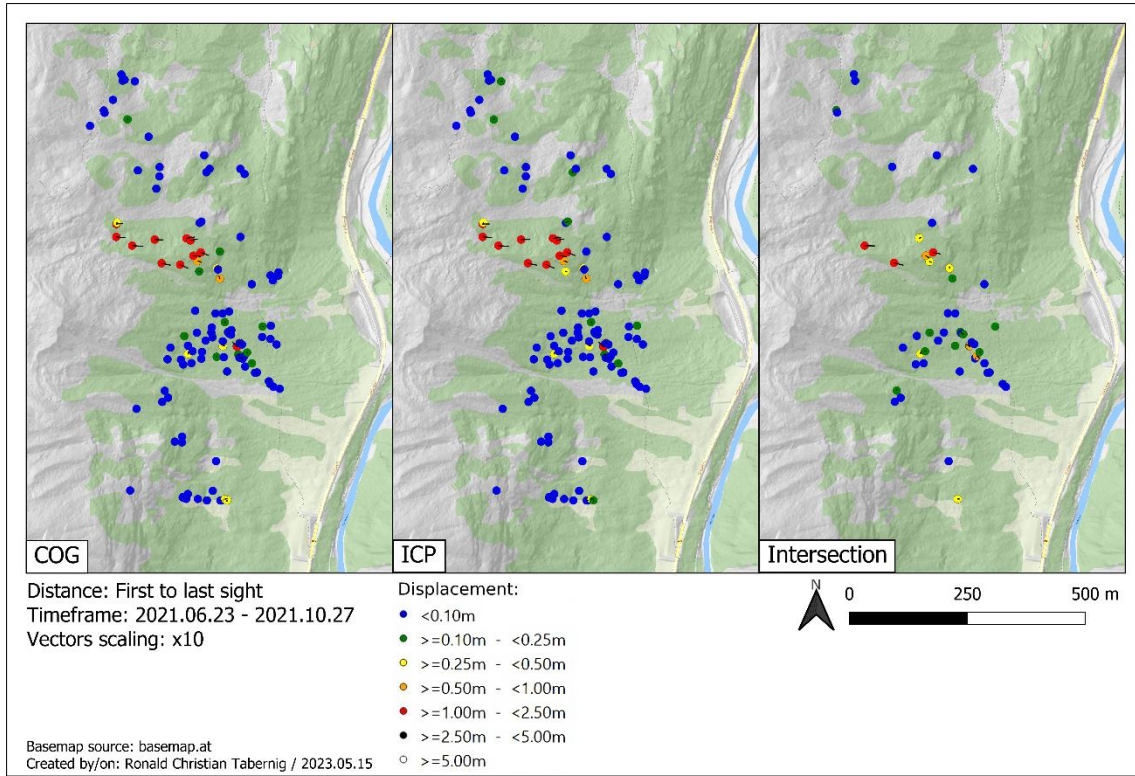


Figure 1: Map showing the displacement of the tree trunks from their first sight to their last sight. Compared are the COG, ICP, and Intersection method. Points indicate the location of the trunk at its first sight and are coloured based on the displacement magnitude. Vectors show the 2D displacement and are scaled with the factor 10.

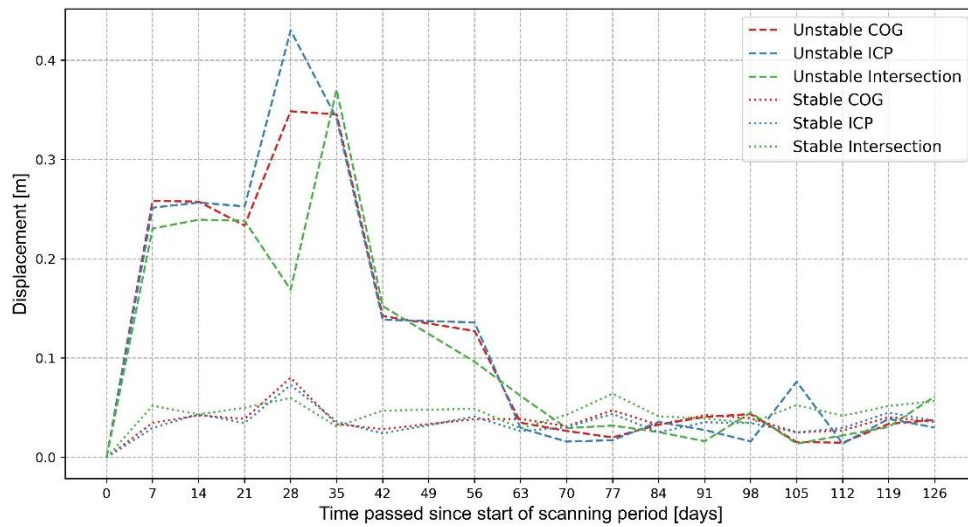


Figure 2: Average displacement of tree trunks during the full scanning season. The data is split into trunks within the stable (dotted) and unstable (hatched) area. Displacement is calculated each for COG (red) ICP (blue) and the Intersection (green). The displacement is relative to the prior date.

# Using Machine Learning to filter point clouds from artificial rainfall simulations

Oliver Grothum\*, Anne Bienert, Mikesch Blümlein & Anette Eltner  
 Technical University of Dresden, [Oliver.Grothum1@tu-dresden.de](mailto:Oliver.Grothum1@tu-dresden.de)

**Key words:** Soil erosion measurement, point cloud processing, machine learning, random forest, PointNet++

Understanding soil erosion processes is crucial for managing landscapes and mitigating environmental impact. One innovative and well-established approach involves utilizing digital elevation models (DEMs) to quantify and model erosion. In a recent study, this technique was employed to track changes in soil topography. During controlled artificial rainfall simulations, cameras captured images of exposed soil, which were then transformed into highly detailed point clouds using Structure-from-Motion and Multiview-Stereo (SfM + MVS) techniques. However, these point clouds contained not only bare soil information but also unintended vegetation data.

To tackle this challenge, the study focused on automating the process of removing vegetation from the point clouds. The research explored three distinct strategies:

1. **Knowledge-based Thresholding:** This technique involved setting thresholds based on various features such as color, height, and roughness to differentiate vegetation from soil. For instance, specific color thresholds were used to distinguish between green vegetation and soil.
2. **Machine Learning based Classification:** Machine learning algorithms were employed to determine thresholds automatically, utilizing features like color and multi-scale attributes of the points. Classifiers like random forest (RF; BREIMANN, 2001) were integrated into this approach.
3. **End-to-end Deep Learning:** The study also considered a deep learning approach, employing the PointNet++ architecture (QI ET. AL., 2017). This method directly classified points as either soil or vegetation, eliminating the need for predefined features.

Comparing the performance and limitations of these approaches provided valuable insights (Figure 1). The overarching aim was to establish an efficient and (semi-) automated technique for accurately removing

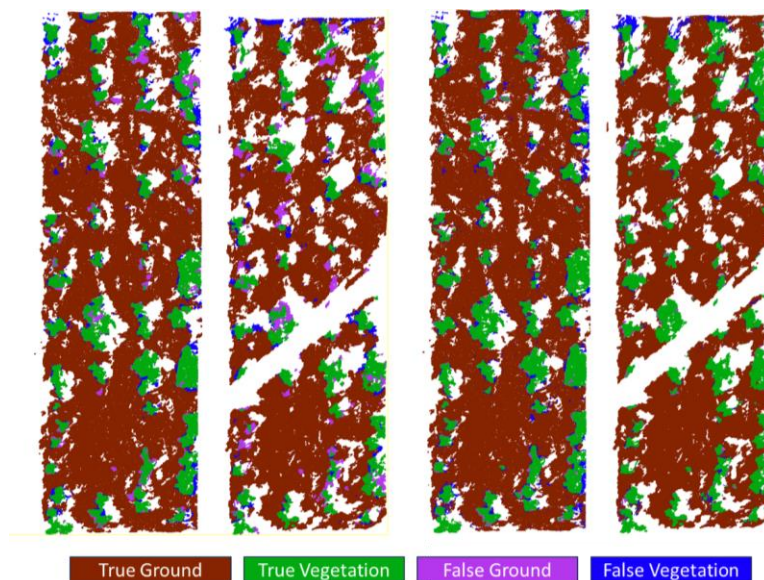


Figure 8: Classification results on two point clouds from one rainfall experiment with Random Forest (both left) and PointNet++ (both right)

vegetation from point clouds of the soil surface. This refinement sought to improve the reliability of erosion measurements while minimizing the need for manual intervention and the associated time and effort.

In conclusion, this study represents a significant step towards advancing soil erosion analysis through the integration of cutting-edge image analysis and machine learning methodologies. By automating vegetation removal from point clouds, researchers and environmentalists can gain more accurate insights into soil erosion processes, enhancing our ability to manage and protect vital natural resources.

## References

- BREIMANN, L., 2001. Random Forests. *Machine Learning* 45, 5–32. <https://doi.org/10.1023/A:1010933404324>
- QI, C. R., YI, L., SU, H., & GUIBAS, L. J., 2017. PointNet++: Deep Hierarchical Feature Learning on Point Sets in a Metric Space. *ArXiv*. /abs/1706.02413

# Processing large amounts of time-lapse imagery for geomorphic research: an AI-based approach

Hanne Hendrickx<sup>1\*</sup>, Xavier Blanch<sup>1</sup>, Mario Kummert<sup>2</sup>, Antonio Abellan<sup>3</sup>, Reynald Delaloye<sup>4</sup>, Anette Eltner<sup>1</sup>

<sup>1</sup> *Institute of Photogrammetry and Remote Sensing, Technische Universität Dresden, Germany*  
([hanne.hendrickx@tu-dresden.de](mailto:hanne.hendrickx@tu-dresden.de))

<sup>2</sup> *Geographisches Institut, Universität Bern, Switzerland*

<sup>3</sup> *Center for Research on the Alpine Environment (CREALP), Sion, Switzerland*

<sup>4</sup> *Department of Geosciences, University of Fribourg, Switzerland*

**Key words:** *Artificial Intelligence (AI), Time-lapse camera, Automatic image processing, Climate change, Erosion processes, mountain geomorphology.*

Fixed monoscopic webcams or time-lapse cameras can capture geomorphic processes at high temporal resolution and operate independently in remote areas. In the European Alps, the availability of extensive and diverse datasets from such cameras, spanning a decade or more (KUMMERT, DELALOYE, & BRAILLARD, 2018), make them an ideal and cost-effective tool for studying various geomorphic processes. These datasets are crucial for validating process-based models and gaining comprehensive insights into the drivers of mountain sediment transfers. However, managing the vast volume of hourly photographs generated by time-lapse cameras requires efficient automatic image processing. In that regard, Artificial Intelligence (AI) techniques, such as deep learning (DL), provide great potential. Unfortunately, geoscience datasets with labelled ground-truth data for training DL models are scarce (DAWSON, DUBRULE, & JOHN, 2023). To address this challenge, we prepare three large datasets that are available from highly erosive study sites (BLANCH, ELTNER, GUINAU, & ABELLAN, 2021; HENDRICKX ET AL., 2022; KUMMERT ET AL., 2018). Pre-processing steps include filtering cyclic change (such as diurnal and seasonal light variation) and augmenting data to increase the amount of training datasets. Afterwards, we test AI-based optical flow models, such as GMFlow (XU, ZHANG, CAI, REZATOFIHI, & TAO, 2022), to detect changes in the image sequences (Fig. 1).

This research aims to establish guidelines for managing large image datasets for geomorphic interpretation, including strategies of collect training and test data collections to achieve optimal results. Ultimately, we aspire the creation of a low-cost tool that can provide valuable information about the temporal and spatial evolution of geomorphic processes on a large scale. By doing so, this study seeks to improve mountain-specific research and monitoring, considering the socio-economic developments in mountain areas worldwide, the vulnerability of mountain cryosphere components to climate change, and the impact of geomorphic processes on tourism, mountaineering activities, water quality, and downstream ecosystems.



Figure 1: A first test, adopting the GMFlow model to detect geomorphic change at bi-temporal images of Gugla rock glacier front.

## References

Blanch, X., Eltner, A., Guinau, M., & Abellan, A. (2021). Multi-epoch and multi-imagery (Memi) photogrammetric workflow for enhanced change detection using time-lapse cameras. *Remote Sensing*, 13(8). <https://doi.org/10.3390/rs13081460>

Dawson, H. L., Dubrule, O., & John, C. M. (2023). Impact of dataset size and convolutional neural network architecture on transfer learning for carbonate rock classification. *Computers & Geosciences*, 171, 105284. <https://doi.org/10.1016/J.CAGEO.2022.105284>

Hendrickx, H., Le Roy, G., Helmstetter, A., Pointner, E., Larose, E., Braillard, L., ... Frankl, A. (2022). Timing, volume and precursory indicators of rock- and cliff fall on a permafrost mountain ridge (Mattertal, Switzerland). *Earth Surface Processes and Landforms*, 47(6), 1532–1549. <https://doi.org/10.1002/esp.5333>

Kummert, M., Delaloye, R., & Braillard, L. (2018). Erosion and sediment transfer processes at the front of rapidly moving rock glaciers: Systematic observations with automatic cameras in the western Swiss Alps. *Permafrost and Periglacial Processes*, 29(1), 21–33. <https://doi.org/10.1002/ppp.1960>

Xu, H., Zhang, J., Cai, J., Rezatofghi, H., & Tao, D. (2022). GMFlow: Learning Optical Flow via Global Matching. *Proceedings of the IEEE Computer Society Conference on Computer Vision and Pattern Recognition, 2022-June*, 8111–8120. <https://doi.org/10.1109/CVPR52688.2022.00795>

# Automated Ground Control Point Identification using Deep Learning Techniques

Xabier Blanch<sup>1\*</sup>, Melanie Elias<sup>1</sup>, Almut Jäschke<sup>1</sup>, Oliver Grothum<sup>1</sup>, Jens Grundmann<sup>2</sup>, Anette Eltner<sup>1</sup>

<sup>1</sup> Institute of Photogrammetry and Remote Sensing, Technische Universität Dresden, 01062 Dresden, Germany. xabier.blanch@tu-dresden.de

<sup>2</sup> Institute of Hydrology and Meteorology, Technische Universität Dresden, 01062 Dresden, Germany

**Key words:** Ground Control Points, Convolutional Neural Network, AI Detection, Keypoint detection

Ground Control Points (GCPs) play a crucial role in photogrammetry, providing essential information for georeferencing, registration and scaling of aerial and satellite imagery. These reference points, with known coordinates, are strategically placed and precisely measured on the ground to achieve accurate georeferencing in the photogrammetric process. The increasing importance of automatic GCP detection stems from technological advancements that have facilitated automated image acquisition, resulting in a significant growth in available datasets.

We adapted the Keypoint R-CNN with ResNet50-FPN to automatically detect and localize ground control points in the images. During the training phase, the model learns to recognize characteristic visual patterns associated with the ground control points. It achieves this by optimizing its parameters using annotated datasets that contain images with pre-labelled ground control points. The labelling of the images consists of the indication of each GCP detected in the image, the coordinates of the boundary box of the GCP (the object), and the coordinates of the centre of the GCP (the keypoint).

For the evaluation, we utilized three different datasets, each implementing different cameras and GCP setups. All three datasets consist of images captured by fixed cameras, which may experience displacements due to installation conditions, temperature, and weather conditions such as wind or rain. Given the variations in image resolution and the lack of homogeneity in the GCPs across the datasets (Figure 2), we conducted dataset-specific fine-tuning to optimize the model's performance for each case. As a result, we obtained three distinct models tailored to the respective datasets.

To assess the results obtained through the AI approach, a comparison is conducted with the results inferred from manually labelled ground truth data. In addition to the classic comparison between true labels and inferred labels, we have also applied a comparison regarding the inferred coordinates and the coordinates obtained using the ellipse fitting method (Figure 1).

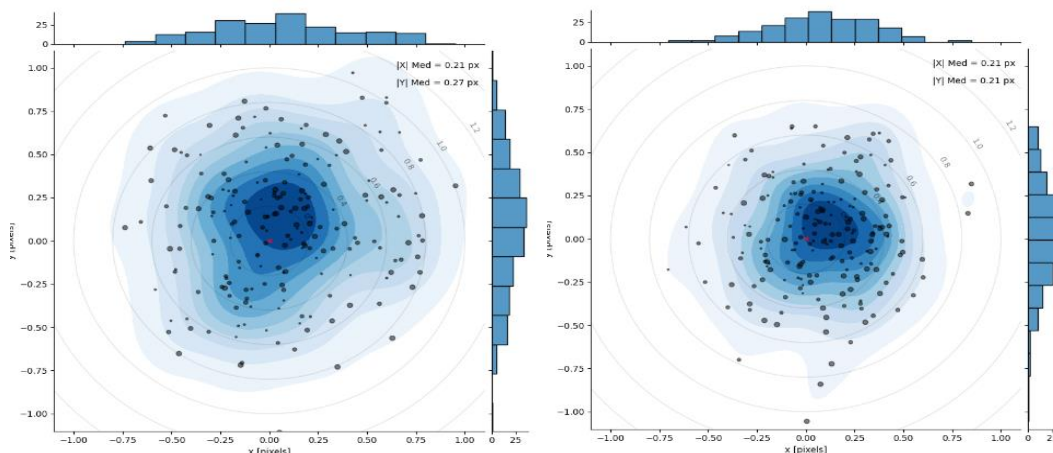


Figure 1: Results obtained for dataset Figure 2a. a) Comparison between AI values and the ellipse fitting method. b) Comparison between AI values and manual labelling.

The accuracy of the coordinates depends on the utilized dataset because the eventual automatic GCP image identification is correlated with the image quality, the image resolution, and the quality of the manual labelling used in the training among others. However, median distances of less than 0.5 px along both axes with respect to the manually labelled coordinates are possible. The evaluation, i.e., performed on test datasets (different from those used during training and evaluation), resulted in a median deviation of less than 0.4 px along both axes with respect to the manually labelled value, which is a value similar to the training metric. Finally, when comparing the values obtained by the AI method with the ellipse fitting (which is used to derive sub-pixel accurate GCP positions in the image), we have obtained a median deviation of only 0.3 px in the best dataset analysed (Figure 1).



Figure 2. Datasets used to evaluate the performance of the automatic detection of GCPs. Dataset A) Black circles on white background. Dataset B) White circles on black background. Dataset C) Black, red and white crosses on white or black background.

## Surface elevation monitoring in northern Tunisia using multi-temporal photogrammetric imagery

Imen Brini<sup>1,2\*</sup>, Denis Feurer<sup>1</sup>, Riadh Tebourbi<sup>2</sup>, Damien Raclot<sup>1</sup>, Fabrice Vinatier<sup>1</sup>, Riadh Abdelfattah<sup>2</sup>

<sup>1</sup> UMR LISAH, Univ. Montpellier, AgroParisTech, INRAE, IRD, Institut Agro Montpellier, Montpellier, France, imen.brini@ird.fr

<sup>2</sup> Higher School of Communications of Tunis COSIM Lab, University of Carthage, Tunis, Tunisia

**Key words:** Photogrammetry, SfM-MVS, DEM, change detection, topography, watershed.

The southern shore of the Mediterranean is likely to face environmental and demographic constraints in the future that can be even more vulnerable than those already observed in the last decades. Those constraints are mainly induced by anthropogenic activities, population growth, and climate change. The landscape pattern and topography are in a continuous interaction with climatic, hydrological, geomorphological, and ecological processes (Wilson, 2012) that contribute to some changes in the land surface. Detecting and estimating these topographic changes is crucial for understanding the historical state of the Earth surface, for environmental monitoring, and for future projections. The main aim of this research is to estimate and monitor the changes in the 3D Earth surface and vegetation in order to facilitate the study of the topography of the watersheds, and the connectivity of material flow (water, soil, and debris flow) in the Lebna watershed, in the Tunisian peninsula. This watershed is vulnerable to soil erosion and subsequently to reservoir siltation, increased mainly by agricultural practices (Desprats et al., 2013; Mekki et al., 2018). Although the study area hosts a long-term on-site observatory (Molenat et al., 2018), remote sensing surveys are useful to complement the monitoring of the potential changes enhanced by agricultural activities and Mediterranean climate. Efficient change detection requires recurrent surveys of the area of interest to estimate the relevant rate of change (Cook, 2017). Historical aerial images, recording global land-cover information, are acquired in a stereoscopic configuration with high spatial resolution. These images provide the prospect to derive digital elevation models (DEMs) and ortho-images, allowing a long-term land surface monitoring and 3D dynamic change detection (Knuth et al., 2023; Zhang et al., 2021). High-quality 3D models based on photogrammetric techniques (Structure from Motion, SfM, and Multi-View Stereo, MVS) require accurate ground control points (GCPs) for model georeferencing and camera interior parameters, positions and orientations calculation (Cook & Dietze, 2019). Recently, work on the SIFT-like algorithms has demonstrated that the exploitation of data at different spatial and temporal scales is possible (Feurer & Vinatier, 2018). This method allows the estimation and the temporal monitoring of fine relief over large areas and with a reduced need for costly calibration data. Novel SfM-MVS approaches rely almost exclusively on image information, and simple camera models to iteratively solve the camera parameters (interior and exterior orientation) using thousands of automatically detected feature matches between overlapping images. This improvement produces a crucial foundation toward automated processing of historical archive imagery with limited camera information and GCPs. In this study, both aerial and satellite images acquired between 2010 and 2018, covering the Lebna watershed, were used to generate Digital Elevation Models (DEMs) and detect potential changes based on the SfM-MVS approach. Different data combinations (multi-temporal, multi-sensor) are tested in order to evaluate the potential of the above-mentioned algorithms. In the following illustration (Fig. 1), some changes can be identified between DEMs derived from Pleiades images acquired in 2015 and 2018 using SfM-MVS algorithm. These changes correspond to houses built during the period (circled in Fig. 1) that have been confirmed visually using the before and after photographs.

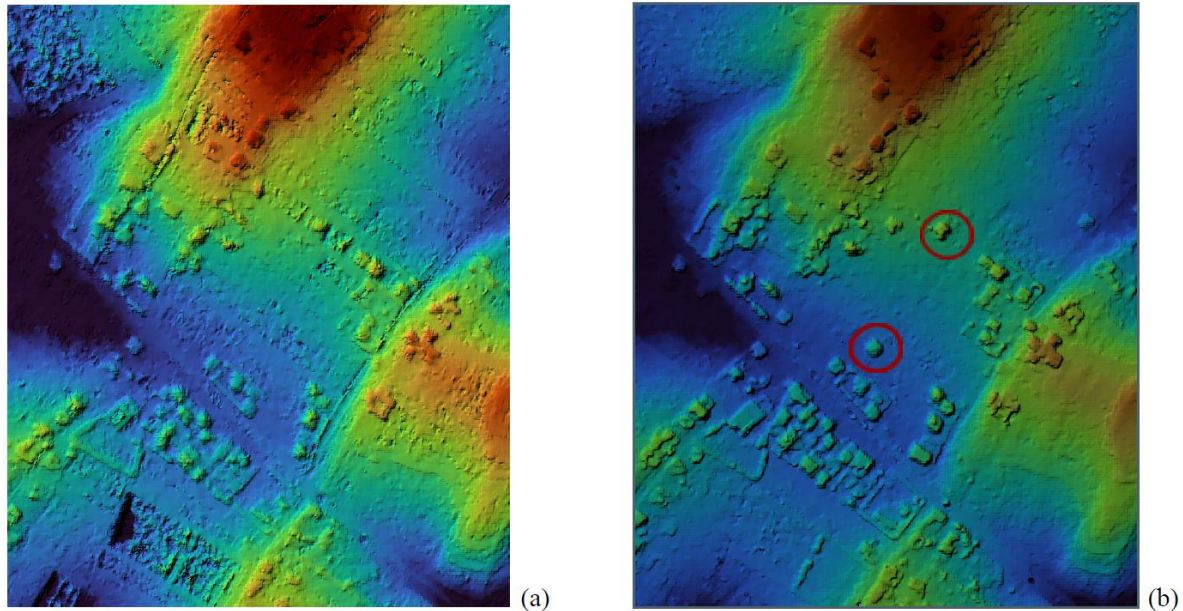


Figure 1: Zoom-in of the derived DEM from Pleiade images, acquired in (a) 2015 and (b) 2018, using SfM-MVS.

## References

- Cook, K. L. (2017). An evaluation of the effectiveness of low-cost UAVs and structure from motion for geomorphic change detection. *Geomorphology*, 278, 195–208. <https://doi.org/10.1016/j.geomorph.2016.11.009>
- Cook, K. L., & Dietze, M. (2019). *Short Communication: A simple workflow for robust low-cost UAV-derived change detection without ground control points*. 1009–1017.
- Desprats J.F., Raclot D., Rousseau M., Cerdan O., Garcin M., Le Bissonnais Y., Ben Slimane A., Fouche J., Monfort-Climent D. (2013). Mapping linear erosion features using high and very high resolution satellite imagery. *Land Degradation & Development*, 24(1), 22-32.
- Feurer, D., & Vinatier, F. (2018). Joining multi-epoch archival aerial images in a single SfM block allows 3-D change detection with almost exclusively image information. *ISPRS Journal of Photogrammetry and Remote Sensing*, 146(July), 495–506. <https://doi.org/10.1016/j.isprsjprs.2018.10.016>
- Knuth, F., Shean, D., Bhushan, S., Schwat, E., Alexandrov, O., Mcneil, C., Dehecq, A., Florentine, C., & Neel, S. O. (2023). *Historical Structure from Motion (HSfM): Automated processing of historical aerial photographs for long-term topographic change analysis*. 285 (November 2022).
- Mekki, I., Bailly, J. S., Jacob, F., Chebbi, H., Ajmi, T., Blanca, Y., ... & Biarnès, A. (2018). Impact of farmland fragmentation on rainfed crop allocation in Mediterranean landscapes: A case study of the Lebna watershed in Cap Bon, Tunisia. *Land use policy*, 75, 772-783.
- Molenat, J., Raclot, D., Zitouna, R., Andrieux, P., Coulouma, G., Feuer, D., ... & Voltz, M. (2018). OMERE: A long - term observatory of soil and water resources, in interaction with agricultural and landmanagement in Mediterranean hilly catchments. *Vadose Zone Journal*, 17(1), 1-18.
- Wilson, J. P. (2012). Digital terrain modeling. *Geomorphology*, 137(1), 107–121. <https://doi.org/10.1016/j.geomorph.2011.03.012>
- Zhang, L., Rupnik, E., & Pierrot-Descelligny, M. (2021). Feature matching for multi-epoch historical aerial images. *ISPRS Journal of Photogrammetry and Remote Sensing*, 182(April), 176–189. <https://doi.org/10.1016/j.isprsjprs.2021.10.008>

# Assesment of Soil Degradation: Water Erosion under Systematic UAV Supervision

Tomáš Laburda<sup>1\*</sup>, Josef Krása<sup>1</sup>, Jakub Stašek<sup>1</sup>, Markéta Báčová<sup>1</sup> & Tomáš Dostál<sup>1</sup>  
<sup>1</sup> Czech Technical University in Prague, Departement of Landscape Water Conservation, Thákurova 7,  
 16629, Praha 6, 16629, Czech Republic, tomas.laburda@fsv.cvut.cz

**Key words:** soil, degradation, erosion, sfm-mvs, photogrammetry

This contribution presents the principles of long-term monitoring of experimental sites in terms of accelerated soil degradation caused by water erosion. Within several different projects, agricultural land near the villages of Býkovice and Nučice in the Central Bohemian Region is monitored for a long time. Data on rainfall, temperature and soil moisture are monitored using meteorological stations on the defined soil plots. At regular intervals or after a significant rainfall event (above 10 mm/24 h), field surveys are carried out, including monitoring of the areas by UAVs. Since the start of systematic monitoring in 2017, a total of 124 monitoring campaigns using UAVs have been carried out until the end of 2022. Approximately 1-6 flights have been conducted per campaign, with an average area per flight of 0.25 km<sup>2</sup> and an average resolution of 2.2 cm/px. The primary drone used for the flights since 2022 is a DJI M300 with a Zenmuse P1 camera and 24 mm lens. A DJI Phantom 4 RTK is also used for smaller land areas. These new drones are used in RTK mode, which makes it possible to obtain positional and height accuracy within 10 cm, compared to several meters for older drones (DJI Phantom 4) without RTK and without additional georeferencing.

The processing of the flight images is done in Agisoft Metashape software. Using this software, digital terrain models and an orthophotomap (Fig. 1) in raster TIFF format in the S-JTSK coordinate system (EPSG: 5514) and Bpv elevation system (EPSG: 5705) are obtained by partial steps (Align photos - Detect markers - Build Dense Cloude - Filter by Confidence or Manually - Build DEM - Build Ortohomosaic). These outputs are further processed in a GIS environment to identify erosion features such as rills, furrows, sheet erosion or sedimentation.

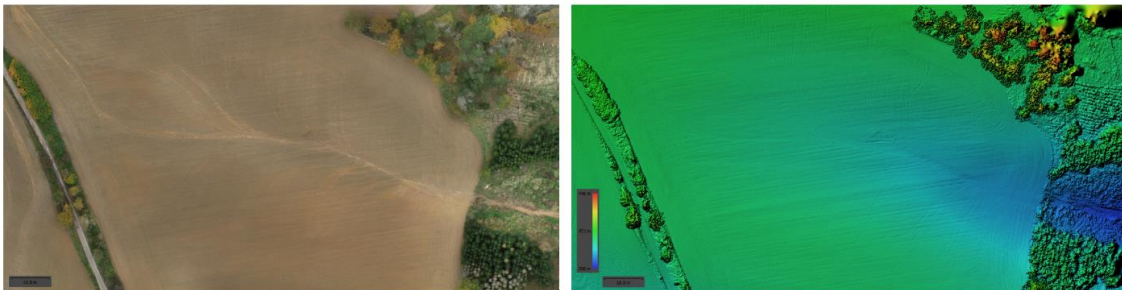


Figure 1: Orthomosaic and DEM of agricultural field with erosion rill.

This step is automated by the GIS tool using the method according to Báčová et al. (2019), (Fig. 2). The input to the tool is a digital terrain model and a polygon layer with rill boundaries, which is created manually. The tool then creates a TIN from the rill boundary and the terrain model, from which it then subtracts the terrain model with the rill to obtain the rill volume, or the volume of rill erosion.

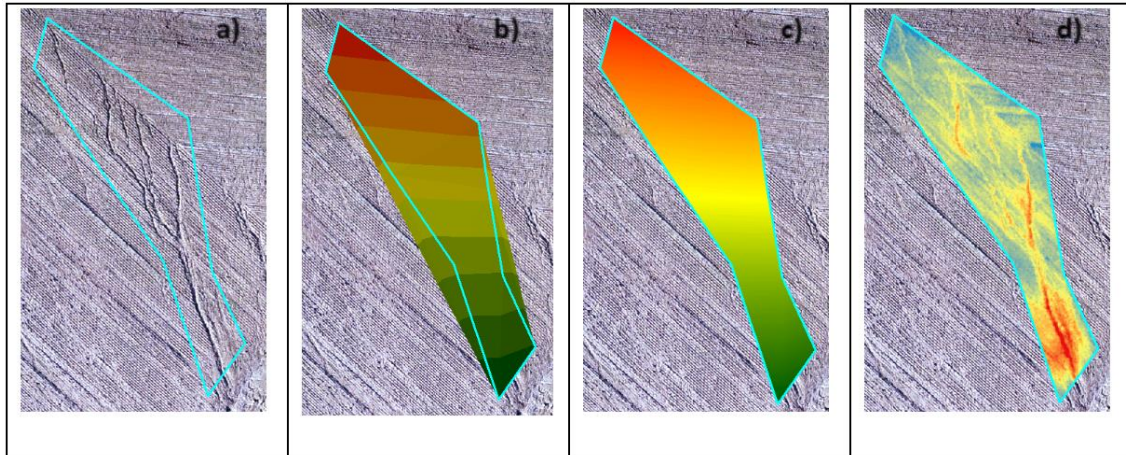


Figure 2: The principle of operation of the tool: a) Polygon of rill boundaries, b) TIN model of rill area and terrain model, c) Smoothed surface model.

The resulting soil erosion volume in the rills only, ranged from 26 to 285 m<sup>3</sup>. The conversion to the commonly used unit t/ha depends on the area to which the rills relate. In the case of the single rill polygon these values range from 215 to 566 t/ha, in the case of the corresponding LPIS parcel from 2.2 to 17.8 t/ha and in the case of the corresponding sub-basin from 5.5 to 56.8 t/ha. From this basic overview it can be seen how much soil is lost to rill erosion. In this way, all the areas where evidences of rill erosion are visible and for which rainfall data are available are processed in turn. In the next stages of the solution, it is planned to continuously acquire additional data and compare the measured soil erosion volumes with the erosion models and with the data measured using rainfall simulators.

**Acknowledgements:** Research has been supported by project TUDI (European Union's Horizon 2020 research and innovation programme under grant agreement No 101000224), SS05010180: Updating concept of the tolerable soil loss from arable land and SGS23/155/OHK1/3T/11: Experimental research and monitoring of rainfall-runoff and erosion processes on agricultural soils.

## References

BÁČOVÁ, M., KRÁSA, J., DEVÁTÝ, J., & KAVKA, P.,. 2019. "A GIS METHOD FOR VOLUMETRIC ASSESSMENTS OF EROSION RILLS FROM DIGITAL SURFACE MODELS." EUROPEAN JOURNAL OF REMOTE SENSING 52(1): 96–107. [HTTPS://DOI.ORG/10.1080/22797254.2018.1543556](https://doi.org/10.1080/22797254.2018.1543556).

# Improving Soil Infiltration Assessment with Deep Learning for Water Segmentation Applied to Time-Lapse Imagery

Mikesch Blümlein<sup>1</sup>, Pedro Zamboni<sup>2</sup>, Jonas Lenz<sup>1</sup>, Anette Eltner<sup>1</sup>

<sup>1</sup> Institute of Photogrammetry and Remote Sensing, Technical University Dresden, Germany, [mikesch.bluemlein@posteo.de](mailto:mikesch.bluemlein@posteo.de)

<sup>2</sup> Faculty of Engineering and Geography Federal University of Mato Grosso do Sul, Brazil

**Keywords:** *convolutional neural networks, water ponding, image segmentation, soil infiltration and runoff*

Infiltration and runoff processes play a crucial role in hydrology and agriculture, influencing water management and environmental conservation. In recent years, the integration of deep learning methods, such as convolutional neural networks (CNNs), has greatly impacted multiple scientific disciplines, including geosciences.

This study aimed to examine the potential of using CNNs to segment ponding areas on bare soils to gain a better understanding of infiltration and runoff processes.

To conduct our research, we artificially irrigated three runoff plots, each measuring 3 m<sup>2</sup> under varying rainfall intensities. The discharge captured in the outlet was recorded every minute, and images were taken every 10 seconds to obtain different stages of the infiltration process. The experimental infiltration rate (IR) was calculated based on the discharge and rainfall intensity. Our dataset contained 1380 images with corresponding masks. Three different CNNs (VGG-16, U-Net ResNet101, and U-Net EfficientNetB0) were trained for the segmentation task.

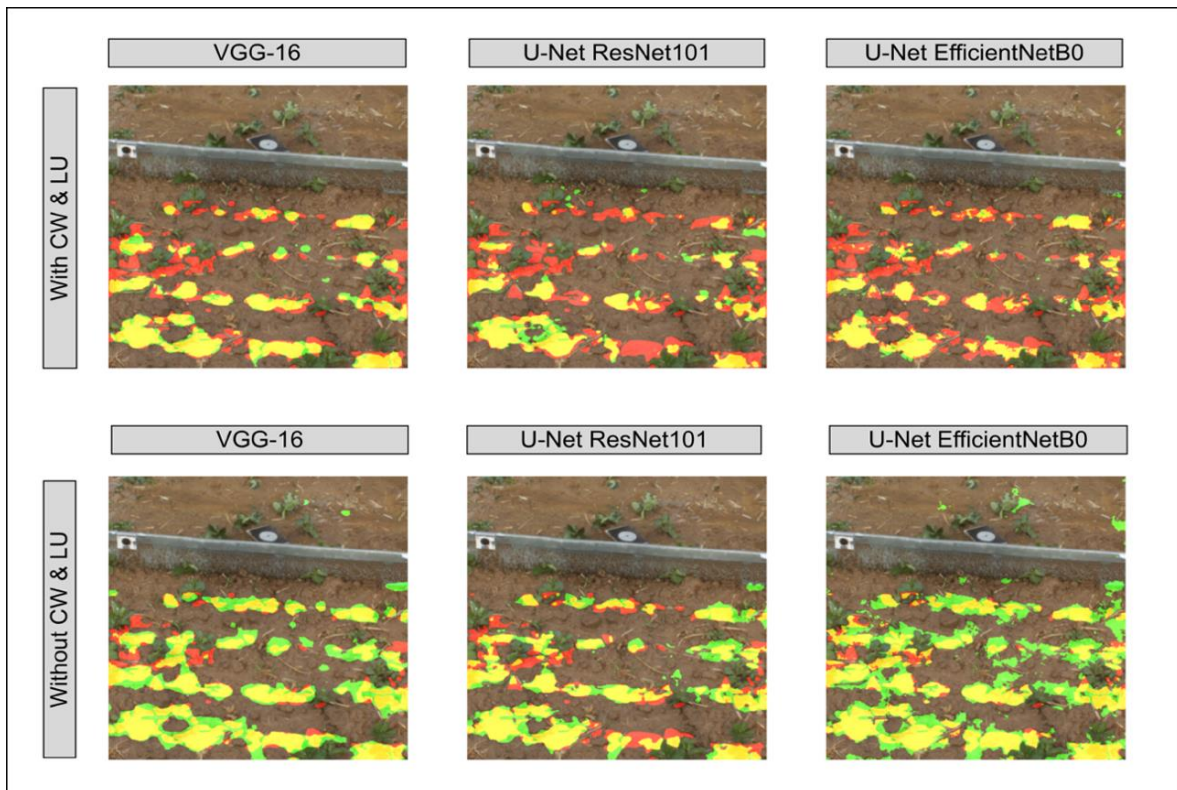


Figure 1: Example segmentation output of CNNs with and without considering CW and LU. The green pixels show the predicted water area by the CNN whereas the red pixels represent the manually annotated ground truth.

Subsequently, the impact of class weight imbalance (CW) and label uncertainty (LU) on model performance was analyzed, and a loss function proposed by BRESSAN *et al.* (2022) was implemented to address these issues. In addition, we created various ensembles based on the models that considered CW and LU. We used pixel accuracy (ACC) and intersection over union (IoU) as evaluation metrics. The best model was used to compute the water coverage area (WCA), which was compared with the discharge, experimental IR, and modeled IR obtained from the Green and Ampt equation.

The ACC and IoU of the CNNs that did not consider CW and LU ranged between 0.499 - 0.535 and 0.332 - 0.453, respectively. By implementing the loss function, ACC increased on average by 28.9 % and IoU by 1.3 %, demonstrating a high potential for addressing CW and LU. The best overall model performance was achieved by an ensemble combining all three models, which were trained considering CW and LU, with an ACC of 0.822 and an IoU of 0.509.

The comparison of experimental IR and WCA shows the tendency of runoff plots to overestimate the initial IR in the field, as they neglect the depression storage capacity (DSC). This emphasizes the importance of DSC for accurate infiltration modeling. The modeled IR showed better correspondence with the WCA, indicating a more accurate approximation of the initial IR.

Our study findings suggest that the application of CNNs is a promising tool for segmenting water ponding areas and capturing their spatiotemporal evolution. Depending on the dataset it is crucial to address CW and LU which in our study was more important than the selection of the CNN. Overall, the results show that ensembles can lead to improved model performance. Based on our findings, we conclude that our CNN-based approach holds great promise for approximating the ponding time and can be seen as an initial step toward estimating the infiltration capacity at the plot scale. Additionally, detecting ponding areas and analyzing their spatiotemporal evolution can facilitate the estimation of runoff onset, enhancing runoff and erosion modeling.

## References

BRESSAN, P.O., JUNIOR, J.M., CORREA MARTINS, J.A., DE MELO, M.J., GONÇALLVES, P., FREITAS, D.M., MARQUES RAMOS, A.P., GARCIA FURUYA, M.T., OSCO, L.P., DE ANDRADE SILVA, J., LUO, Z., GARCIA, R.C., MA, L., LI, J., GONÇALVES, W.N., 2022. Semantic Segmentation with Labeling Uncertainty and Class Imbalance Applied to Vegetation Mapping. *International Journal of Applied Earth Observation and Geoinformation*, 108: 102690.

## Investigating the interrelations between of rainfall characteristics and gully erosion processes

Fentahun Bezie<sup>1,2</sup>, Kwinten Van Weverberg<sup>2</sup>, Amaury Frankl<sup>2,\*</sup>

<sup>1</sup> Institute of Land Administration, Bahir Dar University, P.O.Box 5001, Bahir Dar, Ethiopia

<sup>2</sup> Department of Geography, Ghent University, Krijgslaan 281 (S8), B-9000 Gent, Belgium

\* Corresponding author: A. Frankl, e-mail: Amaury.Frankl@UGent.be

**Key words:** *High-Resolution Topography, Gully, Soil Erosion, Vegetation*

In Ethiopia, the occurrence of gullies is closely linked to unsustainable land use practices driven by poverty in a vulnerable mountainous environment, where intense rainfall poses significant challenges to the physical integrity of the landscape. While decadal trends in gully development and their controlling factors are relatively well understood, there remains a knowledge gap regarding the precise dynamics at seasonal to event scales. This research aims to address this gap in order to inform targeted restoration approaches, as previous interventions have inadvertently exacerbated the situation. For example, gullying in valley-bottom positions has been related to increased infiltration resulting from land terracing on hillslopes. Advancing land management practices necessitates a deeper understanding of event-based rainfall characteristics and gully erosion processes that affect the gully banks (i.e. soil piping, slumping, undercutting). To investigate the correlation between rainfall characteristics and gully erosion dynamics, this study proposes a combined approach involving pluviometer measurements, LiDAR scanning, and time-lapse photography at three gully heads featuring contrasting environmental settings. The anticipated findings and their relevance to triggering environmental changes have the potential to provide valuable insights for sustainable development in Ethiopia and beyond, as well as providing valuable data for process-based modelling.

## Generating ensembles of karst conduit surfaces of varying roughness and complexity with Gaussian random fields

Celia Trunz\*, Tanguy Racine, Julien Straubhaar, Philippe Renard

*University of Neuchâtel, 11 Rue Emile Argand, 2000 Neuchâtel, Switzerland, \*celia.trunz@gmail.com*

**Keywords:** *Karst, 3D triangulated surface, wall roughness*

Karst aquifers represent a quarter of the freshwater resources in the world, making accurate modeling of water flow and sediment/contaminant transport critical for water resource management. Modeling water flow in karst is complex due to the nature of turbulent flow as well as the lack of constraints in the geometry of the conduits. Specifically, wall properties and conduit roughness play a major role in flow velocity. Current models represent conduits in karst as connected tubes with a singular roughness parameter. However, wall and conduit roughness are heterogenous along the aquifers and are scale dependent. In addition, in situ measurements of roughness are challenging. To improve this lack of data and go beyond this single roughness simplification, we need a reliable method for generating realistic but random ensembles of cave conduits of increasing complexity.

Here we utilize a protocol for generating ensembles of cave conduits with well-defined spatial statistics e.g., the normalized rugosity parameter used within the Colebrook-White formula - but random variability. To achieve this, we combine level sets and geostatistical techniques to model triangulated 3D surfaces. To generate a karst conduit surface, we first compute the distance to the conduit centerline as a 3D field and then model the conduit interior with a conditional random field. Once the mean and covariance of this Gaussian random field are inferred from the dataset, we can generate an ensemble of conduit geometries. By modifying these statistical parameters, we can obtain a range of geometries with controlled shapes from the smoother to the more complex. Adapting these techniques to our ground truth data sets collected in the field, we present a preliminary suite of 3D triangulated surfaces with karst-like conduit geometry. Finally, we modulate the experiments with various degrees of roughness and investigate whether they are suitable for running analog or computational fluid dynamics experiments.

The generation of karst-like triangulated surfaces is a stepping stone for flow and transport analog and digital experiments, which we will carry out in the future using 3D-printed conduits and computational fluid dynamics.

# Improving the resolution of mineralogical maps through the use of ANN with hyperspectral datasets of different resolution

Yehor Surkov<sup>1\*</sup> & Urs Mall<sup>1</sup>

<sup>1</sup> Max Planck Institute for Solar System research, surkov@mpg.mps.de

**Key words:** *the super-resolution, hyperspectral imaging, data fusion, spectral indices, geomorphology, Moon*

Various applications in satellite remote sensing require high spatial and high spectral resolution. Imaging spectrometers rarely meet these two requirements simultaneously. Hyperspectral sensors acquire high-spectral-resolution and low-spatial-resolution hyperspectral images (HSIs), while multispectral sensor acquires low-spectral-resolution and high-spatial-resolution multispectral images (MSIs). Due to various practical constraints, it is in most cases impossible to build hardware which is able to deliver the required data in a single data frame. One is therefore challenged with the task to combine two different datasets from two instruments which have different spatial and spectral resolution through data fusion. In the field of geomorphological surface investigations, where it is often required to measure small-scale surface features, attempts have been made to improve the available image quality through the implementation of super-resolution algorithms. Super-resolution refers to the use of correlation and complementarity between multiple low-resolution images of the same observed scene to make up for the lack of information recorded in one single image in order to construct a high-resolution image. However, data fusion from two sensors is a difficult endeavor when the images to be aligned originate from different viewpoints in space and have been recorded under different illumination conditions.

In this study related to the identification of minerals from lunar reflection spectroscopic data, we propose a new method to use data acquired by the Moon Mineralogy Mapper (M<sup>3</sup>) scanning spectrometer onboard the Indian Chandrayaan-1 spacecraft and the Multiband Imager (MI) onboard the Japanese SELENE spacecraft to circumvent problems arising from image registration. The M<sup>3</sup> data have a spatial resolution of about 150 m/pixel and cover the wavelength range between 540 and 2950 nm in 83 narrow spectral channels [Green et al., 2011]. The MI data cover the range from 750 to 1550 nm in 7 spectral bands, but have much greater spatial resolution (30 m/pixel). The logic of our approach is based on the idea to use the high spectral resolution capabilities of the M<sup>3</sup> instrument to identify the mineralogical composition of an imaged lunar surface elements and the high spatial resolution of the MI to obtain the best possible spatial resolution of the observed surface area.

We demonstrate how to use our proposed method to create an olivine index with the two lunar multispectral datasets to map lunar surface features with greater spatial resolution which allows one to analyse the mineralogical composition and its surface morphology context. The architecture of our neural net uses a five parameters input layer, two hidden layers equipped with the logistic activation (5 and three ‘neurons’, correspondently) function, and a single-neuron output layer with linear response. The color ratios, basically the ratios of albedo at different wavelength  $C(\lambda_2/\lambda_1) = A(\lambda_2)/A(\lambda_1)$ , were taken as the input spectral parameters. The output layer is the olivine index. We chose the ratio of integrated band depths (IBDs) of absorption features near 1 and 2  $\mu\text{m}$  as the reliable spectral marker of the olivine presence [Isaacson et al., 2011] in the lunar regolith. The Copernicus crater (9.62°N20.08°W) was chosen as the region of interest. This lunar site is well known for its multiply olivine deposits with diverse origins which have been studied in details [e.g., Dhingra et al., 2015].

Figure 1 shows the region of interest (ROI)s and key results of high-resolution olivine index mapping. As the studied ratio cannot be directly reproduced with MI SELENE data, we merged the images from both datasets and used the M<sup>3</sup> data as the training set to find all weights and biases of the net. It should be noted that we do not need a very high precision of the co-registration primarily due to the significantly lower spatial resolution of M<sup>3</sup>. Then we applied the trained net to the original MI SELENE data to obtain high-resolution distribution of the olivine index over the Copernicus central peak (fig. 1b). These results are depicted at the same range (0-30) as the original M<sup>3</sup> data below (Fig. 1c). The comparisons between them show that the ANN-MI image product has the same range of values; however, it reveals additional surface morphology details on the olivine index distribution like sharp contours of olivine deposits or landslides of olivine-reach materials. Also, distinct

olivine spectral signatures on the ANN-MI map reveal the association with tubes of lava flows and melted basalt ponds on the north-western part of the crater wall (Fig. 1d), outlined on Fig. 1a with the white rectangle, whereas the original  $M^3$  data (Fig. 1e) only allows to hypothesize this affinity.

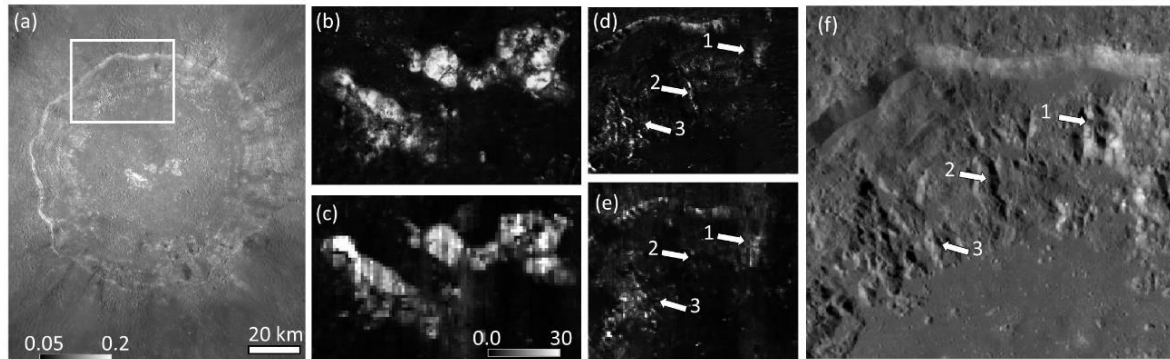


Figure 1: The  $M^3$  Chandrayaan-1 and MI SELENE datasets integration process and results. (a) The MI Kaguya albedo of ROI at 750 nm spectral channel. (b) and (c) represent the results of IBD's ratio distribution over the peak using ANN-MI data and  $M^3$  data, correspondently. (d) and (e) are the same maps for the north-western part of the crater wall with intensive lava ponds and flows. The high-resolution overview scene for this part of the wall is shown on (f). The arrows point to the correspondent locations with the olivine spectral signature.

**Acknowledgements:** The authors *acknowledge* financial support from the Max-Planck Society.

## References

- GREEN, R.O., PIETERS, C., MOUROULIS, P., ET AL., 2011. The Moon Mineralogy Mapper ( $M^3$ ) imaging spectrometer for lunar science: Instrument description, calibration, on-orbit measurements, science data calibration and on-orbit validation. *Journal of Geophysical Research: Planets*, 116:E10, E00G19.
- ISAACSON, P.J., PIETERS, C., BESSE, S., ET AL., 2011. Remote compositional analysis of lunar olivine-rich lithologies with Moon Mineralogy Mapper ( $M^3$ ) spectra. *Journal of Geophysical Research: Planets*, 116:E6, E00G11.
- DHINGRA, D., PIETERS, C., & HEAD, J., 2015. Multiply origins for olivine at Copernicus crater. *Earth and Planetary Science Letters*, 420, 95-101.

# Integrating surface spectral and subsurface geophysical data for comprehensive resource characterisation of mining residues

Moritz Kirsch<sup>1\*</sup>, Ana Bautista Gascueña<sup>1,5</sup>, Samuel Thiele<sup>1</sup>, Akshay Kamath<sup>1</sup>, Andrea Viezzoli<sup>2</sup>, Arianna Rapiti<sup>2</sup>, Roberto De La Rosa<sup>1,5</sup>, Per Gisselø<sup>3</sup>, Angelo Farci<sup>4</sup> & Richard Gloaguen<sup>1</sup>

<sup>1</sup> *Helmholtz-Zentrum Dresden-Rossendorf, Helmholtz Institute Freiberg for Resource Technology, Freiberg, Germany, m.kirsch@hzdr.de*

<sup>2</sup> *Aarhus Geophysics, Aps, Risskov, Denmark*

<sup>3</sup> *SkyTEM Surveys ApS, Aarhus, Denmark*

<sup>4</sup> *Atalaya Mining, Minas de Riotinto, Spain*

<sup>5</sup> *Beak Consultants GmbH, Freiberg, Germany*

**Key words:** *hyperspectral, 3D modelling, mineral exploration*

Airborne hyperspectral imaging (HSI) provides a means to obtain high-resolution mineralogical information across exposed surfaces, while low-frequency electromagnetics (AEM) yields multi-parameter geophysical properties at depth. Individually, these datasets are crucial tools for mineral exploration, but their combined use holds even greater potential, especially for assessing surface-exposed volumetric entities like mining residues and stockpiles. However, integrating surface spectral properties with subsurface geophysical data presents many challenges due to differences in resolution, coverage and other data characteristics. In this study, we integrate AEM and HSI data, supplemented by LiDAR and ground validation, in a machine learning framework to integrate and maximise the predictive capacity of these datasets. We showcase this synergistic fusion using sulfidic waste rocks associated with volcanic-hosted massive sulfide (VMS) deposits of the Iberian Pyrite Belt in southern Spain. These discarded extraction remnants, often overlooked for their economic potential, have gained recent importance due to favourable metal prices and improved processing techniques.

Our methodology involves classifying airborne imaging spectroscopy data across various optical wavelengths using a support vector machine. This classifier, trained on ground data and expert-based labelling, effectively categorises distinct materials exposed on the waste rock deposit based on spectral properties. The resulting classified hyperspectral information seamlessly combines with LiDAR-derived point cloud data, creating a high-resolution 3D dataset that vividly represents the surface composition of the deposit.

To extend this characterisation into the subsurface, an airborne AEM dataset was processed using a layered earth model that accounts for induced polarisation effects, providing a three-dimensional volume of resistivity and chargeability. We then integrate these disparate datasets using kernel density estimates derived from the imaging spectroscopy data and surface AEM inversion values. These estimates are employed to train a classifier for the subsurface AEM data, yielding information on the 3D distribution of three material categories contained in the rock waste deposit. Validation of this integrated methodology against drill hole assays shows a good correlation with logged waste rock categories and with copper and sulfur grades. We conclude that these non-invasive, remote sensing methodologies pave the way for a comprehensive, three-dimensional understanding of waste rock deposits, reducing the need for extensive drilling efforts and contributing to a more sustainable and informed approach to resource management and land use.

**Acknowledgements:** This research received funding from the European Union's Horizon 2020 research and innovation program under grant agreement No 776487.

# Digitalising Svalbard with Svalbox: towards a baseline survey of one of the world's fastest warming places

Kim Senger<sup>1,\*</sup>, Lilith Kuckero<sup>1</sup>, Peter Betlem<sup>1,2</sup>, Rafael Kenji Horota<sup>1,3</sup>, Aleksandra Smyrak-Sikora<sup>1</sup>, Nil Rodes<sup>1</sup>, Anna Sartell<sup>4,1</sup>, Anders Dahlin<sup>1,2</sup>, Tereza Mosociova<sup>1</sup>, Marius Jonassen<sup>1</sup>

<sup>1</sup> Department of Arctic Geology, The University Centre in Svalbard, 9171 Longyearbyen, Norway,

\*corresponding author: [kims@unis.no](mailto:kims@unis.no)

<sup>2</sup> Department of Geosciences, University of Oslo, Sem Sælands vei 24, Blindern, 0371 Oslo, Norway

<sup>3</sup> Department of Earth Science, University of Bergen, Allégaten 41, 5020 Bergen, Norway

<sup>4</sup> Department of Geosciences and Geography, University of Helsinki, Gustaf Hällströmin katu 2, 00560 Helsinki, Finland

**Key words:** Arctic, photogrammetry, digital outcrop model, data integration

Svalbard is one of the fastest warming places in the world, with implications on amongst others geohazards and infrastructure. Even within the past few decades the landscape change is evident, with retreating glaciers, rock and debris flows and enhanced erosion. These changes are projected to continue in the future, and it is critical that the present-day landscape is preserved for time-lapse studies and re-evaluation and reproducibility of observations.

The Svalbox project started in 2016 at UNIS, the world's northernmost educational institution. Svalbox's main goal is to acquire, process, and share digital outcrop models (DOMs, Figure 1) from Svalbard, making it accessible to both our students and the wider geoscientific community (SENGER *et al.*, 2021; BETLEM *et al.*, 2023). Svalbox includes both an open map-based portal, [www.svalbox.no/map](http://www.svalbox.no/map), and a subsurface portal built in Petrel where also subsurface data (e.g., wells, seismic) are included and thematic data packages can be generated (HOROTA *et al.*, 2023). Most of the DOMs are generated using UAV-based photogrammetry. Through Svalbox we put these data in a regional geological context, and allow for downloading not only the models but also the input data (i.e. photographs), Metashape projects (with detailed processing reports), and complementary output files (e.g., high-resolution digital terrain models and orthomosaics). All data contain rich metadata and are FAIRly stored on the Zenodo repository, facilitating free and open re-use for instance in big data/AI studies.



Figure 1: Example of one of the digital outcrop models available on Svalbox, illustrating mixed sandstone-shale succession in the Early Cretaceous on the upper slopes of Janusfjellet. The model is available from BETLEM (2021).

While acquiring photographs for generating georeferenced DOMs we also systematically take 360° images (i.e. photospheres), both aerially using drones and from the ground using 360° cameras. These photospheres are inter-connected in the context of thematic virtual field guides accessible through the [www.vrsvalbard.com](http://www.vrsvalbard.com) platform, as well as available through Svalbox's open map-based portal, [www.svalbox.no/map](http://www.svalbox.no/map). Photospheres, in contrast to DOMs, do not facilitate quantitative interpretation but their rapid acquisition, minimal processing and all-encompassing viewpoints make them an important geoscientific tool.

Svalbox is, however, more than just a repository of DOMs and photospheres (Figure 2). We continuously push the boundaries to facilitate the usage of such digital tools in education, research and societal involvement. This involves user training beyond the department of Arctic Geology, showcasing what is feasible with such methods to fellow scientists and the general public in Longyearbyen and systematically acquiring data in the near-town area that the local community can relate to. We have initiated a programme for systematic time-lapse acquisition of DOMs in easily accessible sites near Longyearbyen to provide documentation of how the landscape changes over time. In parallel, we run large-scale boat-based campaigns each summer and snowscooter-based campaigns each spring to systematically digitalise outcrops around Svalbard.

In this contribution we present some highlights from the Svalbox project, focussing on near-town and remote data acquisition case studies, data processing, data management and data visualisation. We also outline our long-term vision of using the Svalbox platform to obtain a high-resolution digital version of Svalbard's key outcrops and the entire near-town area by the International Polar Year in 2032-33.

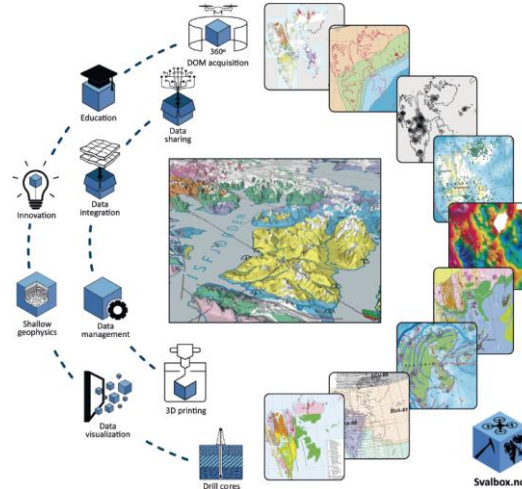


Figure 2: Key elements of the Svalbox concept, illustrating both the integration of different data sets and the innovative aspects of Svalbox. These include data acquisition (digital models, shallow geophysics, outcrop studies), data harvesting (from wells, geophysical data, remote sensing, publications etc.), data management (in a geospatial database), data integration (from basin to thin section scale, and across geoscientific disciplines and data types) and data presentation (both online but also through 3D printing). Figure from SENER et al. (2022).

**Acknowledgements:** Svalbox is organically funded through several collaboration projects, notably from the University of Arctic, the Research Council of Norway (through Svalbard Strategic Grants and Arctic Field Grants) and the Petroleum Research School of Norway. Furthermore, UNIS has provided internal funding for data acquisition, data handling and data visualisation. Students from UNIS and other institutions are thanked for help during both acquisition and processing stages.

## References

- BETLEM, P., 2021. Svalbox-DOM\_2020-0002\_Janusfjellet [Data set]. Zenodo. <https://doi.org/10.5281/zenodo.5134999>
- BETLEM, P., RODES, N., BIRCHALL, T., DAHLIN, A., SMYRAK-SIKORA, A. and SENER, K., 2023. The Svalbox Digital Model Database: a geoscientific window to the Arctic. *Geosphere*, <https://doi.org/10.1130/GES02606.1>.
- HOROTA, R.K., SENER, K., RODES, N., BETLEM, P., SMYRAK-SIKORA, A., JONASSEN, M.O., KRAMER, D. and BRAATHEN, A., 2023. West Spitsbergen fold and thrust belt: A digital educational data package for teaching structural geology. *Journal of Structural Geology*, 167: 104781, <https://doi.org/10.1016/j.jsg.2022.104781>.
- Senger, K., Betlem, P., Birchall, T., Buckley, S.J., Coakley, B., Eide, C.H., Flaig, P.P., Forien, M., Galland, O., Gonzaga Jr, L., Jensen, M., Kurz, T., Lecomte, I., Mair, K., Malm, R., Mulrooney, M., Naumann, N., Nordmo, I., Nolde, N., Ogata, K., Rabbel, O., Schaaf, N.W. and Smyrak-Sikora, A., 2021. Using digital outcrops to make the high Arctic more accessible through the Svalbox database. *Journal of Geoscience Education*, 69: 123-137. <https://doi.org/10.1080/10899995.2020.1813865>.

# Creative and Funny Use of Unmanned Aerial Systems and Mobile Devices in Hydraulic: A Project-Based Learning Approach

Hana Nekrep<sup>1</sup>, Matjaž N. Perc<sup>2\*</sup>

<sup>1</sup> TU Wien, Faculty of Architecture and Planning, Austria

<sup>2</sup> University of Maribor, FGPA, Slovenia, [matjaz.nekrep@um.si](mailto:matjaz.nekrep@um.si)

**Key words:** *project-based learning, active learning, interdisciplinary projects, UAS, mobile devices, hydraulics*

This paper presents some examples of project-based learning at the University of Maribor, the University of Ljubljana, and TU Wien. The focus lies on the innovative use of Unmanned Aerial Systems (UAS) and mobile devices in hydraulic mapping and hydrometry.

These projects highlight the practical and educational implications of employing UAS and mobile phones in hydraulic studies, thereby linking technology, hydrology, and pedagogy. The theoretical foundations of project-based learning are outlined, emphasizing the benefits such as enhanced student engagement, active learning, and the cultivation of critical thinking skills.

Case studies across the three universities illustrate the implementation of this learning methodology at various academic levels, showcasing the versatility of this approach across different disciplines. These projects offer insights into how technology can be harnessed to meet varying learning objectives within the realm of geosciences, specifically hydraulics.

Through an interdisciplinary lens, this paper emphasizes the challenges and benefits of implementing project-based learning in higher education, especially when engaging with complex scientific phenomena and advanced technology. The experiences and outcomes of these projects indicate the potential for further integrating UAS and mobile devices into geoscientific study and teaching.

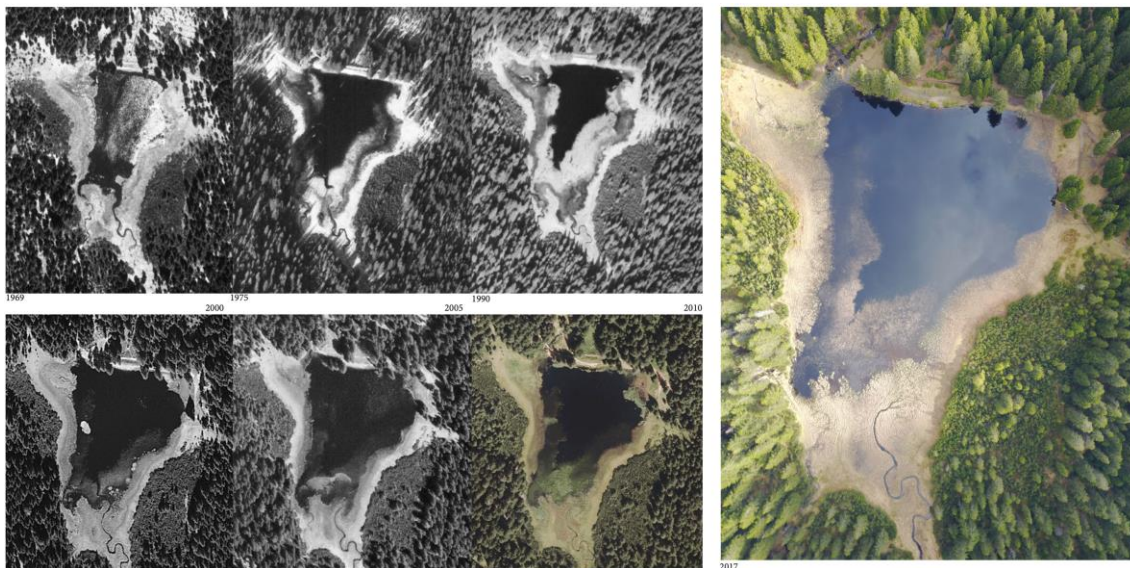


Figure 1: Study of Črno jezero through the time

## Water level estimation comparison: UAV vs satellite altimetric data

Grzegorz Walusiak<sup>1\*</sup> & Matylda Witek<sup>1</sup>

<sup>1</sup> *Department of Geoinformatics and Cartography, Institute of Geography and Regional Development,  
University of Wrocław,  
Pl. Uniwersytecki 1, 50-137, Poland, grzegorz.walusiak@uwr.edu.pl*

**Keywords:** *unmanned aerial vehicle, water level, coastline detection, LiDAR*

Flood management is very important task in the context of rapid climate changes. Increasing the frequency of extreme weather and fluvial phenomena, such as droughts, water shortages or floods determines that detecting water bodies and boundaries between them and surrounding surface is an important and challenging issue. Moreover, the decrease in global amounts of water gauges is the factor that limits conducting regular, hydrological measurements. Remote sensing sensors and data may be very helpful and may densify observation network on ungauged sections of river channels. This work is the part of project, in which we try to verify whether the altimetric data can be used to determine water level on ungauged river sections.

Satellite altimetric measurements have many advantages. The network of ground tracks is dense so it may constitute the gap filling between water gauges. However there is necessity to verify the accuracy of altimetric water level survey. In this case we use UAV platform both with RGB camera and LiDAR sensor. Low altitude data is relatively cheap and fast to acquire. The flight may be done almost on demand (except for bad weather conditions) and in near real time (according to the revisit time of satellite).

We compared estimations of water levels on eight sites on the Oder river (west Poland) based on satellite altimetric and UAV data. As there is no *in-situ* water gauge at so called *virtual stations* (locations of altimetric measurements), there is no reference data. We used GNSS RTK receiver to measure reference water levels at the moment when satellite passes over the river. Using UAV data (both RGB images and LiDAR dense point cloud) we try to delineate river coastline and, in further step, water level. Obtained values were compared against altimetric water level in order to confirm assumption that altimetric data can be used for water level monitoring.

# Multi-drone experimental campaign for shallow river bathymetry

Matylda Witek<sup>1\*</sup> & Grzegorz Walusiak<sup>1</sup>

<sup>1</sup> *Department of Geoinformatics and Cartography, Institute Geography and Regional Development, University of Wrocław, pl.Uniwersytecki 1, 50-137 Wrocław, Poland, matylda.witek@uwr.edu.pl*

**Key words:** *unmanned aerial vehicle, Structure-from-Motion, bathymetry, shallow river*

Knowledge about underwater riverbed topography and river cross-sections remains essential input data for hydrology and fluvial geomorphology, for instance in hydrodynamic modelling as they enable to compute the cross sectional areas. There are a lot of method to survey river bathymetry but they are time- and labour-consuming. The development of drone techniques has led to the creation of various sensors, such as LiDAR or radar, which, however, are expensive. WOODGET et al. (2015) were the first to describe the UAV-SfM method in the context of river bathymetry, and the novelty of the approach was not only the application of UAV photogrammetry to submerged river areas, but also the use of the refraction correction. The question is, whether the UAV-SfM method is repeatable (i.e. if it produces similar underwater topography in repeated flights performed in nearly identical environmental and technical conditions) and reproducible (i.e. if it produces similar bathymetry under modified measurement conditions). Also, there is no knowledge about the similarities or differences between the effectiveness of the UAV-SfM when different types of UAV platforms and cameras are utilized to acquire imagery.

We conducted the multi-drone experimental campaign in SW Poland/N Czechia, Izera river channel, where one fixed-wing drone (eBee by SenseFly) and three multi-rotors (DJI Matrice 210-RTK V2, DJI Mavic 2 Pro, DJI Phantom 4 Pro) were utilized. Riverbed topography was reconstructed on 2 sites using 4 platforms in 3 resolutions and 2 repetitions. We measured reference riverbed elevations with the use of levelling. The error of river bottom reconstruction falls within typical error known for through-water photogrammetry. We found that multi-rotors were the most stable platforms as well as the river bottom reconstruction method, using the Structure-from-Motion algorithm and the refractive index, is robust, especially in terms of its repeatability and reproducibility. Reconstructed river bottom do not fit perfectly in the reference data but the shape of profiles are preserved.

## References

WOODGET, A.S., CARBONNEAU, P.E., VISSER, F. & MADDOCK, I.P., 2015. Quantifying submerged fluvial topography using hyperspatial resolution UAS imagery and structure from motion photogrammetry. *Earth Surface Processes and Landforms* 40(1): 47–64.

# Exploring the potential of UAV for plant biodiversity monitoring in farmland

Caterina Barrasso<sup>1</sup>, Robert Krüger<sup>2\*</sup>, Lisanne Hölting<sup>1</sup>, Anette Eltner<sup>2</sup> & Anna Cord<sup>1</sup>

<sup>1</sup> Chair of Computational Landscape Ecology, Dresden University of Technology, Germany

<sup>2</sup> Junior Professorship in Geosensor Systems, Dresden University of Technology, Germany

\* Corresponding author: R. Krüger: robert.krueger@tu-dresden.de

**Key words:** Ecology, UAV Imagery, Machine Learning

The intensification of agriculture through the application of high fertilization rates is leading to the decline of wild arable herbs with significant natural value (HNV). This decline, in turn, is having a series of adverse ecological consequences. One approach to encourage the preservation of HNV wild arable herbs is to implement result-based payment schemes that compensate farmers based on the observable biodiversity improvements within their fields.

However, the major obstacle facing these programs is the substantial cost and time required for biodiversity monitoring, typically carried out by field surveyors (SIMONCINI ET AL., 2019). Consequently, such initiatives are infrequently adopted within the European Union's Common Agricultural Policy. Satellite and Unmanned Aerial Vehicle (UAV) remote sensing have already displayed promising results for biodiversity monitoring across various ecosystems. In agricultural landscapes, this task is particularly challenging due to the diminutive size of the plants and their partially overlapping spectral signatures (YANG ET AL., 2021). Nevertheless, the combination of multiple UAV based sensors has begun to reveal possibilities in this research domain (PÖTTKER ET AL., 2023; TORRESANI ET AL., 2023; MARCINKOWSKA-OCHTYRA ET AL., 2018).

Using the latest advances in deep learning, this study will explore the potential of UAVs for monitoring plant biodiversity on agricultural land. Our focus is on a farmland area situated in the UNESCO biosphere reserve known as the "Upper Lusatian Heath and Pond Landscape" in Saxony, Germany. In this area, fields with intensive and extensive farming have been assessed to study the usability of different UAV sensors in distinguishing and identifying HNV plant species.

In this research we will focus on the following aspects: i) identification of wild arable herbs for which training data can easily be created from RGB images, ii) Strategies for optimizing sensor selection and flight altitudes to enhance classification accuracy, iii) aspects of fusion of datasets from different UAV based sensors, iv) identification of difficult to map/classify wild arable herbs, and v) Exploring the potential for implementing outcome-based payment programs for other plant species not observed in the study area but considered significant for the application of such schemes in Germany.

## References

MARCINKOWSKA-OCHTYRA, A., JAROCIŃSKA, A., BZDEGA, K., AND TOKARSKA-GUZIŁ, B.: Classification of Expansive Grassland Species in Different Growth Stages Based on Hyperspectral and LiDAR Data, *Remote Sensing*, 10, 2019, <https://doi.org/10.3390/rs10122019>, 2018.

PÖTTKER, M., KIEHL, K., JARMER, T., AND TRAUTZ, D.: Convolutional Neural Network Maps Plant Communities in Semi-Natural Grasslands Using Multispectral Unmanned Aerial Vehicle Imagery, *Remote Sensing*, 15, 1945, <https://doi.org/10.3390/rs15071945>, 2023.

SIMONCINI, R., RING, I., SANDSTRÖM, C., ALBERT, C., KASYMOV, U., AND ARLETTAZ, R.: Constraints and opportunities for mainstreaming biodiversity and ecosystem services in the EU's Common Agricultural Policy: *Insights from the IPBES assessment for Europe and Central Asia, Land Use Policy*, 88, 104099, <https://doi.org/10.1016/j.landusepol.2019.104099>, 2019.

TORRESANI, M., KLEIJN, D., DE VRIES, J. P. R., BARTHOLOMEUS, H., CHIEFFALLO, L., CAZZOLLA GATTI, R., MOUDRÝ, V., DA RE, D., TOMELLERI, E., AND ROCCHINI, D.: A novel approach for surveying flowers as a proxy for bee pollinators using drone images, *Ecological Indicators*, 149, 110123, <https://doi.org/10.1016/j.ecolind.2023.110123>, 2023.

YANG, D., ZHAO, J., LAN, Y., WEN, Y., PAN, F., CAO, D., HU, C., AND GUO, J.: Research on farmland crop classification based on UAV multispectral remote sensing images, *International Journal of Precision Agricultural Aviation*, 4, 29–35, <https://doi.org/10.33440/j.ijpaa.20200401.153>, 2021.

# Demonstrating the OPTRAM soil moisture model over pasture areas in drylands

Arnon Karnieli\* & Micha Silver

The Remote Sensing Laboratory, Institutes for Desert Research, Ben Gurion University of the Negev, [karnieli@bgu.ac.il](mailto:karnieli@bgu.ac.il), [silverm@post.bgu.ac.il](mailto:silverm@post.bgu.ac.il)

**Keywords:** Water content, Sentinel-2, Senegal.

Soil moisture is crucial in hydrological, agricultural, and ecological processes. Remote sensing is essential for retrieving spatiotemporal soil moisture data near the land surface over large areas. Water content has been found to be correlated with optical, thermal, and microwave regions of the electromagnetic spectrum, and therefore corresponding models have been extensively used. Besides, a novel physical-based model, Optical TRApEZoid Model (OPTRAM), was recently proposed and validated by (Babaeian et al. 2018); Sadeghi et al. (2017) to address the need to estimate soil moisture over vast areas in watershed and regional scales. OPTRAM is based on the physical relationship between the shortwave infrared (SWIR) transformed reflectance (STR) and spectral vegetation index (VI), such as the Normalized Difference Vegetation Index (NDVI) or the Soil Adjusted Vegetation Index (SAVI) (Fig. 1). The model can be applied to various earth observation systems with visible, near-infrared, and SWIR bands (e.g., Landsat, Sentinel-2).

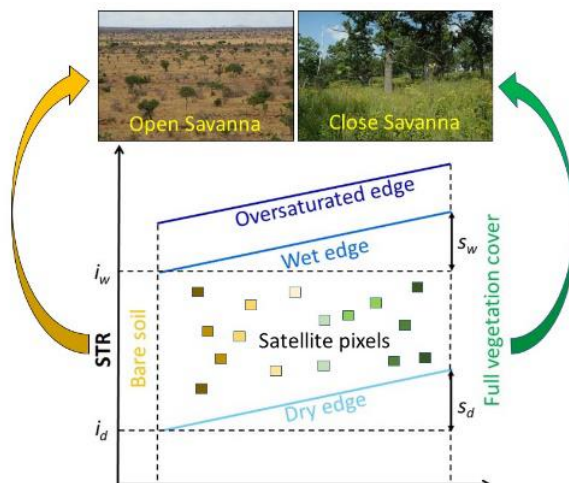


Figure 1: Schematic illustration of the OPTRAM model

The OPTRAM model was programmed in R and implemented in several pasture sites in dryland environments (Israel, Senegal, China, and Kenya) for assessing soil moisture over large regions at several seasonal time slots. Sentinel-2 images were used to differentiate seasonal moisture variations and describe divergent soil conditions between wet and drought years. Landsat images provided a long-term time series, from the 1980s, of water content, which was used, in conjunction with precipitation, for climate change studies.

A ground-based hyperspectral sensing camera was applied for in-situ calibration/validation of the model, along with volumetric soil water content measurements using Time-Domain Reflectometer (TDR), as well as a cosmic ray instrument. The proposed model was implemented with Sentinel-2 images for 2022 in an area of 16.3 sq. km. within the Reserve Sylvo Pastorale Barkedji Dodji, east of Linguere, Senegal (Fig. 2).

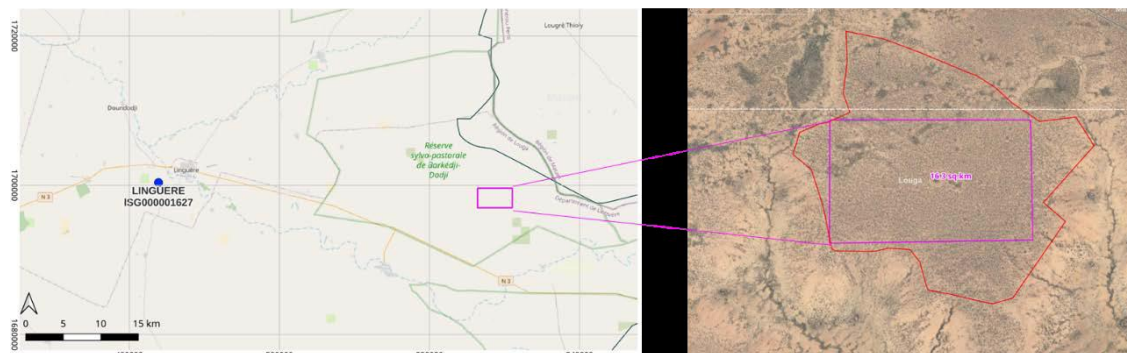


Figure 2: Study area within the Reserve Sylvo Pastorale Barkedji Dodji, east of Linguere, Senegal

The computed monthly trajectory shows the relationship between STR and NDVI for 2022 (Fig. 3):

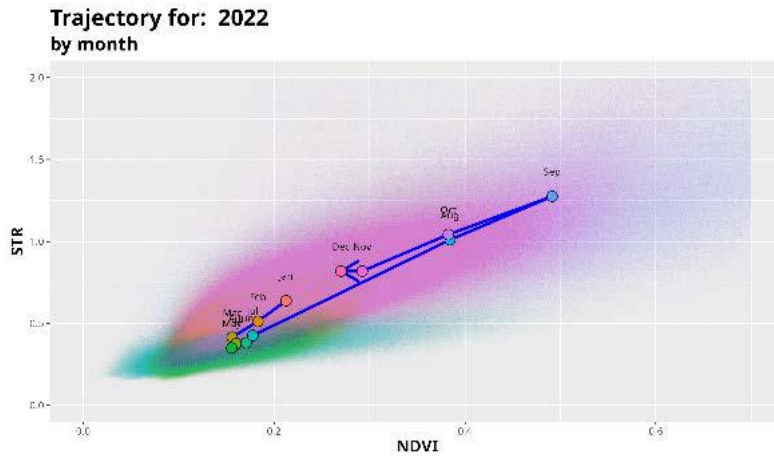


Figure 3: Monthly trajectory shows the relationship between STR and NDVI for 2022.

The model revealed the following monthly average volumetric soil water content, presented with the monthly rainfall, acquired from the Linguere meteorological station (Table 1, Fig. 4).

Table 1: Monthly average volumetric soil water content and the monthly rainfall

Month	Water content (cm <sup>3</sup> /cm <sup>3</sup> )	Rainfall (mm)
Jan	0.43	0
Feb	0.32	0
Mar	0.28	0
Apr	0.20	0
May	0.17	2
Jun	0.19	75.7
Jul	0.22	72.6
Aug	0.41	57.8
Sep	0.43	159.1
Oct	0.45	29.2
Nov	0.40	0
Dec	0.48	0
		<b>396.4</b>

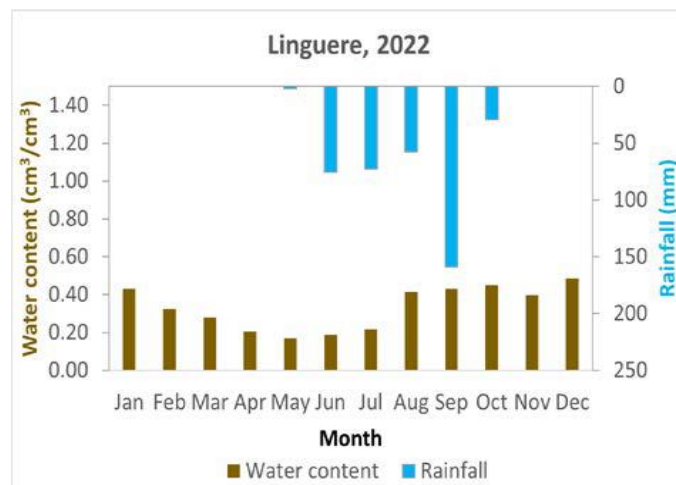


Figure 4: Monthly average volumetric soil water content and the monthly rainfall.

## References

- Babaeian, E., Sadeghi, M., Franz, T.E., Jones, S., & Tuller, M. (2018). Mapping soil moisture with the OPTical TRAppezoid Model (OPTRAM) based on long-term MODIS observations. *Remote Sensing of Environment*, 211, 425-440
- Sadeghi, M., Babaeian, E., Tuller, M., & Jones, S.B. (2017). The optical trapezoid model: A novel approach to remote sensing of soil moisture applied to Sentinel-2 and Landsat-8 observations. *Remote Sensing of Environment*, 198, 52-68